

Radiotherapy & Oncology

Journal of the European Society for
Radiotherapy and Oncology

ICTR-PHE 2014
International Conference on Translational
Research in Radiation Oncology /
Physics for Health in Europe

February 10-14, 2014
Geneva, Switzerland



ICTR-PHE **2014**

Radiotherapy & Oncology

Journal of the European Society for
Radiotherapy and Oncology

INFORMATION FOR AUTHORS

ARTICLES should deal with original research or reviews of topics defined in the aims of the journal. Radiotherapy and Oncology publishes original material only. It is therefore understood that the content of the paper has not previously been published in the same or a similar form and that it is not under consideration for publication elsewhere. The act of submitting a manuscript to the journal carries with it the right to publish that paper.

Radiotherapy and Oncology uses an online manuscript submission and peer review process.

Papers and correspondence should be submitted online at <http://www.ees.elsevier.com/ro> and the instructions on the site should be closely followed. Authors may submit manuscripts and track their progress to final decision. Reviewers can download manuscripts and submit their reports to the Editors electronically.

The full contact details for the Editorial Office are shown below:

Professor Jens Overgaard, M.D., Radiotherapy and Oncology Secretariat, Department of Experimental Clinical Oncology, Aarhus University Hospital, Nørrebrogade 44, Building 5, DK-8000 Aarhus C, Denmark (Tel.: +45 78 46 26 29; Fax: +45 86 19 71 09; E-mail: ro@oncology.dk)

TYPES OF PAPERS

1. Full length original papers (max. 3000 words)

Describe original scientific work in the field of radiation oncology or related areas. The content of the paper should be sufficient to reach valid conclusions. Full papers should include a structured abstract and be divided into sections (Introduction; Materials and Methods; Results; Discussion; References; Tables; Figures) and should not normally exceed 6 printed pages, including references and a maximum of 6 tables/figures. Additional material can be submitted as supplementary files.

2. Short communications and Technical notes (max. 2000 words)

Provide a brief but complete account of a particular piece of work, e.g. Phase I or II study, and should in total be no longer than 4 printed pages, normally including a maximum of 2 figures or tables. A summary of not more than 50 words should be included (not a structured abstract), but the manuscript can have fewer subheadings (e.g. short introduction; materials and methods; results and discussion). Authors are advised to see a recent issue of the journal for size and lay-out.

3. Review articles

Rigorous critical assessment of clinical and/or laboratory research in a field of interest to the journal and its subscribers. Reviews are normally solicited by the editors, and it is suggested that authors wishing to contribute a review article contact the editor-in-chief.

4. Editorials and commentaries

Editorials and commentaries relate to articles in the journal or to issues of relevance for the readership. This type of communication is normally solicited by the editors.

5. Letters to the Editor

On topics of current interest or comment upon material previously or simultaneously published in the journal. They should be limited to 500 words and may include 1 table or figure.

6. Announcements

The inclusion of announcements, etc. is at the discretion of the Editors and the Publisher and subject to space availability. Request for inclusion of meeting announcement should be sent to the ESTRO secretariat (see address in journal).

Author inquiries

For inquiries relating to the submission of articles (including electronic submission where available) please visit this journal's homepage at <http://www.elsevier.com/locate/radonc>. For detailed instructions on the preparation of electronic artwork, please visit <http://www.elsevier.com/artworkinstructions>. Contact details for questions arising after acceptance of an article, especially those relating to proofs, will be provided by the publisher. You can track accepted articles at <http://www.elsevier.com/trackarticle>. You can also check our Author FAQs at <http://www.elsevier.com/authorFAQ> and/or contact Customer Support via <http://support.elsevier.com>

Language services. Authors who require information about language editing and copyediting services pre- and post-submission please visit <http://webshop.elsevier.com/languageediting> or our customer support site at <http://support.elsevier.com>.

A full and complete Guide for Authors is available online at
<http://www.thegreenjournal.com>

Printed by Henry Ling Ltd., Dorchester, United Kingdom

∞ The paper used in this publication meets the requirements of ANSI/NISO Z39.48-1992 (Permanence of Paper)

Radiotherapy & Oncology

Journal of the European Society for
Radiotherapy and Oncology

Volume 110 Supplement 1 (2014)

Editor-in-Chief: J. Overgaard

**ICTR-PHE 2014
International Conference
on Translational Research in Radiation Oncology /
Physics for Health in Europe**

February 10-14, 2014 • Geneva, Switzerland



Recommended by



Endorsed by



Under the auspices of



In collaboration with



Radiotherapy & Oncology is available online:
For ESTRO members: <http://www.thegreenjournal.com>
For institutional libraries: <http://www.sciencedirect.com>



© 2013 Elsevier Ireland Ltd. All rights reserved.

This journal and the individual contributions contained in it are protected under copyright by Elsevier Ireland Ltd., and the following terms and conditions apply to their use:

Photocopying

Single photocopies of single articles may be made for personal use as allowed by national copyright laws. Permission of the Publisher and payment of a fee is required for all other photocopying, including multiple or systematic copying, copying for advertising or promotional purposes, resale, and all forms of document delivery. Special rates are available for educational institutions that wish to make photocopies for non-profit educational classroom use.

For information on how to seek permission visit www.elsevier.com/permissions or call: (+44) 1865 843830 (UK)/(+1) 215 239 3804 (USA).

Derivative Works

Subscribers may reproduce tables of contents or prepare lists of articles including abstracts for internal circulation within their institutions. Permission of the Publisher is required for resale or distribution outside the institution.

Permission of the Publisher is required for all other derivative works, including compilations and translations (please consult www.elsevier.com/permissions).

Electronic Storage or Usage

Permission of the Publisher is required to store or use electronically any material contained in this journal, including any article or part of an article (please consult www.elsevier.com/permissions).

Except as outlined above, no part of this publication may be reproduced, stored in a retrieval system or transmitted in any form or by any means, electronic, mechanical, photocopying, recording or otherwise, without prior written permission of the Publisher.

Notice

No responsibility is assumed by the Publisher for any injury and/or damage to persons or property as a matter of products liability, negligence or otherwise, or from any use or operation of any methods, products, instructions or ideas contained in the material herein. Because of rapid advances in the medical sciences, in particular, independent verification of diagnoses and drug dosages should be made.

Although all advertising material is expected to conform to ethical (medical) standards, inclusion in this publication does not constitute a guarantee or endorsement of the quality or value of such product or of the claims made of it by its manufacturer.

Orders, claims, and journal inquiries: please contact the Elsevier Customer Service Department nearest you:

St. Louis: Elsevier Customer Service Department, 3251 Riverport Lane, Maryland Heights, MO 63043, USA; phone: (800) 6542452 [toll free within the USA]; (+1) (314) 4478871 [outside the USA]; fax: (+1) (314) 4478029; e-mail: JournalsCustomerService-usa@elsevier.com

Oxford: Elsevier Customer Service Department, The Boulevard, Langford Lane, Kidlington, Oxford OX5 1GB, UK; phone: (+44) (1865) 843434; fax: (+44) (1865) 843970; e-mail: JournalsCustomerServiceEMEA@elsevier.com

Tokyo: Elsevier Customer Service Department, 4F Higashi-Azabu, 1-Chome Bldg, 1-9-15 Higashi-Azabu, Minato-ku, Tokyo 106-0044, Japan; phone: (+81) (3) 5561 5037; fax: (+81) (3) 5561 5047; e-mail: JournalsCustomerServiceJapan@elsevier.com

Singapore: Elsevier Customer Service Department, 3 Killiney Road, #08-01 Winsland House I, Singapore 239519; phone: (+65) 63490222; fax: (+65) 67331510; e-mail: JournalsCustomerServiceAPAC@elsevier.com

Funding Body Agreements and Policies

Elsevier has established agreements and developed policies to allow authors whose articles appear in journals published by Elsevier, to comply with potential manuscript archiving requirements as specified as conditions of their grant awards. To learn more about existing agreements and policies please visit <http://www.elsevier.com/fundingbodies>



Radiotherapy & Oncology

Journal of the European Society for
Radiotherapy and Oncology

AIMS AND SCOPE

Radiotherapy and Oncology publishes papers describing original research as well as review articles. It covers areas of interest relating to radiation oncology. This includes clinical radiotherapy, combined modality treatment, experimental work in radiobiology, chemobiology, hyperthermia and tumour biology, as well as physical aspects relevant to oncology, particularly in the field of imaging, dosimetry and radiation therapy planning. Papers on more general aspects of interest to the radiation oncologist including chemotherapy, surgery and immunology are also published.

EDITOR-IN-CHIEF

Jens Overgaard, Aarhus, Denmark

EDITORS

<i>Clinical</i>	<i>Clinical</i>	<i>Clinical</i>	<i>Clinical</i>	<i>Physics</i>	<i>Biology</i>
M. Baumann Dresden, Germany	E. Lartigau Lille, France	R. Pötter Vienna, Austria	P. Hoskin Northwood, UK	D.I. Thwaites Sydney, Australia; Leeds, UK L.P. Muren, Aarhus, Denmark (Assistant Physics Editor)	A.J. van der Kogel Nijmegen, The Netherlands

PAST EDITORS

E. van der Schueren, Leuven, Belgium; H. Bartelink, Amsterdam, The Netherlands

EDITORIAL BOARD

R.P. Abratt, Cape Town, South Africa	D. De Ruyscher, Maastricht, The Netherlands	J.H.M. Kaanders, Nijmegen, The Netherlands	P. Poortmans, Tilburg, The Netherlands
K.K. Ang, Houston, TX, USA	J. Denham, Newcastle, Australia	T. Knöös, Lund, Sweden	H.P. Rodemann, Tübingen, Germany
A.C. Begg, Amsterdam, The Netherlands	W. Dörr, Vienna, Austria	M. Krause, Dresden, Germany	F. Sanchez-Doblado, Seville, Spain
S.M. Bentzen, Madison, WI, USA	G. Duchesne, Melbourne, Australia	T. Kron, Melbourne, Australia	R. Sarin, Mumbai, India
S. Bodis, Zurich, Switzerland	C. Fiorino, Milan, Italy	P. Lambin, Maastricht, The Netherlands	M. Saunders, Northwood, UK
M. Bolla, Grenoble, France	D. Georg, Vienna, Austria	J.A. Langendijk, Groningen, The Netherlands	P. Scalliet, Brussels, Belgium
T. Bortfeld, Boston, MA, USA	B. Glimelius, Uppsala, Sweden	A. Lee, Hong Kong, China	H.D. Suit, Boston, MA, USA
J. Bourhis, Villejuif, France	C. Grau, Aarhus, Denmark	J.W.H. Leer, Nijmegen, The Netherlands	I. Tannock, Toronto, ON, Canada
M. Brada, Surrey, UK	V. Grégoire, Brussels, Belgium	D. Lefkopoulos, Villejuif, France	H. Thames, Houston, TX, USA
R.G. Bristow, Toronto, ON, Canada	J. Harris, Boston, MA, USA	C.C. Ling, New York, NY, USA	W. Tome, New York, USA
W. Budach, Düsseldorf, Germany	K. Haustermans, Leuven, Belgium	B. Maciejewski, Gliwice, Poland	I. Turesson, Uppsala, Sweden
F.A. Calvo, Madrid, Spain	B.J. Heijmen, Rotterdam, The Netherlands	B.J. Mijnheer, Amsterdam, The Netherlands	V. Valentini, Rome, Italy
N. Coleman, Bethesda, MD, USA	M. Hiraoka, Kyoto, Japan	M. Molls, Munich, Germany	M. Verheij, Amsterdam, The Netherlands
J.M. Cosset, Paris, France	J.Cl. Horiot, Geneva, Switzerland	D.R. Olsen, Oslo, Norway	D. Vordermark, Halle, Germany
J.D. Cox, Houston, TX, USA	P. Hoskin, Northwood, UK	B. O'Sullivan, Toronto, ON, Canada	B.G. Wouters, Toronto, ON, Canada
B.J. Cummings, Toronto, ON, Canada	J. Jaal, Tartu, Estonia	L.J. Peters, Melbourne, Australia	D. Zips, Dresden, Germany
O. Dahl, Bergen, Norway	J. Jassem, Gdansk, Poland		
J. Debus, Heidelberg, Germany			

Publication information: *Radiotherapy & Oncology* (ISSN 0167-8140). For 2014, volumes 110–113 (12 issues) are scheduled for publication. Subscription prices are available upon request from the Publisher or from the Elsevier Customer Service Department nearest you or from this journal's website (<http://www.thegreenjournal.com>). Further information is available on this journal and other Elsevier products through Elsevier's website (<http://www.elsevier.com>). Subscriptions are accepted on a prepaid basis only and are entered on a calendar year basis. Issues are sent by standard mail (surface within Europe, air delivery outside Europe). Priority rates are available upon request. Claims for missing issues should be made within six months of date of dispatch.

USA mailing notice: *Radiotherapy & Oncology* (ISSN 0167-8140) is published monthly by Elsevier Ireland Ltd. (Elsevier House, Brookvale Plaza, East Park, Shannon, Co. Clare, Ireland). Periodicals postage paid at Jamaica, NY 11431 and additional mailing offices.

USA POSTMASTER: Send change of address to *Radiotherapy & Oncology*, Elsevier Customer Service Department, 3251 Riverport Lane, Maryland Heights, MO 63043, USA.

AIRFREIGHT AND MAILING in USA by Air Business Ltd., c/o Worldnet Shipping Inc., 156-15, 146th Avenue, 2nd Floor, Jamaica, NY 11434, USA.

Advertising information. Advertising orders and enquiries can be sent to: **USA, Canada and South America:** Elsevier Inc., 360 Park Avenue South, New York, NY 10010-1710, USA; phone: (+1) (212) 633 3974. **Europe and ROW:** Advertising Sales, Elsevier Pharma Solutions, 32 Jamestown Road, London NW1 7BY, UK; phone: (+44) (0) 20 7424 4259; fax: (+44) (0) 20 7424 4433; e-mail: elsevierpharma.uk@elsevier.com

CONFERENCE CHAIRS

Jacques Bernier, *Genolier Geneva*
Manjit Dosanjh, *CERN*

ADVISORY BOARD

Ugo Amaldi
Kian K. Ang
Michael Baumann
Soeren M. Bentzen
Jacques Bernier
Jean Bourhis
David Brizel
Denis Dauvergne
Alberto Del Guerra
Manjit Dosanjh
Marco Durante
Wolfgang Enghardt
Zvi Fuks
Yoshiya Furusawa
Thomas Haberer
Ulli Köster
Philippe Lambin
Paul Lecoq
Anthony Lomax
Alejandro Mazal
Steve Myers
Dag Rune Olsen
Jens Overgaard
Kevin Prise
Osman Ratib
Sandro Rossi
Vincenzo Valentini
Marcel Verheij
Brad Wouters

SESSION ORGANISERS

(Session chairs in black)

Biology

M. Durante, *Darmstadt*
K. Prise, *Belfast*
Ph. Lambin, *Maastricht*
B. Wouters, *Toronto*

Pre-clinical & clinical strategies

K.K. Ang, *Houston*
M. Baumann, *Dresden*
Z. Fuks, *New York*
M. Verheij, *Amsterdam*

Nuclear medicine

O. Ratib, *Geneva*
U. Köster, *Grenoble*
T. Beyer, *Vienna*
J-F. Chatal, *Nantes*

Detectors & imaging

D. Dauvergne, *Lyon*
A. Del Guerra, *Pisa*
T. Haberer, *Heidelberg*
P. Lecoq, *CERN*

New technologies

W. Enghardt, *Dresden*
A. Lomax, *PSI, Villigen*
B. Mazal, *Curie Institute*
S. Rossi, *Pavia*

Radiotherapy

S.M. Bentzen, *Madison*
J. Bourhis, *Lausanne*
D.R. Olsen, *Oslo*
D. Brizel, *Durham*

EXECUTIVE COMMITTEE

Ugo Amaldi, *TERA*
Jacques Bernier, *Genolier & Geneva*
Jean Bourhis, *Lausanne*
Alberto Costa, *Milano*
Manjit Dosanjh, *CERN*
Raymond Miralbell, *Geneva*
Steve Myers, *CERN*

AUTHORS INDEX

Aadnevik, D	1	Gianoli, C	77	Patera, V	152
Abbas, MI	2	Giannotti, F	78	Peeters, S	153
Abellan, C	3	Girst, S	79	Pella, A	154
Akulinichev, S	4	Giubilato, P	80	Petit, B	155
Albertini, F	5	Gregoire, V	81, 82	Pinto, M	156
Amaldi, U	6	Grevillot, L	83	Pizzichemi, M	157
Ares, C	7	Hansen, DC	84	Podesta, M	158
Arico, G	8	Helmbrecht, S	85	Pouget, J-P	159
Arteaga- Marrero, N	9	Herranz, E	86	Prezado, Y	160
Asadi, S	10	Hilaire, E	87	Prise, KM	161
Attili, A	11, 12	Hoffmann, HF	88	Pruschy, M	162
Auffray, E	13	Hopewell, J	99	Rancati, T	163
Balosso, J	14	Horsman, M	89	Rao, BSS	164
Baroni, G	15	Hueso-Gonzalez, F	90	Rath, AK	165
Bassler, N	16	Hughes, C	91	Rescigno, R	166
Battistoni, G	17	Hugtenburg, R	92	Rimoldi, A	167
Bauer, J	18	Janssen, F	93	Rodriguez-Lafrasse, C	168
Baumann, M	19	Janssens, G	94	Rottenberg, S	169
Berbeco, R	20	Jastrzebski, J	95	Rouschop, K	170
Bernatowicz, K	21	Jeraj, R	96	Rucinski, A	171
Bertrand, D	22	Johnstone, PAS	97	Saikouk, H	172
Blakely, EA	23	Jones, B	98, 99	Sakumi, A	173
Bortfeld, T	24	Kam, W	100	Sala, P	174
Bourgeois, M	25	Kamp, F	101	Sarti, P	175
Bourhaleb, F	26, 27	Kim, H	102	Scaife, J	176
Bracinni, S	28, 29	Knäusl, B	103	Schaart, DR	177
Brevet, R	30	Komaki, R	104	Schmid, TE	178
Brizel, DM	31	Koritzinsky, M	105	Scifoni, E	109
Brochu, F	32	Kormoll, T	106	Servoli, L	179
Broggini-Tenzer, A	33	Köster, U	107	Severin, GW	180
Brüningk, S	34	Koumeir, C	108	Shah, E	181
Brunner, S	35	Krämer, M	109	Sidhique, H	182
Bucciantonio, M	36	Krause, M	110	Simmons, M	183
Buchegger, F	37	Krimmer, J	111	Smeets, J	184
Bueno, G	38	Kuess, P	112	Smits, KM	185
Burigo, LN	39	Kulich, I	113	Soleimani, M	186
Busk, M	40	Labalme, M	114	Solevi, P	187
Carillo, V	41	Lambin, P	115	Sørensen, BS	188
Casella, C	42	Landry, G	116	Stachura, M	189
Cella, L	43	Laursen, LV	117	Stora, T	37
Cerello, P	44	Lavagno, M	59	Stützer, K	190
Cirrone, GAP	45	Lecoq, P	118	Tamborini, A	191
Coleman, N	46	Leming, EJ	119	Thirolf, P	192
Conte, V	47	Lepareur, N	120	Thorwarth, D	193
Constanzo, J	50	Lestand, L	121	Tian, Y	194
Crespo, P	48	Ley, J-L	122	Toader, A	195
da Silva, J	49	Litov, L	123	Townsend, D	196
Dauvergne, D	50	Magallanes, L	124	Trani, D	197
Debus, J	51	Magrin, G	125	Trbojevic, D	198
Dedes, G	52	Maingon, P	126	Trovato, M	199
DeLaney, TF	53	Mancini Terracciano, C	127	Tsujii, H	200
Delorme, R	54	Manescu, P	128	The ULICE Consortium	201
Dendooven, P	55	Maneval, D	129	Valdagni, R	202
Deutsch, E	56	Martinez-Rovira, I	130, 131	Van der Meulen, N	203
Ding, K	57	Martisikova, M	132	van Gisbergen, M	204
Doerr, W	58	Maughan, T	133	van Herk, M	205
Donetti, M	59	Maxim, V	134	Velarde, E	206
Dosanjh, M	60	Meier, G	135	Velthuis, JJ	207
Dubois, L	61	Melenevska, N	113	Verheij, M	208
Edgecock, R	62	Ménager, J	136	Vestergaard, A	209
El Kanawati, W	63	Milz, S	137	Viana Miranda Lima, T	210
El Khayati, N	172	Miralbell, R	138	Vidal, M	211
Elas, M	64	Mohan, R	139	Viertl, D	212, 213
ENTERVISION	65	Mori, M	140	Vooijs, M	214
ENVISION	66	Moskal, P	141	Vozenin, M-C	215
Ertl, S	67	Moyal, EC	142	Wang, KK-H	216
Faccini, R	68	Muanza, TM	143	Weichselbaum RR	217
Fassi, A	69	Nazarpavar, B	144	Wilmsen, D	218
Fiorini, F	70	Nesteruk, M	145	Wittenborn, T	219
Fix, M	71, 145	Orecchia, R	146	Wong, J	220
Fleta, C	72	Ovejero, MC	147	Wouters, BG	221
Gallego, L	73	Paillass, S	148	Yagnyukova, A	222
Garcia Ortega, P	74	Park, W-Y	149	Yang, CL	223
Garonna, A	75	Parodi, K	150	Zegers, CML	224
Georgantzoglou, A	76	The PARTNER Training Network	151	Zenhausen, F	225
				Zhang, Y	226

ICTR-PHE 2014
 International Conference on Translational Research in Radiation Oncology/Physics for Health in Europe
 Uniting Physics, Biology and Medicine for better healthcare
 Geneva International Conference Center, February 10 - 14, 2014

Abstract nr	Page
1 Extremely high-granularity digital tracking calorimeter for the detection of charged and neutral radiation in hadron therapy <i>Aadnevik, D, Norway</i>	1
2 Calibration of lanthanum bromide scintillation detectors <i>Abbas, MI, Egypt</i>	1
3 A μ TCA Data Acquisition System and its application for Hadrontherapy Monitoring using a Compton Camera <i>Abellan, C, France</i>	1
4 New design of ytterbium sources for brachytherapy <i>Akulinichev, S, Russia</i>	2
5 The use of 'planned overshoot' for reducing dose to healthy tissue and improve treatments robustness for scanned proton beams <i>Albertini, F, Switzerland</i>	2
6 Physics is beautiful and useful <i>Amaldi, U, Italy</i>	3
7 Spot-scanning Proton Therapy for Pediatric Parameningeal Rhabdomyosarcomas: Clinical Outcome of 39 Patients Treated at PSI <i>Ares, C, Switzerland</i>	3
8 Verification and Application of a new method for Ion Spectroscopy in Heavy Ion Radiotherapy <i>Arico, G, Germany</i>	3
9 DCE-MRI and DCE-US quantification in CWR22 prostate tumour xenografts <i>Arteaga-Marrero, N, Norway</i>	4
10 Choroidal Melanoma brachytherapy enhancement with gold nanoparticles using a full Monte Carlo modelling of human eye <i>Asadi, S, Iran</i>	5
11 Direct evaluation of ion beam radiobiological parameters from clinical data: an alternative approach to the RBE <i>Attili, A, Italy</i>	5
12 Impact of uncertainties in ion beam therapy on the optimality of irradiation condition and fractionation schedule <i>Attili, A, Italy</i>	5
13 A multimodal ultrasound and time of flight PET endoscope for developing new biomarkers for the prostate and pancreatic cancers <i>Auffray, E, Switzerland</i>	6
14 France HADRON: national infrastructure for hadrontherapy research including ETOILE, ARCHADE and protontherapy centers <i>Balosso, J, France</i>	6
15 Oxygen ions achieve better tumour control probability in hypoxic tumours than carbon ions do <i>Bassler, N, Denmark</i>	7
16 Measurement of charged particle yields emitted during irradiation with therapeutic proton and Carbon beams in view of the design of a new tool for the monitoring of hadrontherapy treatments <i>Battistoni, G, Italy</i>	8
17 MCTP: a new Monte Carlo-based treatment planning tool for hadrontherapy <i>Battistoni, G, Italy</i>	9
18 PET/CT-based verification of scanned proton and carbon ion treatment at HIT - an overview <i>Bauer, J, Germany</i>	9
19 Individualized Radiation Oncology - harnessing clinics, biology and high technology <i>Baumann, M, Germany</i>	10

20	Targeted Gold Nanoparticles as Vascular Disrupting Agents during Radiotherapy <i>Berbeco, R, USA</i>	10
21	Performance of layered and volumetric rescanning for different scanning speeds of proton beam <i>Bernatowic, K, Switzerland</i>	11
22	Pre-clinical validation of a beam model designed for treatment planning computation of scanned proton and carbon ion beams <i>Bertrand, D, Belgium</i>	12
23	Ion Beam Radiobiology: From the Lab to the Clinic <i>Blakely, EA, USA</i>	12
24	Evolution of technology to optimize the delivery of proton therapy: the third generation <i>Bortfeld, T, USA</i>	12
25	Preclinical studies and radiopharmaceutical developments with ⁶⁴ Cu produced by ARRONAX facility <i>Bourgeois, M, France</i>	13
26	PlanIt: Planning Ion therapy open platform for treatment plans testing and comparing <i>Bourhaleb, F, Italy</i>	13
27	Augmented Reality tools for particle therapy facilities <i>Bourhaleb, F, Italy</i>	14
28	An innovative on-line beam-monitoring detector based on the emission of secondary electrons <i>Braccini, S, Switzerland</i>	14
29	Dose distribution characterization in the halo of proton pencil beams with emulsion film detectors <i>Braccini, S, Switzerland</i>	15
30	Studying inter- and intrafraction motion mitigation with sequential 4DCTs of lung tumor patients <i>Brevet, R, Germany</i>	15
31	Predictive and prognostic role of functional imaging of head and neck squamous cell carcinomas <i>Brizel, DM, USA</i>	16
32	Evaluation of Late Toxicity Risk for RT Patients through Geant 4 Simulation of X-Ray Dose Deposition <i>Brochu, F, UK</i>	16
33	Combined Radiochemotherapeutical Strategies for Microtubule Stabilizing Agent (MSA)-Resistant Tumors <i>Brogini-Tenzer, A, Switzerland</i>	17
34	Equivalent uniform dose (EUD) based biological optimization for carbon ion therapy <i>Brüningk, SC, Germany</i>	17
35	Potential of Detection of fast Cherenkov Photons for Improved Time of Flight Positron Emission Tomography <i>Brunner, S, Austria</i>	18
36	Development of Advanced Quality Assurance Instrumentation for Hadrontherapy <i>Bucciantonio, M, Italy</i>	18
37	¹⁵² / ¹⁶¹ Tb-DOTA-RM6 biodistribution studies in prostate cancer bearing SCID mice and ¹⁴⁹ Tb sources from CERN-MEDICIS <i>Buchegger, F, Stora, T, Switzerland</i>	18
38	Segmentation and Tracking of ROIs for Image-Guided Fractionated Radiotherapy <i>Bueno, G, Spain</i>	19
39	Properties of therapeutic He, Li and O beams studied with Geant4 <i>Burigo, LN, Germany</i>	19
40	Do physiological relevant doses of biguanides have any role in cancer treatment? <i>Busk, M, Denmark</i>	20
41	Modelling acute urinary toxicity after radiotherapy for prostate cancer <i>Carillo, V, Italy</i>	20
42	Usage of long axial crystals for PET applications: the AX-PET demonstrator and beyond <i>Casella, C, Switzerland</i>	21

43	Detection of ionizing radiation by intrinsic optical fiber sensors: preliminary results <i>Cella, L, Italy</i>	21
44	Simulation of Hadrontherapy In-beam monitoring at CNAO with the INSIDE detector <i>Cerello, P, Italy</i>	22
45	The ELIMED (Multidisciplinary and Medical applications at the ELI-Beams) network perspectives for laser driven beam applications <i>Cirrone, GAP, Italy</i>	23
46	International Cancer Expert Corps, Inc. (ICEC) <i>Coleman, N, USA</i>	23
47	Nanodosimetric descriptors of the therapeutic quality of light-ions: new experimental measurements <i>Conte, V, Italy</i>	24
48	From Radiotherapy Dose Monitoring to Low-Dose Morphologic Imaging with Scanned Megavoltage X-rays <i>Crespo, P, Portugal</i>	24
49	Fast pencil beam dose calculation for hadron therapy on GPU <i>da Silva, J, UK</i>	25
50	Radiograaff: a medium energy proton irradiation platform for radiobiological studies. Presentation and first results <i>Dauvergne, D, France</i>	25
51	Carbon Ion Therapy: Actual and Future Strategies at HIT <i>Debus, J, Germany</i>	26
52	Assessment and improvements of Geant4 models in the context of prompt-gamma hadrontherapy monitoring <i>Dedes, G, Germany</i>	26
53	Proton Radiation Therapy: Current Status of Clinical Trials <i>Delaney, TF, USA</i>	27
54	Development of a Transparent Photon Detector for the Online Monitoring of IMRT Beams <i>Delorme, R, France</i>	27
55	TOF-PET scanner configurations for quality assurance in proton therapy: a patient case study <i>Dendooven, P, The Netherlands</i>	28
56	Impact of tumor autophagy on solid tumors response to IR ; role of the tumor stroma <i>Deutsch, E, France</i>	29
57	Positron emission tomography (PET) isotope production from laser-driven proton <i>Ding, K, USA</i>	29
58	Oral mucosal radiation response (mouse) - relevance of ceramide-induced apoptosis? <i>Doerr, W, Austria</i>	29
59	Dose Delivery System of CNAO: a new medical device <i>Donetti, M, Lavagno, M, Italy</i>	30
60	Collaborating for the future: the ENLIGHT Network <i>Dosanjh, M, Switzerland</i>	30
61	Immunosensitization through radiotherapy: the example of immunocytokines <i>Dubois, L, The Netherlands</i>	30
62	The development of a low energy facility for clinical trials of Boron Neutron Capture Therapy <i>Edgecock, R, UK</i>	31
63	Fast Monte Carlo simulator for the distribution of prompt-gamma emitters in protontherapy <i>El Kanawati, W, France</i>	31
64	DNA damage, protein expression and migration of melanoma cells irradiated with proton beam <i>Elas, M, Poland</i>	32
65	Education and training in medical imaging for conventional and particle radiation therapy: the ENTERVISION training network <i>The ENTERVISION Training Network</i>	32

66	Quality assurance for hadron therapy: the ENVISION project <i>The ENVISION Consortium</i>	33
67	Development of a novel ELISA for detecting inducible Hsp70 in serum <i>Ertl, S, Germany</i>	33
68	A Novel Radioguided Surgery Technique Exploiting α - decays <i>Faccini, R, Italy</i>	33
69	Intra-fraction tumor tracking based on a surrogate-driven 4D CT motion model in particle radiation therapy <i>Fassi, A, Baroni, G, Italy</i>	34
70	Varian Eclipse TPS and FLUKA Monte Carlo proton dose deposition comparison <i>Fiorini, F, UK</i>	35
71	Verification of dynamic trajectory radiotherapy based on Monte Carlo <i>Fix, M, Switzerland</i>	35
72	First investigations of Ultra-Thin 3D silicon detectors as microdosimeters <i>Fleta, C, Spain</i>	36
73	The XEMIS2 prototype <i>Gallego, L, France</i>	36
74	Development of a PET scanner simulation package for FLUKA <i>Garcia Ortega, P, Switzerland</i>	37
75	A Biomedical Research Facility at CERN based on the Low Energy Ion Ring <i>Garonna, A, Switzerland</i>	37
76	Digital Image Processing Techniques for Application in a Microbeam End-Station Microscopy <i>Georgantzoglou, A, UK</i>	38
77	Motion compensated reconstructions in PET-based ion beam treatment verification for moving target <i>Gianoli, C, Germany</i>	38
78	The Higgs boson and our life <i>Gianotti, F, Switzerland</i>	38
79	Reduced side effects by proton microchannel radiotherapy - study in a human skin model <i>Girst, S, Germany</i>	39
80	ProXY - High performance monolithic pixel tracker for proton tomography <i>Giubilato, P, Italy</i>	39
81	Adaptive radiotherapy for head & neck squamous cell carcinoma <i>Gregoire, V, Belgium</i>	40
82	An example of the integrated model: the EORTC DAHANCA-1219 trial <i>Gregoire, V, Belgium</i>	40
83	Evaluation of existing ripple filter designs for clinical use at the MedAustron ion beam therapy facility <i>Grevillot, L, Austria</i>	40
84	Comparing Ion Computed Tomography under clinical constraints <i>Hansen, DC, Denmark</i>	41
85	Prediction of β^+ -activity distributions from PT-PET by means of a yield approach <i>Helmbrecht, S, Germany</i>	41
86	Iterative Reconstruction of Clinical Electron Beam Phase Space for Intra-Operative Radiation Therapy <i>Herranz, E, Udías, JM, Spain</i>	42
87	Compton imaging in proton therapy: reconstructed images compared to simulated prompt- γ distribution <i>Hilaire, E, France</i>	43
88	ESI's Scientific Schools: a privileged place for knowledge transfer <i>Hoffmann, HF, Switzerland</i>	43
89	The vascular supply and micro-environment of tumours and their significance for cancer therapy <i>Horsman, M, Denmark</i>	43

90	Comparison of Scintillation Detectors based on BGO and LSO for Prompt Gamma Imaging in Particle Therapy <i>Hueso-González, F, Germany</i>	44
91	Harnessing laser-plasma accelerated ion beams for applications using Gabor lenses <i>Hughes, C, UK</i>	44
92	Monte Carlo modelling of whole-body secondary cancer risk for conventional and emergent radiotherapy <i>Hugtenburg, R, UK</i>	45
93	Robustness of range prediction in proton therapy using prompt gamma emission <i>Janssen, F, The Netherlands</i>	45
94	Precision in prompt gamma-based range monitoring of proton pencil beams in heterogeneous media <i>Janssens, G, Belgium</i>	46
95	Medical radioisotopes from the Heavy Ion Laboratory, University of Warsaw <i>Jastrzębski, J, Poland</i>	46
96	Target definition based on functional imaging <i>Jeraj, R, USA</i>	47
97	Proton Clinical Correlates: Patient Throughput & Cyclotron Availability <i>Johnstone, PAS, USA</i>	47
98	Towards simpler and better prediction of relative biological effect (RBE) <i>Jones, B, UK</i>	48
99	Radiobiological Considerations for Retreatment of Central Nervous System Tumours <i>Jones, B, Hopewell, J, UK</i>	48
100	Delayed and Persistent Response of Human Mitochondria after Single Exposure to 0.5 to 4 Gy of Gamma Radiation <i>Kam, W, China</i>	49
101	Variance Based Sensitivity Analysis of Biological Uncertainties in Carbon Ion Therapy <i>Kamp, F, Germany</i>	50
102	Expression of common or species specific DNA damage-repair pathway related genes in thymus of low-dose-rate irradiated AKR/J and ICR mice <i>Kim, HS, Republic of Korea</i>	50
103	Can particle beam therapy be improved using helium ions? - A treatment planning study focusing on pediatric patients <i>Knäusl, B, Austria</i>	51
104	Vimentin (EMT Marker Protein) Score As One of Predictors Resistance to Erlotinib and Radiotherapy for Patients with Stage III Non-Small Cell Lung Cancer on A Prospective Phase II Trial <i>Komaki, R, USA</i>	51
105	Reprogramming metabolism with metformin to improve radiation response <i>Koritzinsky, M, Canada</i>	52
106	A Beam Control System for an Experimental Beam Line Operated Parallel to a Therapeutic Beam Line <i>Kormoll, R, Germany</i>	52
107	Radioisotopes: the “fuel” for nuclear medicine <i>Koster, U, France</i>	53
108	Beam monitoring and dosimetry tools for radiobiology experiments at the cyclotron ARRONAX <i>Koumeir, C, France</i>	53
109	New challenges for biologically adapted ion beam treatment planning: single and multi-ion approaches <i>Krämer, M, Scifoni, E, Germany</i>	54
110	Biomarker for stratification in radiotherapy - preclinical and early clinical models <i>Krause, M, Germany</i>	54
111	Real-time monitoring of the ion range during hadrontherapy: An update on the beam tagging hodoscope <i>Krimmer, J, France</i>	54
112	Dosimetric considerations to determine the optimal technique for localized prostate cancer <i>Kuess, P, Austria</i>	55

113	The Advantages of Improved Gd DRZ Screens Compared to Gd ₂ SO ₂ and CsI in Patients Exposure Dose Reduction during the Chest Radiography <i>Kulich, I, Melenevska, N, Ukraine</i>	55
114	95 MeV/A carbon fragmentation studies for hadrontherapy: measurements and comparisons with GEANT4 simulations <i>Labalme, M, France</i>	56
115	Targeting carbonic anhydrase IX by nitroimidazole based sulfamides enhances the therapeutic effect of tumor irradiation and doxorubicin treatment: a new concept of dual targeting drugs <i>Lambin, P, The Netherlands</i>	57
116	Dual energy CT to reduce range uncertainties in hadrontherapy <i>Landry, G, Germany</i>	57
117	Identification of DNA sequence variants associated with a gene expression profile predictive for radiation induced fibrosis <i>Laursen, LV, Denmark</i>	58
118	Ultimate Time Resolution in Time-of-Flight PET <i>Lecoq, P, Switzerland</i>	58
119	Simulation of a coupled Silicon Photomultiplier & LYSO scintillator detector system for prototype PET detector development <i>Leming, EJ, UK</i>	59
120	From bench to bedside: development and early clinical results of 188Re-SSS/Lipiodol for HCC treatment <i>Lepareur, N, France</i>	59
121	Trigger optimization for in-beam PET dedicated to particle therapy range verification <i>Lestand, L, France</i>	59
122	Development of a Time-Of-Flight Compton Camera for Online Control of Ion Therapy <i>Ley, J-L, France</i>	60
123	Multigap Resistive Plate Chambers as a Positron Emission Tomography detector <i>Litov, L, Bulgaria</i>	60
124	Ongoing investigations on ion-based radiography and tomography <i>Magallanes, L, Germany</i>	61
125	Interstitial Detectors for Synchronized Radiation Quality and Range Verification in Ion-Beam Therapy <i>Magrin, G, Austria</i>	61
126	The Radiation Oncology Group of EORTC: From the past to the future <i>Maingon, P, France</i>	62
127	Development of a technique to speed up the simulation of PET and SPECT <i>Mancini Terracciano, C, Switzerland</i>	62
128	4D dose calculations and 4D PET image reconstruction using deformable tetrahedral models of moving organs <i>Manescu, P, France</i>	62
129	Implementation of a GPU Monte Carlo protons transport code for dose calculations: methods and challenges <i>Maneval, D, Canada</i>	63
130	Rediscovering grid therapy: new approaches <i>Martínez-Rovira, I, France</i>	64
131	Effect of the washout processes in quality assurance of carbon therapy treatments by means of PET: a Monte Carlo study <i>Martínez-Rovira, I, France</i>	64
132	Monitoring of carbon ion beams using secondary ions: investigations in inhomogeneous targets <i>Martiskova, M, Germany</i>	65
133	How will we develop the evidence base for biologically individualised radiotherapy? <i>Maughan, T, UK</i>	65
134	Data models for the Compton camera acquisition and their influence on the reconstructed images <i>Maxim, V, France</i>	66

135	Log file based dose calculations as a quality assurance tool in scanned beam proton radiotherapy <i>Meier, G, Switzerland</i>	66
136	Adoptive T cell therapy potentiates efficacy of alpha radio-immunotherapy <i>Ménager, J, France</i>	67
137	A new elastic image fusion model for lung deformation simulation in 4D dose calculations <i>Milz, S, Germany</i>	67
138	Rectal cancer and fractionation sensitivity in the neo-adjuvant radiation therapy setting: a project of meta-analysis and radiobiological modeling from individual patient data in randomized and observational data-sets <i>Miralbell, R, Switzerland</i>	68
139	Robust Optimization of IMPT Dose Distributions <i>Mohan, R, USA</i>	68
140	Parameterization of lateral dose profiles for proton therapy application at CNAO <i>Mori, M, Italy</i>	69
141	A novel TOF-PET detector based on organic scintillators <i>Moskal, P, Poland</i>	69
142	From Bench to bedside: experience of the glioblastoma model for optimization of radiosensitization <i>Moyal, EC, France</i>	70
143	Potential of radiation response by a novel EGFR/DNA targeting molecule in a triple negative breast cancer model <i>Muanza, TM, Canada</i>	70
144	Head motion correction in positron emission tomography using point source tracking system <i>Nazarparvar, B, Iran</i>	70
145	Comparison of 4 MV and 6 MV photons for whole breast irradiations <i>Nesteruk, M, Fix, MK, Switzerland</i>	71
146	Present status of CNAO <i>Orecchia, R, Italy</i>	71
147	First results with a new detection system for complex radiotherapy treatment verification <i>Ovejero, MC, Spain</i>	71
148	Auger electron emitters labeled to monoclonal antibodies trigger cell membrane-mediated bystander effects <i>Pailas, S, France</i>	72
149	Nuclear translocation of FTS (Fused Toes Homolog) is required for EGFR phosphorylation and confers radiation resistance on uterine cervix cancer <i>Park, W-Y, Republic of Korea</i>	72
150	Experimental characterization of acoustic detection and imaging for Bragg peak localization in proton therapy <i>Parodi, K, Germany</i>	73
151	Training the next generation of experts in hadron therapy: the PARTNER training network <i>The PARTNER Training Network</i>	73
152	An integrated monitoring system for the on-line assessment of particle therapy treatment accuracy <i>Patera, V, Italy</i>	73
153	Antitumor activity of combination therapy with TH-302 and irradiation in a rat rhabdomyosarcoma model <i>Peeters, S, The Netherlands</i>	74
154	Clinical testing of an in-room imaging system for patient setup verification in particle therapy <i>Pella, A, Italy</i>	75
155	Cardiac toxicity induced by radiotherapy. Role of the GEF, Epac, in hypertrophy and amyloidosis but not in fibrosis <i>Petit, B, Switzerland</i>	75
156	Research and development of a TOF-based multi-slit collimated camera for online hadrontherapy monitoring <i>Pinto, M, France</i>	76
157	ClearPEM-Sonic: a multimodal PET-ultrasound mammography system <i>Pizzichemi, M, Italy</i>	76

158	Time resolved portal dosimetry for Volumetric Modulated Arc Therapy (VMAT) in lung cancer patients with atelectasis <i>Podesta, M, The Netherlands</i>	77
159	²¹² Pb-labeled mAbs targeting CEA or HER2 during α -RIT of small peritoneal carcinomatosis - Dose effect relationship? <i>Pouget, J-P, France</i>	78
160	Nanoparticles and protontherapy: disentangling possible physical effects <i>Prezado, Y, France</i>	78
161	RBE and DNA damage variation along monoenergetic and modulated Bragg peaks of a 62 MeV therapeutic protons beam <i>Prise, KM, UK</i>	79
162	Radiosensitization of Non-Small Cell Lung Cancers by Targeting Ionizing Radiation-Induced Activation of ADAM17 <i>Pruschy, M, Switzerland</i>	79
163	The REQUITE project: validating predictive models and biomarkers of radiotherapy toxicity to reduce side-effects <i>Rancati, T, Italy</i>	80
164	Influence of Double Strand Breaks Repair on Radiotherapy Induced Acute Skin Reactions in Breast Cancer Patients <i>Rao, BSS, India</i>	80
165	Particle therapy in India: A feasibility study <i>Rath, AK, India</i>	81
166	Proton Interaction Vertex Imaging for carbon therapy quality control <i>Rescigno, R, France</i>	81
167	Geant4 simulation of a dedicated beam line at the CNAO facility for the study of uveal melanomas <i>Rimoldi, A, Italy</i>	82
168	Gadolinium based nanoparticles for radiosensitization of head and neck squamous cell carcinoma <i>Rodriguez-Lafrasse, C, France</i>	82
169	Homologous recombination deficiency and radio-curability in mouse models for BRCA1/2-deficient breast cancer <i>Rottenberg, S, The Netherlands</i>	83
170	Targeting hypoxia through autophagy <i>Rouschop, K, The Netherlands</i>	83
171	Initial Qualification of the Irradiation Uncertainties in Ion Beam Therapy of Prostate Cancer <i>Rucinski, A, Germany</i>	83
172	Quantitative study of clinical SPECT: image reconstruction and sensitivity <i>Saikouk, H, El Khayati, N, Morocco</i>	84
173	Dosimetric comparison between Agility and MLCi heads for nasopharyngeal IMRT plans created by two different treatment planning systems <i>Sakumi, A, Japan</i>	84
174	The recent developments of the FLUKA Monte Carlo code oriented to its applications in hadrontherapy <i>Sala, P, Italy</i>	85
175	Measurements of Carbon ion fragmentation on thin C and Au targets from the FIRST collaboration at GSI <i>Sarti, A, Italy</i>	85
176	Daily variation in rectal size and position during prostate radiotherapy measured from helical tomotherapy CT scans <i>Scaife, J, UK</i>	86
177	Ultrafast PET Detectors Based on Digital SiPMs and Their Use in In-Situ PET and Prompt Gamma Ray Imaging <i>Schaart, DR, The Netherlands</i>	87
178	Enhanced RBE of sub-micrometer focused low-LET protons <i>Schmid, TE, Germany</i>	87

179	Characterization of wireless personal dosimeter prototype for Interventional Radiology medical operators <i>Servoli, L, Italy</i>	88
180	A radionuclide generator of Erbium-165, an isotope for Auger Therapy <i>Severin, GW, Denmark</i>	88
181	The new business model of the European Organization for Research and Treatment of Cancer (EORTC) <i>Shash, E, Belgium</i>	89
182	Octavius 4D measurements For RapidArc™: What are clinically Acceptable Gamma- Index Pass Rates? <i>Sidhique, H, India</i>	89
183	The use of the Golden Triangle paradigm for Knowledge Exchange for Computational Radiotherapy: a Case Study <i>Simmons, M, UK</i>	90
184	Prompt gamma imaging of proton pencil beams at clinical beam current <i>Smeets, J, Belgium</i>	90
185	Fat percentage and hand grip strength in lung cancer: the influence on survival and toxicity <i>Smits, KM, The Netherlands</i>	91
186	A combined electrical impedance tomography and cone beam CT for radiation therapy monitoring <i>Soleimani, M, UK</i>	91
187	Different detector concepts for several imaging scenarios: from hadrontherapy monitoring to clinical imaging <i>Solevi, P, Spain</i>	92
188	Hpv Status and Effect on Radiosensitivity in Head and Neck Cancer Tumor Xenografts <i>Sørensen, BS, Denmark</i>	92
189	Nuclear techniques for studying soft matter at ISOLDE/CERN <i>Stachura, M, Switzerland</i>	93
190	The (non-) detectability of failures in motion mitigated ion beam delivery by means of in-beam PET <i>Stützer, K, Germany</i>	93
191	Automatic beam dose profiler for scanned pencil beams (protons and carbon ions) at the CNAO hadrontherapy facility <i>Tamborini, A, Italy</i>	94
192	Development of a Compton Camera for online range monitoring of laser-accelerated proton beams <i>Thirolf, P, Germany</i>	94
193	Imaging for Prescription Function <i>Thorwarth, D, Germany</i>	95
194	Investigation of Irregular Motion Influence for Future 4D In-Beam PET Imaging <i>Tian, Y, Germany</i>	95
195	PIP: A compact recirculating accelerator for the production of medical isotopes <i>Toader, A, UK</i>	96
196	From CERN to PET/MR <i>Townsend, D, Singapore</i>	96
197	Preclinical Assessment of Efficacy of Radiation Dose Redistribution Based on Intratumoral FDG-PET Uptake <i>Trani, D, The Netherlands</i>	97
198	Large Momentum Acceptance NS-FFAG superconducting gantry for Carbon Ion Cancer Therapy for PAVIA <i>Trbojevic, D, USA</i>	97
199	Compton Telescope Prototype Based on Continuous LaBr3 Crystals and Silicon Photomultipliers <i>Trovato, M, Spain</i>	97
200	Current Status of Carbon-Ion Radiotherapy at NIRS <i>Tsujii, H, Japan</i>	98
201	The ULICE project <i>The ULICE Consortium</i>	98

202	Mediators associated to the inflammatory response in prostate cancer patients undergoing RT: preliminary results <i>Valdagni, R, Italy</i>	99
203	Moving forward in radionuclide development in Switzerland <i>Van der Meulen, N, Switzerland</i>	99
204	Influences of aberrant mitochondrial DNA in cancer and cancer therapy <i>van Gisbergen, M, The Netherlands</i>	100
205	New insights in IGRT for prostate cancer <i>van Herk, M, The Netherlands</i>	100
206	A single device for mechanical and radiation Quality Assurance measurements of medical accelerators <i>Velarde, E, USA</i>	101
207	An Intensity Modulated Radiotherapy Beam Monitoring System using a Monolithic Active Pixel Sensor <i>Velthuis, JJ, UK</i>	101
208	The ART of translation <i>Verheij, M, The Netherlands</i>	102
209	Clinical experience with adaptive radiotherapy for muscle invasive bladder cancer <i>Vestergaard, A, Denmark</i>	102
210	ENTERVISION WP4. Biological Dosimetric Phantom. Proof of Concept Preliminary results <i>Viana Miranda Lima, T, Switzerland</i>	103
211	Realistic on-the-fly dose calculation for low energy X-rays Intra-Operative Radiation Therapy <i>Vidal, M, Spain</i>	103
212	The SMAC-mimetic Debio 1143 efficiently enhanced radiotherapy in head and neck squamous cell carcinoma models <i>Viertl, D, Switzerland</i>	104
213	Radiosensitizing effect of a RasGAP derived peptide on cell survival in human cancer cells in vitro and in vivo <i>Viertl, D, Switzerland</i>	104
214	NOTCH and radiotherapy: does it matter? <i>Vooijs, M, The Netherlands</i>	104
215	Novel strategies to spare normal tissues from radiation damage <i>Vozenin, M-C, Switzerland</i>	105
216	A novel dual-modality optical tomography and x-ray system for small animal radiation research platform <i>Wang, KK-H, USA</i>	105
217	Host and Tumor Immunity: Local and Systemic Opportunities to Enhance Tumor Curability by Radiotherapy <i>Weichselbaum, RR, USA</i>	105
218	The doorway to high specific activity of ^{195m} Pt <i>Wilmsen, D, Germany</i>	106
219	Inhibition of tumour growth using the small molecule Cathepsin L inhibitor, KGP94 <i>Wittenborn, T, Denmark</i>	107
220	Advancing the small animal radiation research platform for pre-clinical radiation research <i>Wong, J, USA</i>	107
221	Identification of new therapeutic targets <i>Wouters, BG, Canada</i>	108
222	Gamma Probe Based on Scintillation Crystal and Silicon Photomultiplier <i>Yagnyukova, A, Russia</i>	108
223	Frequency difference electrical impedance tomography for imaging lung tumour <i>Yang, CL, UK</i>	108
224	[¹⁸ F]HX4 PET imaging of tumour hypoxia in HNSCC patients <i>Zegers, CML, The Netherlands</i>	109

225	Circulating biomarkers for determining absorbed ionizing radiation dose & risk for radiation induced toxicity in humans <i>Zenhausen, F, USA</i>	109
226	Noninvasive Imaging of Radiation-Induced Lung Inflammation with Positron Emission Tomography (PET) in a Murine Model <i>Zhang, Y, USA</i>	110

ICTR-PHE 2014
International Conference on Translational Research in Radiation Oncology/Physics for Health in Europe
Uniting Physics, Biology and Medicine for better healthcare
Geneva International Conference Center, February 10 - 14, 2014

1

Extremely high-granularity digital tracking calorimeter for the detection of charged and neutral radiation in hadron therapy

D. Aadnevik¹, E. Rocco², D. Röhrich¹, T. Peitzmann²

¹University of Bergen, Institute of Physics, Bergen, Norway

²Utrecht University, The Netherlands

A compact, high-granularity digital calorimeter detector will allow the real-time in-vivo monitoring of the irradiated volume position by detecting the trajectory of secondary radiation (charged particles and photons) in ion therapy for cancer treatment. This technique will prove beneficial both in terms of spatial resolution and cost. Furthermore, as an improvement compared to e.g. CT or PET, the information will be available in real-time, thus offering a possibility for continuously adjusting the treatment. The proposed detector will be a single device performing tracking, particle identification and energy measurements simultaneously. Because of the extremely large number of cells the device will be able to cope with large particle multiplicities, thus providing a breakthrough in rate capabilities.

The development of this device profits from R&D performed for high-energy physics experiments. In this context, a small prototype, a silicon/tungsten sandwich calorimeter (4 cm x 4 cm x 10 cm total volume) with 24 layers of Monolithic Active Pixels Sensors (30µm x 30µm pixel size) has been constructed and has been tested with high-energetic pion and electron beams [1,2,3]. We will present the design principles of this detector and discuss its general performance. First measurements have demonstrated that the detector is able to resolve details of electromagnetic shower distributions on scales as small as 100 µm. Data from proton beams at a few GeV are available and will be used to study the performance related to proton radiography.

As a proof of principle for its application in therapy, the prototype will be irradiated with a therapeutic proton beam. The detector response to a 180-250 MeV proton beam, which is stopped inside the detector, is simulated by the Monte Carlo simulation package FLUKA. The implementation of a highly segmented sensor with a pixel size of 30 µm x 30 µm into FLUKA and the conversion of an energy signal into a binary response pattern will be discussed. Results on the tracking precision and the Bragg-peak position determination will be shown.

Keywords: Calorimeter, Hadron Therapy, Pixel Sensors

References:

- [1] T. Peitzmann, Prototype studies for a forward EM calorimeter in ALICE, Proceedings of CHEF2013, preprint arXiv:1308.2585.
- [2] G.-J. Nooren and E. Rocco, First results of beam tests of a MAPS based ElectroMagnetic calorimeter, RD13 - 11th Intern. Conf. on Large Scale Applications and Radiation Hardness of Semiconductor Detectors.
- [3] D. Fehlker et al., Electronics for a highly segmented electromagnetic Calorimeter prototype, JINST 8 (2013) P03015.

2

Calibration of lanthanum bromide scintillation detectors

M.I. Abbas

Physics department, Faculty of Science, Alexandria University, Alexandria, Egypt

A new analytical method of efficiency calibration is proposed for cylindrical lanthanum bromide (LaBr₃:Ce) scintillation detectors. This method depends on the accurate analytical calculation of two important factors; the path length d , the photon traverses within the active volume of a gamma detector, and the geometrical solid angle Ω , subtended by the source to the detector at the point of entrance. In addition, the attenuation of photons by the detector housing materials is also treated by calculating the photon path length through these materials. The comparisons with the experimental and Monte Carlo method data reported in the literature indicate that the present method is useful in the efficiency calibration of the cylindrical lanthanum bromide (LaBr₃:Ce) scintillation detectors.

3

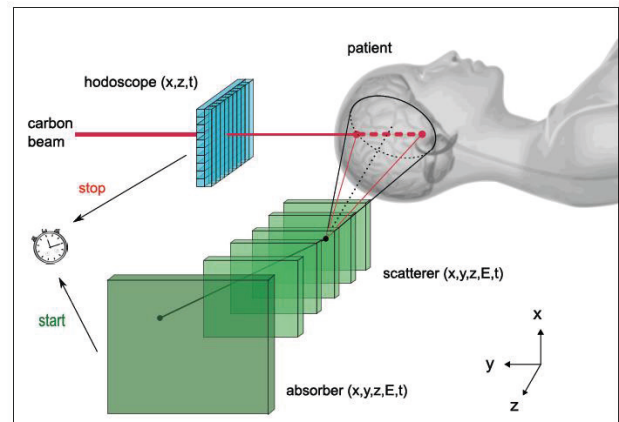
A µTCA Data Acquisition System and its application for Hadrontherapy Monitoring using a Compton Camera

C. Abellan¹, J.-P. Cachemiche¹, D. Dauvergne¹, C. Morel¹, F. Réthoré¹, Y. Zoccarato²

¹CPPM, Marseille, France

²IPNL

This presentation describes a data acquisition system developed within the European project Envision. Our aim is to build a device capable of monitoring dose delivery, during a patient treatment with a proton or carbon ion beam by means of prompt gamma detection using a time-of-flight Compton camera. Indeed, prompt-gamma longitudinal profiles are correlated to the ion range.



The system is composed of a hodoscope (512 PM channels), a stack of double-sided strip silicon detectors scatterer (1280 channels) and a BGO absorber detector (400 PM channels). The front-end electronics is composed of 4 boards for the hodoscope, 10 for the silicon scatterer and 17 for the absorber. Each of these boards is connected to the data acquisition system through optical fibers to allow high bandwidth communications.

The monitoring of the beam range needs to be performed in real time and hardware data processing is needed in order to cope with an aggregated sustained rate of the order of 45 Gbps. We developed a µTCA based data acquisition system that is able to sustain such high data flow rates.

Event selection is based on particle detection times used to search for coincidences. For this, clock jitter of the system must provide a precision better than 100 ps.

Data readout, clock distribution, triggering and a part of the data processing are performed by a set of μ TCA boards developed in the early phase of the Envision project: namely the processing board AMC_Envision and a crossbar module implementable on top of a commercial MCH board. Several types of optical mezzanines attached to this board then enable all the different I/O configurations required by the system.

We will describe how these μ TCA boards are used to address this very demanding application and present results from early measurements with the setup.

4

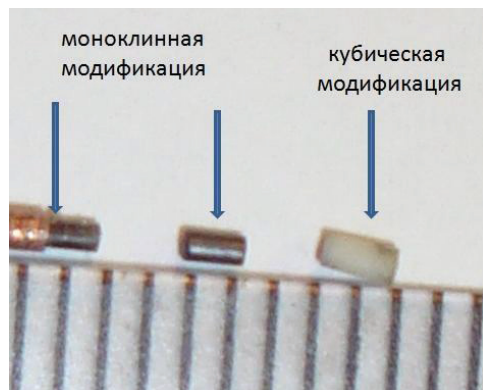
New design of ytterbium sources for brachytherapy

S. Akulinchev, V. Derzhiev

Institute for nuclear research of RAS, Moscow, Russia

Three radioisotopes are now used for the high dose rate (HDR) brachytherapy sources: cobalt-60, iridium-192 and ytterbium-169. The isotope Yb-169 has the average photon emission energy of 93 KeV and the half-life of 32 days. Compared to other isotopes for HDR brachytherapy, iridium and cobalt, the isotope Yb-169 has a significantly lower emission energy and requires a much lighter shielding. However, the ytterbium sources are still a rare exotics for radiologists, partially due to the lack of standard technology of the source production. We have developed an original and cheap laser technology of the production of primary isotope Yb-168 enriched up to 20% and higher. This technology requires much less electrical power than standard electromagnetic technology, normally used for the Yb-168 enrichment.

In order to increase the activity of ytterbium sources, we improved the design of these sources. Characteristic new property of a new source is an extremely high density of its ceramic core containing ytterbium. Using the isostatic pressing at high pressures with a simultaneous or subsequent sintering of ytterbium-oxide powders, we produced samples of ceramic cores of the density 9-10 g/cm³. In the Figure the ytterbium cores with cubic (light core, density 9.247 g/cm³) and monoclinic structure (dark cores, density of 10.08 g/cm³!) are shown on the millimeter scale. This result allows not only to increase the activity of the sources above 10 Ci, but also to avoid the inner container of the source due to the ceramics properties.



Keywords: brachytherapy, ytterbium sources

5

The use of 'planned overshoot' for reducing dose to healthy tissue and improve treatments robustness for scanned proton beams

F. Albertini¹, C. Ares², L.V. van Dijk³, A.C. Knopf², A.J. Lomax²

¹Paul Scherrer Institute, Villigen, Switzerland

²Department of Technical Medicine, Twente, The Netherlands

³PSI, Villigen, Switzerland

Purpose: Range uncertainty is an important consideration in proton therapy, due to the sharp dose gradient at the distal end of the proton Bragg peak. In addition, as range uncertainty is a systematic error it will propagate through the course of the therapy. This makes it a particularly worrying error. Additionally set-up errors are randomly distributed and can affect the target volumes in all directions. To deal with both errors, it is common practice to expand the clinical volume (CTV) by a given safety margin. In passively scattered proton therapy, patient specific hardware like compensators and apertures are used to account for the set-up and range errors separately. For active scanning therapy this has been often done by isotropically expanding the CTV. However, the range uncertainty for any given field will not be isotropic, as it will predominantly affects the distal end of the field, and not the lateral borders. Therefore, in general, a volume larger than needed is irradiated. In this work we investigated the advantage of using field specific planning target volume (fsPTV) to reduce the dose to healthy tissue and to improve treatment robustness to range uncertainties.

Materials and Methods: A field specific target volume (fsPTV) has been constructed as illustrated in Figure 1 by considering margins accounting for setup and range uncertainty separately. Firstly, to deal with set-up errors, the CTV has been isotropically expanded by 2mm (PTV^{set} in figure); then the dose calculation (and optimization) of the pencil beams have been performed on an artificially modified CT data set such that all the CT values are increased by 3%. When the dose is finally calculated on the proper CT data set, this results in what we call a 'planned-overshoot' of the beam. That is, the dose for an individual beam is deliberately calculated to extend further at the distal end than is required, thus making the use of an artificial margin (at least for this error) redundant (fsPTV in figure).

The advantage of using the fsPTV was tested on ten clinical cases calculated with both Single Field Uniform Dose (SFUD) plans and Intensity Modulated Proton Therapy (IMPT) plans. Additionally the plan robustness has been evaluated.

Results: An overall proportional reduction of dose to healthy tissue of 13±3.5% and 15±2.5% was achieved for SFUD and IMPT, respectively. In Table 1 the detailed results of the 10 SFUD plans are reported. Although this value is larger for IMPT plans, SFUD plans were found to benefit more from the approach, due to an increased robustness to range uncertainties when fsPTVs were used. Finally, despite the reduction of the volume treated, the clinical target (CTV) was generally well covered.

Conclusions: In general the fsPTV design shows a great potential for reducing dose to healthy tissue and thereby improving the morbidity of patients. In addition, for SFUD plans, the use of fsPTV improves the plan robustness to range uncertainties.

Figure 1. Schematic representation of the different target volumes for a field coming from the left. The blue line represents the isotropic PTV^{int} accounting for setup uncertainties. The blue area, with the visible distal margin extension, represents the fsPTV.



Table 1. Clinical parameters for evaluating the target coverage and the integral dose to the healthy tissue for ten SFUD plans optimized on the initial isotropic PTV and the fsPTV.

Patient	CTV						Healthy Tissue			Proport.
	D ₉₅	D ₉₅ ^{fsPTV}	Δ	V ₉₅	V ₉₅ ^{fsPTV}	Δ	Int	Int ^{fsPTV}	Δ	
1	98.2	97.6	-0.6	100.0	100.0	0.0	15.19	13.22	-1.97	-5.9 %
2	98.1	97.4	-0.7	100.0	100.0	0.0	9.62	8.26	-1.36	-14.1 %
3	98.0	98.0	0	100.0	100.0	0.0	12.70	11.56	-1.14	-9.0 %
4	98.5	97.8	-0.7	100.0	99.9	0.0	13.10	10.80	-2.29	-17.5 %
5	98.9	97.8	-1.1	100.0	100.0	0.0	12.16	10.55	-1.61	-15.4 %
6	98.1	97.0	-1.1	99.8	99.6	-0.2	21.66	20.39	-1.27	-13.0 %
7	98.4	98.0	-0.4	100.0	100.0	0.0	7.97	7.15	-0.82	-13.1 %
8	98.3	97.4	-0.9	100.0	99.8	-0.2	4.67	3.95	-0.72	-13.2 %
9	97.9	97.1	-0.8	99.9	99.7	-0.3	11.99	10.02	-1.97	-16.4 %
10	98.6	97.2	-1.4	100.0	99.8	-0.2	15.22	13.23	-1.99	-10.3 %
			-0.8 ±0.4			-0.1 ±0.1			-1.5 ±0.5	-13±3.5

Keywords: proton therapy, robustness, field specific target volume

6

Physics is beautiful and useful

U. Amaldi

TERA, Novara, Italy

The year 2014 marks the 60th anniversary of CERN, the largest particle physics laboratory in the world, and of the first cancer treatment with protons done at Berkeley. This is no coincidence: indeed, the beauty of particle physics has always been going hand in hand with useful applications.

These “useful” activities follow from the technical developments in particle accelerators and radiation detectors that have brought to the discoveries of neutral currents (1973), of its mediator, the Z boson (1984) and of the Higgs (2012).

The beginning of 2014 is thus the proper time to first describe these “beautiful” physics results, together with their consequences in our description of the events that took place in the first millionth of a second of the Universe life. The second part of the lecture will review CERN contributions to both diagnostics and therapy and conclude with an overview of possible future developments.

7

Spot-scanning Proton Therapy for Pediatric Parameningeal Rhabdomyosarcomas: Clinical Outcome of 39 Patients Treated at PSI

C. Ares¹, F. Albertini¹, M. Frei-Welte², F. Niggli², G. Goitein¹

¹Center for Proton Therapy - Paul Scherrer Institute, Villigen, Switzerland

²University Children's Hospital Zurich, Switzerland

Purpose: To assess the clinical outcome and late side effect profile of spot-scanning proton therapy (PT) in the treatment of pediatric patients with parameningeal embryonal rhabdomyosarcoma (PM-eRMS).

Materials and Methods: Between September-2000 and July-2012, 39 consecutive children with PM-eRMS received neoadjuvant chemotherapy according to international protocols, followed by PT at Paul Scherrer Institute, Switzerland with concomitant chemotherapy. The median age was 5.8 years (range, 1.2 - 16.1 years). Twenty five patients (64%) required general anesthesia for the irradiation procedure due to young age.

The high risk features were as follows: 29 patients (74%) presented with intracranial extension, 7 (18%) with positive regional lymph nodes and 7 (18%) with distant metastasis at diagnosis.

The median time from the start of chemotherapy to PT was 13 weeks (range, 3 - 23 weeks). Median prescription dose was 54 Gy(RBE) (range 50.0 - 55.8 Gy(RBE)) in 1.8 - 2 Gy(RBE) fractions to the primary tumor and involved lymph nodes. Late toxicity was assessed according to CTCAE version 4.0.

Results: With a mean follow-up of 41 months (range, 9 - 105 months) 10 patients failed: 8 patients experienced in-field local recurrence only, 1 patient developed local relapse and distant lung metastasis and 1 patient developed a meningeal carcinomatosis. The actuarial 5 year local and loco-regional control were 73% respectively and the 5 year overall survival was 77%. In a univariate analysis the time from the begin of chemotherapy to the start of proton therapy with a cut-off point at 13 weeks was the only prognostic factor for local control. Four patients presented with high grade (\geq grade 3) late side effects related to proton therapy: three patients developed unilateral cataract requiring surgery and one patient required a hearing aid. Repeated general anesthesia was delivered safely and without complications.

Conclusions: Our data indicate the safety and the efficacy of spot-scanning based PT for pediatric patients with PM-eRMS. The rates of tumor control and survival are comparable to that in historical controls with similar poor prognostic factors. Furthermore, rates of late effects from PT compare favorably to published reports of photon-treated cohorts. A large series and additional follow-up is warranted.

Keywords: Pediatric, rhabdomyosarcoma, proton therapy

8

Verification and Application of a new method for Ion Spectroscopy in Heavy Ion Radiotherapy

G. Arico^{1,2}, B. Hartmann^{1,2}, J. Jakubek³, S. Pospisil³, O.

Jäkel^{1,2}, M. Martisikova^{1,2}

¹Heidelberg University Clinic, Heidelberg, Germany

²German Cancer Research Center, Heidelberg, Germany

³Institute of Experimental and Applied Physics, Czech Technical University in Prague, Czech Republic

Purpose: Heavy ion beam therapy allows high dose conformation to the target volume. However, heavy ions undergo nuclear fragmentation within the patient, and the created light fragments affect the dose distribution. A deep knowledge of the nuclear interactions is required to reduce the uncertainties in the dose calculation. Thanks to its small size, manageability and rapidity in data acquisition, the semiconductor TimePix detector enables new approaches to investigate the resulting ion spectra.

Materials and Methods: The pixelated TimePix detector [Llopert et al. NIM A 581, 2007], developed by the MediPix Collaboration, is capable to detect single particles and to measure their impact time. Ionizing particles, depositing energy in the silicon sensor, produce a signal in one or more adjacent pixels, giving rise to the so called clusters (see insert in figure 1). The cluster properties depend on the energy and particle species. We have shown that 2D histograms of cluster signal and cluster size enable to recognize different ion species in mixed radiation fields, as illustrated in figure 1.

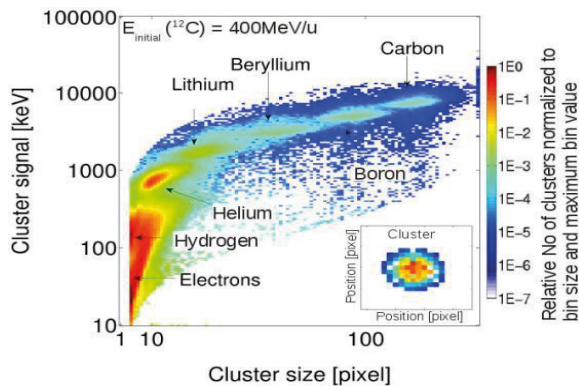


Figure 1: The distribution of the detected clusters (see insert) in terms of size and signal shows concentrations of ion species resulting from fragmentation of carbon ions in a water phantom [Hartmann B. (2013), PhD thesis, U Heidelberg].

Experiments and Results: To compare the novel method to common approaches, the fragmentation of a carbon ion beam in a water target was studied at 2° , 4° and 6° with respect to the beam axis. The experimental set-up was chosen in analogy to a reference experiment with an established method [Haettner E. (2006), in XFOR database]. A good agreement of the relative fractions of ion species with the reference measurements was found [Hartmann B. (2013), PhD thesis, U Heidelberg].

Moreover, the novel method was applied to study the fragmentation of a carbon ion beam in different materials: we used a plastic (similar to body tissue) and a steel phantom, with the same water equivalent thickness. On the beam axis, the relative number of detected fragments was found to be higher behind the plastic than behind the steel (differences up to 50%).

Using several detector layers in coincidence, correlations of the fragments with the incoming carbon ions were studied directly behind the phantom.

Conclusions: For the investigated configurations, the TimePix detector enables the identification of different ion species. The presented method is favorable to measure close to the fragmentation location and can be used to complement larger experimental set-ups. In perspective, it is promising to gain data for improvement of the beam models used in the treatment planning systems.

Keywords: TimePix detector, Ion type distinction, Ion tracking

Acknowledgment: This research is performed in frame of the MediPix Collaboration at CERN.

9

DCE-MRI and DCE-US quantification in CWR22 prostate tumour xenografts

N. Arteaga-Marrero¹, J.F. Mainou-Gomez², K. Nylund³, D.R. Olsen⁴, C.B. Rygh⁵

¹Institute of Physics and Technology, University of Bergen, Norway ²Department of Clinical Medicine, University of Bergen, Norway

³National Centre of Ultrasound in Gastroenterology, Haukeland University Hospital, Bergen, Norway

⁴University of Bergen, Norway

⁵Department of biomedicine, University of Bergen, Norway

Dynamic Contrast-Enhanced Ultrasound (DCE-US) and Dynamic Contrast-Enhanced Magnetic Resonance Imaging (DCE-MRI) are non-invasive, functional imaging techniques which allow us to obtain information about the tumour

phenotype. Subsequent quantification with pharmacokinetic models provides means to characterize tumour vasculature. The capabilities of both techniques to provide reliable image biomarkers have been studied.

In vivo images of the CWR22 human androgen-sensitive xenograft were acquired at day 1 and day 20. The central slice of the tumour, in the sagittal plane, was selected for imaging. First, nonlinear contrast perfusion was performed using a Vevo 2100 ultrasound scanner in combination with 50 μ l bolus injection of microbubbles (MicroMarker, Visualsonics, Amsterdam, The Netherlands). Subsequently, DCE-MRI was acquired using a small animal, horizontal bore 7.0 Tesla Pharmascan (Bruker Biospin MRI, Ettlingen, Germany). The dynamic acquisition consisted of a T1-weighted FLASH sequence in combination with Gadomer 17 (in vivo Contrast, Berlin, Germany), a polysine dendrimer with intermediate molecular weight (35 kDa), which was administered at a dose of 0.1 mmol/kg body weight.

DCE-US and DCE-MRI analysis were performed by in-house developed software using Matlab R2011b (MathWorks, Inc, Natick, MA). A region of interest was delineated around the entire tumour in both image sequences. Signal intensities were converted into relative signal intensity and fitted, voxel-by-voxel, to the Brix pharmacokinetic model [1]. This linear two-compartmental model allows the estimation of the microvascular parameters A, Kep, and Kel. A is the amplitude scaling constant, Kep is the exchange rate constant from the extracellular extravascular space (EES) to plasma, and Kel is the elimination constant of the contrast agent from the central compartment. Figure 1 shows an example of the DCE-US data analysis illustrating the delineation of the tumour (A) and the derived microvascular parameters A (B), Kep (C) and Kel (D).

Preliminary DCE-MRI and DCE-US analysis shows that A mean values decrease with increasing tumour size. Kep mean values resulting from DCE-MRI increase with tumour size. However, Kep mean values obtained from DCE-US remain approximately constant. This difference in the evolution of the Kep parameter could be explained attending to the molecular size of each contrast agent. Although both contrast agents are considered intravascular, and minimal contribution is expected from the EES, the nanometre size of the Gadomer molecules facilitates the leakage. Therefore, Kep values resulting from DCE-MRI are affected by the increment in tumour size. Regarding the Kel parameter, no clear trend was observed in any of the techniques.

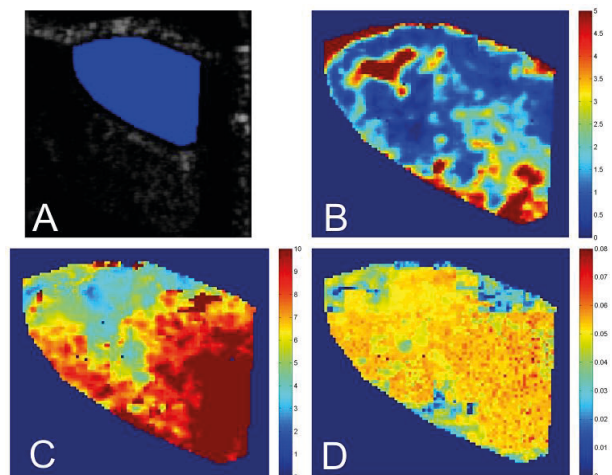


Figure 1.

Keywords: DCE-MRI, DCE-US, prostate

References:

[1] Brix et al. J Comput Assist Tomogr 1991; 15:621-8

10

Choroidal Melanoma brachytherapy enhancement with gold nanoparticles using a full Monte Carlo modelling of human eye

S. Asadi

K.N.Toosi University of Technology, Tehran, Iran

Purpose: To examine the GNPs effects on choroidal Melanoma dosimetry by Monte Carlo study. Hear, the Monte Carlo simulation using MCNP code has been implemented to investigate the application of gold nanoparticles in dose enhancement in brachytherapy of Choroidal melanoma. Monte Carlo Ophthalmic brachytherapy dosimetry usually, is studied by simulation of water phantom. Considering the composition and density of eye material instead of water in these simulations may make a difference in calculations especially when the tumor loaded with GNPs.

Methods: A realistic model of human eye and water phantom have been simulated. The dose delivered to tumor and healthy tissue have been calculated in both phantoms in the presence and absence of GNPs. Making the comparison between results demonstrated the significant effects of GNPs on dose enhancement in tumor area.

Results: The dose to tumor is increased by increasing the GNPs concentration inside the target in both phantoms. The results showed that GNPs within the tumor can enhance the absorbed dose by the tumor without increasing the radiation dose delivered externally. Accordingly, the required time for tumor irradiation decreases as the estimated adequate radiation dose for tumor is provided following this method. The dose delivered to healthy tissue is reduced when the time of irradiation is decreased. Furthermore, making the comparison of the dosimetry calculations in the presence of GNPs between the water phantom and eye model noted the importance of the eye material in ophthalmic brachytherapy dosimetry.

Conclusions: In cancer therapy, the object of brachytherapy as a kind of radiotherapy is to deliver adequate radiation dose to tumor while sparing surrounding healthy tissue. GNPs as radiosensitizers can be used in dealing with this challenge. Also, defining the eye model instead of water phantom leads to more accurate calculations of the GNPs radiation effects in ophthalmic brachytherapy dosimetry.

11

Direct evaluation of ion beam radiobiological parameters from clinical data: an alternative approach to the RBE

A. Attili¹, A. Cometto², G. Russo¹, F. Bourhaleb³, F. Marchetto¹, S. Giordanengo¹, R. Cirio⁴

¹INFN, Torino, Italy

²Politecnico Torino, Italy

³I-See, Torino, Italy

⁴Università degli Studi di Torino, Italy

Purpose: The relative biological effectiveness (RBE) is commonly used in treatment planning for ion beam therapy to help to prescribe the appropriate dose, by mapping the effects of ions to photons, for which the radiotherapist has accumulated a sufficient clinical experience.

Several issues can be easily identified within this approach. Large uncertainties are involved in the currently in-vitro RBE estimation; it was also pointed out that these fluctuations are irreducible: the spread in RBE values cannot be reduced by further experiments [1]. Furthermore, there is the fundamental question about how well survival data obtained in-vitro translate to in-vivo and to clinical conditions. Moreover, the very same biological parametrization used in photon radiotherapy presents a large variance, introducing an additional layer of uncertainty.

In this work an alternative method, based on an effective cell survival parametrization derived from ion beam clinical data, is presented. The method was applied to the analysis of prostate cancer trials with protons and carbon ions.

Materials/methods: A search of the literature was carried out to identify relevant published prostate cancer trials with ion beams reporting Local Control at 5 yr (LC5) and G3 or more normal tissue toxicity rates (TOX).

Complete treatment simulations were performed on a subset of the patients. The aim of these simulations was to produce representative dose and LET distributions to be used as explicative physical variables for the radiobiological modelization. The RBE-weighted dose optimization was carried out using the "Plan-KIT" TPS developed and validated at INFN-IBA.

We investigated three different models with varying degree of complexity and number of free parameters: the Microdosimetric Kinetic Model (MKM) [2], a simplified version of the MKM and a linear model [3]. These models were used in combination with the TCP and NTCP models [4] to fit the LC5 and TOX data. The optimal set of parameters was obtained through a likelihood maximization. A model ranking, based on the Akaike information criterion, was also performed.

Results: The results show large confidence intervals, due to the limited data and the small variety of available treatment schedules. RBE values, such as RBE=1.1 for protons in the target volume, were derived as a by-product of the method, showing a consistency with current approaches.

Conclusions: The possibility to obtain an effective survival parametrization to modulate the dose in treatment planning, from a set of clinical data, was presented. As more ion beam clinical data will be available, this approach could be used to better exploit the specificity and potentiality of ion beam therapy.

Keywords: RBE, Ion Beam Therapy, Treatment Planning

References:

[1] JS Loeffler and M Durante, Nat. Rev. Clin. Oncol., v.10-7 (2013)

[2] RB Hawkins, Radiat. Res., v.160-1 (2003)

[3] A Carabe et al., Phys. Med. Biol., v.57 (2012)

[4] P Källman et al., Int. J. Radiat. Biol., v.62-2 (1992)

12

Impact of uncertainties in ion beam therapy on the optimality of irradiation condition and fractionation schedule

A. Attili¹, F. Bourhaleb², A. Svanetti³, M. Casale³, D. Bottigliengo³, F. Mas Milian^{1,4}, G. Russo¹, A. Kraan¹, F. Marchetto¹, R. Cirio³

¹INFN, Torino, Italy

²I-See, Torino, Italy

³Università degli Studi di Torino, Italy

⁴UESC

Purpose: The well-defined range of ions, enabling precise dose localization, makes them favorable for highly conformal treatments but also sensitive to uncertainties during planning and delivery. Standard approaches to manage these uncertainties include methods based on safety margins and worst-case optimizations [1], or, alternatively, on probabilistic algorithms [2]. However, all these methods are limited to finding optimal conditions for a single fraction, i.e. the overall effect in terms of tumor control has not been evaluated. In this work, a general probabilistic method to evaluate the optimality for the full fractionation schedule, by means of TPC/NTCP evaluations, was presented. The method was used to evaluate the effects of patient setup errors and CT stochastic noise, in the case of pediatric brain tumor.

Materials/methods: The method reproduced a realistic workflow of treatment planning and delivery. Two kinds of uncertainties were included: 1) in planning, due to erroneous input data such as noisy CT, resulting in a systematic error; and 2) in delivery, due to patient setup errors, in which the effects for each fraction are mostly statistically independent. We performed a Monte Carlo/bootstrap sampling over treatment fraction simulations (400, with protons and carbon ions), aimed to model the full PDF of the treatment outcome. Patient setup errors were included by applying random isocenter shifts, sampled from a Gaussian distribution with $\sigma = 1, 2, 3$ and 4 mm (PTV margin = 3 mm). CT spatially correlated noise was generated from a measured noise power spectrum.

The PDFs of several quality indexes, such as conformity, homogeneity, and DVHs, were evaluated. P-value 3D maps for over/underdosage probabilities were also derived (see fig.A-B). A generalization of the TCP/NTCP models was introduced to estimate the full treatment effect as a function of number of fractions and dose per fraction, accounting for interfraction dose and RBE fluctuations.

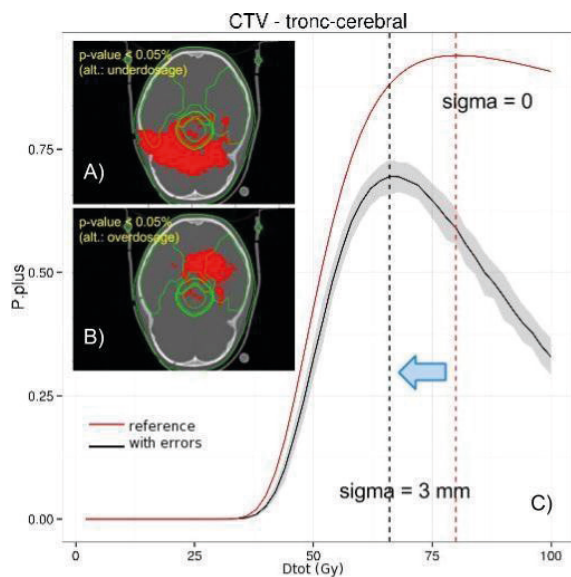
Results: We found that treatments with $\sigma > 2$ mm produce a TCP reduced by 15% or more with respect to the treatment without errors. Also, the optimality of the treatment, quantified by the maximization of the probability of local control without complications (P+), is shifted towards different fractionation schedules (see fig.C). A systematic overestimation of the range of particles (1-2 mm), due to the noise in CT images, was also found. Interestingly, this deviation had the same order of magnitude, but different sign, as the RBE correction to the proton range.

Conclusions: A method was implemented to estimate the effects of stochastic uncertainties on treatment optimality for the full fractionation schedule in ion beam therapy. The method could be used in a treatment procedure to perform robust planning, including also the optimization in fractionation schedule.

Keywords: Patient setup, Ion Beam Therapy, Treatment Planning

References:

- [1] Pflugfelder D et al., Phys Med Biol, 53 (2008)
 [2] Unkelbach J et al., Med Phys, 36 (2009)



13

A multimodal ultrasound and time of flight PET endoscope for developing new biomarkers for the prostate and pancreatic cancers

E. Auffray

CERN, Ph-CMX, Geneva, Switzerland on behalf of the EndoTOFPET-US collaboration

Purpose: The early detection of cancer is known to be of key importance in order to increase the chance of successful treatment and thus to reduce mortality and cost. This has consequently led to a growing activity of developing high performance multimodal imaging devices capable of detecting small early stage tumors. As part of this approach, the EndoTOFPET-US project, a European FP7 program, aims at developing new biomarkers for the pancreatic and prostatic cancers. For this purpose, the EndoTOFPET-US collaboration is building a multi-modal imaging tool combining an ultrasound endoscope with a Time-Of-Flight Positron Emission Tomograph. The objective of this project is to achieve a coincidence time resolution better than 200ps FWHM and a spatial resolution of 1mm for the PET head, while at the same time integrating all components in a very compact detector suitable for endoscopic use. This scanner aims to be used for diagnostic and surgical oncology, as well as at being instrumental for the clinical test of new biomarkers targeted to prostate and pancreatic cancer. The development of targeted biomarkers is a task on which the consortium is working and has already produced first results.

Materials/methods: The EndoTOFPET-US system consists of two separate PET detectors: one external plate of $23 \times 23 \text{ cm}^2$ total area (placed outside the body) with 256 arrays of 4×4 LYSO crystals of $3.5 \times 3.5 \times 15 \text{ mm}^3$ size coupled to Hamamatsu MPPC discrete arrays of $3 \times 3 \text{ mm}^2$ single sensors (S12643-050CN), and an internal (endoscopic) PET probe made of an array of 9×18 LYSO pixels with a size of $0.71 \times 0.71 \times 15 \text{ mm}^3$ coupled to a fully digital SiPM developed by the consortium. The internal PET probe is combined with an endoscopic ultrasound probe. A time-of-flight electronic collimation technique between the external PET plate and the internal PET probe provides the necessary sensitivity through efficient background rejection. This, however, requires a coincidence time resolution of at least 200ps FWHM, allowing the selection of a region of interest of 3cm along the Line Of Response. A high spatial resolution of better than 1mm can be achieved through a very high granularity of the endoscopic PET probe.

Results: First prototypes of both internal and external probe have been produced and tested. A coincidence time resolution of 240ps has been obtained close to our target value of 200ps. Furthermore new biomarkers for targeting the pancreatic and prostate cancer are under study, in particular on $[^{68}\text{Ga}]\text{-PSMA}$ (Prostate specific membrane antigen), while the glycosylated antigen mAb16D10 has been selected as marker for pancreatic cancer, yielding very promising results in preclinical tests.

Conclusions: Most of the components to build EndoTOFPET-US have been received and are currently characterized, the assembly of external plate and internal probe will start in the next months. The design of the system and the current status of the project will be presented.

14

France HADRON: national infrastructure for hadrontherapy research including ETOILE, ARCHADE and protontherapy centers

J. Balosso¹, J.L. Habrand², G. Montarou^{3,4}, R. Ferrand⁵, D. Dauvergne^{3,6}

¹GCS-ETOILE, Lyon, France

²Assoc. ARCHADE, Caen, France

³IN2P3

⁴LPC

⁵Institute Claudius Regaud, France

⁶IPNL

Hadrontherapy is an advanced form of radiotherapy able to cure very radioresistant tumors. It is developing since two decades mainly in Japan and Europe in Germany, Italy and Austria. The input of CERN has been important in its development in Europe. France is involved in that domain since 20 years thanks to its two protontherapy centers, ICPO in Orsay and Médicyc in Nice. This experience as well as the exploratory development of carbon ion therapy in the U.S.A., and the further clinical use in Japan and Europe, have given rise to projects in France for both a treatment center (ETOILE in Lyon) and a research center (ARCHADE in Caen). Different applied research programs have been associated to these projects involving many different teams located in different towns in France.

To boost this domain of R&D a long term grant has been solicited to the French government in the frame of the National Program of Investments for the Future. To obtain this grant a great effort of coordination and gathering of all the involved teams, laboratories and projects had to be done. The result has been the “national infrastructure” **France HADRON** (FrHA) one unique organization constituting a *distributed* multicenter infrastructure. FrHA has been nominated and financed in 2012, up to 15M€, to spend from 2013 to 2019. FrHA includes 5 centers able to provide now or in the future hardware and beam time. These are Lyon (ETOILE), Caen (ARCHADE), Orsay (ICPO), Nice (Medicyc and IMPACT) and Toulouse (PERICLES). More than 20 scientific teams are federated in FrHA to develop a 4 WP's scientific program encompassing all the former individual programs (see figure).

This entity will be able to lead and promote this area of research and medical application by: coordinating and driving the national research and training program in hadrontherapy which ranges from particle fragmentation to clinical research, through dosimetry, radiobiology, imaging, control of target positioning, radiation protection and quality control instrumentation; organizing, facilitating and financing researchers' access to the particle beams required for the development of experimental work; financing part of the equipment of the research platforms.

And ensuring the participation in international programs such as those already existing and actively invested by the French teams: ENLIGHT, Partner, ULICE, ENVISION, ENTERVISION. FrHA had its T0 the 1st March 2013 for financial items and on the 14th October 2013 for its activities. The Pr J.Balosso and JF.Habrand are the coordinators of FrHA. In the frame of FrHA, projects as ETOILE and ARCHADE are devoted to ensure an output to all these research efforts. The first one relies on a governmental decision (not yet obtained) as the national center for carbon ions radiotherapy for the French patients, and the second one, on local decisions as a R&D project based on the development of a new heavy ions cyclotron specie, the C400 of IBA.



Keywords: Carbontherapy, Applied research, National infrastructure

15

Oxygen ions achieve better tumour control probability in hypoxic tumours than carbon ions do

N. Bassler¹, O. Jäkel², M. Krämer³, A. Lühr^{4,5}, J. Overgaard⁶, L. Saksø Mortensen⁶, E. Scifoni³, B. Singers Sørensen⁶, J. Toftegaard¹

¹Department of Physics and Astronomy, Aarhus University, Denmark

²Heidelberg Ion Therapy, Universitätsklinikum Heidelberg, Germany

³Biophysics Department, GSI Helmholtzzentrum für Schwerionenforschung, Darmstadt, Germany

⁴National Center for Radiation Research in Oncology, OncoRay University Hospital, Dresden, Germany

⁵Medical Faculty C.G. Carus Technische Universität Dresden, Dresden, Germany

⁶Department of Experimental Clinical Oncology, Aarhus University Hospital, Denmark

Purpose: In vitro experiments have demonstrated a well-established relationship between the oxygen enhancement ratio (OER) and linear energy transfer (LET), where OER approaches unity for high-LET values. However, high-LET radiation is also associated with an elevated risk for late effects in normal tissue. LET-painting restricts high-LET radiation to compartments that are found to be hypoxic, while applying lower LET radiation to normoxic tissues, thereby minimizing the risk for late effects.

Methods: Carbon-12 and oxygen-16 ion treatment plans with four fields and with homogeneous dose in the target volume, are applied on an oropharyngeal cancer case with an identified hypoxic entity within the planning target volume (PTV). First we assume a fully normoxic tissue and optimize the target dose to a tumour control probability (TCP) of 95%. The primary particle energy fluence needed for this plan is pinned, and TCP is recalculated for three cases assuming hypoxia:

- 1) using the previously obtained conventional plan with homogeneous fields
- 2) LET-painting while varying the hypoxic tumour volume in order to investigate the threshold volume where TCP can be established
- 3) LET-painting while adding a slight dose boost (5-20%) in the hypoxic subvolume to assess its impact on TCP.

Results: The homogenous plan (1) yielded 0% TCP as expected. LET-painting with carbon-12 ions (2) can only achieve tumour control for hypoxic subvolumes smaller than 0.5 cm³. Using oxygen-16 ions, ~50 % TCP can be achieved for tumours with hypoxic subvolumes of up to 1 or 2 cm³.

Tumour control can be achieved for tumours with even larger hypoxic subvolumes, if a slight dose boost is allowed in combination with LET-painting (3).

Conclusion: A substantial TCP increase can be achieved when applying the LET-painting concept using oxygen-16 ions on hypoxic tumours, ideally with a slight dose boost.

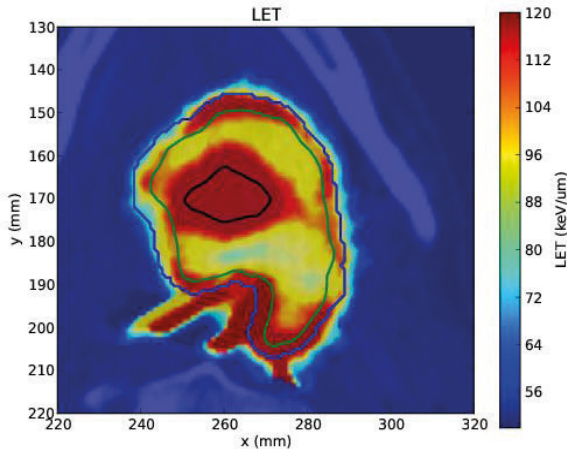


Figure 1. TCP can be achieved in LET-painted plans such as this one. Within the CTV (green line) a hypoxic target is identified (black line). Using partially ramped fields, the LET is redistributed so the hypoxic volume is covered by high-LET radiation, lowering the OER herein.

Keywords: LET-painting, heavy ion therapy

16

Measurement of charged particle yields emitted during irradiation with therapeutic proton and Carbon beams in view of the design of a new tool for the monitoring of hadrontherapy treatments

G. Battistoni¹, V. Patera^{1,2,3}, I. Mattei^{1,2}, M. Marafini³, A. Sarti^{1,2}, A. Sciubba^{1,2}, R. Faccini^{1,2}, L. Piersanti^{1,2}, C. La Tessa⁴, M. Van Stalle⁴, C. Schuy⁴

¹INFN Milano, Italy

²Univ. Roma 1, Italy

³Centro Fermi, Italy

⁴GSI

Purpose: The interaction of the radiation with the patient body in ion therapy yields to the production of secondary charged and neutral particles, whose detection can be used to monitor hadron therapy treatments. Experimental tests have been performed, and others are planned, to verify expectations and to guide the design of specific detectors. We have focused our interest on the detection of charged particles [1,2,3].

Experimental tests have been performed with Carbon and proton beam on a simple homogeneous tissue-like target (PMMA), at GSI and CNAO respectively.

The emission region of particles has been detected with a drift chamber while a LYSO scintillator provided the time-of-flight and residual energy, from which the kinetic energy spectra have been obtained. The measurements were performed with the setup at different angle with respect to the primary beam direction.

Results have been analyzed and compared to Monte Carlo expectations based on the FLUKA Monte Carlo code [4].

The accuracy on the reconstruction of the emission profile of the fragments has been measured and its relationship with the position of the primary Bragg peak has been investigated. Based on the results, a method to monitor the dose profile and the position of the Bragg peak inside the target is proposed

Materials/Methods: A scheme of the experimental setup is shown in Fig. 1. The beam rate has been monitored using plastic scintillator counters. Charged tracks have been identified and measured by means of a 21 cm long Drift Chamber (DC). Given the DC geometry, a particle traveling from the target to the LYSO detector will cross most of its twelve tracking planes. It has been operated with 1.8 kV sense wire voltage, Ar/CO₂ (80/20) gas mixture and 30 mV discriminating threshold for the signals, achieving ~200 μm single cell spatial resolution and ~96% single cell efficiency. A scintillation detector, composed of an array of 4 LYSO crystals, 1.5x1.5x12 cm³ each, was placed downstream the drift chamber. The scintillation light of the crystals was detected with an EMI 9814B PMT. The energy and time calibration of the LYSO crystals have been previously studied and reported in literature.

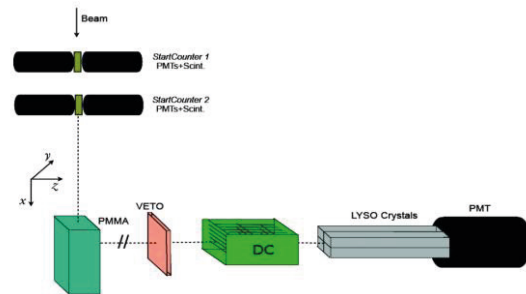


Figure 1.

To select events with charged particles arriving on the LYSO scintillator we exploited the information collected by the Drift Chamber. Given the DC geometry, an ion traveling from the target to the LYSO detector will cross most of its twelve tracking planes. The time of flight (TOF) between a signal recorded by the Start Counters and the LYSO array was measured with a Time-to-Digital Converter (TDC). The combination with energy deposition in LYSO and TOF allowed identification of particles.

Results: Fluxes and velocity spectra of emitted particles have been obtained. The spatial distribution of the fragments has been characterized to investigate a possible correlation between its shape and the dose profile inside the target.

These distributions can be also used to validate Monte Carlo predictions

Conclusions: An important outcome of the emission shape study is that the experimental single track resolution needed to exploit the charged monitoring can be safely of the order of few millimeters without spoiling the precision achievable on longitudinal shape. The results obtained should be considered as preliminary to assess a practical application of this technique to the clinical practice. A first design of a profile detector is presented.

Keywords: hadrontherapy, monitoring, detector

References:

- [1] Agodi C. et al., "Charged particle's flux measurements from PMMA irradiated by 80 MeV/u carbon ion beam", JINST 7 (2012) P03001;
- [2] Henriquet P. et al., "Interaction vertex imaging (IVI) for carbon ion therapy monitoring: a feasibility study". Physics in Med. And Biol. 54 (2012) 4655;
- [3] Gwosch K. et al., "Non invasive monitoring of therapeutic carbon ion beams in a homogeneous phantom by tracking of secondary ions", Physics in Med. And Biol. 58 (2013) 3755;
- [4] A. Ferrari, P. R. Sala, A. Fasso, and J. Ranft, "FLUKA: a Multi-Particle Transport Code," CERN, INFN, SLAC, CERN-2005-10, INFN/TC_05/11, SLAC-R-773, 2005.

17

MCTP: a new Monte Carlo-based treatment planning tool for hadrontherapyG. Battistoni¹, T.T. Böhlen², A. Mairani³, A. Schiavi^{1,4}, V. Patera^{1,4}¹INFN Milano, Italy²MedAustron, Vienna, Austria³CNAO, Italy⁴Universita "La Sapienza", Roma, Italy

Purpose: In the field of radiotherapy Monte Carlo particle transport calculations are recognized for their superior accuracy in predicting dose and fluence distributions in patient geometries compared to analytical algorithms which are generally used for treatment planning due to their shorter execution times. In the present work, a newly-developed MC-based treatment planning (MCTP) tool for hadron therapy is proposed to support treatment planning studies and research applications. It allows for single-field and simultaneous multiple-fields optimization in realistic treatment scenarios both for proton and light ion ($Z < 8$) treatments and is based on the MC code FLUKA[1]. Relative biological effectiveness (RBE)-weighted dose can be optimized using a variable RBE according to radiobiological input tables.

Examples of treatment plans in water phantoms and in patient-CT geometries together are presented and compared to commercial analytical TP calculations. The MCTP tool is aimed to be used in future for research and to support treatment planning at state-of-the-art ion beam therapy facilities.

Materials/Methods: The MCTP tool is composed of various program components that require a range of treatment- and facility-specific input information. The basic input information can be provided by an existing Treatment Planning System or by a fast simulation code, so to provide the starting guess to generate a full set of pencil beam simulation of a patient specific case by means of a complete Monte Carlo model. In this work the FLUKA Monte Carlo [1] code has been adopted. Final optimization is performed using Monte Carlo dose and fluence kernels.

A new fast simulation and skimming code, called FRED, has been developed as alternative for the input generation to the Monte Carlo optimization.

The FLUKA code can be coupled to a radiobiological model so to provide results in terms of dose weighted by Radiobiological Effectiveness (RBE).

Results: The MCTP tool has been tested for a number of patient cases both with proton beams at CNAO and with carbon beams at HIT. The results of the Monte Carlo based optimization have been compared with the output of the Treatment Planning Systems in the quoted facilities.

Fig. 1 shows the results of the calculation for a proton treatment (chordoma) with three ports in terms of RBE-weighted Dose. The distributions are depicted in panels (a), (b) and (c) for the axial, sagittal and coronal view respectively. The first row shows the results of the commercial TPS. The second row is the results of the MC forward calculation starting from (a) results. The third row shows instead the results from MCTP.

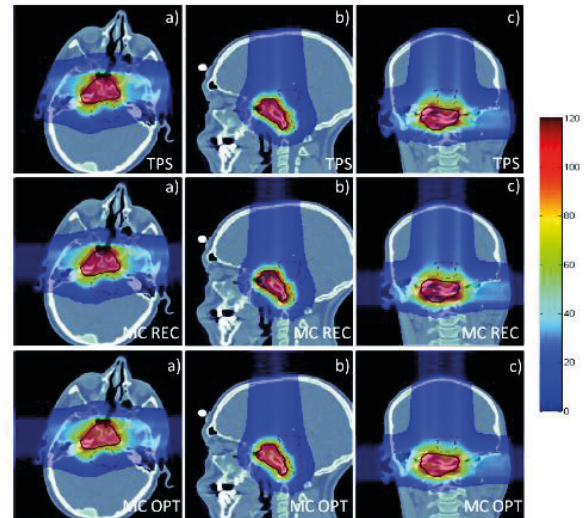


Figure 1

Conclusions: MCTP results have been successfully compared against analytical TPS plans and also experimental dosimetric data. The differences between TPS and MC-based recalculations can be mostly attributed to the different handling of scattering effects. The MCTP approach accounts in particular for a much more accurate description of scattering effects with respect to an analytical approach.

The developed MCTP tool can calculate RBE-weighted dose either using a constant RBE or using a variable RBE according to radiobiological input tables. In addition, beyond dose prescriptions, this tool can generate at the same time also predictions to be used for monitoring, like for instance a positron annihilation map for in-beam PET application. The MCTP tool is at present mainly aimed to be used for research and to support treatment planning at state-of-the-art ion beam therapy facilities. In particular, studies comparing treatment plans created using different ion species and optimization techniques are envisaged.

Keywords: Treatment Planning, hadrontherapy, Monte Carlo

References:

[1] A. Ferrari, P. R. Sala, A. Fasso, and J. Ranft, "FLUKA: a Multi-Particle Transport Code," CERN, INFN, SLAC, CERN-2005-10, INFN/TC_05/11, SLAC-R-773, 2005.

18

PET/CT-based verification of scanned proton and carbon ion treatment at HIT - an overviewJ. Bauer^{1,2}, C. Kurz^{1,2}, D. Unholtz^{1,2,4}, K. Frey³, S.E. Combs^{1,2}, J. Debus^{1,2}, K. Parodi^{2,3}¹Heidelberg Ion-Beam Therapy Center, Heidelberg, Germany²Radiation Oncology, Department of Radiology, Heidelberg University Hospital, Germany³Ludwig-Maximilians University, Munich, Germany⁴Leica Microsystems CMS GmbH, Mannheim, Germany

Purpose: At the Heidelberg Ion-beam Therapy Center (HIT) a commercial full-ring PET/CT scanner is used for post-therapeutic verification of scanned proton and carbon-ion treatment. By measuring the β^+ activation of the irradiated tissue, conclusions can be drawn about the quality of the applied treatment, especially in terms of beam range, possible anatomic changes in the target region and positioning uncertainties.

Material/methods: A Siemens Biograph mCT is installed in a room next to the treatment places and selected patients are either walked to the scanner or transferred by a dedicated

shuttle system to receive a post-therapeutic PET/CT scan. The measured volumetric PET images are then compared to an expectation derived from a Monte Carlo (MC) simulation of nuclear interactions between the delivered beam particles and the irradiated tissue nuclei.

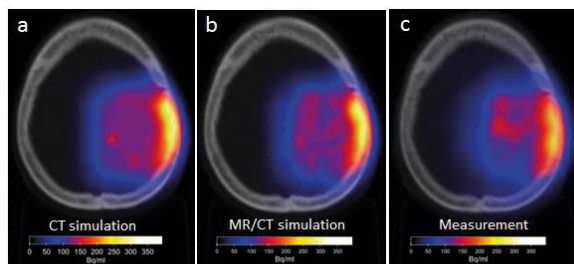
Various aspects of the MC modeling have been improved with respect to commonly used methods, in particular for the monitoring of proton treatment: (i) experiment-driven minimization of uncertainties in the cross-section data for proton induced radionuclide production and (ii) extension of the usual CT-based patient model by considering MRT information to improve the modeling of carbon abundance in the brain region. Quantitative and qualitative analysis of the measured and simulated PET/CT data is realized in a dedicated framework providing visual 3D comparison functionality and a beam range verification evaluating the profile difference between two activity distributions in beam's eye view.

Results: More than 100 patients with various indications within the broad therapeutic spectrum covered at HIT received one or more post-therapeutic PET/CT measurements. Especially for proton induced activity, we could considerably improve the predictive power of the activity calculation by the refinement of the used cross-sections for radionuclide production and, for brain tumour subjects, a refinement of tissue classification based on a novel multi-modal patient model. The initial clinical experience allows identifying the anatomical locations which benefit most from PET-based verification, as well as the shortcomings of the offline data acquisition.

Conclusions: Post-therapeutic PET/CT-based treatment verification is fully integrated into the clinical workflow at HIT. Despite the comparatively low signal due to decay and washout during the transfer time distinct to the offline workflow, valuable treatment quality information can be extracted in favorable tissue regions. Current research efforts aim at a more sophisticated washout modeling and the establishment of a decision support system to provide a prompt and reliable feedback about treatment delivery to the physicians.

Keywords: Ion beam therapy, PET-based treatment verification, Monte Carlo simulations

Acknowledgement: The work has been supported by the BMBF project DOTMOBI (grant 01IB08002F); JB and CK also acknowledge financial support from the FP7 project ENVISION.



Example for improved multi-modal patient model: Simulated activity distribution using (a) the standard CT-based patient model and (b) a combined MR/CT-based model compared to the post-therapeutic PET measurement (c) of a brain tumor patient treated with a single proton field. Activity distributions are overlaid onto the planning CT image (a, b) or the CT acquired during the PET examination (c).

19

Individualized Radiation Oncology - harnessing clinics, biology and high technology

M. Baumann

Department of Radiation Oncology, Technische Universität Dresden, Germany

OncoRay National Center for Radiation Research in Oncology, Medical Faculty and University Hospital Carl Gustav Carus, Technische Universität Dresden, Germany

Radiotherapy has proven efficacy to inactivate cancer stem cells in the primary tumor and locoregional lymph node metastases and therefore has become a mainstay of curative treatment in a variety of tumors. Radiation oncology also is a highly personalized treatment modality, tailoring treatment plans for each individual patient based on precise anatomical information on tumor size and location as well as on normal tissues in the irradiated volume. Models based on radiation physics, radiobiology and clinical data are routinely used in radiotherapy for generating individualized space-resolved radiation dose distributions, as well as for assessment of tumor control probability- vs. normal tissue complication-models. Enormous progress in high-precision radiation delivery and planning technology has been achieved during the past decades and rapidly been translated into clinical practice. Examples for technological advances to be expected to become clinically available in the coming years include fast dose planning algorithms for adaptive radiotherapy, image guided motion control or implementation of fully image-guided particle therapy. Individualized radiotherapy in the future will be significantly spurred by integrating biological information on the specific tumor and on surrounding normal tissues in the treatment strategy of patients. Biological imaging is of particular relevance for advancing personalized radiation oncology, but other predictive and prognostic markers also demonstrate high potential in preclinical and clinical studies. This holds true for stratified selection of the best total dose, dose-distribution and fractionation parameters but also for the combination of radiation with specific drugs. A specific feature of personalized radiation oncology is that already broad biological stratification of patients in two or few groups can substantially promote individualization as this information adds a power-function to the fully anatomically-personalized dose-distributions achieved today. This ESTRO lecture will review preclinical and clinical examples of potential strategies to increase cure rates by adding a biology dimension to personalized radiation oncology.

MB receives support by the Bundesministerium für Bildung und Forschung (BMBF, BMBF-ZIK program 01KS9602).

20

Targeted Gold Nanoparticles as Vascular Disrupting Agents during Radiotherapy

R. Berbeco¹, H. Korideck¹, R. Kumar², S. Sridhar², M. Makrigrigos¹

¹Brigham and Women's Hospital, Dana-Farber Cancer Institute and Harvard Medical School, Boston, Massachusetts, USA

²Northeastern University, Boston, Massachusetts, USA

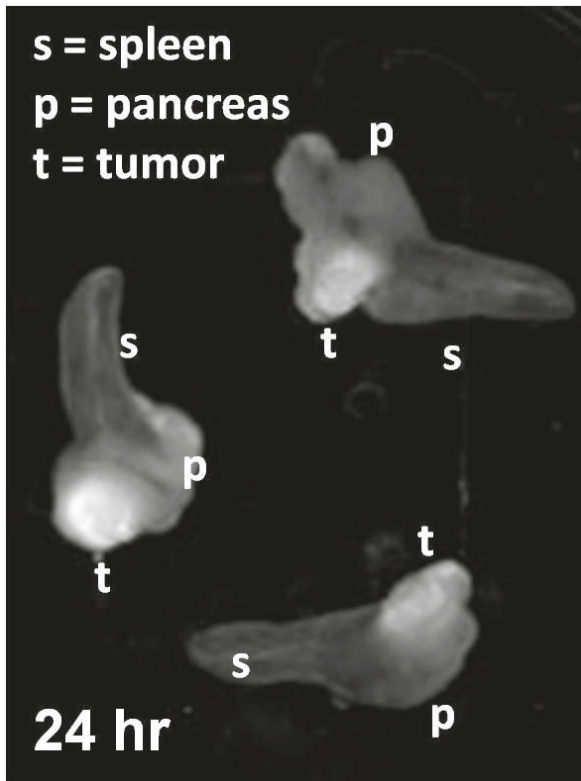
Purpose: Recent developments in anti-angiogenic and vascular-disrupting therapies have shown the great potential of tumor vasculature as a therapeutic target for cancer medicine. We have an original idea for using targeted gold nanoparticles as vascular disruptive agents in conjunction with clinical megavoltage photon beams. Unlike competing proposals, we recognize that gold nanoparticles tend to accumulate in, and can even be targeted for, tumor blood vessels and that these structures may be more important for anti-cancer therapy than clonogenic cell death alone. Due to the short distance traveled by x-ray induced photoelectrons,

the endothelial cells of the tumor will receive a sizable boost in dose, even for clinical megavoltage (MV) photon irradiation.

Materials and methods: We have developed and characterized a novel 4th generation gold nanoparticle platform which includes PEGylation for long circulation, Arginylglycylaspartic acid (RGD) for neovascular targeting and AF647 for fluorescence imaging. Theoretical studies were performed using a combination of Monte Carlo and analytical methods. In vitro experiments were performed using a clinical 6 MV photon beam with the HeLa cell line. In vivo imaging experiments were performed in an orthotopic pancreatic cancer model.

Results: The targeted gold nanoparticle platform was stable over 6 months. TEM imaging demonstrated consistent gold nanoparticle size of 2-3 nm and confocal microscopy showed robust in vitro cell uptake. Theoretical studies predict a 50% dose enhancement to adjacent tumor endothelial cells. Experimental studies in a 6 MV beam found 40-60% damage enhancement with the effect greatest for deeper targets, larger field sizes and with the flattening filter removed. Imaging studies confirmed preferential uptake in the tumor (see figure), infiltration of the tumor endothelial cells and renal clearing of the gold nanoparticles.

Conclusions: Our studies have demonstrated that a significant therapy enhancement is expected when gold nanoparticles are targeted to tumor endothelial cells prior to clinical radiation therapy. Our concept is highly compatible with current clinical practice and could offer a substantial clinical benefit with minimal patient risk.



Keywords: Nanoparticles, vascular disrupting agents

21

Performance of layered and volumetric rescanning for different scanning speeds of proton beam

K. Bernatowicz^{1,2}, A.J. Lomax^{1,2}, A.C. Knopf^{1,2}

¹Department of Physics, ETH Zurich, 8092 Zurich, Switzerland.

²Proton Therapy Center, Paul Scherrer Institute, 5232 Villigen PSI, Switzerland.

Purpose: The principle of rescanning using actively scanned proton beams has been recognized as potentially beneficial for mitigation of motion interplay effects. In this study, we compare layered and volumetric rescanning techniques for four realistic proton delivery designs exhibiting different Beam Position Adjustment Times (BPATs).

Materials and Methods: Volumetric and layered rescanning were compared for four different scenarios - a combination of fast and slow BPATs laterally (4ms & 10ms) and in depth (80ms & 1s); and 9 different treatment plan arrangements for two clinical liver cases with varying tumor size i.e. clinical target volume (CTV) of 98 and 264 cm³. 4D dose calculations were performed using regular, sinusoidal rigid motion assumed as the worst-case motion scenario to model interplay effects. Calculations were sampled over 3 different starting phases resulting in a total of 432 dose distributions. Effectiveness of rescanning was quantified in terms of dose homogeneity (D₅-D₉₅ values) and mean dose to CTV. Additionally, treatment delivery times were compared.

Results: For slow scanning systems, D₅-D₉₅ values were lower by up to 16% with layered rescanning and the estimated treatment delivery time was reduced by up to 300s. Analysis of dose homogeneity showed that layered rescanning leads to a smoother decrease in dose inhomogeneity as a function of the number of rescans than volumetric rescanning, which shows larger fluctuations. However, layered rescanning appears to be more sensitive to the starting phase. When analyzing the performance of both approaches and different scanning speeds as a function of delivery time, layered rescanning appears to be the only viable approach for systems with a slow energy changes, even approaching the performance of faster systems, as long as lateral scanning speeds are kept high. Similar results were found for multiple field plans and when analyzing different field directions.

Conclusions: In summary, there might not be a dedicated best design for the treatment of moving targets, instead it seems to be important to choose an adequate rescanning technique for a specific proton delivery system design. Our work suggests layered rescanning, as the method of choice for slow scanning systems, both in terms of dose homogeneity and treatment delivery time.

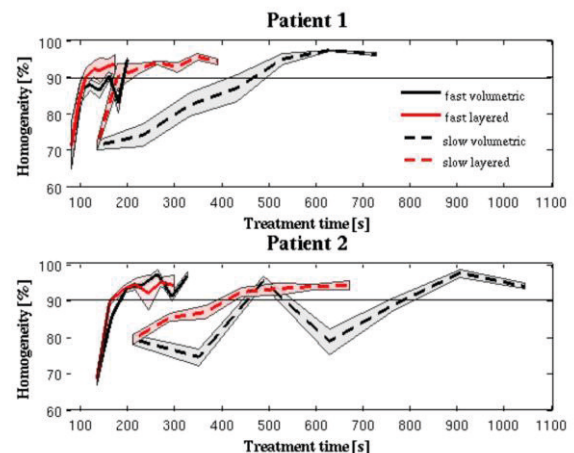


Figure: Increasing dose homogeneity ($= 1 - D_5-D_{95}$ value in percent) to CTV as a function of the treatment time, when different rescanning techniques are employed (i.e. volumetric - black, layered - red). Two scenarios with fast (solid line) and slow (dashed line) beam position adjustment times are shown.

Keywords: proton therapy, interplay effect, rescanning

22

Pre-clinical validation of a beam model designed for treatment planning computation of scanned proton and carbon ion beams

D. Bertrand¹, G. Russo², F. Marchetto², M. Ciocca³, T. Orts¹

¹IBA, Belgium

²INFN, Italy

³CNAO Foundation, Italy

An innovative beam model, the Beamlet Superposition (BS) model, has been proposed to describe the physical and radiobiological properties of therapeutic protons and carbon ion. The physics performances of this model have been assessed by an extensive validation procedure, aimed at demonstrating the suitability of this computation method for treatment planning purposes.

Measurements have been conducted in the CNAO facility, irradiating homogeneous targets with proton and carbon ion beams. The BS model has been commissioned on the used beam lines, exploiting pre-existing experimental data. The BS model has been incorporated in a TPS computing kernel, the Planning Kernel for Ion Therapy (PlanKIT), used to design the irradiations and predict the resulting dose distributions. Irradiation patterns included single spots, monoenergetic uniform layers, and cubic homogeneous volumes. Single spot profiles were characterized using a scintillator-based detector placed after variable amounts of PMMA slabs. Dose at the centre of monoenergetic fields was measured with a small ionization chamber. Cubic volumes were characterized both longitudinally by measuring depth-dose profiles along the irradiation axis with a multi-layer ionization chamber, and transversally by means of scintillator and PMMA slabs.

A general agreement between the predictions of the BS model and the measured data are observed. The model describes correctly the single spots as a function of penetration depth, except in positions far from the isocentre. Field size dependency is smaller than 2% in all configurations except at lowest proton energy. Comparison over carbon ion cubes is satisfactory, with more than 98% of the volume passing 3%-3mm gamma index criteria. Proton cubes exhibit dose ripple in deep positions slightly underestimated in the simulation, leading to a gamma index score of about 95%. Such observations match with the discrepancies observed for single spots.

The predictions obtained with the BS model have been found to closely match the measurements. The few observed discrepancies can probably be ascribed to limitations in the commissioning procedure rather than indicating failures of the model itself. Furthermore, observed differences are typically located far downstream in positions of minor clinical relevance, and generally lead to an overestimation of the model. The outcome of the comparisons gives positive indications regarding the clinical usability of the BS model.

Keywords: TPS, PBS, validation

23

Ion Beam Radiobiology: From the Lab to the Clinic

E.A. Blakely

Lawrence Berkeley National Laboratory, Berkeley, CA 94720 USA

Particle radiobiological data emerged from the laboratory to provide hadron therapy essential guidance on effective ion dose levels and dose-rates to eradicate targeted tumors, and safe ion dose tolerances for normal tissues. Radiobiological measurements continue to contribute an important validation element in the development of new beam delivery methods and particle treatment protocols combined with pharmaceutical for controlling radioresistant mechanisms, as well as chemotherapeutic agents for controlling metastatic disease. However the full potential of hadron therapy is yet to be fully realized for a number of reasons, including (1) particle radiobiology research is currently significantly underfunded in most locations worldwide, despite numerous lines of biophysical and molecular evidence of intriguing biological responses that potentially could lead to transforming breakthrough applications in particle therapy, and (2) inadequate radiobiological funding and access to beams has hampered the international resolution of differences in technical approaches to incorporate radiobiological effectiveness measurements into hadron treatment planning, without which clinical trial comparisons will be more difficult.

Simplicity often provides the best solution to problems. But our modern approach to medical care has developed sophisticated tools with high caliber computerized controls to enhance outcome, but with the essential requirement for more detailed basic information on the systems involved. Hadron therapy has made significant strides in the last decade, but struggled with the thorny practical problem of identifying a complex matrix of RBE values for various biological parameters to document a prescribed clinical dose, and to allow a reference comparison with conventional low-LET modalities. Now is the time to propose creative simple solutions that can unify the international protocol for ion beam therapy. This presentation will review the current status and future directions of radiobiological input to the clinic, and will discuss several options to resolve some of the problems in order to facilitate the full future potential of hadron therapy.

Keywords: hadron treatment planning issues, potential applications of new biology

Acknowledgement: Supported by the Office of Science (BER), U.S. Department of Energy Low Dose Radiation Research Program under Contract No. DE-AC02-05CH11231, NASA Grant #NNJ11HA941, and the University of California, San Francisco, Department of Radiation Oncology, San Francisco, CA.

24

Evolution of technology to optimize the delivery of proton therapy: the third generation

T. Bortfeld, J. Flanz

Massachusetts General Hospital, Department of Radiation Oncology, Boston, USA

While proton therapy is on the rise worldwide, it still plays a very small role compared with other treatment modalities in radiation therapy. The two primary reasons are: 1. the much bigger, heavier, and more costly equipment, and 2. The lack of clear clinical evidence that proton therapy is significantly better than conventional radiation therapy with x-rays. The second point is partially related to technical limitations of the current proton therapy technology, which leads to reduced lateral "sharpness" of the beam, and substantial uncertainties in the proton range.

In this presentation we will put forward plans to develop the next generation of proton therapy equipment that will be much smaller, cheaper, and fit in conventional bunkers. At the same time it will not suffer as much from those technical limitations. It will push proton therapy towards what is

physically possible as opposed to what is technically feasible. As for point 1, we will discuss methods to shrink proton gantries, to use fixed beams in combination with positioning robots, and disease site-specific solutions. We will show examples of proton therapy equipment that can almost be retrofitted in a conventional treatment room. Regarding point 2, we will discuss what is left to be done to sharpen the proton beam laterally, and to reduce range uncertainties such that the beam can be stopped in front of critical structures. We will argue that those new technologies are not that far off and may become clinically available in the next decade.

25

Preclinical studies and radiopharmaceutical developments with ^{64}Cu produced by ARRONAX facility

M. Bourgeois¹, J. Barbet¹, M. Chere², N. Chouin³, A. Faivre-Chauvet⁴, M. Frindel², F. Haddad¹, S. Supiot⁴

¹ARRONAX Cyclotron, Saint Herblain, France

²INSERM U892, France

³ONIRIS

⁴ICO

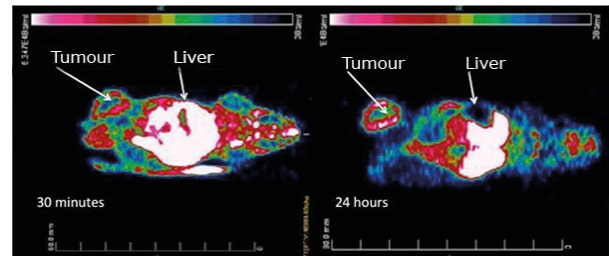
Purpose: Copper-64 is one of the most promising PET emitters currently studied in nuclear medicine. The well-established coordination chemistry of copper and the physical properties of copper-64 allows a wide use in nuclear medicine where copper could be radiolabeled with a large range of radiopharmaceutical compound from small organic molecules to large biological origin proteins like monoclonal antibody compounds. The present work is focused on the collaborative work around the ARRONAX cyclotron based at Nantes (France) in the field of copper-64 radiolabeling for tumour hypoxia mapping, haematopoietic radiotoxicology and phenotypic imaging.

Materials and Methods: ARRONAX is a multi-particle accelerator that can accelerate deuterons for ^{64}Cu production (d,2n reaction) with an optimal energy around 15 MeV on enriched nickel-64 target prepared by electroplating enriched nickel-64 on a gold backing.

The copper-64 is then extracted using a strong base anion exchange resin in HBr medium. More than 90% of the copper activity is recovered within 20 mL. Quality control of the final product includes an activity measurement using our dose calibrator, a γ -spectrometry to infer radioactive contaminants and an ICP-OES for stable contaminants (Zn, Co, Fe, Ni and Cu).

From this production of ^{64}Cu , the different research teams around the ARRONAX cyclotron are working on the radiolabelling of bishiosemicarbazone molecule like ATSM for giving a preclinical response on radiotherapeutic need on the tumour hypoxia status for xenografted human prostate cancer on mice. Another part of copper-64 work has given, after a bisphosphonate complexation, a compartmental model of haematopoiesis in the context of bone marrow radiotoxicity after injection of a bone vectorized radionuclide. At last, phenotypic imaging is an important field of work in nuclear medicine and we work on the optimisation of monoclonal antibody radiolabeling with copper-64 with classical bifonctionnal chelating agents like DOTA derivated structure or with new picolinate agents.

Results: Currently, the radiolabeling of ATSM was optimized and we obtained a first image of hypoxia in prostate cancer with a good correlation between the image contrast and biological hypoxic parameters.



The study on haematopoietic radiotoxicity conduces to a best knowledge on radiobiologic process of the most important nuclear medicine adverse effect.

Finally, our work on antibody radiolabelling permit to obtain an in vivo more stable radioimmunoconjugate

Conclusions: A repeatable production of ^{64}Cu on ARRONAX cyclotron is currently done. This is the first step to a pharmaceutical production and we work now on clinical trial project with ^{64}Cu -ATSM on two oncologic localisations (head and neck, prostate) for hypoxia tumour imaging. This project is in relation with the national French grant "LABEX Innovative Radiopharmaceuticals in Oncology and Neurology".

Keywords: copper-64, preclinical, cancer

26

PlanIt: Planning Ion therapy open platform for treatment plans testing and comparing

F. Bourhaleb^{1,2}, F. Dalmasso^{1,3}, A. Attili², F.M. Milian^{2,4}, G. Russo²

¹I-See, Torino, Italy

²INFN, Italy

³University of Turin, Italy

⁴UESC

Purpose: The aim of this work is to present the potentiality of web platform called PlanIt implemented for collecting treatment plans realized by experts in planning external radiation therapy to create planning templates for typical pathologies.

Indeed, we are proposing a common platform for data exchange and plans inter-comparison for different cancer pathologies and different radiation techniques. This platform can be also used as an online training tool and for plans verification with Monte Carlo simulations.

Materials/methods: We introduced examples of plans for typical pathologies treated with different radiation therapy techniques and verified with a Monte Carlo treatment plan simulation.

The main evaluation tools given by PlanIt platform are parameters to evaluate the plan quality: target coverage index (CI), inhomogeneity coefficient (IC) and relative dose-Volume-Histograms (DVHs).

We use typical study cases for real patients, in addition this system is providing an alternative approach enabling trainings using a virtual patient (VPatient): an antropomorphic phantom for generating virtual case studies with complete set of CT images and contours of volumes of interest. This is a peculiar value that is performing the possibility of investigating properly and focusing on specific problem with different techniques for treatment planning.

Results: We have a number of typical plans compared and verified within PlanIt system that we are presenting in this work. It is summarizing the potentiality of such system.

The PlanIt value will increase and grow in time and with the continued use of experienced professional figures, testing and evaluating different treatments and different pathologies.

Conclusions: PlanIt is an open platform for research institutions that can help, contribute and share their knowledge for one common objective: clinical endpoint. It is a platform giving an impartial and objective tool for optimizing the planning for typical cases of cancer pathologies and verifying which is the best convenient radiation therapy. This avoids an inopportune use of sophisticated advanced radiation techniques when it is not giving clinically any real advantage. VPatient module provides a powerful tool for testing and comparing plans on fully realistic phantom with the potentiality of creating virtual different pathologies.

Keywords: Treatment Planning, radiation therapy, Ion Beam Therapy, Virtual patient.

27

Augmented Reality tools for particle therapy facilities

F. Bourhaleb^{1,2}, G. Petrone³

¹I-See, Torino, Italy

²INFN, Italy

³Department of computer science, University of Turin, Italy

Purpose: Particle therapy facilities represent excellence centers that are results of advanced multidisciplinary research and high-technology equipments. A need of a Augmented Reality (AR) dedicated tools to integrate the important and sophisticated amount of information is an evident advantage in the optimization of the facility workflow.

Such tool set provides better management of information that usually are collected but not used due to difficulties in manipulating and accessing information.

According to the operator task the AR software infrastructure activate different level and kind of data and information.

A look at augmented reality features emphasizes a strong and better use of the potentialities of all the applications contributing for a better treatment.

Materials/methods: Our AR application has a software infrastructure that is managing different level of access.

All information related to the patient and the medical environment are hosted in a private cloud platform and the only needed access is a wi-fi connectivity.

Information are stored and ordered according different levels and relevance to the purpose considered.

According to the role of the user, the access is redirected to a predetermined kind of relevant information and use.

The only hardware needed for the final user is a simple tablet.

Results: The AR application we present is a prototype for particle therapy center since they are typical case of facilities where an optimized virtual medical environment makes the communication easier and so the facility workflow managed better.

In this work we present an example with three levels of use of the same AR application: medical doctor, medical physicists and technical engineer.

Conclusions: AR is nowadays a powerful tool for integrating information and giving in real time all knowledge needed to get the best management of resources dedicated to the patient.

Particle therapy centers are perfect candidates for taking full advantage for the potentiality of AR as an application and a service in the e-healthcare field.



Keywords: Augmented Reality, radiation therapy, Ion Beam Therapy.

References:

Photo courtesy of Medical Augmented Reality

28

An innovative on-line beam-monitoring detector based on the emission of secondary electrons

S. Braccini¹, D. Bergesio², A. Ereditato¹, E. Kirilova¹, G. Molinari², K.P. Nesteruk¹, P. Scamporrì^{1,3}, U. Amaldi²

¹AEC-LHEP University of Bern, Switzerland

²TERA Foundation, Novara, Italy

³Department of Physics University of Naples Federico II, Italy

Purpose: The BISE (Beam Imaging with Secondary Electrons) detector was designed and built by TERA for the on-line control of the intensity and shape of ion beams along transfer lines. It is aimed at operating in a large range of beam currents, from fractions of nA typical of particle therapy to several μ A used in radioisotope production.

Materials and methods: BISE is based on the detection of low energy (< 50 eV) secondary electrons emitted by a thin aluminum foil (of about $0.8 \mu\text{m}$) traversed by the ions. It represents the evolution of an apparatus previously developed by TERA [1]. The foil is placed at 45 degrees with respect to the beam direction and simulations show that the particles are subject only to a negligible perturbation. In this way, the detector can be continuously kept in the beam. The detector operates under vacuum and consists of an electrostatic lens used to focalize and accelerate the secondary electrons at the energy of 20 keV. The electric field produced by the lens is such that the electrons reach a plane where an inverted de-magnified image of the primary ion beam is formed. Here a sensor is located to detect the image. Simulations were performed using SIMION and COMSOL to study the optimal configuration of the electrostatic lens, the magnification and the resolution of the images. The sensor was chosen on the basis of its simplicity, reliability and cost-effectiveness. A phosphor screen (P47) read out by a CCD camera is used. In case of beam currents below the nA range, a micro channel plate can be added in front of the phosphor to amplify the signal. BISE is now under development and test in collaboration with LHEP at the new Bern cyclotron laboratory, where a specific beam transfer line ending in a separate bunker has been constructed to perform research activities [2]. The experimental set-up is shown in Fig. 1 (left).

Results: The first images of an 18 MeV proton beam are reported in Fig. 1 (right). They demonstrate that the detector equipped only with a phosphor screen is able to operate in wide range of beam intensities. The measurement of the magnification is ongoing and is performed by interposing a multi-hole collimator in front of the thin foil. The possibility of using a laser beam for the precise

assessment of possible distortions is also considered. For the calibration and measurement of the beam intensity through the analysis of the detected images, a specific high-sensitivity Faraday cup has been constructed and will be installed at the end of the beam line.

Conclusions: An on-line beam-monitoring detector based on the emission of secondary electrons was designed, constructed and tested. On the basis of the first beam tests, further developments are ongoing.



Figure 1. The BISE detector installed in the beam transfer line of the Bern cyclotron (left). Images of an 18 MeV proton beam at different intensities (right).

Keywords: Beam monitoring; Radioisotope production; Particle therapy

References:

- [1] L. Badano et al., IEEE Trans. Nucl. Sci. 51 (2004) 2990
 [2] S. Braccini et al., Proc. of IPAC2011, 3618.

29

Dose distribution characterization in the halo of proton pencil beams with emulsion film detectors

S. Braccini¹, A. Ariga¹, T. Ariga¹, A. Ereditato¹, F. Giacompo¹, C. Pistillo¹, P. Scamporrà^{1,2}

¹AEC-LHEP University of Bern, Switzerland

²Department of Physics University of Naples Federico II, Italy

Purpose: This work is aimed at the experimental characterization of the dose distribution in the beam halo region of a clinical proton pencil beam using a novel method based on nuclear emulsion detectors.

Materials and methods: Nuclear emulsion films allow for high-precision tracking of charged particles. Specific detectors can be built by interposing double-sided emulsion films with a tissue equivalent material to measure proton tracks in the proton therapy energy range. This technique has been recently used for proton radiography [1]. A 15 cm long detector composed by 60 emulsion films and PMMA plastic sheets was constructed and exposed to a 138 MeV proton pencil beam directed towards its center using the Gantry 1 at PSI. While the track density is too high to be measured in correspondence of the pencil beam, this method allows counting single proton tracks in the halo along the depth of the detector. This region is particularly interesting since the corresponding dose can be located outside the target volume and could potentially lead to undesired secondary effects. A Monte Carlo simulation was performed using Geant4 to optimize the design of the detector and to assess the average dose delivered by each proton in the halo. Following the chemical development and the automatic microscopic scanning of the emulsion films, three areas in the halo region were selected at about 2 cm distance from the beam axis (Fig. 1 - left). Here, proton tracks were identified and efficiently separated from the background by means of their high ionization loss.

Results: Data were analyzed at several depths and the corresponding angular distributions showed that the protons in the halo region could be subdivided into two components (Fig. 1 - right). The former is dominating at small depths and is almost parallel with respect to the beam axis. It is generated up-stream with respect to the detector, in the gantry and in the nozzle. The latter is characterized by large

angles and is due to the multiple scattering of the protons inside the tissue equivalent material of the detector. This second component dominates at larger depths. The identification of the proton tracks, together with the corresponding dose estimated by Monte Carlo, allows assessing an upper limit of the dose in the beam halo region. It was found to be less than 3×10^{-4} Gy for a delivery of 2 Gy in the spot region.

Conclusions: A new method to measure the dose in the beam halo region of a clinical proton pencil beam based on nuclear emulsion detectors is proposed and successfully tested.

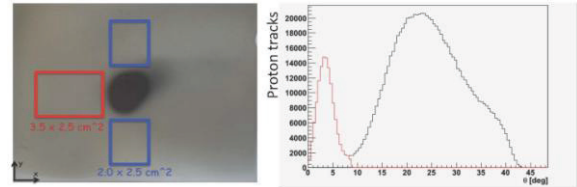


Figure 1. A nuclear emulsion film exposed to a 138 MeV proton pencil beam where the selected regions for the analysis are indicated (left). Angular distribution of the proton tracks at 7.3 cm depth. The first almost parallel component is indicated in red while the one due to multiple scattering in black (right).

Keywords: Radiation dose; Nuclear emulsion detectors; Proton therapy

References:

- [1] S. Braccini et al., First results on proton radiography with nuclear emulsion detectors, Journal of Instrumentation 2010 JINST 54 P09001.

30

Studying inter- and intrafraction motion mitigation with sequential 4DCTs of lung tumor patients

R. Brevet¹, C. Bert^{1,2}, M. Durante¹, C. Graeff¹, D. Richter^{1,2}

¹GSI, Darmstadt, Germany

²UK Erlangen, Germany

Compared to conventional radiotherapy, physical and biological properties of scanned carbon ion beam therapy can allow a more accurate irradiation. Treatment of moving tumors can be problematic due to range sensitivity and interplay effects. Purpose of this study is to investigate if dedicated optimization of treatment planning parameters and ITV-PTV margins provide a solution.

For 5 NSCLC lung tumor patients from MDACC (The University of Texas MD Anderson Cancer Center), a total of 38 weekly 4DCT datasets were available. Reference phases of each subsequent CT were registered rigidly to mimic patient setup. Motion phases of each 4DCT were registered non-rigidly. Single field gating plans were simulated using the GSI treatment planning system TRiP4D, including 4D-dose reconstructions. Plans were initially optimized to the ITV without additional margins but considering motion related range changes. First, the impact of variations in focus size and length of the gating window (GW) on dose coverage (V95) and conformity number (CN) was analyzed. Three beam foci (6, 10 and 15 mm full width at half maximum) and three GW (11.9, 30 and 50% of the amplitude) were studied. Then, the influence of range (3mm water-equivalent + 3%) and isotropic (3mm) ITV-PTV margins on V95 and CN were investigated. Combination of both margins was also analyzed.

The initial treatment plans resulted in V95 of 98.8% (96.6% to 100%) and CN of 0.6 (0.53 to 0.7). Anatomic variations such as patient misalignment or tissue drifts caused the largest effects on dose coverage. For all patients, such variations

yielded V95 below 85% for some weeks and all studied parameter combinations. A larger beam focus and a shorter GW increased the homogeneity of the dose, but not sufficiently to compensate the anatomic changes. The worst configuration of longest GW and smallest focus yielded a mean V95 value of 72.7% (42.8% to 94.5%) and a mean CN of 0.39 (0.15 to 0.62), while the best configuration of shortest GW and largest focus yielded V95 = 89.2% (67.5% to 99.7%) and CN = 0.45 (0.17 to 0.66). Then largest focus and shortest GW were combined with the two types of ITV-PTV margins. For isotropic margins, V95 increased to 94.2% (76.8% to 100%) but CN decreased to 0.38 (0.18 to 0.52). For range margins, V95 increased to 96.4% (80.7% to 100%) with a CN of 0.38 (0.2 to 0.53). Combination of both yielded V95 = 97.6% (81.8% to 100%) and CN = 0.33 (0.19 to 0.45). Details are listed in table 1 and illustrated in figure 1.

For inter-fractional settings, dose coverage deteriorated due to anatomic changes as well as patient setup. GW and beam focus could partially recover 4D-dose coverage, but ITV-PTV margins appear necessary. Target coverage appeared to increase significantly by adding isotropic and range margins resulting in slightly decreasing CN due to increased dose to normal tissue. Rescanning and multiple fields will be investigated as a next step to further improve target coverage.

Margins	Focus (mm)	Gating window (% of amplitude)	V95 (% of dose) (range)	CN (range)
ITV	6	50	72.7 (42.8 to 94.5)	0.39 (0.15 to 0.62)
ITV	15	11.9	89.2 (67.5 to 99.8)	0.45 (0.17 to 0.66)
ITV + 3mm isotropic	15	11.9	94.2 (76.8 to 100)	0.38 (0.18 to 0.52)
ITV + 3mm+3% range	15	11.9	96.4 (80.7 to 100)	0.38 (0.2 to 0.53)
ITV + 3mm isotropic + 3mm+3% range	15	11.9	97.6 (81.8 to 100)	0.33 (0.19 to 0.45)

Table 1: Impact of focus, gating window and margins on V95 and CN

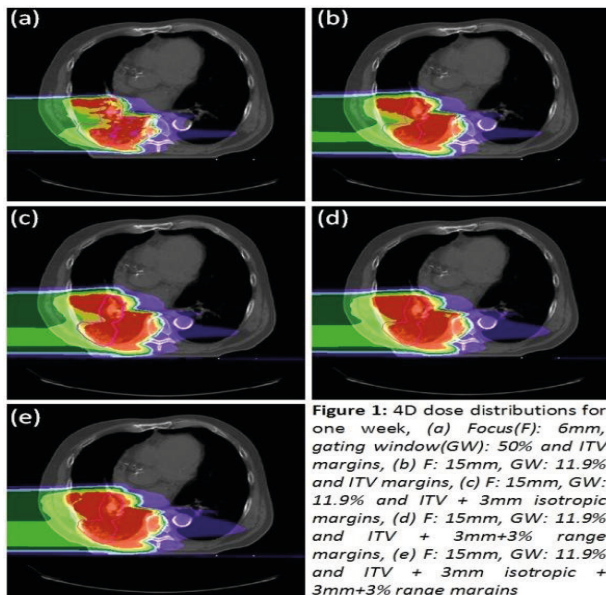


Figure 1: 4D dose distributions for one week, (a) Focus(F): 6mm, gating window(GW): 50% and ITV margins, (b) F: 15mm, GW: 11.9% and ITV margins, (c) F: 15mm, GW: 11.9% and ITV + 3mm isotropic margins, (d) F: 15mm, GW: 11.9% and ITV + 3mm+3% range margins, (e) F: 15mm, GW: 11.9% and ITV + 3mm isotropic + 3mm+3% range margins

Keywords: ion beam therapy, adaptive treatment planning, robustness study

31

Predictive and prognostic role of functional imaging of head and neck squamous cell carcinomas

D.M. Brizel

Department of Radiation Oncology, Duke Cancer Institute, Durham, NC, USA

Novel non-invasive functional imaging methods are necessary to predict therapeutic outcome and thereby improve the ability to properly select patients for treatment with both conventional and targeted therapies, to better evaluate

therapeutic effectiveness during the early phases of treatment, and to enhance a priori risk assessment for treatment induced toxicity. Functional metabolic imaging typically involves a pretreatment baseline MRI and/or PET scans. A second scan may be performed during or after treatment. Imaging parameter changes are routinely attributed to the intervening therapy and clinical outcomes subsequently correlated with these changes. If the second scan is performed during therapy, then an opportunity exists to modify the treatment plan based on changes in tumor and/or normal tissue.

The physiologic parameter(s), which best correlate with clinical outcome or risk of complications are unknown, however. Furthermore, unlike anatomy, which is static, tumor physiology is a heterogeneous and dynamic process. Large daily fluctuations in metabolic processes occur in a significant proportion of patients without any intervening treatment. The magnitude of this temporal variability is not established for MRI nor for PET. Optimal integration of functional imaging into treatment planning and response assessment requires understanding and quantification of the intrinsic variability of the underlying biological processes and a demonstration that treatment induced changes exceed intrinsic temporal variation. The state of the art for the clinical use of functional imaging in head and neck cancer will be reviewed and ongoing investigational efforts will be discussed.

Keywords: PET scanning, functional imaging, adaptive radiotherapy

32

Evaluation of Late Toxicity Risk for RT Patients through Geant 4 Simulation of X-Ray Dose Deposition

F. Brochu¹, N.G. Burnet², R. Jena³, M.A. Parker¹, S.J. Thomas⁴

¹University of Cambridge, HEP Group, UK

²University of Cambridge Department of Oncology, Cambridge Biomedical Campus, UK

³Oncology Centre, Addenbrooke's Hospital, Cambridge, UK

⁴Department of Medical Physics, Addenbrooke's Hospital, Cambridge, UK

Radiotherapy is an important component of treatment for many cancers, but the unavoidable delivery of dose to the tissue surrounding the target area can lead to toxicity associated with the treatment, which may become manifest several months or years after the treatment.

Image-guided radiotherapy is a technique which has been successfully employed to improve the accuracy of the beam delivery and attempt to increase tumour cures and reduce the associated toxicity effects. However it usually involves X-rays taken daily throughout the treatment, and therefore carries a risk of second malignancy which is poorly understood and difficult to quantify.

We describe the modelling of two image guided radiotherapy treatment machines (linear accelerator), the Elekta Synergy and Tomo Therapy Hi-Art in use in Addenbrooke's Hospital, with the simulation software Geant 4 and its validation against measured calibration data.

We also present some 3D dose distributions obtained by simulation, using voxel models obtained by conversion of diagnostic radiotherapy planning scans of some clinical cases. A full-body dose map of an image guidance CT is shown in Figure 1, based on simulation using a diagnostic radiotherapy planning scan of a patient.

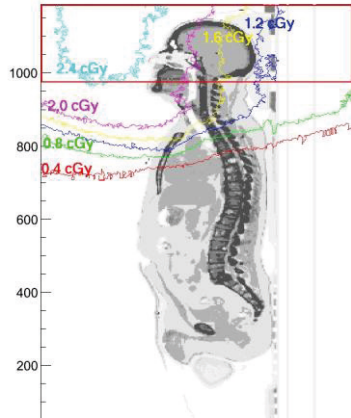


Figure 1: Dose distribution in whole body after a simulated image guidance CT scan to the head region (red box), using 150 mAs and 120 kVp as beam parameters.

As one can see, the doses obtained do not exceed 2.5 cGy, which is roughly 100 times smaller than the typical dose from an individual daily fraction.

The dose maps obtained over an entire treatment plan, including the daily image guidance CT scans and the daily treatments can be combined for analysis and estimation of the overall risk rate to develop late complications related to the radiotherapy treatment.

Keywords: Simulation, dose deposition, late toxicity

33

Combined Radiochemotherapeutical Strategies for Microtubule Stabilizing Agent (MSA)-Resistant Tumors
A. Broggini-Tenzer, A. Sharma, K. Nytko-Karouzakis, V. Vuong, M. Pruschy
University Hospital Zürich, Radiation Oncology, Laboratory for Molecular Radiobiology, Switzerland

Purpose: Tumor cells are the major targets for classic anticancer treatment modalities such as radiotherapy or chemotherapy, but tumor cells with a mutated genetic background are often the cause for inherent or acquired treatment resistances. At the same time other cell types including fibroblasts and endothelial cells, which build up the tumor microenvironment, are co-targeted and co-determine the tumor treatment response. Tumor growth control by aiming at such elements of the microenvironment is especially desirable in tumors with a mutated genetic background. Here we present a rationally designed combined treatment modality to overcome treatment resistance against microtubule stabilizing agents (MSA) in combination with ionizing radiation.

Material and Methods: Single and combined treatment regimens of ionizing radiation, microtubule stabilizing agents (patupilone and taxol) and anti-angiogenic agents (Rad001 (everolimus) and avastin) were investigated in genetically-defined MSA-resistant lung and colon adenocarcinoma tumor cells (A549EpoB40 and SW480 respectively), in endothelial cells (HUVECs) and in the corresponding tumor-cell derived tumor xenografts.

Results: While MSAs were potently inhibiting MSA-sensitive tumor cell and endothelial cell proliferation, no antiproliferative effect was observed against the MSA-resistant tumor cells. Furthermore, MSAs only reduced growth factor-secretion from MSA-sensitive but not from MSA-resistant tumor cells. Endothelial cells showed an additive antiproliferative response to MSAs in combination with ionizing radiation and Rad001, respectively, which could not

be observed in the MSA-resistant tumor cells. Interestingly, MSA-resistant tumor xenografts (A549EpoB40-xenografts) were strongly re-sensitized to patupilone when combined with Rad001. In contrast, the combination of IR and patupilone did not even lead to an additive tumor growth delay. Thus, Rad001 specifically sensitized treatment-resistant tumors to patupilone, most probably by a mechanism involving tumor-cell derived auto-/paracrine signaling. Rad001 strongly inhibited the secretion of VEGF from tumor cells, which could be a potential mechanism leading to an anti-vasculature effect, thereby controlling tumor growth. Indeed, MSA-resistant tumor xenografts derived from A549EpoB40 or SW480 cells could be re-sensitized to patupilone and taxol, respectively, when combined with the anti-VEGF inhibitory antibody avastin.

Conclusions: These data demonstrate that the interaction between the tumor cell compartment and tumor microenvironment strongly determines the radiochemotherapy treatment response and can be exploited to re-sensitize MSA-resistant tumors to clinically relevant agents.

34

Equivalent uniform dose (EUD) based biological optimization for carbon ion therapy
S.C. Brüningk, F. Kamp, J.J. Wilkens
Department of Radiation Oncology, Technische Universität München, Klinikum rechts der Isar, Germany

Purpose: Since its formulation by Niemierko in 1997, the concept of the equivalent uniform dose has successfully been used for comparing and optimizing IMRT plans. We transfer this concept to carbon ion therapy and use it as a basis for the biological optimization of treatment plans. The aim is to relate the optimization closer to the biological outcome by considering each structure as a whole in the optimization process, rather than optimizing the equivalent dose (relative biological effectiveness (RBE) x dose) in each voxel. Additionally we investigate the interplay of structure- and voxel-based objective functions and constraints.

Materials and methods: To simplify the optimization process of carbon therapy plans we propose an equivalent uniform effect (EUE) instead of RBE-weighted conversion of the physical dose. Following Niemierko's EUD, the EUE is defined as the biologically equivalent uniform effect that will result in the same probability of injury as the inhomogeneous effect distribution under consideration. Its mathematical formulation is based on the generalized mean effect:

$$EUE = \left(\frac{1}{N} \sum_{i=1}^N E_i^a \right)^{\frac{1}{a}}$$

Here N denotes the number of voxel in the structure under study, E_i is the biological effect ($aD + bD^2$, with linear quadratic parameters a and b) in voxel i and a is a tissue-specific parameter indicating the dose-volume effect. Two EUE-based objective functions, using a sum of squared differences or a sum of log-sigmoids respectively, were implemented into a research treatment planning system (CERR). Constraint functions were designed to choose for each structure between biological effect constraints per voxel and EUE constraints per structure. Here an EUE constraint is accompanied by a fictive exponent a emphasizing the under- or overdosed volume of a structure. This enables limiting the dose and the corresponding volume, while optimizing for the biologically meaningful EUE. Treatment plans were calculated for a head-and-neck patient for multiple combinations of objective functions and

constraint sets. Plans were evaluated regarding multiple dosimetric criteria as target coverage, homogeneity, conformity, as well as the final EUD (based on RBE x dose) for the target and organs at risk (OAR).

Results: In terms of target coverage, homogeneity and conformity it was possible to achieve comparable plans for voxel- and EUE-based optimization. However, regarding the biological outcome, it was more intuitive to apply the EUE-based objective function, since voxel-based approaches are rather try and error processes. Especially in the case of inhomogeneous dose distributions in OARs, where it was difficult to meet the voxel-based effect constraints, the optimization could easily be steered in the desired direction by applying EUE-constraints.

Conclusions: Our investigation showed that EUE based optimization for carbon ion therapy can be a useful tool to optimize more specific in the sense of biological outcome.

Keywords: EUD, carbon ions, treatment plan optimization

35

Potential of Detection of fast Cherenkov Photons for Improved Time of Flight Positron Emission Tomography

S. Brunner¹, T. Beyer², L. Gruber¹, A. Hirtl³, J. Marton¹, K. Suzuki¹

¹Stefan-Meyer-Institute for Subatomic Physics, Austrian Academy of Sciences, Vienna, Austria

²Center for Medical Physics and Biomedical Engineering, Medical University of Vienna, Austria

³Department of biomedical imaging and image-guided therapy, Medical University of Vienna, Austria

Purpose: The time of flight (TOF) method is used successfully to improve the signal-to-noise ratio (SNR) of positron emission tomography (PET). State of the art systems have been developed by major PET manufacturers and reach coincidence time resolutions (CTR) of 500 ps FWHM. By improving the time resolution further, the obtained information could be used for even better SNR of PET-images. Moreover, achieving time resolutions much smaller than 100 ps, the spatial resolution of PET could be further improved, resulting in higher resolution of PET images together with shorter examination duration for patients.

Materials and methods: We study the potential of ultra-fast Cherenkov-photons in scintillators and Cherenkov radiators for improving the time resolution of TOF-PET. Proof-of-principle measurements using standard lead-glass have been performed successfully. The results of the measurements have been compared with Monte Carlo simulations (using Geant4). Variations of geometrical and optical parameters such as crystal size, transmission wavelength or refractive index, help to determine their impact on the total time resolution and allow a better understanding of optimum material and geometry properties for best time resolutions of annihilation-photon-detectors for PET. Based on the simulation outcomes, basic CTR measurements using several promising materials, detector geometries and detector arrangements using photo-multiplier tubes and Silicon photo-multipliers (SiPMs) have been performed.

Results: We present the latest results of systematic, experimental and simulation studies on the CTR and Cherenkov photon yield of various promising Cherenkov radiators, detector geometries and detector arrangements. Simulation results show CTRs reaching from 32 ps to 144 ps FWHM for certain detector configurations which can be improved by -20 ps by detecting Cherenkov photons yielding to CTRs of 12ps to 125 ps FWHM. Results of a proof-of-concept will show the feasibility of our method to improve the CTR significantly. Furthermore, outcomes of these studies show that small, pixelized photo-detectors such as SiPMs, are most suitable for detection of Cherenkov photons for TOF-PET. Therefore, the single photon time resolution of

different types of SiPM from major vendors has been determined using a picosecond laser. Results will be presented.

Conclusions: Detection of ultra-fast Cherenkov photons helps to improve the CTR in TOF-PET significantly, resulting in improved SNR and furthermore, has the potential to make direct reconstruction of the origin of annihilation photons, using their precise time-stamps, possible.

Keywords: Cherenkov effect, Time of flight positron emission tomography (TOF-PET)

36

Development of Advanced Quality Assurance Instrumentation for Hadrontherapy

M. Bucciantonio^{1,2}, U. Amaldi¹, R. Kieffer¹, F. Sauli¹, D. Watts¹

¹TERA Foundation, Novara, Italy

²University of Bern, Switzerland

We describe the development and preliminary results obtained with two dedicated instruments aiming at improving the quality of patient monitoring before and/or during beam exposure at forthcoming hadron therapy centers.

The first system, named Proton Range Radiography (PRR), relies on a method to obtain the integrated density distribution in the target recorded in-beam before or after the treatment, at reduced beam intensity; the second, the Time Of Flight PET (TOF-PET), aims at providing in real-time dosimetry information during the therapy exploiting the detection of the positron emission of isotopes created during the irradiation, restricting the region of interest by a sub-nanosecond timing using as fast gaseous detectors stacks of Multigap Resistive Plate Chambers (MRPC).

Proton transmission radiographic images are produced by measuring with a pair of position-sensitive detectors (GEM chambers) the direction of the protons transmitted through the patient, and with a stack of scintillators the residual range of the protons leaving the patient. After the successful tests of a small prototype (PRR10, with 10x10 cm² active area), a larger system named PRR30, has been built and tested. with a complete redesign of the front-end and data handling electronics capable to acquire data at rates exceeding 1 Megahertz and therefore suited to match the requirements of near-real time high-resolution imaging with a few seconds of exposure.

Integral part of the cooperative ENVISION project, the TOF-PET has succeeded developing the technology for the realization of medium-size, compact MRPC detector prototypes with an optimum active/total area ratio as demanded by a PET application. Based on the use of stacks of high resistivity glass serving both as electrodes and photon converters, the detectors are readout with fast multi-channel integrated discriminators having intrinsic time dispersions below 40 ps. A thorough optimization of the components and the use of inter-calibration algorithms permit to anticipate TOF resolutions between 100 and 200 ps, comparable or better than those that can be achieved with the use of fast scintillators.

37

152/161Tb-DOTA-RM6 biodistribution studies in prostate cancer bearing SCID mice and 149Tb sources from CERN-MEDICIS

F. Buchegger¹, S. Baechler¹, L. Bühler², E. Deshayes¹, A. Gottberg³, M. Kosinski¹, H.R. Maecke⁴, R. Mansi⁴, C. Müller⁵, J.O. Prior¹, R. Schibli⁵, T. Stora³

¹CHUV, Switzerland

²HUG, Switzerland

³CERN, Switzerland

⁴Universitaetklinikum Freiburg, Germany

⁵PSI, Darmstadt, Germany

Introduction: At ICTR-PHE2012 conference the project of a facility for the production of isotopes for medical research at CERN was presented: the CERN-MEDICIS project. Here we report on results obtained recently on animal models and on the details of the construction of the CERN-MEDICIS facility.

Background: Gastrin releasing peptide receptors (GRPr) are highly expressed in prostate and breast cancer. DOTA-RM6 is a new GRPr antagonist, prepared and selected by two of us (RM, HRM). Terbium (Tb) radioisotopes would allow the comparative study (Müller et al 2012 J Nucl Med p1951) of systemic radiolabeled therapies with either low energy beta-radiation (^{161}Tb) or alpha-radiation (^{149}Tb) using 2 perfectly matched radioisotopes and correlate the therapy with PET imaging (^{152}Tb).

Materials and Methods: Biodistributions in PC-3 tumor bearing SCID mice were performed (n=3, unless specified otherwise) 20min to 16h post i.v. injection. DOTA-RM6 (30 ug) radiolabeling with 1.7MBq ^{152}Tb (CERN, pilot batch prepared before accelerator revision shut-down) or 200 MBq ^{161}Tb (Paul Scherrer Institute, Villigen) was performed with 20min boiling at pH 4 to 5.

Results: Labeling of DOTA-RM6 with $^{152/161}\text{Tb}$ yielded $^{152/161}\text{Tb}$ -DOTA-RM6 of >98% purity without further purification. Tumor and pancreas uptake of ^{152}Tb -DOTA-RM6 1h post injection was 24.0 ± 2.8 and $11.4\pm 1.8\%$ ID/g, respectively, and it was 19.2 ± 0.8 and $1.9\pm 0.3\%$ ID/g at 3h, respectively (n=2). ^{152}Tb -DOTA-RM6 co-injected with excess unlabeled peptide (0.03 mg, n=2) showed at 1h 1.7 and 0.7%ID/g in tumor and pancreas, respectively. A kinetic biodistribution study with ^{161}Tb -DOTA-RM6 showed highest pancreas uptake of $50.7\pm 5.5\%$ ID/g at 20min, while tumor uptake peaked at 1h with $28.1\pm 2.6\%$ ID/g, pancreas decreasing at 1h to $19.9\pm 1.5\%$ ID/g. Unlabeled peptide in excess co-injected with ^{161}Tb -DOTA-RM6 inhibited tumor and pancreas uptake at 1h by >90%. ^{161}Tb SPET/CT imaging 3h post i.v. injection (3MBq) of a Fox nude mouse grafted with PC-3 tumor (0.2g) showed high tumor uptake and low background activity in normal tissues, also confirmed in the biodistribution post sacrifice with tumor measured at 12%ID/g.

Conclusion: $^{152/161}\text{Tb}$ -DOTA-RM6 showed high and specific GRPr mediated tumor uptake with a long retention while an initially high pancreas uptake lasted only a short time. The results show that this peptide radiolabeled with Terbium isotopes could allow performing SPECT and PET/CT controlled, strictly comparative systemic alpha- and low energy beta-radiation therapies.

Keywords: Targeted radiotherapy, prostate cancer, Terbium isotopes

38

Segmentation and Tracking of ROIs for Image-Guided Fractionated Radiotherapy

G. Bueno, O. Déniz, J. Salido

VISILAB - E.T.S: Ingenieros Industriales, Universidad de Castilla-La Mancha

Purpose: Organ motion should be taken into account for image-guided fractionated radiotherapy. Organ modelling is of key importance to improve the conformation of the dose delivered to the target (tumoral tissues), whatever its shape, in order to spare surrounding tissues. It may be applied for several purposes including segmentation, registration and tracking.

In this work a novel method for performing deformable segmentation and tracking was developed for inter- and intra-fraction organ motion planning and evaluation.

Materials and Methods: Energy minimizing active model were synthesized for tracking a set of organs delineated by regions of interest (ROI) in radiotherapy treatment. The initial model consists of a surface deformed to match the ROI contour by geometrical and morphological properties, following a heat

flow model driven by region, boundary and shape information.

The deformable segmentation model was applied to prostate and lung cancer for a database composed of 300 CT images belonging to 25 patients.

Results: In order to assess the performance of the segmentation, the results were compared against those obtained by manual segmentation, carried out with the TPS ADAC Pinnacle, and quantitative measures including sensitivity and specificity were obtained. Three metrics have been also used to quantitatively compare the results obtained with the proposed method and the manual delineation, namely, Jaccard index, Dice coefficient and Hausdorff distance.

Experimental evaluation of automated versus manual segmentation was done for the cardiac, thoracic and pelvic regions for real CT data. It was also tested using a Shepp-Logan head CT simulation and CT with added noise and partially occluded organs.

The quantitative validation gave an average of 98.23% and 99.35% for the sensitivity and specificity, respectively, 92.81% for the Jaccard index, 97.55% for the Dice coefficient and 0.98%mm for the Hausdorff distance.

Conclusions: Model-based deformable segmentation and ROI tracking was developed and tested for image-guided radiotherapy treatment planning. The method is efficient, robust and has sufficient accuracy for 2D CT data without markers. We increase the robustness of the segmentation result using the additional shape information that represents the desired structure.

Using the implemented geodesic active region model to accurately track the clinical target volume, a full implementation of IGRT is possible using only the 2D CT data without markers. Additionally, it may be used for accurate segmentation in the CT, all of which results in adaptive radiotherapy. In this process, intra/inter-fraction changes in tumour shape and position can be accurately detected and tracked. Thus, the dose delivery for treatment fractions can also be adaptively modified to compensate for inaccuracies.

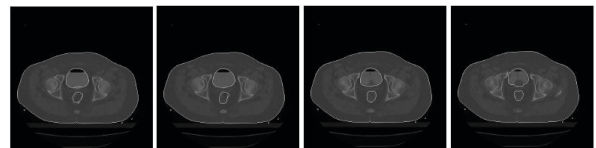


Figure 1.- Results of the segmentation model applied to ROI tracking of a pelvic CT sequence.

Keywords: ROI segmentation and tracking, geodesic active model

39

Properties of therapeutic He, Li and O beams studied with Geant4

L.N. Burigo^{1,2}, M. Bleicher^{1,2}, I.N. Mishustin^{1,3}, I.A. Pshenichnov^{1,4}

¹Frankfurt Institute for Advanced Studies, Goethe-Universität, Frankfurt am Main, Germany

²Institut für Theoretische Physik, Goethe-Universität, Frankfurt am Main, Germany

³Kurchatov Institute, Russian Research Center, Moscow, Russia

⁴Institute for Nuclear Research, Russian Academy of Sciences, Moscow, Russia

Purpose: Protons and carbon ions have been successfully applied to treat localized tumors by delivering an elevated dose to the target volume while sparing healthy tissues. Which cancer cases benefit more from carbon treatment compared to proton therapy is still under discussion.

Questions can be raised whether other light nuclei as helium, lithium or oxygen could be advantageous in particular cases. Therefore, the physical and biological properties of these projectiles are considered in the present work in view of their possible applications in cancer therapy.

Materials and methods: Our Monte Carlo model for Heavy-Ion Therapy (MCHIT) [1,2] is used to calculate dose profiles and microdosimetry quantities for p, He, Li, C and O nuclei of therapeutic energies in tissue-like media. MCHIT is based on the Geant4 toolkit [3] and takes into account fragmentation of beam nuclei leading to secondary fragments with their radiobiological properties different from primary nuclei. MCHIT is coupled with the Microdosimetric Kinetic (MK) model [4,5] in order to estimate the Relative Biological Effectiveness (RBE) for Human Salivary Gland (HSG) cells at various positions inside a complex radiation field created by primary and secondary nuclei inside the irradiated medium.

Results: RBE for HGS cells are calculated and folded with dose distributions providing biological dose profiles for the considered beams. The calculated biological depth-dose distributions for helium, lithium and carbon beams are found to be similar to each other. All three ions demonstrate a high ratio of the dose at the Bragg peak to the dose at the plateau thus indicating a possibility to spare healthy tissues located in the beam entrance channel.

Conclusions: The MCHIT model coupled with the MK model makes possible to calculate the physical and biological dose-depth profiles for proton, helium, lithium, carbon and oxygen ions in tissue-like media. A proper modeling of nuclear fragmentation reactions is important for describing radiation effects of light ion beams and their secondary fragments. Favorable biological dose-depth profiles for helium and lithium beams are predicted. Since such profiles are similar to those known for carbon beam, helium and lithium nuclei can be considered as promising options for cancer therapy.

Keywords: hadrontherapy, Geant4, RBE

References:

- [1] I. Pshenichnov et al., Nucl. Instr. Meth. B, 266 (2008) 1094-1098.
- [2] L. Burigo et al., Nucl. Instr. Meth. B, 310 (2013) 37-53.
- [3] J. Allison et al., IEEE T. Nucl. Sci., 53 (2006) 270-278.
- [4] R. Hawkins, Int. J. Radiat. Biol., 69 (1996) 739-755.
- [5] Y. Kase et al., Radiat. Res., 166 (2006) 629-638.

40

Do physiological relevant doses of biguanides have any role in cancer treatment?

M. Busk¹, J. Frøkiær², M.R. Horsman¹, S. Jakobsen², N. Jessen³, J. Overgaard¹

¹Department of Experimental Clinical Oncology, Aarhus University Hospital (AUH), Aarhus, Denmark

²PET centre, Aarhus University Hospital, Aarhus, Denmark

³Department of Internal Medicine and Endocrinology, AUH

Purpose: The anti-diabetic biguanide drugs metformin (MET) and phenformin (PHE), which work by mild self-limiting inhibition of mitochondrial complex I and activation of the energy-sensing LKB1/AMPK pathway in the liver, may also have antineoplastic effects. Anticancer effects may relate to changes in insulin/glucose, but inhibition of respiration and compensatory increased glycolytic flux in tumor cells may also cause (i) death of nutrient-deficient tumor cells which are particularly susceptible to further elevated metabolic stress or (ii) tumor reoxygenation and sensitization to radiotherapy. Surprisingly and unfortunately, nearly all cancer studies used irrelevant, non-physiological biguanide concentrations in vitro. Biguanides are cell membrane impermeable and uptake depends critically on organic cation transporters (OCTs), but this fact has also been ignored in most cancer studies. The purpose of this study was to provide

evidence for (or against) directly mediated metabolic tumor effects using in vivo achievable biguanide concentrations.

Materials and methods: Dose-response effects of MET and PHEN on cell proliferation/viability and glucose metabolism were studied in vitro in lung, mammary, colon, head and neck, prostate and cervix cancer cells differing in OCT expression and LKB1 status. Furthermore, to assess drug bioavailability, we developed ¹¹C labeled biguanides which allowed assessment of in vitro cellular drug uptake and, importantly, in vivo biodistribution assessment using PET scans/organ dissection. Based on the in vitro screening for cell sensitivity, two cell lines (SiHa and A549) were grown as xenografts in mice, and effects of repeated MET (250 mg/kg, i.p.) or PHEN (100 mg/kg) treatment on cell viability, glucose metabolism and hypoxia was studied using repeated FDG/hypoxia PET scans and invasive analysis of tissue markers of proliferation, glucose use and hypoxia.

Results/Conclusions: Cells retained ¹¹C-labeled biguanides in vitro and uptake was slowed by adding unlabeled biguanides. High levels of biguanides stimulated glucose uptake and the response was similar to the effect of anoxia suggesting that biguanides works via mitochondrial inhibition. This was further supported by the observation that adding biguanides to anoxic cells did not further stimulate glucose flux. The lung cancer cell line A549 was particularly sensitive and showed metabolic and proliferative responses down to 0.5 mM MET, but even this level was higher than peak blood values (<0.2 mM) as estimated from ¹¹C-MET. PHEN was 100 times more potent and produced metabolic changes similar to N₂ down to 50 μM. For A549 this was also true for 5 μM. Since the in vivo tolerable dose was only 2.5 times lower for PHEN than for MET further in vivo testing focus on PHEN. Preliminary PET data suggests that SiHa tumor oxygenation was acutely improved in PHEN treated mice. Further data analysis is ongoing.

Keywords: Biguanides, metabolic targeting, reoxygenation

41

Modelling acute urinary toxicity after radiotherapy for prostate cancer

V. Carillo¹, A. Botti², V. Casanova Borca³, G. Cattari⁴, F. Civardi⁵, C. Cozzarini¹, C. Degli Esposti⁶, C. Fiorino¹, P. Franco⁷, G. Girelli³, A. Maggio⁴, A. Muraglia², M. Palombarini⁶, A. Pierelli⁸, E. Pignoli⁵, T. Rancati⁵, R. Valdagni⁵, V. Vavassori⁸, S. Villa⁵, M. Zeverino⁷

¹Fondazione Ospedale San Raffaele, Milan

²Arcispedale S. M. Nuova, Reggio Emilia

³Ospedale ASL9, Ivrea

⁴IRCCS-Candiolo, Candiolo

⁵Fondazione IRCCS Istituto Nazionale dei Tumori

⁶Ospedale Bellaria, Bologna

⁷Ospedale Regionale U. Parini-AUSL Valle d'Aosta, Aosta

⁸Cliniche Gavazzeni Humanitas, Bergamo

Purpose: DUE-01 is a multi-centric observational study aimed at developing predictive models of genito-urinary (GU) toxicity and erectile dysfunction for prostate cancer patients treated with conventional (1.8-2Gy/fr, CONV) or moderate hypofractionation (2.5-2.7Gy/fr, HYPO). Current analysis focused on modelling the relationship between the risk of IPSS₁₅≥15 (IPSS15end) at the end of radiotherapy and clinical/dosimetric risk factors.

Material and methods: Planning data and relevant clinical factors were prospectively collected, including DVH/DSH referred to the whole treatment and to the weekly delivered dose (DVHw/DSHw). Best discriminating DVH/DSH parameters were selected by the differences between patients with/without IPSS15end=1 (t-test).

Bootstrap variable selection techniques (300 resamples) in the framework of logistic backward feature selection was used to improve model building (see El Naqa, IJROBP 2006). Graphical and quantitative analyses of the variable selection

process applied to bootstrap data replicates was used to avoid underfitting/overfitting and to assess the final multi-variable model.

Results: Data of 247 patients were available (CONV:116, HYPO:131). 71/247 (28.7%) reported IPSS_{15end}=1.

The most predictive dosimetric tools (as assessed through t-test) were the absolute weekly delivered dose (DSHw and DVHw). DSHw and DVHw were alternatively inserted in the bootstrap variable selection flow, together with clinical risk factors.

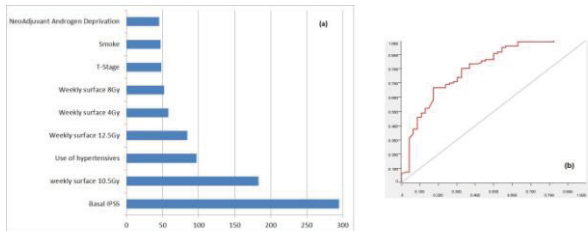
Due to the number of events, a logistic model containing 6 variables was accepted. The panel (a) of the figure displays the frequency of appearance of variables in the top 6 explanatory factors (with a cut-off on variable appearing at least 1/10 of times).

On the basis of observed frequency a model including basal IPSS (median OR=1.22, median p=0.00001), use of antihypertensives (median OR=2.7, median p=0.01), absolute bladder surface receiving more than 10.5 Gy/week (s10.5w, median OR=1.16, median p=0.0001), and absolute bladder surface receiving more than 12.5 Gy/week (s12.5w, median OR=1.07, median p=0.005), was chosen. AUC of this model was 0.80 (panel (b) of the figure).

Similar results were obtained when using weekly absolute DVH instead of DSH.

Conclusions: Basal IPSS, use of hypertensive drugs, s10.5w/v10.5w and s12.5w/v12.5w are the main predictors of IPSS_{15end}>=1 at the end of radiotherapy.

Bootstrap variable selection technique gives the modeler more insight into the importance and stability of the different variables selected and allows development of more robust models.



Keywords: Prostate cancer, acute GU toxicity, clinical/dosimetric predictors

42

Usage of long axial crystals for PET applications: the AX-PET demonstrator and beyond

C. Casella¹, M. Heller², O. Holme¹, C. Joram¹

¹ETH Zurich - Institute for particle physics

²CERN

The usage of long and axially-oriented scintillator crystals for PET scanners has been shown by the AX-PET experiment to be a viable solution towards a parallax free PET system, where spatial resolution and sensitivity could be both optimized at the same time. The recent advent of digital SiPM (dSiPM) from Philips, with their compactness and high level of integration, combined with the excellent timing performance, opened interesting possibilities for future PET detectors and motivated the study of small scale prototypes modules of long, axially-oriented crystals coupled to dSiPM.

The AX-PET is a fully operational PET demonstrator, based on axially arranged matrices of LYSO crystals (3x3x100 mm³ each) and wavelength shifting strips. Two modules have been constructed and used in coincidence in a dedicated gantry system. After extensive characterization measurements, the AX-PET demonstrator has been used for the reconstruction of images of several phantoms and a few small animals (one mouse and two rats), filled and injected with F-18 based solutions.

Small scale PET prototypes, readout by dSiPM, but otherwise based on the same geometry and detector elements as in the AX-PET, have been tested. The performance of these “digital axial modules” have been compared with the ones achieved by the AX-PET. In addition, coincidence timing performance have been assessed, both with single- and dual-sided readout of the crystals with dSiPM. In parallel, possibilities to reconstruct the axial coordinate from the dual-sided readout of long crystals, using light sharing techniques combined with a mechanical etching on the crystals surface, have been explored.

The AX-PET detector showed competitive performance in terms of energy ($\Delta E/E$ - 12% FWHM at 511 keV) and spatial (R < 2 mm FWHM in all three dimensions) resolutions. Combined with a dedicated software, it allowed the reconstruction of high quality images of small rodents, see Figure 1.

The same detector performance already achieved by the AX-PET has been reproduced by small scale setups with dSiPM readout. Excellent coincidence timing resolution of ~ 210ps have been achieved from dSiPM dual-sided readout of 100 mm long LYSO bare crystals. Spatial resolution of the order of 3-4 mm FWHM, constant all along the length of the crystal, are obtained, with crystals with etched surfaces (5 mm pitch, staggered in the four faces) and ESR wrapping.

The present paper proposes a review of the AX-PET working principle and its main results, including the recent image reconstruction of small animals. The studies on 100 mm long LYSO crystals readout on both sides by dSiPM, will also be presented, focusing both on the achieved timing performance (non-etched, bare crystals) and axial spatial resolution (etched and wrapped crystals).



Figure 1 : AX-PET reconstructed rendered image of a young rat injected with F-18

Keywords: (up to 3 excluding session name): PET, axial crystals, digital SiPM

43

Detection of ionizing radiation by intrinsic optical fiber sensors: preliminary results

L. Cella¹, S. Avino², V. D'Avino¹, P. De Natale², G. Gagliardi², A. Giorgini², R. Liuzzi¹, R. Pacelli³

¹Istituto di Biostrutture e Bioimmagini, Consiglio Nazionale delle Ricerche, Napoli, Italy

²Istituto Nazionale di Ottica, Consiglio Nazionale delle Ricerche, Italy

³Dipartimento di Scienze Biomediche Avanzate, Università di Napoli Federico II, Italy

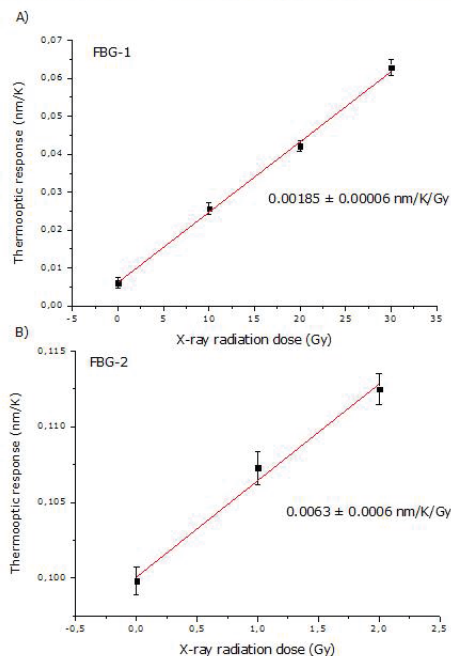
Purpose: Recent technological advances in radiation delivery techniques, such as particle therapy and IMRT, have reinforced the demand for novel dosimeter technology. Purpose of our study is to develop a totally passive miniature radiation sensor based on optical fiber resonant cavity with potential applications in radiation therapy and in radiobiology studies.

Materials and Methods: We employed totally passive $\text{Ge}_{6\%}^{\text{mol}}$ -doped optical fiber sensors based on special Bragg-grating (FBG) cavity reflectors. The FBGs were irradiated at different doses by a 6MV linac photon beam and then interrogated by a high resolution interferometric technique. The detection principle consists in measuring the wavelength shift of the modes of the fiber cavity when irradiated. Radio-induced wavelength shift measurements were performed with the fiber kept under temperature controlled conditions in an insulated chamber. Interaction mechanisms of radiation within the sensor material were studied. The mass attenuation coefficients (μ_m) and the effective atomic number (Z_{eff}) of the sensors were calculated using WinXCOM in function of the photon energy in the range 1-6 MeV.

Results: The effective interaction volume of the sensor is $6 \times 10^{-4} \text{ mm}^3$. The weighted average μ_m and the Z_{eff} resulted to be $0.044 \text{ cm}^2/\text{g}$ and 10.04 , respectively. A first sensor (FBG-1) was irradiated, with 10-Gy increments, up to 30 Gy. A second sensor with a higher envelope reflectivity (FBG-2) was irradiated at smaller doses of 1 and 2 Gy. A net wavelength shift was measured after each irradiation. We experimentally observe an additional phenomenon: a radio-induced change of the fiber thermo-optic response that is measured by tuning the resonant mode wavelengths with temperature. Figures A-B show the linear trend of the radiation-induced thermo-optic response change vs the dose, with a coefficient of $0.00185 \pm 0.00006 \text{ nm/K/Gy}$ for FBG-1 and of $0.0063 \pm 0.0006 \text{ nm/K/Gy}$ for FBG-2. Dividing the dose response coefficient by the average value of the uncertainty on the single measurement of the thermo-optic response (1 pm/K) we obtain a final resolution of 160 mGy (FBG-2).

Conclusions: We demonstrated radiation detection by means of a totally-passive, nearly tissue equivalent, miniaturized sensor based on an optical fiber resonator. The effect of the radiation delivered to the sensor was twofold: a change of the refractive index and a change of the thermo-optic response of the intra-cavity fiber. Further investigations are warranted.

Thermo-optic responses as a function of the radiation dose for FBG-1(A) and FBG-2 (B)



Keywords: dosimeter, optical fiber sensor, laser

44

Simulation of Hadrontherapy In-beam monitoring at CNAO with the INSIDE detector

P. Cerello¹, G. Battistoni², N. Belcarì^{3,4}, M.G. Bisogni^{3,4}, N. Camarlinghi⁴, F. Cicirello^{5,6}, G.A.P. Cirrone⁷, S. Coli¹, F. Corsi^{5,6}, G. Cuttone⁷, E. De Lucia⁸, A. Del Guerra^{3,4}, P. Delogu^{3,4}, R. Faccini^{9,10}, S. Ferretti^{3,4}, E. Fiorina^{1,11}, G. Giraudo¹, A. Kraan^{3,4}, F. Licciulli^{5,6}, B. Liu^{3,4}, N. Marino⁴, C. Marzocca^{5,6}, G. Mataresse^{5,6}, C. Morone^{12,13}, M. Morrocchi^{3,4}, S. Muraro², R. Nicoloni², F. Pennazio¹, C. Peroni^{1,11}, L. Piersanti^{9,10}, M.A. Piliero^{3,4}, G. Pirrone^{3,4}, A. Rivetti¹, F. Romano⁷, V. Rosso^{3,4}, P. Sala², A. Sarti⁸, A. Sciubba^{9,10}, G. Sportelli^{3,4}, R. Wheadon¹

¹INFN Torino, Italy

²INFN Milano, Italy

³University of Pisa, Italy

⁴INFN Pisa, Italy

⁵Politecnico Bari, Italy

⁶INFN Bari, Italy

⁷INFN LNS

⁸INFN LNF

⁹University Roma La Sapienza, Italy

¹⁰INFN Roma La Sapienza, Italy

¹¹University of Torino, Italy

¹²University Roma Tor Vergata, Italy

¹³INFN Roma Tor Vergata, Italy

Hadrontherapy's remarkable precision could be impaired if the hadrons range varies from the planned one, due for example to temporary modifications of the organ or tumour. Thus, a method to control to 1 mm the particle range during treatment is required.

The INSIDE (INnovative Solutions for Dosimetry in hadrontherapy) project is starting the construction of a PET segment and a fiber tracker to be installed at CNAO, so as to acquire in-beam data and evaluate the actual dose distribution (PET) and the primary vertex position (tracker) in real-time.

The PET detector consists of two symmetric planar heads, each one formed by 8 blocks ($\sim 5 \times 5 \text{ cm}^2$) of 16×16 elements of LSO scintillator read out with Hamamatsu MPPC. The prototype electronics will be based on the TOFPET ASIC developed by the Endo-TOFPET collaboration.

The tracker consists of 6 layers of thin plastic scintillator, each made of two orthogonal planes of $0.5 \times 0.5 \text{ mm}^2$ optical fibres, and a position sensitive calorimeter for the measurement of the proton energy, made of 4×4 LYSO pixelated crystal arrays ($5 \times 5 \times 2 \text{ cm}^3$) read out by MultiAnode PMT.

The software simulation, performed with state-of-the-art tools like FLUKA and GEANT4, was a key factor in optimizing the detector design and predicting its performance. Data analysis will be based on correlation studies of tracker and PET data, so as to further improve the precision.

The FLUKA beam simulation was validated with experimental data acquired at CNAO. The secondary particles are tracked to the detectors and provide interaction points that are processed to simulate its response. With the inclusion of noise and dark counts, a reliable simulation of the actual rates is obtained and a set of information equivalent to the output of a DAQ system is generated and forwarded to the event reconstruction module.

The expected data rate (fig. 1), based on the actual and foreseen CNAO beam parameters, was used to optimize the detector position and the overall layout, including the selection of the front-end electronics and the DAQ design.

The simulation results of a proton pencil beam ($5 \cdot 10^9$ pps) forecasts an average particle rate of 3.5 kHz for each PET detector channel, while the optimal time window for reconstruction is in the 1-5 ns range. After a 5 minutes treatment with the CNAO facility duty cycle a total number

of 10^7 coincidences is expected, indicating the feasibility of PET imaging.

The detailed simulation of the tracking layers and the LYSO crystal calorimeter includes the geometry and materials of the mechanical structure. The energy release inside active detectors, as well as the optical photons impinging on the active photodetector is recorded and stored for further analysis.

Monte Carlo simulations validated on real data suggest the feasibility of in-beam monitoring both for the PET and the tracker subsystem.

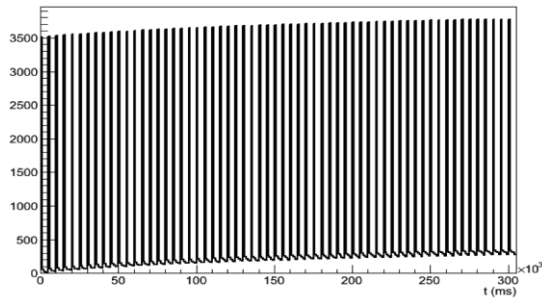


Figure 1. An example of the simulated trigger rate on PET SiPM channels for the CNAO beam. Peaks and valleys correspond to the spill delivery and asynchronous decays of B^+ emitters followed by e^+e^- annihilations, respectively.

Keywords: hadron therapy, in-beam PET, silicon photomultiplier (SiPM)

45

The ELIMED (Multidisciplinary and Medical applications at the ELI-Beams) network perspectives for laser driven beam applications

G.A.P. Cirrone¹, M. Borghesi², M. Carpinelli³, G. Cuttone¹, D. Doria², G. Korn⁴, T. Licciardello¹, M. Maggiore⁵, L. Manti⁶, D. Margarone⁴, P. Pisciotta¹, I. Petrovic⁷, F. Romano¹, A. Ristic Fira⁷, F. Schillaci^{1,4}, V. Scuderi^{1,4}, C. Stancampiano¹, A. Tramontana¹

¹INFN-LNS, Catania, Italy

²Centre for Plasma Physics School of Mathematics and Physics The Queen's University of Belfast, Belfast BT7 1NN

³INFN Sezione di Cagliari, c/o Dipartimento di Fisica, Università di Cagliari, Cagliari, Italy

⁴Institute of Physics of the ASCR, ELI-Beamlines project, Na Slovance 2, Prague, Czech Republic

⁵Istituto Nazionale di Fisica Nucleare, Laboratori Nazionali di Legnaro, Viale dell'Università 2, Legnaro (Pd), Italy

⁶INFN Sezione di Napoli, c/o Physics Department, University of Napoli, Napoli, Italy

⁷University of Belgrade, Vinca Institute of Nuclear Sciences, Mihajla Petrovica 12-14, Belgrade, Serbia

Nowadays, laser-driven proton beams generated by the interaction of high power laser with solid targets represent a fascinating attractive in the field of the new acceleration techniques. In the last decades a great effort, both from theoretical and experimental point of view, has been devoted to charged particle acceleration using high power lasers. Several acceleration regimes have been investigated so far in literature aiming to overcome the experimental limits achieved up to now and to generate proton beams characterized not only by very high intensity and high energy but also by small energy and angular spread [1-7]. Moreover, in order to characterize in terms of focusing, transmission and energy selection the laser-generated ion beams and to make them suitable for multidisciplinary applications, investigating also the possibility of using laser-driven proton

beams in the clinical field, an adequate beam transport line must be developed and tested.

In the framework of the ELIMED project [8], we started to design and realize a first prototype of a beam transport line (BTL) that will allow to deliver laser-accelerated proton beams with optimized properties and sufficient repetition rates in order to perform first dosimetric and radiobiological irradiations with such kind of beams [9-10]. In particular, we have already developed a first prototype of a key element of the beam transport system, i.e. an Energy Selector System (ESS), based on permanent dipoles, capable to control and select in energy laser-accelerated proton beams. Monte Carlo simulations and some preliminary experimental tests have been already performed to characterize the device. A calibration of the ESS system with a conventional proton beam has been performed in September at the LNS in Catania. A first experimental test run with our ESS prototype using a laser-driven ion beam will be performed at the Queen's University in Belfast with the TARANIS laser-driven proton beam [11] starting from November 2013.

In this contribution a description of different solutions studied for the BTL development depending on transmission efficiency and on energy spread and preliminary results regarding the experiment with the ESS performed at the TARANIS facility together with the Monte Carlo simulations performed on the ESS will be discussed.

Keywords: Laser-driven beams, beam handling, medical applications

46

A critical challenge for 21st century radiation oncology: reaching the underserved in Low-Middle Income Countries

C.N. Coleman¹, M. Daphtary¹, B. Vikram¹,
¹Radiation Research Program, Division of Cancer Treatment and Diagnosis, National Cancer Institute, USA Richard R. Love, MD²,

²Int'l Breast Cancer Research Foundation, Madison, WI, USA

Globally, cancer is a growing and progressively urgent problem. The World Health Organization projects that Low- and Lower-middle income countries (LMICs) will have 50% of the global cancer in 2015 rising to 70% by 2030. The importance of addressing the rising cancer incidence was highlighted in by the United Nations Declaration on non-communicable diseases (NCDs) in 2011. The larger problems in which cancer exists are daunting including healthcare systems that are disorganized, dysfunctional and underfunded; human right issues including poverty and discrimination; and governance issues including corruption and misspent funds. The term "public health oncology" (Ann Oncol 2:3040, 2012) has been proposed to help recognize that cancer is both a key problem and also manifestation of larger societal problems.

Data bases such as GLOBOCAN 2012 (<http://globocan.iarc.fr>) and IAEA-DIRAC (<http://www-naweb.iaea.org/nahu/dirac/map.asp>) can help determine shortfalls and the UICC is presently conducting an in-depth study as to what is needed to close the gap, which is known to be quite substantial. While metrics are critical for assessing the efficacy of an intervention, what are needed are action steps to begin to address the shortfalls. A number of well-intended efforts exist by agencies such as IAEA with its PACT, VUCCnet and imPACT programs (<http://www.iaea.org/>) as well as efforts by individual institutions and professional societies for educational and twinning programs; however, these are often intermittent efforts due largely to shortage of personnel and time.

A systemic solution including increased collaboration among countries and disciplines and increase in local initiatives is proposed. This would involve multinational partnerships, public-private investment and collaboration with research

institutes for implementation science, development of “bottom-up” local champions, and translational and clinical research. New business models are needed so that the poor can access treatment. Given the central and cost-effective role of radiation oncology and the ability to use telemedicine and other technological advances to enhance outreach, our discipline has the potential to be world leaders in this effort. Qualified people are limited in number in both the LMIC and also in the resource-rich settings because this type of effort is not often valued as a *bona fide* part of an academic career. Therefore, among the potential solutions, a proposed solution to be presented, the International Cancer Expert Corps (ICEC) (www.iceccancer.org) could help bring together international resources and efforts built on radiation oncology to address one of the most critical challenges of the 21st century- healthcare disparities and the rising burden of cancer in LMICs.

Keywords: cancer disparities; international; global cancer

47 Nanodosimetric descriptors of the therapeutic quality of light-ions:

new experimental measurements

V. Conte, P. Colautti, B. Grosswendt
LNL-INFN Legnaro, Italy

The biological effectiveness of ionizing particles is clearly related to their track-structure properties on a nanometric scale. It was therefore the aim of this work to develop a method and a detector which allow to measure directly the track structure properties of light ions of therapeutic interest.

The track-nanodosimeter installed at the TANDEM-ALPI accelerator complex of LNL (Legnaro National Laboratories) counts the number of ionizations produced inside a small gas volume by ionizing particles directly crossing it, or passing nearby at given impact parameter. From the point of view of ionizing interactions, the gas volume simulates a cylindrical water target volume of nanometric dimensions (for a detailed description see V. Conte et al., *Track structure of light ions: experiments and simulations*. New J. Phys. 14, 093010, 2012).

Considering the great interest for light ions in radiotherapy, the study of particle track structure properties was concentrated on protons, Li-ions and C-ions. Ionization cluster-size distributions were measured and simulated by a dedicated Monte Carlo simulation code. Some descriptors of the track structure can be derived from these distributions. They describe particular aspects of the track structure of ionizing particles and hence also of radiation quality.

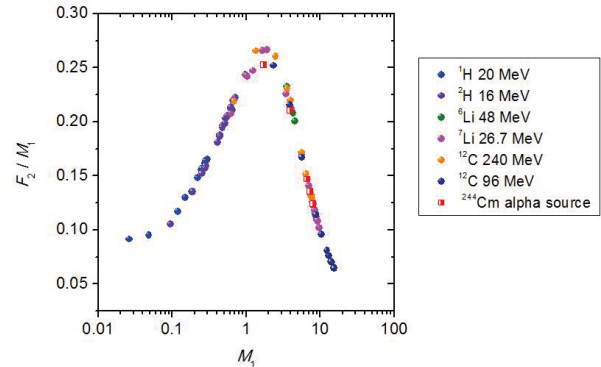
The measured mean cluster-size M_1 is one of the characteristic parameters of track structure and is proportional to the mean number of ionizing processes D/λ_{ion} of the primary particles along the travelling length D (λ_{ion} is the mean free ionization path length).

We also found out that the sum distributions F_k of measuring cluster sizes $v \geq k$ form almost perfect universal curves if plotted versus M_1 , independent of charge state and velocity of the particles.

The distributions F_k behave, as a function of M_1 , similarly to the radiobiological cross sections as a function of *Linear Energy Transfer (LET)*, first increasing with increasing values of M_1 and then showing a saturation effect. As a consequence of this saturation, the ratio F_k/M_1 plotted as a function of M_1 mimics the trend of the *Relative Biological Effectiveness (RBE)* as a function of *LET*.

In the following figure the ratio F_2/M_1 is plotted as a function of M_1 . Here, F_2/M_1 represents the sum probability of measuring at least two ionizations inside the target volume, scaled to M_1 . The probability F_2 of initiating two or more

ionizations is intuitively related to the probability of inducing a double strand break (DSB) in the DNA.



The ratio F_2/M_1 versus M_1 due to different particle type and energy forms an almost perfect universal curve and behaves like the \square -parameter of dose-effect curves as a function of *LET*. The maximum is reached for a mean cluster size M_1 approximately equal to 2.

In consequence, the ratio F_2/M_1 (or ratios F_k/M_1 of higher order to describe radiobiological end-points other than DSBs), is well suited to define the physical quality of radiation.

Keywords: Radiation-Quality, Track-structure-measurements, Nanodosimetry

48 From Radiotherapy Dose Monitoring to Low-Dose Morphologic Imaging with Scanned Megavoltage X-rays

P. Crespo^{1,2}, I. Bravo³, M. Capela⁴, A. Cavaco⁵, R. Ferreira Marques^{1,2}, P. Fonte^{1,6}, M.C. Lopes⁴, H. Pereira³, P.J.B.M. Rachinhas⁵, J. Santos³, P. Soares⁵, J. Silva³, H. Simões¹, P.C.P.S. Simões⁵

¹LIP, Coimbra, Portugal

²University of Coimbra, Portugal

³Oncology Institute of Porto, Portugal

⁴Oncology Institute of Coimbra, Portugal

⁵Coimbra University Hospitals, Portugal

⁶Polytechnic of Coimbra, Portugal

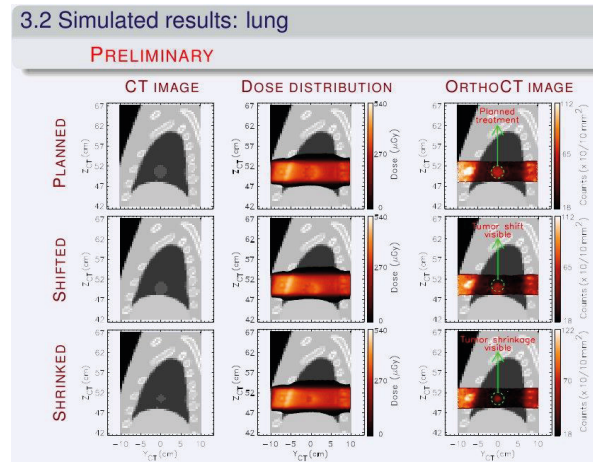
Purpose: To investigate whether orthogonal ray imaging, a new technique that consists in detecting radiation dispersed in the patient and emitted at right angles in respect to the beam axis, is capable of assisting external photon beam radiotherapy by providing images correlated with the effective dose distribution, and by enabling in parallel low-dose morphologic imaging, mainly on-board tumor/patient imaging.

Materials and methods: Monte Carlo simulations were carried out with the anthropomorphic phantom NCAT adapted to Geant4, together with experimental proof-of-principle measurements collected with a heterogeneous phantom made of acrylic/air and irradiated with a 6-MV clinical linac. The Monte Carlo simulations comprise an intensity modulated radiation therapy-like treatment in the region of the pituitary gland, together with the irradiation of a tumor with a diameter of 30 mm located in the lung. The lung tumor irradiation was considered in three possible scenarios: normal treatment, tumor shift of 9.36 mm to caudal, and a tumor diameter shrinkage of 9.36 mm.

Results: The simulated results show that, despite the subtherapeutic, very-low dose simulated (ca 1 mGy), a good visual agreement between the planned dose distribution and the orthogonal ray simulated images is obtained. It is also shown that the filling of the nasal cavity of the patient may account for a dose reduction of up to 10 %, which may be detected with an orthogonal ray imaging system. In the case

of the irradiation of the lung, images allow a tumor shrinkage or dislocation of 9.36 mm to be clearly discernible. The experimental results show that scanned pulse height spectra acquired with a collimated detector allowed for a profile correlation of 0.9911 to be obtained between the measured data and the dose simulated inside the acrylic/air heterogeneous phantom. In addition, a 2-mm phantom displacement was clearly distinguishable by simulation and experiment.

Conclusions: Orthogonal ray imaging is a new imaging concept for assisting external photon beam radiotherapy that shows a good potential for image-guided radiotherapy, adaptive radiotherapy, and low-dose on-board patient imaging.



Keywords: Image-Guided Radiotherapy, Adaptive Radiotherapy

49

Fast pencil beam dose calculation for hadron therapy on GPU

J. da Silva, R. Ansgore, R. Jena
University of Cambridge

Intensity-modulated radiotherapy using charged particles can achieve better dose conformity and more sparing of healthy tissue than other modalities. However, to benefit from this, adaptive radiotherapy (ART) is necessary to handle organ motion, anatomical changes and variations in patient set-up. A crucial component of ART is fast recalculation of dose. As of a few years, one can no longer rely on ever increasing single-core computation power to provide perpetual speedup of serial algorithms. To achieve the dose calculation times necessary for true ART it is therefore essential that the dose calculation can be efficiently parallelised to run on many-core systems, e.g. graphics processing units (GPUs), which continue to show exponential growth in computational power.

We present a pencil beam dose calculation engine for charged particles implemented in CUDA to run entirely on a GPU. The calculation performed is equivalent to commercial treatment planning systems, and include a ray tracer that calculates cumulative water-equivalent path-length and deposits dose, and a convolution/superposition step which accounts for lateral scatter. However, each function has been parallelised so that its performance scales with increasing core number and is optimized through use of fast hardware-implemented functionality, efficient memory operations, and minimising memory copies.

The total computation time for a proton plan consisting of 20 energy layers covering a $10 \times 10 \times 10$ cm³ target 10 cm deep in water using a dose grid of $1 \times 1 \times 1$ mm³ was 1.38 s on a Nvidia Quadro 1000M GPU. The only similar study found in the

literature (R. Fujimoto et al., Phys. Med. Biol. 2011) performs only the computationally heavy superposition step on a five times faster GPU, with a calculation time of 0.41 s for the deepest energy layer alone. In the case of a constant convolution kernel, an approximation that has been used when calculating physical dose from carbon ions, the calculation time for the implementation presented was further reduced to 0.42 s. The calculation engine is in the process of verification against a commercial system for clinically relevant cases, but since it employs equivalent calculation routines a very good agreement is expected.

To the best of our knowledge we present the first complete pencil beam dose calculation engine for charged particles to run on a GPU. In terms of calculation time it outperforms the partial GPU implementation found in the literature, which in turn is significantly faster than the corresponding CPU implementation. Since all steps were successfully parallelised we conclude that although the calculation time might still be too long for real-time ART, we can anticipate continued exponential increase in calculation speed with the development of new many-core devices, making the prospects for real-time dose calculation very good.

Keywords: GPU dose calculation

Acknowledgment: This work was funded by ENTERTVISION, EC FP7 grant 264552.

50

Radiograaff: a medium energy proton irradiation platform for radiobiological studies. Presentation and first results

D. Dauvergne¹, J. Constanzo¹, M. Fallavier¹, G. Alphonse^{2,3}, P. Battiston-Montagne², C. Bernard¹, C. Rodriguez-Lafrasse^{2,3}, M. Beuve¹

¹Université de Lyon; Université Lyon 1; CNRS/IN2P3, Institut de Physique Nucléaire de Lyon, F-69622 Villeurbanne, France.

²Université de Lyon; Université Lyon 1; Faculté de Médecine Lyon-Sud, LRCM, F-69921 Oullins, France.

³Hospices-Civils-de-Lyon, CHLS, F-69495 Pierre-Bénite, France

Radiograaff is a horizontal beam facility for radiobiological experiments with medium-energy protons which has been setup at the 4MV Van de Graaff accelerator of the Institut de Physique Nucléaire de Lyon. At this energy, the Relative Biological Effectiveness (in terms of α/α_X ratio) of protons may amount to 2-6 [1] and RBE at 10% of cell inactivation was reported for V79 cell line to range between 1 and 1.6 [2]. Thus, this platform constitutes a tool to study the specific effects of high Linear Energy Transfer (LET) radiations to cells. For such macroscopic-irradiation facilities, the dose distribution over the cell samples has to be uniform with accuracy better than $\pm 5\%$ with a controlled dose rate (2 Gy/min for clinical interest). In addition, the variation of the LET between the entrance and the exit of the cells does not exceed 10%.

A homogeneous irradiation field with a suitable proton flux is obtained by means of two collimators (various sizes) and two Au-scattering foils arrangements set 62 cm apart from each other. The last arrangement is set 120 cm upstream from the irradiation area. A monitoring chamber contains a movable Faraday cup, a movable quartz beam viewer for controlling the intensity and the position of the initial incident beam, four scintillating fibers for beam monitoring during the irradiation of the cell samples, and is ended by a thin aluminized mylar window (12 μ m thick) for the beam extraction in air. The set-up was simulated by the GATE v6.1 Monte-Carlo platform.

Proton energy measurement, fluence-homogeneity evaluation and monitoring system calibration were tested with 3.5 MeV protons using a silicon PIPS detector, placed in air in the

same position as the biological samples to be irradiated. With the double scattering system, a fluence heterogeneity of $\pm 2\%$ over a circular field of 20 mm diameter was obtained. A preliminary biological experiment was performed to test protocols with two Human Head and Neck Squamous cell lines carcinoma with quite different radiosensitivities.

In order to study the RBE of medium-energy protons, we used two methods. First, the survival of the two HNSCC lines (different radiosensitivities) irradiated with 2.9 MeV protons, corresponding to a LET of 12.5 keV/ μm evaluated at the entrance of the cells (with less than 10% variation throughout the cell thickness), have been studied in the dose range 1-5 Gy at a 2 Gy/min dose rate. As reference, the survival curve obtained with 250 kV X-rays was used. The measured RBE has been found between 1.3 and 1.4. Then, DNA Double Strand Break (DSB) induction and repair were measured by scoring the γ -H2AX foci. Results will be presented and discussed.

References:

- [1] M. Belli et al., Int. J. Radiat. Biol., 74(4), (1998) 501-509.
- [2] H. Paganetti and T. Bortfeld, Int. J. Radiat. Oncol. Biol. Phys. 53 (2002) 407-421.

51

Carbon Ion Therapy: Actual and Future Strategies at HIT
 J. Debus, K. Herfarth
 Dept. of Radiation Oncology, University of Heidelberg,
 Germany

The primary goal of the Heidelberg Ion Treatment center (HIT) is to assess the role of ion irradiation (primarily carbon ions and protons) in cancer treatment. Clinical trials have been established to broaden the evidence for the use of particle therapy and for looking in differences in the use of different particles. This article focuses on the trials that have been started at HIT. Starting with tumors without movement, newer trials also deal with more movement of the target and the surrounding tissue. Future trials will also include a motion management.

Introduction: Heidelberg University treated the first patient with carbon ions in Germany in 1997. In these days, treatments with carbon ions were performed at the German society of heavy ions (GSI) in Darmstadt. There were 3 treatment slots counting 20 days each available for patient treatment each year. 440 patients had been treated at this facility between 1997 and 2008. Most of those patients had chordomas and chondrosarcomas of the skull base or adenoid cystic cancers of the salivary glands in clinical trials. The results of these trials had been published [1, 2] and results the long term outcome will be presented in the near future. Among other arguments, the experience at the GSI initiated the development of the Heidelberg Ion Treatment facility HIT, the first real clinical heavy ion institution. The foundation stone was set in November 2003 and the first patient was treated 6 years later in November 2009. Over 1700 patients have been treated at HIT using carbon ions or protons. Many of those patients were included in clinical trials to proof and to confirm the value of heavy ion radiation therapy in the treatment of cancer. The article will focus on the actual trials at HIT and the future directions.

Methods and Materials: Fifteen clinical trials had been started at HIT since the first patient was treated on November 14, 2009. The trials will be described and future directions will be pointed out in the discussion section.

Results: One of the first initiated trials at HIT were the trials about chordomas and chondrosarcomas of the skull base. Very promising results could have been achieved during our treatment time at the GSI which seemed to be at least equally to the actual standard treatment using protons. Based on those experiences and the possibility to treat patients either with protons or carbon ions at HIT, two randomized phase III trials were established at HIT.

Discussion: After patient start in November 2009, a number of trials were initiated to assess the role of carbon ions and or protons in the treatment of a variety of cancers. The NIRS data set a founding stone in the design of new trials. Many of our trials want to confirm the NIRS data also using raster scanning technique and a more dense fraction schedule. However, other trials also look into the possible different effect of the RBE of protons and carbon ions. Many of the trials will take years for final conclusions, others will collect basic data for the development of larger phase III trials like those for skull base chondrosarcomas and chordomas.

Future trials at HIT will include more and more moving targets. Shortly, the INKA trial for neoadjuvant radiotherapy using raster scanned carbon ions in patients with locally advanced sulcus superior tumors will be initiated. The role of ion radiotherapy in the treatment of pancreatic cancer will also be assessed in trials as the use of carbon ions for inoperable esophageal cancer.

Conclusion: HIT wants to continue the work that NIRS has started: To bring ion radiotherapy of different cancer types to a evidence based level for the benefit of our patients.

References:

- [1] Schulz-Ertner D, Karger CP, Feuerhake A, Nikoghosyan A, Combs SE, Jakel O, Edler L, Scholz M, Debus J: Effectiveness of carbon ion radiotherapy in the treatment of skull-base chordomas. *International journal of radiation oncology, biology, physics* 2007, 68(2):449-457.
- [2] Schulz-Ertner D, Nikoghosyan A, Hof H, Diding B, Combs SE, Jakel O, Karger CP, Edler L, Debus J: Carbon ion radiotherapy of skull base chondrosarcomas. *International journal of radiation oncology, biology, physics* 2007, 67(1):171-177.

52

Assessment and improvements of Geant4 models in the context of prompt-gamma hadrontherapy monitoring

G. Dedes¹, M. Pinto², D. Dauvergne², N. Freud³, J. Krimmer², J. Michel Létang³, C. Ray², E. Testa²

¹LMU, Munich, Germany

²IPNL

³INSA

Purpose: The utilization of protons and carbon ions for radiotherapy purposes provides high conformity and increased biological effectiveness. In order to fully benefit from the advantages, a precise beam range monitoring in real time is vital. The detection of prompt gammas with a collimated scintillating detector makes it possible to locate the Bragg peak position during proton or carbon ion irradiation.

Accurate Monte Carlo simulations are essential both for the further development of an optimized detection array and for the accurate estimation of the applicability of the system in clinical conditions. Purpose of the current work is to assess and improve the performance of the Geant4 toolkit in the description of currently available prompt-gamma data.

Materials/methods: Our Monte Carlo studies have been performed with the GEANT4 9.4 toolkit and validated with experimental data obtained with ¹²C of 80 MeV/u, 95 MeV/u, 310 MeV/u and with 160 MeV protons. We focus on the hadronic models describing nuclear collisions between projectile and target nuclei and the subsequent fragmentation processes. Those models are mainly responsible for the production of secondary particles related to the beam path, such as protons, neutrons, light nuclei, positron emitting nuclei and of course prompt photons.

We studied the applicability of different available models in our hadrontherapy monitoring experiments, in order to define the most suitable set of models to be used. Furthermore, we investigated improvements to the QMD model.

The results of model improvements are reported in a twofold way: Compared with nuclear properties, and thoroughly validated with experimental defined observables such as secondary particle emission yields.

Results: GEANT4 simulations using internal theoretical models overestimate prompt-gamma emission yields by a factor of about 100% to 200%, over an energy range from 80 MeV/u to 310 MeV/u for the case of ^{12}C , and to a lesser extent for 160 MeV protons.

By optimizing the values of the free parameters of QMD and especially of the nucleon Gaussian wave-packet width, an improved description of the available experimental data is achieved: Nuclear binding energies are calculated more accurately, minor improvements are obtained in the nuclear densities, while we maintain a comparable accuracy in charged particle emission rates prediction.

Finally, when using the proposed improvements, Monte Carlo calculations agree with prompt-gamma measurements within a range of 5% to 70%.

Conclusions: In the presented study, we have investigated the performance of some of the most widely used internal nuclear models of Geant4 in the field of hadrontherapy.

A considerable improvement of the description of prompt-gamma data has been achieved with the proposed QMD parameter modifications. At the same time, the proposed changes were justified by comparisons with nuclear properties and fragmentation experimental data.

Keywords: Prompt-gamma, nuclear models, Geant4

53

Proton Radiation Therapy: Current Status of Clinical Trials

T.F. DeLaney

Massachusetts General Hospital, Boston, MA

Purpose/Objective: Because of the absence of exit dose beyond the Bragg peak, protons can improve the radiotherapy physical dose distribution. This offers the potential for dose escalation to improve local control in anatomic sites and histologies where local control of tumor is suboptimal with photons. At the same time, the reduction in the normal tissue dose/volume profile is anticipated to reduce acute and late normal tissue toxicity. The competing technologies include intensity modulated photon radiation therapy (IMRT) as well as heavier charged particles. Because protons and IMRT are both low-LET radiation, tumor control at any given dose level is anticipated to be similar, but protons are expected to have an improved therapeutic ratio because of lower normal tissue dose. Heavier charged particles may have a biologic advantage, but only if the RBE is higher in tumor or lower in normal tissue than protons or photons. An overview of clinical trial strategies designed to assess these technologies will be presented, as will comments about the impact of technology evolution/maturation over the course of a clinical trial.

Materials/Methods: Hospital and clinic-based proton facilities employing cyclotrons or synchrotrons have now been available for over a decade, with multiple new facilities being developed in recent years. These have the technical capabilities to treat all anatomic sites. There is a transition currently underway from passively scattered proton delivery to pencil beam scanning, allowing beam modulation for intensity modulated proton therapy (IMPT). This should allow comparable dose conformality in the high dose region between IMRT and IMPT; IMRT may be more conformal in the high dose region than 3-D passively scattered protons. The theoretical possibility for using spot scanning to modulate the LET distribution in the target and organs at risk has recently been explored. The cost for proton radiation is higher than photon radiation, primarily related to the upfront capital cost of the facility, driven by the higher cost of accelerating and steering protons compared to electrons (employed in

photon linear accelerators). A smaller number of heavier charged particle facilities, primarily using carbon ions, have been developed; cost for carbon facilities is higher than photons.

Results: Because of the potential for significant reduction in the volume of tissue radiated with protons compared to photons, there is general agreement that the focus of clinical trials in the pediatric population can only be phase II studies, designed to demonstrate a reduction in acute and late effects in normal tissue. Phase III studies, randomizing children between photons and protons are not ethically acceptable. Concern has been raised in the past about the possibility for deleterious late effects from secondary neutrons generated with passively scattered protons; clinical and radiobiologic data suggest, however, that protons will still result in fewer second malignancies than photons, and that further reductions will be anticipated with scanned proton beams. A pediatric proton registry has been established to help study efficacy and late effects in children treated with protons. In adult patients, if cost for protons and photons were identical and the technologies had equivalent clinical robustness, there would be little rationale for clinical trials comparing protons as photons. The current differential in cost, however, has generated considerable discussion about the need for comparative trials of protons and photons, as well as the most appropriate endpoints and clinical trial strategies. These have led to randomized trials of IMRT and 3D passively scattered protons in prostate and lung cancers. Several new phase II proton clinical trials are focusing on the use of IMPT, with ongoing discussion about future randomized studies of IMRT vs. IMPT. Additional issues to be discussed include the differences in image guidance at proton and photon facilities, the higher sensitivity of protons to changes in the tumor and normal tissue than photons which necessitates adaptive treatment strategies in some tumor sites, and the importance of robustness in proton treatment planning and delivery. Clinical trials to compare protons and carbon ions have now been initiated. The high local control rate with high dose, low LET radiation at many clinical sites raises the question of which clinical sites might benefit from heavier charged particles and how best to compare protons with heavier charged particles.

Conclusions: Proton radiation therapy offers a number of potential treatment advantages to patients over photons related primarily to differences in physical dose distribution; clinical gain can be assessed in clinical trials which are currently in progress. Rapid changes in technology must be considered in designing and conducting clinical trials in this area. The potential for exploiting higher RBE in tumor with heavier charged particles, currently primarily carbon, can also be evaluated in comparative clinical trials, comparing them with lower LET radiation.

54

Development of a Transparent Photon Detector for the Online Monitoring of IMRT Beams

R. Delorme¹, Y. Arnoud¹, B. Boyer¹, I. Fonteille¹, L. Gallin-Martel¹, M.L. Gallin-Martel¹, J.Y. Giraud², O. Guillaudin¹, A. Pelissier¹, O. Rosetto¹, L. Weber¹

¹LPSC, Université Joseph Fourier Grenoble 1, CNRS/IN2P3, Grenoble INP, France

²Centre Hospitalier Universitaire de Grenoble (CHUG), Inserm U836, équipe 6, France

External beam radiotherapy performance has been increased by the emergence of state-of-the-art techniques, such as Intensity-Modulated Radiation Therapy (IMRT) and rotational IMRT. They require consistent Quality Assurance (QA) programs. In the framework of the INSPIRA project, the DAME group¹, in collaboration with the Radiotherapy Department of CHUG², is developing an innovative Transparent Detector for Radiotherapy (TraDeRa). The detector aims at monitoring the

modulated beam ahead of the patient in real-time and without dead zone.

Current version of this detector is a 1:4 scale prototype (see Figure), partially instrumented and designed to test the electronics and acquisition chain. The fully instrumented 1:4 scale prototype (324 electrodes) will be operational for December. Basically, TraDeRa consists in a pixelated matrix of ionization chambers with a dot pitch of 3.3 mm in the central area. A specific integrated circuit has been designed by the LPSC microelectronics group allowing to extract the amplitude of each pulse and providing a real-time map of the signal at the pulse scale. The measurements under irradiation are made with a 6 MV X-Ray beam, from a Clinac 600 and a Clinac 2100 (Varian Medical System), at the CHUG. We use the Monte Carlo code PENELOPE for the dose calculations.

With the partially instrumented prototype, we showed that the detector was able to give accurate and stable information at the pulse scale and integrated during all the delivery, as a function of different parameter of irradiation. A 0.6 % attenuation of the beam was measured in the presence of TraDeRa. Furthermore, we validated the new microelectronic acquisition system that will be embedded on the fully instrumented prototype using the very high precision beams of the medical line ID17 of the European Synchrotron Radiation Facility (ESRF). We will show the latest measurements obtained with this new prototype and the results of a PENELOPE dosimetric study done to evaluate the influence of TraDeRa on the photon beam and the electrons produced.

The current version of TraDeRa already shows promising results for IMRT-QA and led to a number of patents being registered [1-2]. It is relatively transparent and should not hinder the irradiation while keeping the beam upstream of the patient under constant control. It will offer both suitable precision on 2D-beam characterization and real-time measurements at the pulse scale. With the fully instrumented prototype, we expect to obtain an equivalence between the images provided by TraDeRa and the dose in the water measured in a water phantom and calculated with PENELOPE. Considering the good results obtained on the medical beam line of ESRF, the TraDeRa structure could be easily adapted to provide a low attenuation and fully homogeneous detector for real time monitoring of the very high photon fluence X-ray beam, ahead of the target.

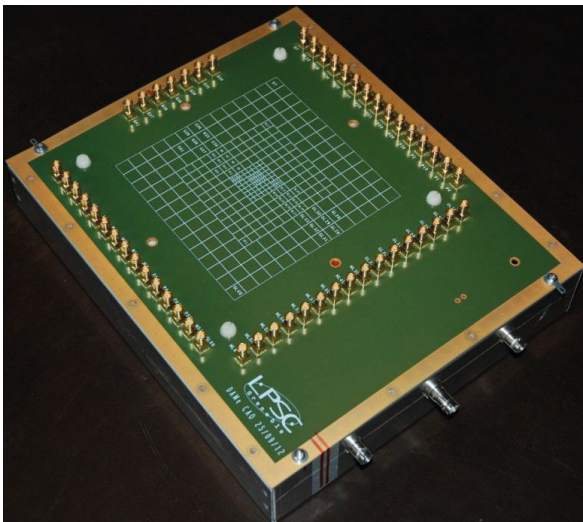


Figure 1 : TraDeRa partially instrumented prototype

Keywords: in-line monitoring, Quality Assurance, Intensity-Modulated Radiotherapy (IMRT)

References:

- [1] Brevet FR N° 11/53254
- [2] Brevet FR N° FR 13/54339

55

TOF-PET scanner configurations for quality assurance in proton therapy: a patient case study

P. Dendooven¹, A.K. Biegun¹, S. Brandenburg¹, H.J.T. Buitenhuis¹, P. Cambraia Lopes², F. Diblen³, D.C. Oxley¹, D.R. Schaart², A.J. van der Borden⁴, M.-J. van Goethem⁴, A. van der Schaaf⁴, S. Vandenberghe³, A.A. van 't Veld⁴

¹KVI, University of Groningen, The Netherlands

²Delft University of Technology, Faculty of Applied Sciences, Radiation Science & Technology Department, The Netherlands

³MEDISIP, Department of Electronics and Information Systems, Ghent University-IBBT-IBiTech, Belgium

⁴University of Groningen, University Medical Center Groningen, Department of Radiation Oncology, The Netherlands

Purpose: In order to determine the clinical benefit of positron emission tomography (PET) for dose delivery verification in proton therapy, we performed a patient case study comparing in-situ with in-room time-of-flight (TOF) PET. For the in-situ option, we consider both a (limited-angle) clinical scanner and a dual-head scanner placed closer to the patient.

Materials and methods: Geant4-based Monte-Carlo simulations of the treatment plan of a typical head & neck patient case result in the distribution of the production of the 7 most relevant PET isotopes. Radioactive decay during irradiation is taken into account; biological washout is not. GATE is used to simulate PET imaging, with coincidence resolving time and limited angular coverage (in case of the in-situ clinical scanner) applied to the GATE output data. Identical PET block detectors containing of 4x4x22 mm³ LSO crystals and the same axial length (18 cm) were considered for all scanners. A scan duration of 120s is considered in all cases. For the in-situ options, scans start with zero delay after the end of the irradiation; for the in-room option, delays of 30 and 60 s are considered.

The original treatment plan was also simulated for patients with artificially introduced anatomical changes. The ability to see the effect of the anatomical changes at the distal edge of the irradiation in the TOF-PET images is related to scanner geometry, scanning protocol and scanner timing resolution.

The improvement in image quality for a dual-head scanner with a detector design optimized for imaging close to the object (smaller LSO crystals and depth-of-interaction (DOI) capability) will be presented.

Results: The maximum number of detected coincidences, 3.36 million for an SOBP physical dose of 0.46 Gy, is obtained for the full-ring in-situ clinical scanner. The dual-head scanner detects only 23% less coincidences, a number comparable to that of a full-ring in-room scanner. An in-situ clinical scanner needs an angular coverage of more than 2/3 to acquire the same number of coincidences as the dual-head scanner.

Conclusions: We conclude that, for the same PET detector design, both an in-situ dual-head and an in-room full-ring clinical TOF-PET scanner deliver comparable image quality: they detect a comparable number of coincidences and state-of-the-art TOF capability can eliminate the limited-angle image artifacts of the dual-head scanner. An optimized dual-head scanner detector design (smaller crystals and DOI capability) will further improve the image quality with respect to the in-room full-ring clinical scanner. The in-situ dual-head configuration has the advantage of minimizing the effect of biological washout. Given that its detector area is just 1/6th that of a full-ring clinical scanner, it is an economic solution as well.

Keywords: proton therapy, TOF-PET, dose verification

56

Impact of tumor autophagy on solid tumors response to IR; role of the tumor stroma

E. Deutsch, A. Ko, J.L. Perfettini

INSERM 1030 Molecular Radiotherapy, Gustave Roussy Cancer Campus & Paris-Sud university, Villejuif France

The role of autophagy in radiation response of tumors remains largely elusive. By using a dual pharmacological and genetic inhibitory approach, we identified a dual role of autophagy in the response of cancer cells to ionizing radiation. First, we observed that the depletion of essential autophagy-relevant gene products, such as ATG5 and Beclin 1, increased the sensitivity of human or mouse cancer cell lines to irradiation, both in vitro (where autophagy inhibition increased radiation-induced cell death and decreased clonogenic survival) and in vivo, after transplantation of the cell lines into immunodeficient mice (where autophagyinhibition potentiated the tumour growth-inhibitory effect of radiotherapy). Secondly, when tumour proficient or deficient for autophagy were implanted in immunocompetent mice, defective autophagy reduced the efficacy of radiotherapy. Indeed, radiotherapy elicited an anti-cancer immune response that was dependent on autophagy-induced ATP release from stressed or dying tumour cells and was characterized by dense lymphocyte infiltration of the tumour bed. Intratumoural injection of an ecto-ATPase inhibitor restored the immune infiltration of autophagy-deficient tumours post radiotherapy and improved the growth-inhibitory effect of ionizing irradiation. Our results reveal that beyond its cytoprotective function, autophagy confers immunogenic properties to tumours, hence amplifying the efficacy of radiotherapy in an immunocompetent context. This has far-reaching implications for the development of pharmacological radiosensitizers.

57

Positron emission tomography (PET) isotope production from laser-driven proton

K. Ding¹, Y. Zhang¹, J.J. Su², K. Kang-Hsin Wang¹, J. Wong¹

¹*Department of Radiation Oncology and Molecular Radiation Sciences, Johns Hopkins University School of Medicine, Baltimore, MD 21231, USA*

²*Department of Physics, University of Maryland, College Park, MD 20742, USA*

Positron emission tomography (PET) plays a critical role in oncology over the last several decades, due to its high sensitivity, capability of quantification, and excellent tissue penetration. The most widely used PET isotopes include ¹⁸F, ¹¹C, ¹⁵O and ⁶⁴Cu. The production of short-lived PET isotopes requires onsite cyclotron, which typically needs extensive radiation shielding and is heavily occupied. Some recent studies suggested that megavoltage protons accelerated by high-power laser can be used for PET isotope generation. Compared with conventional cyclotron, the laser PET (LPET) has several advantages, such as compact size, easy to shield, and on-demand production.

The direct laser acceleration has the potential to deliver accelerating gradient more than 1000 times higher than that conventional accelerator technology, which is the key to reducing the scale of the accelerator. Megavoltage proton beams are produced when an intense $> 10^{19}$ W/cm² laser pulse interacts with a thin solid or gaseous target. The high-power laser of our collaborators at University of Maryland shows encouraging capability in achieving this purpose. The 30 TW, 10 Hz Ti: Sapphire laser system can accelerate proton beam energy up to 20 MeV. A dedicated laser chamber for

PET isotope production has been installed and will be soon available for the preliminary studies. The theoretical yield for ¹¹C is 0.09 mCi/min at current laser repetition rate. And with the current setup, it is possible to carry out proof-of-concept studies. In the near future, a higher power laser with 100 Hz repetition rate and microfluid synthesizer will significantly increase the yield and the resulting product will be more realistic for further applications.

Keywords: Laser, Isotope, PET

58

Oral mucosal radiation response (mouse) - relevance of ceramide-induced apoptosis ?

W. Doerr^{1,2}, E. Bozsaky², V. Limpert¹, C. Mey¹, M. Schmidt¹

¹*Department of Radiation Oncology, Medical Faculty Carl Gustav Carus, Technical University Dresden, Germany*

²*Department for Radiation Oncology & CD Lab. Medical Radiation Research for Radiation Oncology, CCC, Med. University Vienna, Austria*

Oral mucositis is a frequent and dose-limiting adverse event of radiotherapy of head-and-neck malignancies. The relevance of apoptotic processes is currently discussed controversially. Ceramides, formed either de-novo (ceramide synthase, CS) or from sphingomyelin (sphingomyelinases, SMA), are essentially involved in apoptotic processes. The present investigation therefore focused on the modulation of radiation-induced oral mucositis by different ceramide synthesis inhibitors in an established mouse model.

Single dose or fractionated irradiation (5x3 Gy/wk.) over 1 week (days 0-4) or 2 weeks (days 0-4, 7-11) were administered. All fractionation protocols were concluded by a test irradiation (day 7 or 14, respectively). Single dose and test irradiation comprised graded doses (5 dose levels, 10 animals each) in order to generate complete dose effect curves for mucosal ulceration as a clinically relevant endpoint. Three ceramide synthesis inhibitors were alternatively applied: Desipramin (DES, aSMA inh.), Glutathione (GLU, nSMA inh.), or Fumonisin B1 (FB1, CS inh.). The drugs were administered over the following time intervals: Single dose irradiation: day -3 until first diagnosis (-3/D) or healing (-3/H) of all ulcers; 1 week of fractionation: day -3 until day 7 (-3/7), D (-3/D), or H (-3/H); 2 weeks of fractionation: week 1 (-3/7), week 2 (7/14), both weeks (-3/14) or from day -3 to D or H (-3/D, -3/H).

No effect of any of the drugs was found with single doses irradiation. With 1 week of fractionation, only GLU administration including post-irradiation intervals (-3/D, -3/H) resulted in a significant increase in mucosal tolerance, while, in contrast, no effect was observed with 2 weeks of fractionation. DES was exclusively protective in the longest administration protocol (-3/H), while FB1 resulted in only minor effects in all protocols. The time course of ulcers (latent time, ulcer duration) was unaffected by any of the drugs protocols. The functional results (ulcer induction) were confirmed by various histological and immunohistochemical investigations.

The present investigation clearly shows that inhibition of various pathways of ceramide synthesis does impact on the manifestation of oral mucosal ulceration only in very specific experimental protocols. These are associated with radiation-induced regeneration processes ("repopulation") in the epithelium. These results demonstrate that apoptotic processes obviously do not play a (predominant) role in the pathophysiology of radiation-induced ulcerative mucositis.

Keywords: Oral Mucositis, Apoptosis, Fractionation

59

Dose Delivery System of CNAO: a new medical device

M. Donetti¹, M. Lavagno², L. Casalegno¹, A. Di Domenico², M. A. Garella¹, A. Ghigo², S. Giordanengo³, G. Kostyleva², F. Malerba⁴, G. Pittà², S. Rossi¹, S. Toncelli¹, E. Viale⁴

¹CNAO Foundation

²DE.TEC.TOR. S.r.l.

³NFN Torino

⁴SKY-TEAM

Since September 2011 CNAO Foundation has been using the active Dose Delivery System (DDS) developed by CNAO and INFN.

The evolution toward a CE marked medical device with the involvement of industrial partners is presented.

The DDS is composed by: two independent beam monitors (with strip and integral ionization chambers each) with an active area larger than 200x200 mm² and a total water equivalent thickness along the beam path of about 0.9 mm; data transmission system to carry signals away from the treatment room; data acquisition system based on real-time software and designed to manage hadrontherapy treatment, beam measurements and check of the dosimetric parameters. Ancillaries: power supplies of the detection system, gas distribution system, delivered dose recovery (DDR) and interfaces towards patient interlock system, chopper magnet (beam stopper) and scanning magnets.

The acceptance tests to verify the performance of the system and the tests required to demonstrate the compliance with the technical rules related to the 93/42/EEC are described and showed.

The DDS has been produced following the Medical Devices Directive 93/42/EEC - ISO 13485 - medical requirements.

Keywords: medical device certification, dose delivery system, technology transfer

60

Collaborating for the future: the ENLIGHT Network

M. Dosanjh, A. Ballantine, M. Cirilli, H. Dixon-Altaber, I. Floros, S. Navin, M. Puianu, I. Tudosescu (CERN) for the ENLIGHT Network

The European Network for Light Ion Hadron Therapy (ENLIGHT) was launched in 2002 with the goal of establishing a unified approach to hadron therapy in Europe. Hadron therapy is inherently a multidisciplinary field, as it requires know-how from a variety of scientific disciplines, such as medicine, biology, physics, information technology and engineering. Successful translational projects in this field require interaction and information exchange among the different communities.

Funded by the European Commission for its first three years, ENLIGHT has created a multidisciplinary platform, uniting traditionally separate communities so that clinicians, physicists, biologists and engineers with experience in ions could work together with a common goal. At the end of the EU grant, the community felt that ENLIGHT was a key ingredient for future progress, and therefore should be maintained and broadened: this brought to the establishment of the ENLIGHT++ network in 2006. The aim of ENLIGHT++ is twofold: to maintain and enlarge the European network of institutions and specialists which work in the field of Light Ion Therapy, and to sponsor the research in fields of common interests for the development of the cutting edge and technically advanced clinical facilities.

The network provides a common European platform for fostering and coordinating collaborations between national research activities related to hadron therapy, encompassing such various fields as proton and light ion accelerators, detectors, image reconstruction and processing, radiobiology, oncology, and clinical research. ENLIGHT also permits to

maintain a critical mass of physicians, radiobiologists, medical physicists and biomedical engineers from different European countries, involved in the development of hadron therapy. It also fosters innovation and supports partnerships with industry for more affordable treatment centres.

A major goal of ENLIGHT++ is to develop strategies for securing the funding necessary to continue the initiative in these two fundamental aspects, mostly through dedicated EU projects, while the network itself carries on without specific funding.

Indeed ENLIGHT coordinates four EC-funded projects: PARTNER, ULICE, ENVISION and ENTERVISION. These projects focus diverse aspects of the subject: pushing the development of infrastructures necessary for the diffusion of particle therapy; ensuring the possibility for researchers to access the facilities for tests (transnational access) and the data for comparisons and study; improving the monitoring and imaging tools in order to target moving organs and adapt the irradiation to the changing size of the tumour; training the new generations of experts who, thanks to their multidisciplinary education, will be able to work together efficiently for the common goal and to address the challenge from a broader perspective. Detailed information on ENLIGHT, including how to join the network, is available on the website <http://cern.ch/ENLIGHT>

Keywords: hadrontherapy, cancer, radiotherapy

61

Immunosensitization through radiotherapy: the example of immunocytokines

L. Dubois¹, N.H. Rekers¹, C.M.L. Zegers¹, N.G. Lieuwes¹, W.T.V. Germeraad², D. Neri³, E.G.C. Troost¹, P. Lambin¹

¹Dept of Radiation Oncology (MAASTRO)

²Dept of Internal Medicine, GROW - School for Oncology and Developmental Biology, Maastricht University Medical Center, Maastricht, The Netherlands,

³Dept of Chemistry and Applied Biosciences, Swiss Federal Institute of Technology, Zürich, Switzerland

Although radiotherapy (RT) is one of the major cancer treatment modalities to kill malignant cells, advanced-stage disease is often hard to control. Stimulation of the immune system to assist in eliminating cancer cells within, and outside, the radiation field could be beneficial in advanced-stage or metastasized disease. One of the major appeals of immunotherapy is the antigen specificity of T-cells which are able to recognize the differentially expressed antigens between tumor cells and normal cells. Overwhelming evidence is available in recent literature that T-cell mediated immunity is most effective in terms of tumor cell killing. Interleukin-2 (IL2) is one of the essential cytokines for driving proliferation and differentiation of naïve T-cells into active effector T-cells resulting in increased cytotoxic activity, eventually leading to tumor regression. High-dose systemic IL2 treatment has been approved by the FDA and although initial efficacy was proven, acute toxicity, severe side-effects and even deaths lead to its dismissal for most indications.

Radiation-induced tumor cell death provides a plethora of pro-immunogenic effectors associated with inflammation. Although the potential for RT to generate anti-tumor immunity is apparent, the evidence that it does so in the clinical situation is limited. Recently, it has been demonstrated that cancer patients have increased levels of cytotoxic T-cells after radiotherapy, making them eligible for immunotherapy. Furthermore, several pre-clinical studies have shown synergistic anti-tumor effects when combining RT with systemic cytokine treatment strategies, such as IL2, although this strategy was accompanied with systemic toxicity.

To reduce the significant systemic toxicity, monoclonal antibodies have been designed as "targeting vehicle" for the

selective delivery of immune-stimulatory cytokines to the tumor microenvironment while sparing normal tissue. An example is the human recombinant scFv fragment L19, that is specific to the alternatively spliced extra-domain B (EDB) of fibronectin; EDB expression in normal healthy tissues is confined to the female reproductive organs, while it is abundantly expressed in a variety of malignancies. The L19 antibody selectively localizes at these tumor neovascular EDB positive sites following systemic administration and serves as delivery vehicle for IL2. Targeted administration by coupling IL2 with L19 markedly improved the therapeutic index when compared to systemic IL2. Our lab has combined single high-dose RT with systemic L19-IL2 administration in a number of murine xenograft models and found outstanding, long-lasting complete response rates mediated by cytotoxic T-cell activity. L19-IL2 is thus an immunocytokine with strong immune response enhancing properties in EDB-positive tumors.

Keywords: radiotherapy, immunotherapy, immunocytokine

62

The development of a low energy facility for clinical trials of Boron Neutron Capture Therapy

R. Edgecock¹, R. Bennett¹, S. Green², B. Phoenix³, M. Scott³

¹STFC

²Queen Elizabeth Hospital, Birmingham, UK

³Physics Department, Birmingham University, UK

Boron Neutron Capture Therapy (BNCT) is a binary cancer therapy particularly well-suited to treating aggressive tumours that exhibit a high degree of infiltration of the surrounding healthy tissue. Such tumours, for example of the brain and lung, provide some of the most challenging problems in oncology and remain recalcitrant to conventional therapies.

The first element of the therapy is boron-10 which is preferentially introduced into the cancerous cells using one of two carrier compounds, boronophenylalanine (BPA) or sodium borocaptate (BSH). Boron-10 has a very high capture cross-section with the other element of the therapy, thermal neutrons, resulting in the production of a lithium nucleus and an alpha particle. The mean free path of these is about the size of a cell, leading to the destruction of the cell they are created in. The uptake mechanism for BPA has been studied in detail for glioblastoma multiforme (GBM) in Birmingham. It has been shown that although a large fraction of GBM cells take up the BPA, not all do. As a result, a combination of BNCT and another therapy, for example radiotherapy, is required for the treatment. Recently, limited trials of this combination have taken place in Japan, though without using the Birmingham studies to optimise the doses. These have demonstrated a factor of two increase in 2-year survival over the current standard treatment.

For the neutron beam, a flux of around 10^9 neutrons/cm²/s is required for a session of less than 30 minutes. In addition, as well as being mainly at epithermal energies, the beam should not have high energy neutrons, as these add to the dose to healthy tissue in an uncontrollable manner. Until recently, the only source used is a nuclear reactor. It is possible to make the neutrons with an accelerator, but the beam requirements create significant technical problems. In particular, a low energy proton beam with a beam power of ≥ 12 kW is required. The best neutron production reactions are Li(p,n)Be and Be(p,n)B, with a strong preference for the former due to the larger yield at low energy and lower flux of high energy neutrons. However, as the lithium target would only be 40cm away from the patient, health and safety requirements indicate the need to keep the target solid. This is a major challenge due to the 180° melting point. To date, only a 30 MeV beam with a Be target in Japan has been used to treat patients.

In Birmingham, studies of an existing BNCT facility using a 2.8 MeV proton beam and a solid lithium target have found a way to increase the beam power to a sufficient level to allow clinical trials, while maintaining the target solid. This work is now being implemented and proposals are in preparation and submitted to fund the trials.

In this talk, we will introduce BNCT, talk about the recent developments, explain what has been done in Birmingham and what is now planned and compare with other accelerator-driven BNCT projects around the World.

Keywords: BNCT, lithium target

63

Fast Monte Carlo simulator for the distribution of prompt-gamma emitters in protontherapy

W. El Kanawati, N. Freud, J. M. Létang

Université de Lyon, CREATIS ; CNRS UMR5220 ; Inserm U1044; INSA-Lyon, Université Lyon 1, Centre Léon Bérard, France

Purpose: Real-time in vivo control of the ion range in a patient during protontherapy is a major challenge for Quality Assurance of treatments. A few years ago, prompt gamma rays have been investigated for beam range verification with proton¹ and carbon ion beams². Since then, several teams in the world have been progressing toward the construction of first clinical prototypes^{3,4,5}. The imaging concept is usually designed and optimized with the help of Monte Carlo simulations (MC), which have become the gold standard for physical calculations especially for simulations of prompt gammas emitted by proton inelastic interaction in complex geometries. It remains however hindered by its slow statistical convergence.

Materials and methods: In the domain of low energy photons, the track length estimator TLE method is an efficient variance reduction technique and standard of practice in voxel-based dose computation in the kerma approximation^{6,7}.

In order to compute maps of prompt-gamma emission spectra, a TLE-based variance reduction technique for nuclear fragmentation has been implemented in Geant4/GATE.

During patient irradiation with a proton beam, nuclear fragmentation reactions take place. These reactions lead to the emission of prompt gammas (de-excitation of nuclei produced), and various fragments (protons, neutrons and other nuclei in small quantities). Each volume element of the patient becomes a point source emitting these secondary particles. In order to simulate the distribution of prompt-gamma sources, a database of 2D prompt-gamma emission spectra has been established for different types of human tissues and for the useful range of incident proton energy (typ. -1 to 250 MeV). This database of these 2D spectra is built offline with high statistics. Then each proton deposits along its track in the corresponding voxel the expectation of the prompt-gamma spectra from the database according to the proton kinetic energy and the local material composition. **Results:** Benchmarking with analog MC simulation has been carried out for both homogenous and heterogeneous phantoms and shows the gain in efficiency of the proposed prompt-gamma TLE MC technique.

Conclusions: This feasibility study of the proposed variance reduction technique for estimating the distribution of prompt-gamma emitters is very promising and application to CT and RT plan data are envisaged.

Keywords: variance reduction, prompt gamma, Monte Carlo simulation

Acknowledgements:

This research was funded in part by ENVISION (grant agreement no. 241851) FP7 project.

References:

- [1] C.H. Min et al. (2006), Prompt gamma measurements for locating the dose falloff region in the proton therapy. *App Phys Let*, 89(18), p.183517-3.
- [2] É. Testa et al. (2008), Monitoring the Bragg peak location of 73 MeV/u carbon ions by means of prompt gamma-ray measurements. *App Phys Let* 93(9), p.093506.
- [3] J. Smeets et al. (2012), Prompt gamma imaging with a slit camera for real-time range control in proton therapy. *Phys Med Biol* 57(11), p.3371-3405.
- [4] F. Roellinghoff et al. (2011), Design of a Compton camera for 3D prompt-gamma imaging during ion beam therapy. *NIMA* 648(sup.1), p.S20-S23.
- [5] C.H. Min et al. (2012), Development of array-type prompt gamma measurement system for in vivo range verification in proton therapy. *Med Phys* 39(4), p.2100-2107.
- [6] J. DeMarco et al. (2002), An analysis of MCNP cross-sections and tally methods for low-energy photon emitters. *Phys Med Biol* 47, p.1321-1332.
- [7] K. Smans et al. (2010), Simulation of image detectors in radiology for determination of scatter-to-primary ratios using Monte Carlo radiation transport code MCNP/MCNPX. *Med Phys* 37(5), p.2082-2091.

64

DNA damage, protein expression and migration of melanoma cells irradiated with proton beam

M. Elas¹, S. Kędracka-Krok¹, U. Jankowska¹, Ł. Skalniak¹, J. Jura¹, E. Zuba-Surma¹, K. Jasińska¹, A. Pawlak¹, U. Sowa², P. Olko², K. Urbańska¹, B. Romanowska-Dixon³

¹Faculty of Biochemistry, Biophysics and Biotechnology, JU, Poland

²Institute of Nuclear Physics, PAS

³Department of Ophthalmology and Ophthalmic Oncology, Jagiellonian University Medical College.

Purpose: The goal of our study was to determine the cellular response to low, sublethal doses of proton beam irradiation, in particular DNA damage, cell cycle arrest, changes in expression of proteins, and effect on metastases in vivo.

Material/Methods: BLM cells were irradiated with 1-7 Gy of proton beam irradiation. The source of the 58 MeV proton beam was the AIC-144 cyclotron at Institute of Nuclear Physics, Polish Academy of Sciences, Kraków. The dose rate was 0.15 Gy/s. DNA content was evaluated by flow cytometry (Becton Dickinson). The level of DNA damage was tested by electrophoresis of single cells in agarose gel (comet assay). Protein expression were determined by 2D protein electrophoresis and mass spectroscopy. Tumors of Bomirski Hamster Melanoma (BHM) implanted into the anterior chamber of the hamster eye grew aggressively and completely filled the anterior chamber within 8-10 days. Metastases, mainly in the lung, were found in 100% of untreated animals 30 days after enucleation. The protons were accelerated using AIC-144 isochronous cyclotron, operating at 60 MeV and BHM tumors located in the anterior chamber of the eye were irradiated with 10 Gy, for the depth of 3.88 mm.

Results: Slow accumulation of damage was observed reflected in slowing of the proliferation rate, and increase in caspases activity with time. The number of cells in G2/M and >2n increased with proton beam dose. Proton beam irradiation caused upregulation of proteins involved in: DNA repair, RNA functioning (i.e. stress granule and P-bodies components), apoptosis and survival processes and downregulation of enzymes engaged in glycolysis. Of particular interest was heavy downregulation of vimentin (2.4 times), involved in structural integrity of cells and tissues, adhesion and migration, and other processes. Irradiation led to changes in cell migratory properties. Proton beam

irradiation caused inhibition of tumor growth by about 10 days and inhibition of metastatic spread.

Conclusions: Low doses of proton beam irradiation cause significant DNA damage in human melanoma metastatic cells. Arrest in G2/M phase in response to DNA damage may lead to apoptosis (5 and 7 Gy), increase in polyploidy (>2n) or to DNA repair and cell survival (1-3Gy). Four groups of proteins were differentially regulated after proton beam irradiation: i) DNA repair and stress, ii) pro-survival response, iii) metabolic and iv) connected to motility and cytoskeleton. 10 Gy of proton beam irradiation given to melanoma growing in the hamster eye inhibited metastases growth in the lung 4.3 times.

Keywords: proton beam, molecular, DNA

65

Education and training in medical imaging for conventional and particle radiation therapy: the ENTERVISION training network

The ENTERVISION training network.

ENTERVISION is a Marie-Curie Initial Training Network aimed at educating young researchers in online 3D digital imaging for hadron therapy. ENTERVISION brings together ten academic institutes and research centres of excellence and a leading European company in particle therapy, and is coordinated by CERN. Since the kick-off in 2011, the participating institutes have been recruiting a total of 15 researchers, coming from different academic backgrounds.

The multi-disciplinary training programme of ENTERVISION includes a diversified portfolio of scientific courses, complemented by specific courses aimed at developing soft skills that will help the researchers to build successful careers.

The research activities within ENTERVISION are organised in four distinct work packages: hardware and software solutions for signal handling, data acquisition and processing for image based in-vivo dosimetry; modelling of in-beam PET and SPECT imaging devices; nuclear fragmentation studies; integration of treatment related imaging and dosimetry data.

Intercalated into the training programme, the researchers have the opportunity to perform hands-on work in the following fields:

- Development of in-beam Positron Emission Tomography monitoring techniques
- Development of Single Particle Tomography techniques
- Adaptive treatment planning and organ motion
- Optical imaging, cell irradiation, and biological phantom design
- Monte Carlo simulation of in-vivo dosimetry

The actual technology development of this next-generation image based in-vivo dosimetry is being carried out in the EC funded project ENVISION: this project has not been designed to incorporate a platform for knowledge development for future generations of researchers, and ENTERVISION bridges this gap between R&D and training.

Throughout the project, the trainees are encouraged to build a multidisciplinary network which will not only help them with their future careers but ultimately improve the transfer of knowledge and collaboration between the various disciplines of cancer treatment.

The Researchers have made good progress in their individual research projects and have had the opportunity to attend several training courses. These are multidisciplinary and build their scientific knowledge as well as communication and leadership skills greatly enhancing their career development and employment prospects.

The researchers also became part of the European Network for Light Ion Hadron Therapy (ENLIGHT); this allowed them to attend the ENLIGHT and related EU project meetings, where they have presented their work and listened to and interacted with the leading experts in the hadron therapy

field. This privileged situation is providing them with unique learning and networking opportunities.

Keywords: hadrontherapy, cancer, radiotherapy

Acknowledgment: The ENTERVISION project is funded by the European Commission under FP7 Grant Agreement N. 264552.

66

Quality assurance for hadron therapy: the ENVISION project

The ENVISION Consortium
CERN, Switzerland

A key challenge in particle therapy today is quality assurance during treatment, which needs advanced medical imaging techniques. This issue is tackled by the EC funded project ENVISION, an R&D consortium of sixteen leading European research centres and one industrial partner, co-ordinated by CERN and funded by the European Commission. The project aims at developing solutions for real-time non invasive monitoring, quantitative imaging, precise determination of delivered dose, fast feedback for optimal treatment planning, real-time response to moving organs, and simulation studies.

ENVISION pursues the goal of developing accurate and fast in-beam imaging, exploiting both the positron emitting isotopes and prompt single particles produced during therapeutic exposures to ion beams.

In the case of PET, the project aims at improving image quality by limiting the region of interest with a measurement of the time difference between the photons emitted by positron annihilations in the body (Time-of-Flight PET, or TOF-PET). ENVISION is comparing technologies for sub-ns TOF resolution; designing, building and testing dual-head demonstrators; simulating full in-beam TOF PET systems; developing fast image reconstruction algorithms exploiting TOF for in-beam PET.

For prompt radiation components, ENVISION studies the feasibility of single photon imaging for in-vivo dosimetry in ion therapy and develops systems for prompt gamma imaging, both passively and electronically collimated. The implementation of a full in-beam SPECT system also requires a fast position sensitive beam monitor, tomographic reconstruction, and accurate simulation of the imaging process.

The project also investigates the potential of secondary charged light particles for in-vivo dosimetry as an alternative to photon detection.

Quality assurance of particle therapy needs also innovative software and hardware solutions to improve the accuracy of dose delivery in the case of moving targets. ENVISION aims at assessing the feasibility and at enabling optimal performances of time-resolved in-vivo dosimetric imaging for validation of motion-mitigated ion beam delivery to moving targets. At the same time, the project develops accurate and reliable 4D motion monitoring systems and integrates them into the in-vivo dosimetric data acquisition and processing.

ENVISION also works towards a fast and automatic integration of the dosimetric information from in-vivo dosimetry and 4D monitoring into the treatment planning and delivery workflow, in order for these techniques to become clinically useful tools.

Highly realistic calculation models and fast simulation tools are an underlying need for most of these quality assurance tools, and ENVISION aims at developing dedicated simulation tools appropriate for use in hadron therapy applications, in order to reliably predict and understand all possible signals useful for treatment monitoring.

The ENVISION project is co-funded by the European Commission under FP7 Grant Agreement N. 241851.

Keywords: hadrontherapy, cancer, radiotherapy

67

Development of a novel ELISA for detecting inducible Hsp70 in serum

S. Ertl, C. Bayer, G. Multhoff

Department of Radiotherapy and Radiooncology, Klinikum rechts der Isar, Technische Universität München, Munich, Germany

Background: The members of the heat shock protein 70 family are known to play a major role in assisting protein folding, preventing protein aggregation and transporting proteins across membranes. The heat shock cognate protein 70 (Hsc70), which is constitutively expressed in the cytosol of eukaryotic cells, is only moderately up-regulated following stress. The major stress-inducible heat shock protein 70 (Hsp70), which is found at low levels under physiological conditions, is highly up-regulated after various stress conditions, including heat, oxidative stress and/or chemo- and radiotherapy.

Tumor cells, in contrast to normal cells, frequently express Hsp70 also on their plasma membrane and can actively release Hsp70 via exosomes. In accordance with that, elevated levels of Hsp70 have been detected in the supernatant of tumor cell lines and also in the blood of cancer patients.

Method: We developed a novel sandwich ELISA for the detection of inducible Hsp70 in serum. Capture of the protein is achieved with a polyclonal Hsp70 antibody and detected using a biotinylated monoclonal anti-Hsp70 antibody. This antibody binds specifically to Hsp70 and does not cross-react with the highly homologous constitutively expressed Hsc70. After incubation with horseradish peroxidase-conjugated streptavidin, antibody binding is quantified by measuring substrate conversion in an ELISA microplate reader.

Results: When comparing our novel ELISA with a commercially available Hsp70 ELISA kit, we found that we are able to detect higher amounts of Hsp70 in the serum of cancer patients and have better recovery rates in samples spiked with known amounts of Hsp70 protein.

Conclusions: This novel ELISA can be used for the screening of cancer patients to monitor their Hsp70 serum levels before, during and after therapy. By taking into account tumor entity, stage, therapy and clinical outcome, the ELISA can provide a novel diagnostic and prognostic tool for cancer therapy.

Keywords: Hsp70, biomarker, ELISA

68

A Novel Radioguided Surgery Technique Exploiting - b decays

R. Faccini^{1,2}, F. Collamati¹, S. Morganti^{1,2}, V. Patera^{1,2,5}, A. Russomando^{1,4}, A. Sciubba^{1,2}, E. Solfaroli⁴

¹Dip. Fisica, Univ. Di Roma 'La Sapienza', Roma, Italy

²INFN sezione di Roma, Roma, Italy

³Dip. Scienze di Base Applicate all'Ingegneria, Univ. Di Roma 'La Sapienza', Roma, Italy

⁴Center for Life Nano Science, @Sapienza, Istituto Italiano di Tecnologia, Roma, Italy

⁵Centro Fermi, Roma, Italy

Purpose: Radio-guided surgery (RGS) is a technique that enables the surgeon to perform complete lesion resections, minimizing the amount of healthy tissue removed [1]. The basic idea is to administer to the patient, before surgery, a radio-labelled tracer that is preferentially taken up by the tumor and to exploit, during surgery, a specific probe system [2] to detect remnants difficult to identify by the naked eye. Existing methods make use of a γ radiation detection, but its high penetration power limits the applicability of the technique because an eventual uptake of the tracer in nearby healthy tissue would represent a non-negligible background.

We present an alternative technique based on β^- radiation detection that may extend the applicability of the radio-guided surgery. The low penetration of such radiation allows for a lower background rate and lower irradiation of the medical personnel.

Materials and methods: A prototype of the β^- probe was developed: a cylindrical scintillator (diameter 2.1 mm, height 1.7 mm) of poli-crystalline P-terphenyl[3] is shielded from the external light by a thin PVC layer. A 2.8 mm thick ring of PVC protects the device from radiation coming from the sides a thin aluminium body preserves it from mechanical stress. In collaboration with the Istituto Neurologico Carlo Besta and the Istituto Europeo di Oncologia in Milano, we have noted that ^{90}Y labelled DOTATOC is identified as a good candidate for a radio-guided removal of meningioma [4] and therefore it represent an excellent first clinical test. We are in parallel studying further use cases that are more of interest from the clinical point of view.

After performing the first laboratory tests with a ^{90}Sr source, we tested the response of the first prototype to four phantoms filled of ^{90}Y labelled DOTATOC in saline solution, simulating cancerous residuals with different topologies: a 0.1 ml volume phantom, the typical residual of interest, and other three cylindrical phantoms with the same area of a circular face (13 mm²) but different heights (1, 2, 3 mm), to check the effect of the phantom depth in the probe response and in distinguishing the residual edge.

Results: Tuning the electronic threshold of our device to have a background rate of 0.2 cps, we measured rates on the phantoms ranging from 2.3 cps to 18 cps when the solution had an activity of 22kBq/ml.

To translate the observed rates into actual sensitivity to tumor residuals, the impact of the background from the noise coming from uptake in healthy tissues was estimated with FLUKA simulations based on DICOM images of the uptake of ^{68}Ga -DOTATOC PET scans.

With such simulation we conclude that by requiring both the false positive and the false negative rates to be below 1%, for a tumor activity of 22kBq/ml all the samples are visible within 2s, while 5kBq/ml would require to wait at least 10s. Further development is therefore ongoing on the probe to be able to reduce such intervals in order to allow the system to work with 5kBq/ml.

Conclusions: Laboratory tests show that the proposed innovative technique for radio-guided surgery allows for a fast feedback during surgery with minimal irradiation of the patient and the surgeon. We are now preparing the first ex-vivo tests on meningioma patients at the Istituto Neurologico Carlo Besta.

Keywords: radio guided surgery, probe, e- technique

References:

- [1] see, for instance, Mariani G, Giuliano A E, Strauss H W Edts, "Radioguided Surgery: A Comprehensive Team Approach" Springer (2006)
- [2] see, for instance, Hoffman E J, Tornai M P, Janecek M, Patt B E and Iwanczyk J S, "Intraoperative probes and imaging probes", Eur J Nucl Med (1999) 26:913
- [3] M. Angelone et al., "Properties of para-terphenyl as detector for α , β , and γ radiation", arXiv: 1305.0442, submitted to T.N.S.
- [4] Bartolomei M, Bodei L, De Cicco C, Grana C M, Cremonesi M, Botteri E, Baio S M, Aricò D, Sansovini M and Paganelli G "Peptide receptor radionuclide therapy with (^{90}Y)-DOTATOC in recurrent meningioma" Eur J Nucl Med Mol Imaging (2009) 36:1407-1416

69

Intra-fraction tumor tracking based on a surrogate-driven 4D CT motion model in particle radiation therapy

A. Fassi¹, M. Seregini¹, M. Riboldi¹, P. Cerveri¹, D. Sarrut², G. Baroni¹

¹Politecnico di Milano, Italy

²Centre Léon Bérard, Lyon, France

Purpose: The application of tumor tracking techniques for intra-fraction motion compensation in particle radiation therapy is challenging due to the need to account both for target motion and for particle range fluctuations induced by tissue density variations along the beam line. The aim of this work is to develop and investigate a tumor tracking method for an application in particle therapy, providing the daily respiratory dynamics of the entire patient anatomy as a function of an external surface surrogate combined with an a priori motion model.

Materials/methods: The proposed tracking approach is based on a patient-specific breathing motion model, extracted from time-resolved (4D) planning CT images through deformable image registration (DIR) and driven by a respiratory surrogate capturing the external body surface displacement. The model is able to estimate the whole CT volume corresponding to a specific motion state identified by three respiratory parameters (baseline, amplitude and phase), which describe inter- and intra-fraction motion pattern variations. DIR is applied to compensate for baseline shifts in the patient anatomical configuration. Changes in breathing amplitude and phase parameters are corrected from the external surface surrogate. The developed technique was assessed on a dataset of double 4D CT scans acquired from four lung cancer patients. The first 4D CT was used to build the respiratory motion model, which was tested on the second dataset by assessing both geometric reconstruction errors and water equivalent path-length (WEL) variations along a simulated beam line.

Results: The geometric accuracy in identifying tumor position, averaged over all 4D CT frames, ranged between 0.9 and 1.8 mm across all patients (Table). Errors in tracking the surrounding organs at risk (lungs, trachea and esophagus) was on average lower than 1.5 mm. Contour reconstruction uncertainties did not exceed 1.3 mm for all structures of interest, whereas the Dice coefficient for volume overlapping was always higher than 0.8. Mean absolute WEL variations within the target volume did not exceed 1.4 mm-WEL with the proposed tracking method (Figure). A statistically significant improvement (p-value<0.001) was achieved compared to the standard setup procedure based on patient rigid alignment, showing WEL differences up to 7.8 mm-WEL.

Table. Geometric results in reconstructing the position, contour and volume of the different structures of interest (T=Tumor, L=Lungs, Tr=Trachea, E=Esophagus), quantified respectively by the distance between centers of mass (COM), the Hausdorff distance and the Dice coefficient. The Table reports for each patient the mean values of the geometric variables computed over all 4D CT frames.

Patient	COM distance [mm]				Hausdorff distance [mm]				Dice coefficient			
	T	L	Tr	E	T	L	Tr	E	T	L	Tr	E
P1	1.6	0.8	1.0	0.8	0.6	0.6	0.5	0.3	0.80	0.97	0.88	0.91
P2	1.8	1.1	2.0	1.0	0.6	0.6	0.6	0.4	0.82	0.98	0.90	0.93
P3	0.9	2.8	2.2	2.1	0.4	1.3	1.1	1.2	0.93	0.96	0.79	0.76
P4	1.3	0.4	0.7	1.2	0.6	0.4	0.3	0.3	0.80	0.99	0.94	0.92
Mean value	1.4	1.3	1.5	1.4	0.6	0.7	0.6	0.6	0.84	0.98	0.88	0.88

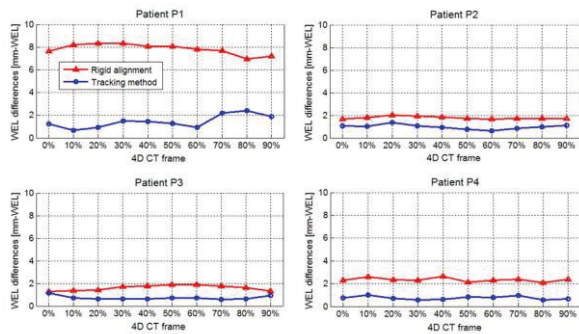


Figure. Mean absolute WEL variations within the tumor volume for each 4D CT frame, measured with the proposed tracking technique and after the rigid alignment of the two 4D CT datasets.

Conclusions: The present work can be regarded as a feasibility study for the potential extension of intra-fraction tumor tracking techniques in extra-cranial particle treatments. Differently from the point-based tracking methods currently applied in conventional photon radiotherapy, the proposed approach allows the dynamic localization of all anatomical structures included in the CT scan, thus providing complete information on density variations required for particle beam range adaptation.

Keywords: Tumor tracking, Particle therapy, 4D CT motion model

70

Varian Eclipse TPS and FLUKA Monte Carlo proton dose deposition comparison

F. Fiorini, B. Jones, M.A. Hill
University of Oxford, UK

The overall aim of the work is the investigation and quantification of factors leading to the deviation between planned, simulated and actual 3D dose distributions for clinical particle beams. The assessment of these differences is important for high quality assurance in particle therapy. Additionally information on the resulting deviations will ultimately be used to make an assessment of their clinical significance.

To facilitate this work, the Varian Eclipse TPS has been used to plan proton beam deliveries in the first instance. The resulting beam delivery data along with the relevant source beam information have been used as an input to the FLUKA Monte Carlo code to enable comparisons between planned and simulated 3D dose distributions. In addition to using water the distributions were also obtained in a range of different materials including air, inflated lung tissue, compact bone tissue, PMMA and aluminium. The comparisons were then extended to include heterogeneous phantoms containing cylindrical rods of a range of different materials to investigate how these perturb the planned and simulated dose distributions. These structures were initially created directly in Eclipse or FLUKA to avoid effects due to CT artefacts. More complex configurations involving real and virtual CT were also used not only to address how Eclipse copes with complex structures but also to investigate the effects of CT artefacts.

Good agreement was obtained between the 3D dose distributions from Eclipse and FLUKA for water, however increased deviations were observed for other materials studied. For example for the phantom with rods configuration, the goodness of agreement was close to 98% for PMMA, ~95% for air, lung and bone, but fell to 70% for aluminium in some regions of the phantom. Increasing the complexity of inhomogeneities caused the goodness of agreement to decrease for almost all the materials used, but particularly for the high density materials. Initial data also

shows the importance of appropriately dealing with CT artefacts.

The extraction of beam data from Eclipse plans to create source input data for FLUKA simulations have been successfully implemented. Although good agreement was found in water, deviations between planned and simulated distributions were observed for other materials. These deviations increased with increasing complexity of inhomogeneities.

The obtained results will be used to guide experimental studies which will compare planned and simulated distributions to those obtained experimentally.

Keywords: Eclipse TPS, proton dose deposition, FLUKA

Acknowledgment: This work is supported by the ENVISION project, grant number 241851.

71

Verification of dynamic trajectory radiotherapy based on Monte Carlo

M.K. Fix, D. Frauchiger, L. Henrich, M. Sassowsky, D. Frei, D. Terribilini, P. Manser

Division of Medical Radiation Physics and Department of Radiation Oncology, Inselspital, Bern University Hospital and University of Bern, Switzerland

Purpose: Volumetric modulated arc therapy (VMAT) is of increasing interest in radiation oncology. In this delivery technique gantry position, multi leaf collimator (MLC) as well as dose rate change dynamically during the application leading to efficient and conformal dose delivery to the patient. However, in general additional components can be changed dynamically throughout the dose delivery such as the collimator or the couch. By this means the degrees of freedom increase allowing almost arbitrary dynamic trajectories for the beam. Whereas the dose delivery of such dynamic trajectories is technically possible, there is currently no dose calculation and validation method available. Thus, the aim of this work is to develop a dose calculation and verification tool for dynamic trajectories based on Monte Carlo (MC) methods.

Materials and methods: The dose calculation for dynamic trajectories is implemented in the previously developed Swiss Monte Carlo Plan (SMCP) [1]. SMCP interfaces the treatment planning system Eclipse with a MC dose calculation algorithm and is already able to handle dynamic MLC or gantry rotations. Hence, the additional dynamic components, namely the collimator and the couch, are described similarly to the dynamic MLC by defining data pairs of positions of the dynamic component and the corresponding MU-fractions. In order to validate the new tool, measurements are performed with the Delta4 phantom using the developer mode on a TrueBeam linear accelerator. These measured dose distributions are then compared with the corresponding calculations using SMCP. First, simple cases applying one-dimensional cases are compared and second, more complex dynamic trajectories with several simultaneously moving components are investigated.

Results: The SMCP is successfully extended in order to allow dose calculations for dynamic trajectories. The comparisons between the measured and calculated dose distributions for the simple as well as for the more complex situations show an agreement which is generally within 2% of the maximum dose or 2 mm. The required computation time for the dose calculation remains the same when the additional dynamic moving components are included.

Conclusions: The results of the dose comparisons for simple and complex situations suggest that the extended SMCP is an accurate and efficient verification tool for dynamic trajectory radiotherapy.

Conflict of Interest: This work was supported by Varian Medical Systems.

Keywords: Monte Carlo, Dose calculation, Quality assurance

References:

[1] M.K. Fix, P. Manser, D. Frei, W. Volken, R. Mini, E.J. Born, *An efficient framework for photon Monte Carlo treatment planning*, Phys. Med. Biol., 52, p. 425-437, 2007.

72

First investigations of Ultra-Thin 3D silicon detectors as microdosimeters

C. Fleta¹, C. Guardiola², S. Esteban¹, G. Pellegrini¹, D. Quirion¹, J. Rodriguez¹, F. Gomez³, A. Carabe-Fernández², M. Lozano¹

¹Instituto de Microelectrónica de Barcelona, IMB-CNM (CSIC)

²University of Pennsylvania, Department of Radiation Oncology

³Dpto Física de Partículas, Universidad de Santiago de Compostela (USC)

IMB-CNM (CSIC) has developed a new type of three-dimensional diode on ultrathin SOI silicon wafers with 3D columnar structures with P-N junctions fabricated with micromachining techniques for plasma diagnostic applications or neutron detection in demanding environments [1, 2]. The three-dimensional electrodes are columns etched through the silicon instead of being deposited on the surface like in the standard planar diodes. The sensitive volume is a silicon membrane only 10 microns thick (fig.1). The ultra-thin sensors have shown to be insensitive to the gamma radiation background, their membrane structure avoids the backscattering contributions from the supporting silicon wafer and the confinement of the electric field given by the columnar electrodes reduces charge sharing. All these characteristics make the ultra-thin 3D devices the perfect candidates for microdosimetry.

Recently, IMB-CNM have carried out the first tests of these devices with beams of 62MeV protons and 95MeV/u ¹²C ions. The results of these first experiments show that, although they were not specifically designed for microdosimetric applications, the detectors with ultra-thin 3D structure are able to characterize the therapeutic hadron beams. Results from these proof-of-concept tests will be presented and compared with Monte Carlo simulations using MCNPX and Geant4 codes.

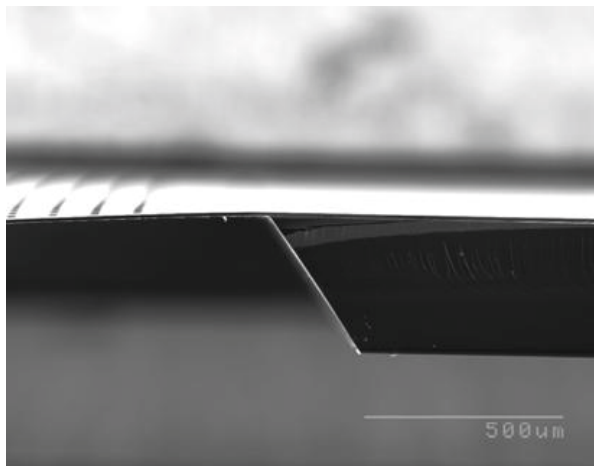


Figure 1. SEM image of a ultra-thin 3D detector showing the 10 micron active membrane and the silicon frame that acts as mechanical support

Keywords: silicon detectors, microdosimetry, particle therapy

References:

[1] G. Pellegrini et al., "Ultra-thin 3D silicon detector for plasma diagnostics at the ITER Tokamak". NSS/MIC, 2011.

[2] C. Guardiola et al., "Neutron measurements with ultra-thin 3D silicon sensors in a radiotherapy treatment room using a Siemens PRIMUS linac". Phys. Med Biol. 58 - 10, pp. 3227 - 3242, 2013.

73

The XEMIS2 prototype

L. Gallego¹, S. Bassetto², P. Briend², J-P Cussonneau¹, J. Donnard¹, M. Gorski², M. Le Calloch¹, P. Le Ray¹, O. Lemaire¹, J. Masbou¹, E. Morteau¹, A. Perier¹, L. Scotto Lavina¹, J-S Stutzmann¹, D. Thers¹.

¹Laboratoire SUBATECH, 4 rue Alfred Kastler, 44307 Nantes cedex 3, France

²AIR LIQUIDE Advanced Technologies Division, 2 rue Clémencière, F-38360 Sassenage, France

The use of liquid xenon as radiation detector medium has been increased in the recent years. Its intrinsic physical properties, high density and atomic number, fast scintillation, high scintillation light yield and large ionization yield, make liquid xenon very efficient for gamma-ray detection in the energy range from hundreds of keV to tens of MeV. For this reason, it has been used in numerous applications in particle physics, astrophysics and medical imaging.

SUBATECH laboratory has successfully developed a liquid xenon time projection chamber, named XEMIS1 (Xenon Medical Imaging System), for 3D imaging. This new medical imaging technique allows to obtain a precise tridimensional location of a radioactive source with good temporal, spatial and energy resolutions.

The latest results obtained with this first prototype show a very good energy and spatial resolutions for the ionization signal in liquid xenon. We have achieved an energy resolution of 8.9% for 1MeV and an electric field of 1 kV.cm⁻¹ and a spatial resolution along the z-axis smaller than 100 μm. The incorporation of a segmented anode of 64 pixels provides a transversal spatial resolution of less than 1 mm. Updates in the technical characteristics have contributed to a high liquid xenon purity and very low electronic noise. Moreover attenuation lengths higher than 1 m are now currently obtained, which implies an important improvement in comparison to the first obtained results. The very positive results obtained for XEMIS1 have led to a second prototype for small animals imaging, XEMIS2, which is now under development (see figure). This second prototype is based on a full liquid xenon cylindrical camera totally surrounding the small animal. A complete Monte Carlo simulation using GATE has been developed for XEMIS2 in order to understand the performance of this new prototype. First results show a sensitivity of 2.7% and a spatial resolution of the order of 1 cm FWHM along the Line of Response (LOR). Good quality images have been obtained by simulated tomographic reconstruction for a very low administered dose. We target to inject only several tens of kBq during 20 minutes to image the whole animal.

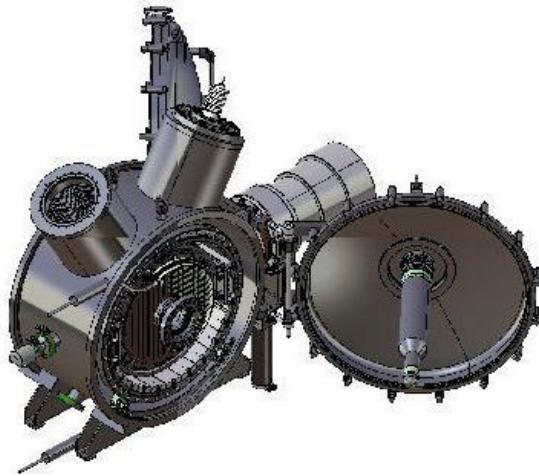


Figure 1. Design of the XEMIS2 Prototype.

Keywords: Compton Imaging, Liquid Xenon, 3 gamma

74

Development of a PET scanner simulation package for FLUKA

P. Garcia Ortega¹, T. Boehlen², F. Cerutti¹, M.P.W. Chin¹, A. Ferrari¹, C. Mancini¹, C. Morone³, P.R. Sala⁴, V. Vlachoudis¹

¹CERN, CH-1211 Geneva, Switzerland

²MedAustron, A-2700 Vienna, Austria

³University Rome Tor Vergata, Rome, Italy

⁴INFN Milano, Italy

Beyond well-established clinical applications, the proposed usage of positron emission tomography (PET) encompasses various applications at an investigational stage. The fast development of new radiotherapy techniques, like hadron-therapy, put in evidence the needs of a more precise diagnostics, achievable by a better image quality. For hadron-therapy, an accurate analysis of the distribution of activated positron emitters is employed to verify treatment delivery. Such novel applications necessitate detector development and design studies. For such purposes, Monte Carlo codes are fundamental tools in the first stages of detector designs. In this work, a dedicated package for PET scanner simulations is presented, using the general purpose Monte Carlo code FLUKA [1].

The simulation of radiation fields produced by ion beams in tissues with Monte Carlo codes, while accounting for nuclear interactions and processes, allows to predict the activity distributions in the field. The comparison of such distributions with the detected ones is the base of range verification using PET scanners. FLUKA is a fully integrated particle physics Monte Carlo simulation package widely used for an extended range of applications (accelerator shielding, detector and target design, calorimetry, activation, dosimetry, medical physics, radio-biology...). Its use for medical applications and activation studies is broad and recent model developments make it a suitable tool for nuclear medicine and hadron-therapy simulations.

The present package consists on an intuitive PET scanner geometry generator and a dedicated scoring routine for coincidence events. The geometry generator eases the construction of a PET detector with general parameters. The user can also benefit from multiple templates of commercial PET scanners provided within the interface. The scoring routine allows the user to store the output of the simulation either on a list mode or a binary *Interfile 3.3* file, which can be later analyzed with external reconstruction algorithms. Both tools are fully integrated in the FLUKA GUI *Flair* [2].

This dedicated package for PET simulations facilitates the simulations of new detectors for hadron-therapy or nuclear medicine, and inherits the predictive power of FLUKA. It helps to build a realistic simulation in an intuitive way, where further studies can be performed. At the same time, this works takes advantage of recent model developments and the inclusion of other medical-related tools in *Flair*, such as the DICOM to FLUKA voxel transformation tool, which allows the user to transform DICOM images into FLUKA geometry for simulation purposes.

Keywords: Monte Carlo codes, FLUKA, PET, Software

References:

- [1] A. Ferrari, P. R. Sala, A. Fasso , and J. Ranft, CERN, INFN, SLAC, CERN-2005-10, INFN/TC_05/11, SLAC-R-773, 2005.
- [2] V. Vlachoudis, Proc. Int. Conf. on Mathematics, Computational Methods & Reactor Physics (M&C 2009), Saratoga Springs, New York, 2009

75

A Biomedical Research Facility at CERN based on the Low Energy Ion Ring

A. Garonna, D. Ablter, C. Carli, J. Stafford-Hayworth, D. Kuchler, M. Dosanjh, S. Myers, P. Collier
CERN, Switzerland

The existing Low Energy Ion Ring (LEIR) at CERN will be maintained as a lead ion accumulator for the Large Hadron Collider (LHC) and for fixed-target experiments with the Super Proton Synchrotron (SPS). An additional secondary use of LEIR for a biomedical research facility was proposed [1-3]. Based on an existing infrastructure, this facility would provide the research community with relevant beams in a collaborative and cost-effective way. Research beam time availability would by far exceed that at other facilities throughout the world and allow more rapid progress in several biomedical areas, such as in: ion beam therapy, medical imaging, dosimetry and radioprotection.

Studies are undergoing to investigate the technical challenges linked to the feasibility of the project. The aim is to implement the simplest and most cost-effective configuration, compatible with the need to maintain the current operational performance of LEIR for LHC and SPS physics operation. Among the investigated solutions, a new dedicated front-end, comprising a commercial ion source and Radio Frequency Quadrupole (RFQ), would provide ion species from hydrogen to neon. These beams would be injected and accelerated in LEIR up to a magnetic rigidity of 6.7 Tm (corresponding to a kinetic energy of 440 MeV/u for fully stripped carbon ions). A new slow extraction scheme would be implemented in LEIR, by installing an electrostatic septum and two magnetic septa [4]. Finally, the construction of a low energy vertical beamline and a horizontal beamline would provide the users with a wide range of possibilities for experiments.

Keywords: Ion Beam Therapy, Hadrontherapy, Radiobiology, Dosimetry, Imaging

References:

- [1] Dosanjh M. et al., Br J Radiol 2013; 86:20120660.
- [2] Holzschetter M.H. et al., Radiother Oncol 2012; 105:1-3.
- [3] Position Paper of the Workshop on Physics for Health in Europe (PHEE-10), 2010.
- [4] Ablter D. et al., J Radiat Res. 2013; 54(Suppl 1) :i162-i167.

76

Digital Image Processing Techniques for Application in a Microbeam End-Station Microscopy

A. Georgantzoglou¹, M.J. Merchant², J.C.G. Jaynes², A.-C. Wera², R. Jena¹

¹Department of Oncology, University of Cambridge, Addenbrooke's Hospital, UK

²Ion Beam Centre, University of Surrey, Guildford, UK

Purpose: Charged particle therapy has emerged as a highly promising technique for cancer treatment. However, it is accompanied by uncertainty in correlation between the fluence of the particle beam and the biological cell damage. This ambiguity motivated the use of charged particle microbeams in the investigation of cellular radiobiological phenomena.

The Surrey Vertical Beamline was specifically designed for such purposes as it is capable of delivering precise amount of dose to single cells. It is supported by an end-station digital microscopy facility for cell imaging and, consequently, assessment of cell radiobiological response. A digital image processing technique has to be designed for automated cell recognition and targeting prior to irradiation as well as imaging of post-irradiation cell evolution.

Materials and Methods: Bright-field illumination microscopy of dish-plated cells was selected as an imaging method avoiding the photo-toxicity effects induced by fluorescence. A sophisticated image processing pipeline was designed to determine the cellular boundaries using the software MATLAB[®] (The MathWorks, Inc., Natick, MA). More specifically, wavelet decomposition with soft thresholding was used to denoise the acquired images, maintaining cellular internal structure. The next step included a combined top-hat transformation with edge detection followed by an adaptive threshold, eliminating the background intensities and undesired frequencies. Cell boundaries were, then, delineated using the convex hull while morphological operators produced the ultimate binary mask. Geometrical descriptors provided phenotypic information while statistical and textural features were extracted for further analysis.

Results: A cell segmentation process was successfully established. Cells were recognised and parameterised for further analysis. The accuracy of cell detection was tested for two different cell phenotypes, flat and round cells; sensitivity was found 0.938 and 0.979, respectively, while specificity was found 0.961 and 0.931, respectively. The processing time was (1.96 ± 0.09) seconds for each 512×512 pixels image providing a sensible performance. The whole process has been optimised for application on a series of images. Cells coordinates can be recorded and used for tracking in time-lapse microscopy.

Conclusions: An automated procedure for cell recognition and segmentation has been developed enabling high-throughput radiobiological experiments with unstained cells. Data from cells response to charged particle irradiation can be integrated in the treatment planning systems for additional optimization of dose delivery to tumours.

Keywords: microbeam, cell biology, image processing

Acknowledgment: The authors gratefully acknowledge the financial support of project ENTERVISION, funded by the European Commission under FP7 Grant Agreement N. 264552.

77

Motion compensated reconstructions in PET-based ion beam treatment verification for moving target

C. Gianoli¹, G. Baroni^{2,3}, J. Bauer^{4,5}, C. Kurz^{4,5}, K. Parodi^{5,6}, M. Riboldi^{2,3}

¹Department of Radiation Oncology, Heidelberg University Hospital, Germany

²Dipartimento di Elettronica, Informazione e Bioingegneria, Politecnico di Milano, Italy

³Bioengineering Unit, National Center for Oncologic Hadrontherapy

⁴Heidelberg Ion Beam Therapy Center, Germany

⁵Department of Radiation Oncology, Heidelberg University Hospital, Germany

⁶Ludwig Maximilian University of Munich, Germany

Purpose: This study investigates the effectiveness of two motion compensated reconstruction strategies in 4D PET-based ion beam treatment verification. Due to the extremely low count statistics, the independent (gated) reconstruction of 4D raw data does not result in clinically meaningful images. Both investigated strategies aim at the reconstruction of a motion compensated image making use of all the acquired raw data.

Materials and methods: The well-known 4D MLEM reconstruction was compared to an innovative motion compensation strategy able to provide motion compensated 4D sinograms. The advantages and limitations of both strategies were assessed and compared. Phantom activation studies were performed and a preliminary study on patient data was also considered.

Results: In presence of regular and rigid motion (Figure 1) the two motion compensated reconstruction strategies demonstrated similar performance. The advantages of the innovative strategy were demonstrated on patient data, where the motion model was characterized by 4D CT artifacts and lack of exact 4D CT-PET co-registration (also due to different 4D CT-PET sampling).

Conclusions: Initial results support the effectiveness of motion compensated reconstruction strategies in 4D PET-based ion beam treatment verification for moving targets. The advantages of the new proposed strategy will be further investigated in an envisioned clinical evaluation, where motion model artifacts due to motion irregularities could be observed.

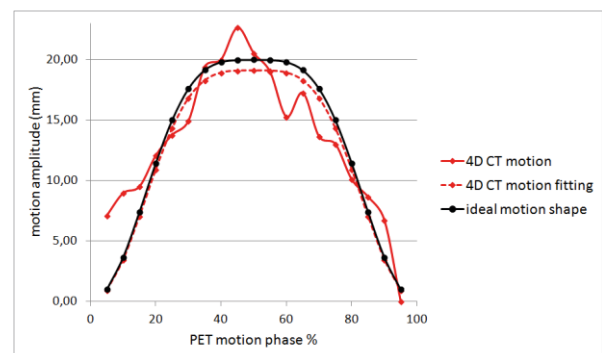


Figure 1. The 4D CT are interpolated on the spatial and temporal grids of the 4D PET, according to the specific motion function (\cos^4 for the reported phantom). The motion is measured by means of image registration.

Keywords: PET-based treatment verification, 4D PET imaging, moving target

Acknowledgements: This work is being supported by ENVISION EU FP7 program.

78

The Higgs boson and our life

F. Gianotti
CERN, Switzerland

On 4 July 2012, the ATLAS and CMS experiments operating at the CERN Large Hadron Collider (LHC) announced the

discovery of a new particle compatible with the Higgs boson (hunted for almost 50 years), which is a crucial piece for our understanding of fundamental physics and thus the structure and evolution of the universe.

This talk describes the unprecedented instruments and challenges that have allowed such an accomplishment, the physics meaning and relevance of this discovery, and the implications for our day-by-day life.

79

Reduced side effects by proton microchannel radiotherapy - study in a human skin model

S. Girst¹, G. Dollinger¹, C. Greubel¹, G. Multhoff², J. Reindl¹, T.E. Schmid², C. Siebenwirth¹, J.J. Wilkens², O. Zlobinskaya²

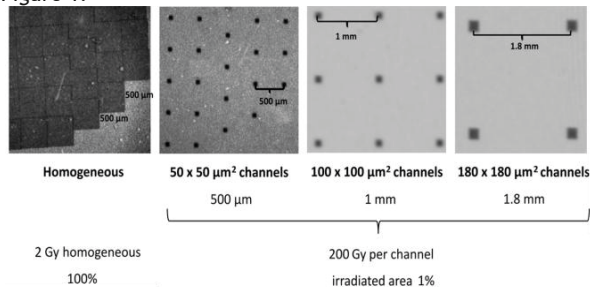
¹Universität der Bundeswehr München, Neubiberg, Germany

²Klinikum rechts der Isar, Technische Universität München, München, Germany

Purpose: Here, we propose a novel strategy to reduce the known side effects of radiotherapy by using proton microchannel irradiation. The goal is to minimize the risk of normal tissue damage by microchannel irradiation, while preserving local tumor control through a homogeneous irradiation of the tumor that is achieved because of beam widening with increasing track length. In order to prove the hypothesis of reduced side effects in normal tissue through microchannel proton irradiation, we report on a comparative study of microchannel and broad beam irradiation of artificial skin tissue.

Methods: 20 MeV protons were administered to human skin models (EpidermFT™) in 10 to 180 μm wide irradiation channels on a quadratic raster with distances of 500 to 1800 μm between each channel (center-to-center) applying an average dose of 2 Gy. For comparison, other samples were irradiated homogeneously by protons at the same average dose. Widened channels as in deeper lying tissues were investigated in skin tissues as well. The figure shows the irradiation fields of 20 MeV protons with a mean dose of 2 Gy visualized by Gafchromic films.

Figure 1.



Results: Normal tissue viability was significantly enhanced after microchannel proton irradiation compared to homogeneous irradiation (~80% vs. ~40% viability (MTT)). Levels of inflammatory markers, such as cytokines and chemokines, were significantly lower in the supernatant of the human skin tissue after microchannel irradiation than after homogeneous irradiation. Furthermore, genetic damage as determined by the measurement of micronuclei (MN) in keratinocytes was also significantly reduced after microchannel irradiation compared to homogeneous irradiation (0.015-0.030 micronuclei per divided cell for microchannel vs. 0.070 ± 0.007 MN/divided cell for homogeneous irradiation).

Conclusion: Our data show that proton microchannel irradiation maintains cell viability while significantly reducing inflammatory responses and genetic damage compared to

homogenous irradiation, and thus might improve normal tissue protection after radiation therapy.

Keywords: proton therapy, microbeam, spatial fractionation

Acknowledgements: Supported by the DFG Cluster of Excellence: Munich-Centre for Advanced Photonics.

References:

Zlobinskaya, Girst et al., Radiat. Environ. Biophys. 52, 123-133 (2013)

80

ProXY - High performance monolithic pixel tracker for proton tomography

P. Giubilato^{1,2}, D. Bisello^{1,2}, S. Mattiazzo¹, D. Pantano¹, N. Pozzobon^{1,2}, W. Snoeys³, J. Wyss^{2,4}

¹Padova University, Italy

²INFN Padova, Italy

³CERN, Switzerland

⁴Cassino University

In recent years the use of hadrons (¹H and ¹²C ions) for cancer radiation treatment has steadily grown in importance. To fully exploit the therapeutic advantages offered by hadron therapy, precise body imaging for accurate beam delivery is decisive. Proton Computed Tomography (pCT) scanners could provide the ultimate in 3D imaging for hadrons treatment guidance. The pCT capability of distinguish tissues density is in fact a key factor to fully exploit the protons intrinsic targeting precision. At the core of a pCT scanner is the protons tracker, which defines the scanner performances and ultimately limits its maximum speed.

This work describes a novel proton tracking detector design (dubbed ProXY) which would increase the current scanning speed by more than a factor 100, being able to handle a particle flux of more than 50 MHz cm⁻² over an area of 250 cm². This leads to record 10⁹ proton tracks (entry point, exit point and exit angle for each particle), the quantity of information necessary to reconstruct the complete 3D image of a head-size target, in less than 1 second. This has to be compared with the minutes-long exposures necessary with present state of the art technology. Together with the increased speed, the proposed detector offers higher tracking spatial resolution (equal or better than 10 μm) and lower material budget (by a factor 10) respect to present tracking sensors, leading to further performances enhancement. Very important for a viable clinic system, the production costs will be lower than for existent and currently in-development systems, as the detector has been designed to be realized with commercially available CMOS technology instead of custom-made processes. The very same commercial technology actually offers the possibility to produce the large area sensor necessary for a pCT scanner directly at the foundry.

Such broad advancement in performances is achieved by employing a completely new proprietary architecture to effectively sparsify the data inside the detector itself and the very latest development in Monolithic Active Pixel Detectors to build high granularity, low material budget large area silicon detectors. Characteristic, performance and the underlying technology of the ProXY design will be illustrated and discussed in the contribution, together with consideration on how they could impact the development of protons Computed Tomography.

Keywords: Proton Therapy, CMOS, Proton Tomography

81

Adaptive radiotherapy for head & neck squamous cell carcinoma

V. Gregoire

Dept. of Radiation Oncology & Center for Molecular Imaging, Radiation & Oncology, Université catholique de Louvain, St-Luc University Hospital, Brussels, Belgium

In Radiation Oncology for Head and Neck tumors, conformal treatment with IMRT has been recently demonstrated to be the standard of care. However, target volumes (TV) and organs at risk (OAR) are typically delineated on pre-treatment CT or MR images. This is obviously a simplification, as patient's external contours, TVs and to a lesser extent OARs will likely change during treatment.

Tracking the reduction in TV during IMRT offers the prospect of a progressive cone down of the irradiated volume, thus leading to a progressive dose reduction in the non-target tissues with potential decrease in treatment morbidity. In addition, adaptive radiotherapy could also potentially allow for a dose increase to the tumor, thus potentially leading to better local control. A proof of concept study performed in our group in a series of HNSCC have shown that after a mean dose of 46 Gy (of 70 Gy) the primary tumor GTV assessed with CT and MR had substantially decreased leading to subsequent reduction of the high dose volume. A subsequent study has shown that the use of FDG-PET, which allows a more accurate delineation of the primary tumor GTV, could further reduce the high dose volume.

Adaptive radiotherapy requires the use of a very strict methodology for image acquisition, image segmentation, and volume and dose registration. For volume segmentation of FDG-PET images, recent data have shown that gradient-based methods are more powerful to distinguish between residual tumor activity and peri-tumoral inflammation induced by treatments. It is likely that non-rigid methods will be required for registering the various sets of images acquired during treatments. Also, the summation of dose during treatment when deformation of anatomic structures is likely to affect the expected dose distribution, still remain an unresolved issue. Last, outcome research to demonstrate the clinical benefit of adaptive IMRT is presently lacking.

During the lecture, the various issues of adaptive IMRT in Head and Neck tumors will be reviewed and illustrated with original data from the presenting author's group.

82

An example of the integrated model: the EORTC DAHANCA-1219 trialV. Gregoire¹, J. Overgaard², E. Shash³

¹Dept. of Radiation Oncology & Center for Molecular Imaging, Radiation & Oncology, Université catholique de Louvain, St-Luc University Hospital, Brussels, Belgium

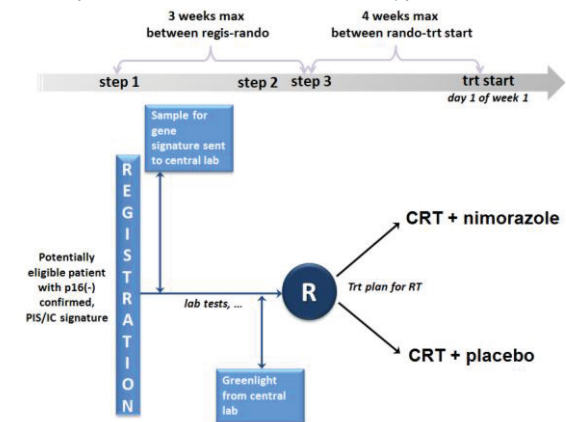
²Department of Experimental Clinical Oncology, Aarhus University Hospital, Aarhus, Denmark

³EORTC Data Center, Brussels, Belgium.

Head and neck cancer is the 5th common malignancy worldwide, and among these tumors locally advanced squamous cell carcinoma of the head and neck (HNSCC) are the most frequent. The treatment of such locally advanced HNSCC is predominately radiotherapy, alone or combined with simultaneous chemotherapy. Several biological modifications of radiotherapy of HNSCC have markedly improved the outcome in form of both locoregional control, disease specific and overall survival. These modifications include the use of altered fractionation (i.e. accelerated and hyperfractionation), hypoxic modification and concomitant chemo-radiotherapy. Recently a 15-gene hypoxia classifier has been identified and tested retrospectively in 323 patients with head and neck carcinoma treated with radiotherapy and either placebo or nimorazole in the DAHANCA-5 protocol. The

classifier has been demonstrated to be an efficient tool to categorize tumors for their hypoxic status and therefore responsiveness to combination treatment with radiation and hypoxic modifier.

In this framework, DAHANCA and EORTC decided to join forces to conduct an international randomized trial aiming at evaluating in a blinded randomized trial, whether the hypoxic cell radiosensitizer nimorazole can improve the effect of primary curative accelerated fractionated concomitant chemo-radiotherapy with concomitant cisplatin given to patients with locally advanced HPV/p16 negative HNSCC. Patients will be stratified according to their gene signature of hypoxia to investigate if the hypoxic gene profile can predict which patient benefit from the use of hypoxic cell sensitizer.



Several translational research studies will be associated to this clinical trial aiming at identifying other molecular markers of radioresponsiveness, and at testing the use of hypoxic PET tracers for patient selection.

83

Evaluation of existing ripple filter designs for clinical use at the MedAustron ion beam therapy facility

L. Grevillot, S. Vatnitsky

EBG MedAustron GmbH, Wiener Neustadt, Austria

Purpose: Ripple filter is commonly used in active scanning delivery systems at carbon ion beam therapy facilities. The main function of this device is to reduce the number of energy layers required to produce a homogeneous dose distribution in the target volume, by increasing the width of pristine Bragg peaks of carbon ions. The purpose of this study was to evaluate different ripple filter designs, focusing on their clinical implementation at MedAustron.

Materials and methods: The existing ripple filter designs implemented at ion beam therapy centers have been reviewed. Preliminary Monte Carlo simulations based on the GATE/GEANT4 code have been performed for the selected ripple filter designs, in order to identify their performances. Further measurements have been conducted for a limited set of carbon ion energies, in order to verify the Monte Carlo investigations. Based on these measurements, a realistic Monte Carlo model of the beam delivery has been developed and used to extrapolate the ripple filter transfer function at any available energy.

Results: Two ripple filter designs have been selected. The design of the ripple filters and the manufacturing process are dependent on carbon ion beam energy and are especially sensitive to low energy carbon ions. Monte Carlo simulation was found to be a very useful tool in the selection process. It allowed to prepare an effective test plan for the evaluation of the selected ripple filter prototypes with clinical beam and also to extrapolate the limited set of measurements to any type of foreseen clinical situation, without use of additional beam time.

Conclusion: The preparation of the medical commissioning process of a new ion beam therapy facility has to be anticipated long before the first beam is available at the facility. Due to the complexity of the ion beam therapy commissioning process, most of the centers are employing independent Monte Carlo calculations, considered as the gold standard in medical physics. The Monte Carlo method has been successfully used at MedAustron in the evaluation of existing ripple filter designs. Further studies including a complete model of the MedAustron nozzle are intended, in order to continue the preparation of the procedures for medical commissioning of the facility and to speed up the execution of the commissioning process, by significantly reducing the amount of required beam time.

Keywords: Ripple filters, Simulation, GATE/GEANT4

84

Comparing Ion Computed Tomography under clinical constraints

D.C. Hansen¹, N. Bassler^{1,2}, J.B. Petersen³, J. Seco^{4,5}

¹Department of Experimental Clinical Oncology, Aarhus University, Denmark

²Department of Physics, Aarhus University, Denmark

³Department of Medical Physics, Aarhus University Hospital

⁴Massachusetts General Hospital, USA

⁵Harvard Medical School, USA

Purpose: To develop a robust methodology for comparing the image quality of ion computed tomography (ion-CT) and use this to compare protons, helium and carbon ions for imaging.

Methods: A digital phantom was created in the Monte Carlo code Geant4. This consisted of 15 cylindrical inserts for estimating stopping power accuracy and one cylindrical box of cortical bone to evaluate resolution. The cylindrical inserts were made of tissue and bone-like materials.

Ion CT scans of the phantom were simulated with 360 distinct angles, using 4 different scenarios: protons at 230 MeV and 330 MeV, helium ions at 230 MeV/u and carbon ions at 430 MeV/u. The energies were chosen based on available energies at particle therapy centers.

Doses for each of the scans were evaluated by the ion CT dose index (ICTDI). This is similarly to the CT dose index (CTDI) used in x-ray CT, but weighted with the LET-dependent quality factor of the ICRP.

Ion CT images were then reconstructed along cubic spline curves, using a proportion of the simulated ions equivalent to an ICTDI of 10mSv, which is similar to the doses given by x-ray CT.

Stopping power accuracy was evaluated from the cylindrical inserts and resolution via the edge spread function (ESF) gained from the box.

Results:

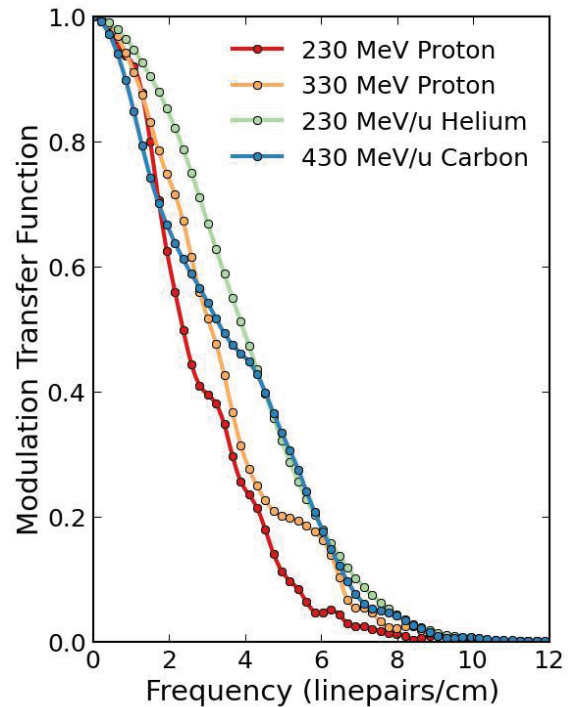
	230 MeV H	330 MeV H	230 MeV/u He	430 MeV/u C
MTF _{10%} (linepairs/cm)	5.15	6.50	6.95	6.67
Maximal systematic error (%)	0.36	0.48	0.34	4.47

230 MeV protons demonstrated the lowest resolution of 5.15 linepairs/cm, with 230 MeV/u helium ions having the highest resolution of 6.95 linepairs/cm. Helium ions had the smallest maximal systematic error (MASE) of 0.34% and carbon ions the highest of 4.47%. The two proton cases had a systematic error 0.36% for the 230 MeV and 0.48% for the 330 MeV.

While carbon ions could be expected to show the highest resolution and smallest error, the it also deposits the most dose per ion track. In addition, a large percentage of the carbon ions are lost to nuclear interactions. At even lower dose levels, it is expected that helium ions would show a similar behavior.

Conclusion: We have presented a new method for comparing ion CT implementations and shown that helium ions yield the

highest resolution and most accurate reconstruction at clinically acceptable dose levels. 330 MeV protons gave a better spatial resolution, but a lower accuracy than 230 MeV protons. Carbon ions were not able to predict the stopping power with an accuracy of less than 1% at these dose levels. This might be alleviated by using more advanced reconstruction techniques such as total variation.



85

Prediction of β^+ -activity distributions from PT-PET by means of a yield approach

S. Helmbrecht¹, W. Enghardt¹, M. Priegnitz², F. Fiedler²

¹TU Dresden, OncoRay - National Center for Radiation Research in Oncology, Germany

²Helmholtz-Zentrum Dresden-Rossendorf, Germany

Purpose: Particle therapy PET (PT-PET) is a clinically approved method for verification of ion beam therapy. The evaluation of the obtained images is performed by means of a comparison of the measurement and a prediction. A new approach for the simulation of the activity distribution using measured yields in reference materials has recently been suggested [1]. This approach provides the possibility to take the elemental composition of the different tissues into account without the use of any nuclear cross section. In this work first results of simulation in real patient cases are presented.

Materials/methods: The amount of β^+ - emitting isotopes, that are created during irradiation with carbon ions has been measured in water, graphite and polyethylene as a function of depth, initial energy and amount of substance [1]. These materials allow the modeling of ¹⁰C, ¹¹C, ¹³N and ¹⁵O.

A pencil beam algorithm for the simulation of the activity distribution, making use of these yields has been implemented. The software code is based upon an existing simulation which does not take into account the individual composition of different tissues [2]. This conventional simulation is a condensed history code, which applies the result of a Monte Carlo calculation of β^+ - emitters in polymethyl methacrylate to patients.

To apply the yields in the reference materials to patient cases, a biunique conversion of the elemental composition of human tissues to a composition from the reference materials has been established.

Since the measured yields do not contain any information on the lateral properties of the beam, a model for the spread caused by multiple Coulomb scattering in thick targets [3] has been implemented. The width of the beam as provided by the accelerator is taken from the accelerator beam parameters. Furthermore, an extended analytical model for the positron range distribution around the emitting isotopes has been included in the software [4].

For comparison in-beam PET measurements were used, which were acquired by means of a detector system installed at the irradiation site in the framework of the carbon therapy project at GSI Helmholtzzentrum für Schwerionenforschung [5].

Results: Figure 1 shows the measured activity distribution (a), the conventional condensed history MC simulation (b) and the yield based simulation (c) of a patient suffering from a skull base tumor in coronary view. The iso-activity lines have a distance of 10%. The PTV is shown in pink. The yield based simulation produces a reasonable activity distribution. Compared to the conventional code, a superior accordance is observed.

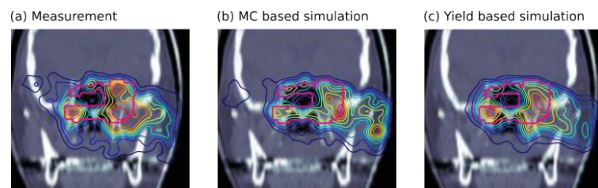


Figure 1.

Conclusions: The prediction of the B^+ activity distribution by means of the yield approach is feasible. The consideration of the elemental composition increases the quality of the activity prediction.

Keywords: PT-PET, simulation, in-vivo dosimetry

References:

- [1] M Priegnitz et al: *IEEE Trans Nucl Sci*, 2012, 59, 77-87
- [2] F. Pönisch et al: *Phys Med Biol*, 2004, 49, 5217-5232
- [3] B. Gottschalk et al: *Nucl Instrum Meth B* 1993, 74, 467 - 490
- [4] M. Palmer et al: *IEEE Trans Nucl Sci*, 2005, 52, 1391-1395
- [5] W. Enghardt et al: *Nucl Instrum Meth A*, 2004, 525, 284-288

86

Iterative Reconstruction of Clinical Electron Beam Phase Space for Intra-Operative Radiation Therapy

E. Herranz¹, J.M. Udías¹, P. Ibañez¹, J.L. Herraiz¹, M. Pérez-Liva¹, M. Vidal¹, P. Guerra²

¹Grupo de Física Nuclear, Dpto. Física Atómica, Molecular Nuclear, UCM, CEI Moncloa, Madrid, Spain

²Department of Electronic Engineering, ETSIT, Universidad Politécnica de Madrid, Madrid E-28040 Spain

Purpose: The Monte Carlo (MC) method is suitable to model realistic electron beams produced by linear accelerators, including those used in Intraoperative Radiotherapy (IORT). However, MC calculations require a realistic and reliable description of the particle beam that delivers the dose, which is not readily available. We introduce a phase space (PHSP) determination procedure driven by dose-measurements in reference (homogeneous) materials. Beam characteristics, i.e. energy spectrum, angular and radial distribution and particle type are derived without detailed information about the accelerator head. Further, the

optimization process and the measurements should be simple enough in order to be performed at a typical medical physics service.

Method: The PHSP is expressed in the following variables: particle type, energy, radial position of emission and angle with respect to the applicator axis. Instead of optimizing only the energy or a reduced set of variables of the PHSP, as it is often done, all the degrees of freedom of relevance are included in the optimization problem. To make the problem amenable for computation, the PHSP is discretized into about 250000 bins or elementary sources (for a given value of energy, radial distance to axis and emission angle), whose individual dose contribution in water or air can be computed once and stored. Dose distributions were pre-computed with the MC code Dose Planning Method (DPM) [1]. Computation time was about a week using 32 cores of modern CPUs (Xeon, 3 GHz). The iterative reconstruction of the PHSP amounts then to determine the linear combination of doses that describes the doses in homogeneous phantoms made either of air or water. To this end, an iterative algorithm (EM-ML) has been employed [2]. This second phase takes a few minutes in 1 core of a 3 GHz CPU.

Results: The PHSP files have been analyzed in terms of energy spectra, angular distribution, and fluency to assess the reliability of the results obtained after minimization. The dose obtained from the PHSP is in good agreement with pseudo-data obtained from simulated accelerators and with reference experimental data. Agreement with data not included in the optimization procedure is also good.

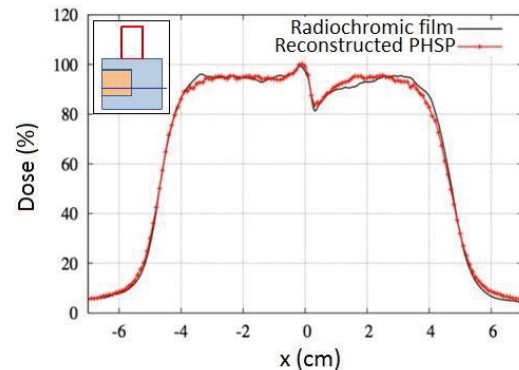


Figure 1. Comparison between the experimental dose profiles measured with Radiochromic EBT2 film, and the one produced by the PHSP reconstructed from measurements in air and water. A profile on an heterogeneous phantom of water and cork (simulating mediastinum region) is shown.

Conclusions: Reasonable PHSP which are in agreement with dose measurement can be obtained in very moderate computational times and, at the reconstruction site, without the need for detailed MC knowledge. The method is a new and powerful technique that can be employed to obtain PHSP files for any accelerator for radiotherapy system.

Keywords: Intraoperative radiotherapy, Monte Carlo simulations, dose calculation

References:

- [1] Sempau J. et al. 2000 *Phys.Med.Biol* 45:2263-91
- [2] Herraiz J.L et al. 2006 *Phys.Med.Biol* 51:4547-65

87

Compton imaging in proton therapy: reconstructed images compared to simulated prompt- γ distribution

E. Hilaire¹, C. Robert², X. Lojaco¹, D. Sarrut¹, I. Buvat², F. Peyrin^{1,3}, V. Maxim¹

¹CREATIS, Villeurbanne, France

²IMNC

³ESRF

Purpose: In proton therapy cancer treatments, interactions between the beam and the patient's body lead to nuclear reactions that produce secondary prompt- γ radiation. It was shown that some correlation exists between those photons and the Bragg peak position, and works are ongoing to design imaging systems in order to monitor the deposited dose by exploiting prompt- γ . Teams obtained encouraging results on the performance of the Compton camera for in vivo dosimetry in hadron therapy.

The Compton camera detects a photon in two steps. The photon is scattered (at least once) in a first detector (in silicon in our case), then it is absorbed in a second detector (in LYSO). The hits, recorded with positions and energies, define an event. For each event, a Compton cone is defined and the incoming path of the initial ray lies on its surface. The image of the source is then calculated by tomographic reconstruction from projections calculated on conical surfaces.

The goal of this work is to assess the ability of the reconstruction algorithms to faithfully calculate the image of the prompt-gamma distribution.

Methods: An isotropic line source emitting 1 MeV photons was placed in a water box. We simulated the acquisition process with GATE (Jan et al, 2011), based on the GEANT4 Monte Carlo toolkit.

Photons that interacted at least once in the scatterer and in the absorber were selected after the end of the simulation. The path of the photon in the camera was calculated from the statistically disturbed measures, by a software called MEGALib (Zoglauer et al, 2006).

Finally, we reconstructed the 3D image using either an analytic filtered back projection method (Lojaco et al, 2011) or a list-mode MLEM (LM-MLEM) method. Unlike the analytic method, the LM-MLEM algorithm allows to include a model for the energy measurement errors.

Preliminary Results:

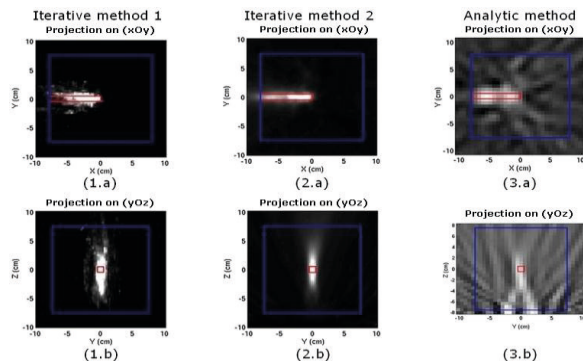


Figure: Projection images of a line source reconstructed from different methods. (1. a-b) Iterative method ignoring measurement errors. (2. a-b) Iterative method modeling energy measurement errors with a Gaussian. (3. a-b) Analytic method.

The reconstruction methods showed promising results, although elongation artifacts, specific to Compton camera imaging, are observed. Because the analytic method involves a tradeoff between resolution and image quality, the results (3) are worse than the LM-MLEM ones (1 & 2). The latter are improved when the uncertainties on the energy measures are modeled (2) compared to not accounting for them (1).

Conclusion: The images of a source in a phantom are promising, although more effort has to be put in the development of the reconstruction algorithms in order to

reduce the artifacts from the images. In a future work, we will investigate the possibility to reconstruct the image of the prompt-gamma distribution from a simulated treatment plan. Imaging the prompt- γ distribution is important in proton and hadron therapy. The comparison between the reconstructed and the simulated distributions will hopefully open a way to validate the ability of Compton imaging to accurately monitor the Bragg peak position.

Keywords: proton therapy, Compton imaging, tomographic reconstruction

88

ESI's Scientific Schools: a privileged place for knowledge transfer

H.F. Hoffmann

ESI, Switzerland

The European Scientific Institute (ESI) at Archamps Technopole offers three schools:

JUAS, the Joint Universities Accelerator School, since 1994, on the physics, technologies and applications of particle accelerators

ESMP, the European School of Medical Physics, since 1998, on medical imaging, medical informatics, radiotherapy and radioprotection, organised together with EFOMP, the European Federation of Organisations in Medical Physics

ESIPAP, the European School of Instrumentation for Particle and Astro-particle Physics, since 2014, on particle detectors, data acquisition and data analysis

The schools profit from the availability and interest of high level experts from CERN, Universities involved CERN programmes, University Hospitals and industry.

The courses address particular subjects in modular fashion, consisting of high level lectures, practical work and examinations and addressing Master or PhD, physics or engineering students interested in the particular subject of their school.

ESI strives to have its formation widely recognised within the European Credit Point System (ECTS) or the European Lifelong Learning programmes.

Since almost 20 years ESI has delivered courses to ~1500 participants from the European Union, Eastern European and Mediterranean Countries.

ESI further considers offering short (long weekend) high level lecture modules for professionals:

Lecturing on the latest theoretical and practical developments in particular fields and

Discussing in panels potential new directions or desired developments in these domains

The poster will present ESI and its schools in detail.

89

The vascular supply and micro-environment of tumours and their significance for cancer therapy

M. Horsman, M. Busk

Dept. Experimental Clinical Oncology, Aarhus University Hospital, Aarhus, Denmark

The growth and development of animal and human solid tumours requires an adequate supply of oxygen and nutrients. When tumours first arise this function is provided by the vascular supply of the host tissue in which the tumour originates. But, as the tumour grows the host vasculature cannot meet these demands, thus tumours form their own vascular supply, from the host vessels, through the process of angiogenesis. However, the essential neo-vasculature that develops is a primitive and chaotic system that has numerous structural and functional abnormalities compared to normal vessels, so it is still inadequate. As a result, micro-regional areas are formed within the tumour which are oxygen deficient, nutrient deprived and highly acidic. Such regions are a characteristic feature of animal and human solid

tumours. Surprisingly, tumour cells can actually survive these adverse conditions and play a crucial role in the development of acquired treatment resistance and are a major driving force for malignant progression by promoting loco-regional invasion of cancer cells and metastatic spread to distant sites. Substantial effort is now being made to image the tumour micro-environment and identify this cell population, thus allowing us to not only predict outcome to therapy, but also select appropriate methods to eliminate these cells. The fact that the tumour vascular supply is grossly different from the normal host vasculature makes it a unique target, thus effort is also being made to image and identify approaches for specifically targeting the vasculature. Current techniques for non-invasively imaging tumour micro-environmental parameters have focused on the use of positron emission tomography (PET), magnetic resonance imaging/spectroscopy (MRI/MRS), or computer tomography (CT). For imaging vasculature the methods of choice appear to be primarily MR based. With regard to targeting tumour vasculature then numerous agents have been developed that either inhibit the angiogenesis process or disrupt the already established tumour vessels and many of these treatments have undergone clinical evaluation. The major target from a micro-environmental perspective is hypoxia and numerous attempts have been made to simply reduce the level, sensitize them to radiation, or just kill this population. More recent suggestions have focused on modifying the radiation treatment to overcome the resistance. While all these approaches will work extremely well against primary tumours, their effects on metastatic disease would be more limited and other approaches, such as inhibition of hypoxia induced signalling mechanisms, are being considered. In this presentation we will review the current status of research on imaging and targeting the tumour micro-environment and vasculature.

90

Comparison of Scintillation Detectors based on BGO and LSO for Prompt Gamma Imaging in Particle Therapy

F. Hueso-González¹, D. Bemmerer², M. Berthel¹, A.K. Biegun³, J. v. Borany², P. Dendooven³, A. Dreyer¹, W. Enghardt^{1,2}, F. Fiedler², C. Golnik¹, K. Heide², T. Kormoll¹, J. Petzoldt¹, K. Römer², K. Schmidt², R. Schwengner², A. Wagner², L. Wagner², G. Pausch¹

¹Technische Universität Dresden, OncoRay, Händelallee 28 / PF 41, 01307 Dresden, Germany

²Helmholtz-Zentrum Dresden-Rossendorf (HZDR), Bautzner Landstraße 400, 01328 Dresden, Germany

³University of Groningen, Kernfysisch Versneller Instituut (KVI), Zernikelaan 25, 9747, The Netherlands

Purpose: Particle range verification is a major challenge for the quality assurance of particle therapy. One approach promising range access and dose quantification in real-time is the measurement of the prompt gamma rays resulting from interactions of the therapy beam with nuclei of the tissue. A Compton camera based on multiple position sensitive gamma ray detectors, together with an imaging algorithm, is expected to reconstruct the prompt gamma ray emission density profile, which is strongly correlated with the dose distribution and particle range.

Materials and Methods: At Helmholtz-Zentrum Dresden-Rossendorf (HZDR) and OncoRay, various Compton-imaging detector setups were tested. Semiconductor CdZnTe cross strip detectors were used for the scatter plane and PET block detectors with Lu₂SiO₅ (LSO) and Bi₄Ge₃O₁₂ (BGO) scintillators as absorbers, respectively. The data acquisition was based on VME electronics and handled by software developed on the ROOT platform. The tests were performed at the linear electron accelerator ELBE at HZDR, at the Tandem accelerator at HZDR and at the cyclotron AGOR at Groningen. The gamma rays measured at the different scenarios have

similarities in energy range and timing structure with the prompt gamma rays expected in a clinical cyclotron beam.

Results: Based on the different measurement campaigns, BGO and LSO scintillators are compared in terms of absorption efficiency, internal activity, price, energy, time and spatial resolution (see figure 1).

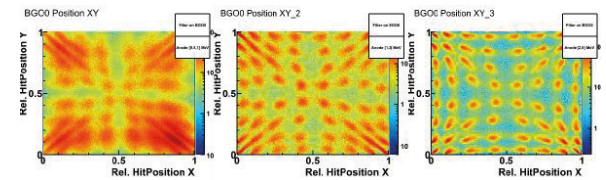


Figure 1 - Flood map of the BGO detector for different prompt gamma energy ranges (0.5-1 MeV, 1-2 MeV, 2-8 MeV), measured at AGOR proton beam with graphite as target. The crystal identification resolution improves significantly for high gamma ray energies (PGI scenario, 2-8 MeV) compared to low energies (PET scenario, <1 MeV).

Conclusions: The performance of BGO and LSO scintillators as absorber detectors is assessed for different energy ranges and the suitability of BGO as an alternative to LSO for a Compton camera aiming at prompt gamma imaging (PGI) is discussed.

Keywords: detectors and imaging, absorber, Compton camera, scintillator comparison

Acknowledgement: Supported by German Federal Ministry of Education and Research (BMBF-03Z1NN12), ENVISION and ENTERVISION (funded by the European Commission under FP7 Grant Agreement N. 241851 and N. 264552 respectively).



91

Harnessing laser-plasma accelerated ion beams for applications using Gabor lenses

C. Hughes¹, N.P. Dover¹, Z. Najmudin¹, J.K. Pozimski¹, J.S. Green², P.A. Posocco^{1,3,4}

¹Imperial College London, UK

²Rutherford Appleton Laboratory

³The Cockcroft Institute

⁴Gunnar Nilssons Cancerstiftelse

Intense beams of ions are generated when a high intensity laser pulse irradiates a solid target. There has been great recent interest in laser-plasma sources for medical applications such as radiotherapy due to the potential to create affordable, compact treatment devices. Laser-plasma ion sources create divergent beams, which may limit their practicality for many applications. Being able to capture and

focus laser-plasma ion sources would greatly increase the attraction of further development towards medical applications. One potential method of achieving this is to use a Gabor lens, which uses the space charge of a magnetically confined electron cloud to focus the laser-plasma accelerated proton beam.

To investigate methods to control the inherent divergence of the beams, we have experimentally characterised the proton beam generated by a laser-plasma source, in particular interactions of the Astra-Gemini laser at the Rutherford Appleton Laboratory with micron scale targets. The spatial and energy spectral characteristics of the beam were carefully measured using RadioChromic Film stacks. This beam distribution was then used as an input for beam transport simulations to optimise the design of the Gabor lens.

The Gabor lens was found to be an effective tool to capture and refocus the proton beam when the parameters of the lens were carefully chosen, and was able to focus a selected energy down to a \sim mm spot size. The beam transport simulations have guided the design of an experiment to fully demonstrate an integrated experiment with an initial aim of using the refocused beam for proton radiobiology experiments, a vitally important area of research in particular for proton therapy.

92

Monte Carlo modelling of whole-body secondary cancer risk for conventional and emergent radiotherapy

R. Hugtenburg, W. M. Al-Saleh
Swansea University, UK

Purpose: Secondary cancer is a significant late-effect associated with radiotherapy that is becoming increasingly prevalent, as improvements in technology lead to earlier diagnosis in younger patients and longer term outcomes. During the course of a radiotherapy, all parts of the body are exposed to doses upwards of 100 mSv, therefore such analysis must consider distal organs and incorporate accurate out-of-field dosimetry.

Methods: Conventional treatment planning algorithms are not sufficiently accurate to predict out-of-field dose, and CT data, used for planning purposes, usually only covers the treatment site. Detailed Monte Carlo model of the source and of the energy deposition in a representative patient are used to calculate whole-body distributions of dose which are converted into risk according to models of cancer induction. The BEAMnrc and EGSnrc codes are used to calculate the dose from a therapeutic linear accelerator in combination with ICRU whole-body CT data-sets. Risk of second cancers as a function of dose are taken from the Life-span Study of the survivors of the A-bomb detonations in Hiroshima and Nagasaki, as well as epidemiological evidence from the use of radiotherapy in young cohorts, such as those receiving treatment for Hodgkin's lymphoma.

Results: The technique is used to analyse the distribution of secondary cancers for conventional and intensity modulated radiotherapy (IMRT) treatments of the prostate, in this case for a simplified model of risk that assumes linearity of risk with dose and homogeneous risk for all tissue (Figure 1). The data supports the observation that secondary cancers occur with the greatest frequency at treatment margins [1]. Risk for out-of-field doses are primarily due to leakage dose, which reflects differences in machine output and influenced by the treatment strategy, including use of small fields and attenuators such as physical wedges. Emergent IMRT therapies often use larger numbers of small fields, but in this the effect is mitigated by an absence of the wedged fields used in the conventional therapy. (Figure 1 to go here).

Conclusions: Methods have been developed for analysing the whole-body risk of secondary cancers. Patterns of incidence of secondary cancers can be analysed and, through an

improved understanding, mitigated in certain circumstances. The use of Monte Carlo modelling enables the dose distributions and contaminating constituents of complex and emergent therapies to be considered, including particle and mixed radiation therapies.

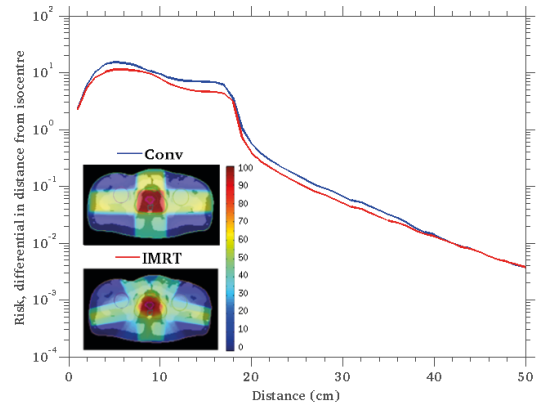


Figure 1: Relative risk as a function of distance from isocentre for typical conventional and IMRT prostate treatments, calculated for the ICRU male whole body phantom using Monte Carlo. The dose distribution at the lateral plane of the isocentre is shown in the inset.

Keywords: IMRT, Monte Carlo treatment planning, secondary cancers

References:

[1] Diallo, I, Haddy, N, Adjadj, E, *et al.* Frequency distribution of second solid cancer locations in relation to the irradiated volume among 115 patients treated for childhood cancer. *Int. J. Radiat. Oncol. Biol. Phys.* 74 (2009) 876-883.

93

Robustness of range prediction in proton therapy using prompt gamma emission

F. Janssen¹, G. Landry¹, K. Parodi², D.R. Schaart³, P. Cambraia Lopes³, F. Verhaegen¹

¹Maastricht Clinic, Maastricht, The Netherlands

²Ludwig Maximilians University, Munich, Germany

³Delft University of Technology, Delft, The Netherlands

In proton therapy, correct dose delivery is sensitive to patient positioning errors and anatomical changes. In-vivo imaging is a strategy to monitor the range of the protons inside the patient. A possible method of in-vivo imaging is detection of secondary 'prompt' gamma-rays outside the body, which are produced by proton-nuclear interactions inside the patient. A good understanding of prompt gamma emission under various circumstances, e.g. in different media and at different beam energies, is essential to develop a clinical technique to detect the range of protons inside the patient during treatment with desirable accuracy.

In this work, Monte Carlo simulations are performed with TOPAS [1], a Geant4 based Monte Carlo code, to determine the correlation between prompt gamma emission and the range of protons inside the body in different scenarios. Simulations are performed for several mono-energetic pencil beams, ranging from 50 MeV to 250 MeV, incident on homogeneous artificial phantoms with variable carbon and oxygen concentration, and changing density, to investigate the influence of those changes on the prompt gamma emission. Prompt gamma profiles are computed in a perfect cylindrical detector outside the phantom, with a filtering

angle of ± 3 degrees. Also prompt gamma profiles for a number of ICRU tissues have been studied.

To extract parameters from the noisy prompt gamma profiles (as in real measurements), a logistic regression model was used to fit the steep fall-off region of the profile, as can be seen in Figure 1.

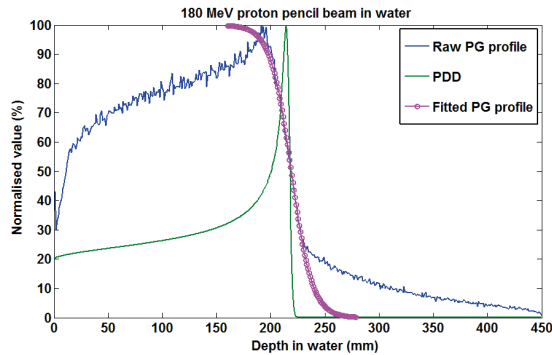


Figure 1: PDD (green), prompt gamma profile (blue) and a fit through the fall-off region of the prompt gamma profile (pink) for a 180 MeV proton pencil beam incident on a homogeneous cylindrical water phantom.

A strong correlation between the prompt gamma profile and PDD can be found in all cases. Nevertheless, this correlation is not identical under various circumstances. For various tissue densities, the shape of the fall-off region of the prompt gamma profile changes in a different way than the PDD.

Altering carbon and oxygen concentrations influence the excitation potential of tissue and the prompt gamma production threshold. This influences the position of the Bragg peak and the shape of the prompt gamma profile. The magnitude of prompt gamma emissions also changes due to the variation in carbon and oxygen concentration.

Varying incident beam energy leads to a small change in shape of the fall-off region of the prompt gamma profile. These results indicate that tissue properties need to be taken into account with care, to be able to make an accurate correlation between prompt gamma profile and proton range inside the body.

Keywords: (up to 3 excluding session name): proton therapy, prompt gamma emission, range prediction uncertainties

References:

[1] J. Perl *et al.*, *Med. Phys.*, 39 (2012) 6818-6837

94

Precision in prompt gamma-based range monitoring of proton pencil beams in heterogeneous media

G. Janssens¹, A. Celani², E. Clementel³, C. Fiorini^{4,5}, T. Frizzi², W. Enghardt⁶, S. Helmbrecht⁶, I. Perali^{4,5}, D. Prieels¹, M. Priegnitz⁷, F. Roellinghoff¹, J. Smeets¹, F. Stichelbaut¹

¹Ion Beam Applications SA, Louvain-la-Neuve, Belgium

²XGLab, Milano, Italy

³iMagX Project, ICTEAM Institute, Université Catholique de Louvain, Louvain-la-Neuve, Belgium

⁴Politecnico di Milano, Dipartimento di Elettronica, Informazione e Bioingegneria, Milano, Italy

⁵INFN, Sezione di Milano, Milano, Italy

⁶OncoRay-National Center for Radiation Research in Oncology, Medical Faculty Carl Gustav Carus, TU Dresden)

⁷Helmholtz-Zentrum Dresden-Rossendorf, Germany

Purpose: Proton therapy has the advantage of sparing the tissues located beyond the Bragg peak. However, this advantage is hampered by the uncertainty on the position of

the Bragg peak due to anatomical changes and tissue composition. In practice, safety margins are used to cope with the range uncertainties. Such margins could be reduced thanks to online range monitoring based on prompt gamma imaging. A precision of 1-2 mm in realistic conditions was previously demonstrated in a homogeneous phantom by means of range monitoring with a slit camera [1]. The purpose of this study was to investigate the impact of typical tissue heterogeneities on the range retrieval precision.

Materials and methods: In this study, we considered a knife-edge slit camera made of a 4 cm-thick tungsten collimator and a detector composed of 20 LYSO slabs of 5 mm. The distance between the beam axis and the detector was of 30 cm, and the collimator was located halfway in-between. Typical clinical cases of head-and-neck as well as lung irradiation have been identified and simplified in order to generate 1D-heterogeneous virtual phantoms. The delivery of pencil beams and the corresponding gamma detection profiles were simulated using the MCNPX Monte-Carlo software. The detection profiles were then filtered in order to reduce the noise. Different range shift estimation methods based on a matching of the simulated detection profile with the expected detection profile were tested and compared. This included absolute difference, root-squared difference, mutual information, local phase difference and single-point matching. Similar configuration was implemented using a PMMA phantom and measurements were performed in clinical conditions using a full-size camera prototype.

Results: The results of the simulations showed that a range retrieval precision (1 sigma) better than 2 mm could be achieved in most cases, down to 3 cGy per pencil beam. Overall, the best performing matching method was based on the squared-root difference between detected and expected profiles after Gaussian smoothing of 20 mm FWHM. However, the best method differed from case to case. Furthermore, the case of a pencil beam expected to stop 4 mm beyond an air cavity lead to systematic failure of all range retrieval methods, due to the lack of signal coming from the cavity. This was confirmed by the measurements.

Conclusion: Prompt gamma imaging is able to monitor range shifts with sufficient precision for a single pencil beam of realistic dose in most cases. This could lead to a reduction of range-specific margins in proton therapy. The choice of the range retrieval method showed a significant impact on the overall performance of the system. However, the range of pencil beams that stop just beyond an air cavity could not be estimated.

Keywords: Proton therapy, Range verification, Prompt gamma imaging

Acknowledgment: This project received funding from the European Union Seventh Framework Program (FP7/2007-2013) under grant agreement nos 241851 (ENVISION) and 264552 (ENTERVISION).

References:

[1] Smeets J *et al.*, "A Prompt gamma imaging with a slit camera for real time range control in proton therapy", *Phys. Med. Biol.* 57 3371-405, 2012.

95

Medical radioisotopes from the Heavy Ion Laboratory, University of Warsaw

J. Jastrzebski¹, A. Bilewicz², J. Choiński¹, J. Chudyka³, K. Kilian¹, M. Łyczko², I. Mazur¹, P.J. Napiorkowski¹, A. Pękal¹, A. Stolarz¹, K. Szkliniarz³, A. Trzcńska¹, B. Waś⁴, W. Zipper³

¹Heavy Ion Lab., Univ. of Warsaw, Poland

²Inst. of Nucl. Chem. and Techn.

³Silesian University

⁴Inst. Nucl. Physics PAN

The Heavy Ion Laboratory of the University of Warsaw (HIL UW) currently operates two accelerators. The older machine, a K=160 home made cyclotron accelerates heavy ions from 4He up to 40Ar with energies up to 10 AMeV. It is used for a fundamental research program in nuclear physics, solid state physics, biology and detector testing. Its application to medical radioisotope production started about three years ago. The recently commissioned GE PETtrace medical cyclotron is intended mainly for the production of radioisotopes for Positron Emission Tomography (PET) but other diagnostic and therapeutic isotopes and radiopharmaceuticals are also being considered. They will be produced in the Radiopharmaceuticals Production and Research Centre belonging to the Laboratory and situated on the premises of HIL (see upper part of the attached figure) and equipped with a number of hot cells, automatic synthesis and dispensing units and quality control equipment.

The ^{211}At isotope is produced on the K=160 cyclotron with an internal target using the $^{209}\text{Bi}(+\text{He},2n)^{211}\text{At}$ reaction at 30 MeV bombarding energy. The production yield as a function of the bombarding particle energy was determined. The produced activity is transported to the Institute of Nuclear Chemistry and Technology where the ^{211}At is extracted from the Bi target and chemical research consisting of binding the ^{211}At to substance P, a peptide with a high affinity to the receptors of glioma cancer cells, is conducted.

Besides the most popular PET radiopharmaceutical fluoro-deoxy-glucose (FDG) which will be produced and distributed in collaboration with a commercial company, the production using the PETtrace cyclotron of other radiopharmaceuticals based on ^{18}F , ^{11}C and ^{15}O is in the preparatory, research phase. The close vicinity (about 500 m) of the Nuclear Medicine Department of the Warsaw Medical University, equipped with a modern PET-CT scanner, will facilitate the development of the diagnostics and research program even including the shortest lived radioisotope ^{15}O after the installation of an underground capillary line (in preparation). An important example of cyclotron beam use for non-PET radiopharmaceuticals will be research into an alternative (via accelerators) way of producing the most popular isotope in nuclear medicine, $^{99\text{m}}\text{Tc}$, presently obtained from the nuclear reactor produced $^{99\text{m}}\text{Mo}$ generator. This activity will be performed within a research contract with the International Atomic Energy Agency and will also be supported by the Polish NCBiR research funding agency.

As in a number of other nuclear physics facilities all around the world the medical applications program becomes of a prime importance for the Heavy Ion Laboratory of the University of Warsaw. We expect that the European Horizon 2020 initiative will facilitate more developed networking opportunities for this program.

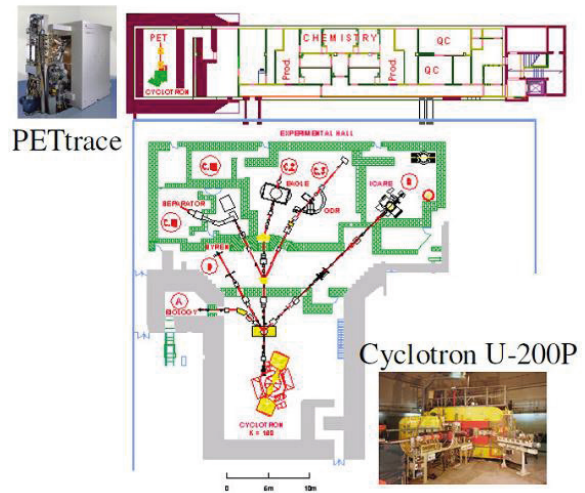


Figure 1: The layout of the University of Warsaw Heavy Ion Laboratory ground floor

Keywords: Medical radioisotopes

96

Target definition based on functional imaging

R. Jeraj

University of Wisconsin - Madison, USA

Accurate definition of the treatment target has been a fundamental problem in radiation therapy. Many decades ago it has been realized that heterogeneous tumors require heterogeneous dose targeting. However, the lack of sensible imaging modalities to assess tumor heterogeneity and the lack of technologies to deliver such highly-heterogeneous dose distributions has hampered developments of the patient-specific approach.

In this lecture we will specifically focus on the question how functional and molecular imaging can help to define which type of therapy should be used, as well as assess the spatial extent and heterogeneity of the tumor, thus providing grounds for more reliable target definition. Functional and molecular imaging has been shown to significantly reduce large inter-observer variability in target definition compared to anatomical imaging. This reduction leads to significant reduction in treatment margin, thereby enabling more accurate and precise tumor targeting.

Furthermore, functional and molecular imaging has the potential to characterize biological heterogeneity within tumors, providing foundations for so-called biologically conformal radiotherapy, or dose painting. While the enthusiasm for employment of functional and molecular imaging techniques to target patient-specific tumor biology remains high, the adoption of biologically-conformal radiation therapy has been rather slow. We will review some of the latest achievements and highlight some of the remaining challenges.

97

Proton Clinical Correlates: Patient Throughput & Cyclotron Availability

P.A.S. Johnstone¹, J. Kerstiens², I.J. Das¹

¹Indiana University, Indianapolis, USA

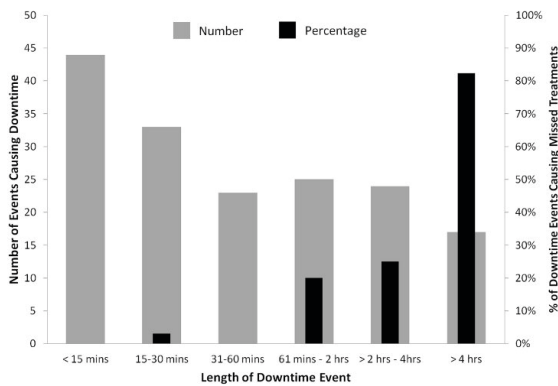
²IU Health Proton Therapy Center

Purpose: The large number of new proton therapy (PrT) facilities being built globally is indicative of the superior dose distribution with PrT; a healthy appreciation for the unique capacity of PrT to treat a broad variety of lesions; and the presumption that those cases will be referred away from

photon centers where they are already generating revenue. While data supporting viability of PrT for lesions throughout the neuraxis, and especially in children in general, are well described, the financial underpinnings of many US centers are rather weak.

Materials/Methods: Using data from the IU Health Proton Therapy Center (Bloomington, IN), we sought to describe the critical aspects of patient mix and treatment room throughput to repayment of construction and other fixed costs. The essential relationship of cyclotron availability to a functional PrT clinic was also investigated.

Results: We have modeled lost revenue by varying from a distinct case load of simple (including prostate cancer) procedures. A case mix involving complex patients or sleeping children has high opportunity costs because of the relatively low patient throughput. Most losses of cyclotron availability are of <1 hour duration; these infrequently cause treatments to be missed. However, about a tenth of down times exceed 4 hours: these have >80% likelihood of causing missed treatments. (Figure from JACMP 2012;13:134-146)



Conclusions: Patient mix and cyclotron availability both relate critically to treatment room throughput, and thus to potential revenue from a proton center.

Keywords: Proton Therapy, Facility financing, Availability

98 Towards simpler and better prediction of relative biological effect (RBE)

B. Jones¹, F. Fiorini¹, P. Posocco², M.A. Hill¹, R.G. Dale².

¹University of Oxford, UK

²Imperial College London, UK

Purpose: To develop a simple and robust method of predicting RBE from linear energy transfer (LET), which is not dependent on large numbers of assumptions and complex microdosimetry.

Materials/methods: The *in vitro* data sets of Todd, Barendsen, Belli and Weyrather *et al* are used since they extend over a large range of LET and include the turnover of RBE with LET, which is critical in the model. Simple energy transfer considerations are applied to optimum lethality probabilities based on LET_U (the LET value at the turnover point), considering increased efficiency at lower LET values beforehand and inefficiency above LET_U. The addition of a stochastic element can also be made using the Poisson distribution for one lethal event (discounting larger numbers of events as leading to increased inefficiency), which effectively caters for the use of a range of LET values within the beam. The required input parameters are the separate low LET α and b parameters of the linear quadratic model and the nuclear charge (z) of the ion species, which controls the LET_U value.

Results: Reasonably good fits are found where monoenergetic ions are used and these are maintained for the symmetrical fall of RBE values with increasing dose (see figure 1 of Barendsen's data). The stochastic variation option is useful to model hadrontherapy delivered by a spectrum of energies as with the clinical example of Carbon ions, the overall RBE curves then being broader with a less distinct peak.

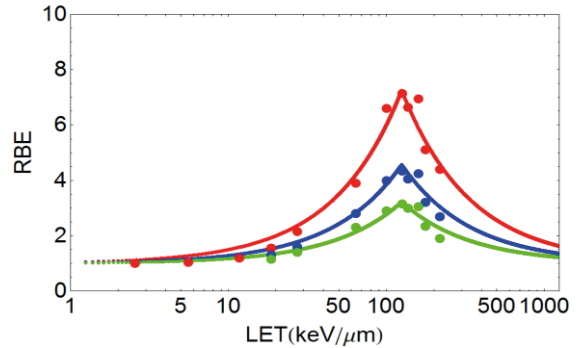


Figure 1. Irradiation of human T cells by monoenergetic helium particles by GW Barendsen in the Netherlands, fitted by the simplest model. The three different colours represent, from above downwards, 80%, 10% and 1% survival respectively.

Conclusions: These results indicate that more LET RBE studies with greater attention to turnover point position should be done for a range of ions with different z values. The importance of a better method of predicting RBE with LET and dose per fraction is self-evident given the expansion in clinical use of ionic beams, along with concerns about RBE that need to be solved in order to produce maximal clinical gains.

Keywords: RBE, Hadrons, predictive models

99 Radiobiological Considerations for Retreatment of Central Nervous System Tumours

B. Jones, J. Hopewell

University of Oxford, UK

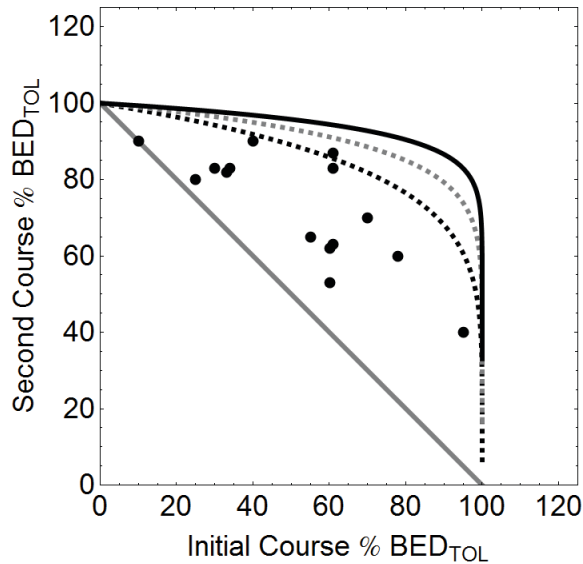
Purpose: To investigate practical models that would allow an increased re-treatment dose, with elapsed time, in brain and spinal cord tissue.

Materials/methods: Analysis of published murine, rat and higher primate spinal cord myelitis data show a non-linear time dependency for the second course 'tolerance' biological effective dose (BED). The presently available data is limited but provides important insights. The time dependency can be fitted using saturation type equations, some derived from simple differential equations, to find the permitted the remaining tolerance within the phase space allowed above the line that connects the 100% tolerance BED of the first and second treatment courses. A simpler model, based on the assumption that fractional recovery is not dose dependent, is also available.

Results: Three modelled approaches are compared, with attention to changes in second course dose when initial radiation dose is low or high. Safeguards can be introduced to reduce the assumptions made from the primate experiments of Ang *et al* (2001) which contain few data points and, in human terms, relatively short follow up times. The accumulated results from the literature, shown in Figure 1, are fitted with three modelled curves for a 1 (brown), 2 and 3 year time interval, based on the Ang *et al* data set. Note that murine and rat models which show more rapid recovery

of tolerance than in the primate. Caution is required in interpretation of the dose after a previous 100% BED exposure.

Figure 1: Plot of initial course percentage BED against that of the second course using a model where slope is inversely proportional to the second dose, raised to a power function, linked to time. Data points are murine and rat data treated at intervals up to 1 year following first exposure. The fitted curves are based on Ang et al (2001), for monkey spinal cord experiments for: black hatched curve 1 year, grey hatched curve 2 years and black 3 years of elapsed time between the exposures, although we assume 95% recovery rather than 100%. The grey straight line represents no recovery with time.



Conclusions: These results show that it is possible to model these time dependent relationships. To give greater confidence as to which of the three presented methods is best, further experiments are required. In the meantime clinicians will need to exert caution and judgement as to the choice of a final BED. This is a pressing dilemma since adults and children receive re-irradiation and so specific funding for properly conducted experiments is essential in order to provide the safest solutions and best clinical outcomes in the future.

Keywords: Re-treatment, Neural Tolerance

100 Delayed and Persistent Response of Human Mitochondria after Single Exposure to 0.5 to 4 Gy of Gamma Radiation

W. Kam¹, R. Banati²

¹Hong Kong Polytechnic University, Hong Kong, China

²Australian Nuclear Science and Technology Organization, University of Sydney, Australia

The cell nucleus is accepted as the primary site of radiation damage. Using both Monte Carlo simulation and qPCR, we have predicted that mitochondria (where extra-nuclear DNA resides) as a preferential site for ionization events to occur and showed an acute mitochondrial gene expression change upon 10 to 100 Gy of ionizing irradiation. A systematic inclusion of mitochondrial responses in addition to that of the cell nucleus, therefore, should provide important information about the cellular response to ionizing radiation. This study extends our previous work on delayed radiation effects of the mitochondria at clinically relevant doses.

Human T lymphocyte JURKAT cells were irradiated at 0, 0.5, 1, 2, 4 Gy, followed by total RNA and DNA extraction 1, 2 or 7 days after the irradiation.

RNA was reversed transcribed to cDNA for qPCR to examine the expression of 18 mitochondrial and 3 nuclear genes, which encode different subunits of the oxidative phosphorylation enzyme complexes (each made up of subunits encoded by mitochondrial and nuclear genomes (except Complex II which is only nuclear-encoded)); and, the expression of some nuclear genes known to regulate mitochondrial gene expression (PGC1 alpha), mitochondrial fission (DRP1) and fusion (Mfn1 and Mfn2). Gene expression was quantified by normalizing to 3 housekeeping genes (GAPDH, beta-actin, 18S).

DNA was directly used for qPCR using a primer set (specificity confirmed by sequencing) targeting the common deletion region, which is known to delete upon stress including ionizing radiation. Mitochondrial DNA integrity, extrapolated from qPCR yield of the common deletion region (damaged template not amplifiable), was quantified by normalizing to the qPCR yield of MtTL1 and MtTV, two mitochondrial genes that locate outside the common deletion region.

On day 1, 12 out of 18 tested mitochondrial genes show a dose-dependent increase in expression. The number of gene showing such an increase increases with the time post irradiation i.e. 14 on day 2; 17 on day 7. However, the tested nuclear genes do not show an expression increase with dose at all tested time points (Fig A).

The tested mitochondrially-related nuclear genes also show a dose-dependent increase in expression: PGC1 alpha, DRP1 and Mfn1 on day 1; DRP1 on day 2 and PGC1 alpha on day 7. Mfn2 does not show any expression change with an increase in radiation dose at all tested time points (Fig B).

Mitochondrial DNA integrity shows a dose-dependent decrease from the 2nd day post irradiation. A more drastic reduction is seen on day 7, and appears to be exponential instead of linear (Fig C).

Our results demonstrate a dose-dependent, delayed and persistent response of mitochondria to a clinically relevant range of radiation exposure (0.5 to 4 Gy). These persistent changes of mitochondrial state after single radiation exposure merit further studies on how they may affect the long-term stability of the nuclear genome.

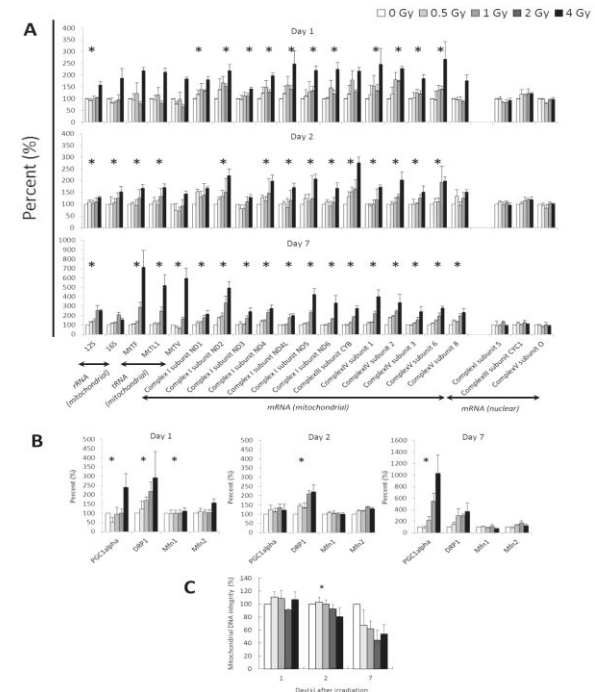


Figure legend: Quantified gene expression of (A) 18 mitochondrial and 3 nuclear genes of the oxidative phosphorylation system, as well as (B) PGC1 alpha, DRP1, Mfn1 and Mfn2, of JURKAT cells on 1, 2, 7 days after irradiation at 0, 0.5, 1, 2, 4 Gy. (C) Mitochondrial DNA integrity is extrapolated from the normalized qPCR yield of the common deletion region. All results are expressed as relative % with reference to 0 Gy control at each time point. An asterisk (*) represents a statistically significant correlation ($p < 0.05$) between the relative % and dose (Gy).

Keywords: Mitochondrial gene expression, Common deletion, Ionizing Radiation

101

Variance Based Sensitivity Analysis of Biological Uncertainties in Carbon Ion Therapy

F. Kamp, J.J. Wilkens

Klinikum rechts der Isar, Technische Universität München, Department of Radiation Oncology, Germany

In ion beam therapy, biological models to estimate the relative biological effectiveness (RBE) or the equivalent dose in 2 Gy fractions (EQD2) are frequently used in treatment planning and plan evaluation. In the context of the linear-quadratic model, these quantities depend on biological parameters (alpha, beta) for ions as well as for the reference radiation and the dose per fraction. The needed biological parameters as well as their dependency on ion species and ion energy typically cannot be determined directly in experiments for in vivo situations. They are often derived from in vitro data and biological modeling and subject to large (relative) uncertainties of up to 20-40% or even more. Therefore it is necessary to estimate the resulting uncertainties in e.g. RBE or EQD2 caused by the uncertainties of the relevant input parameters.

The influences of different input uncertainties can be examined by variance based Sensitivity Analysis (SA) methods. In this Monte Carlo approach a function is evaluated $n=1000$ to 1000000 times, depending on the number of input parameters. For each of those runs all parameters are changed simultaneously, using random numbers according to their associated uncertainties. Variance-based statistic formalisms then rank the input parameter/uncertainty pairs according to their impact on the result of the function. This Sensitivity S on the i -th input parameter X_i is defined as:

$$\text{Eq.(1)} \quad S_i = \frac{\text{var}(\text{mean}(Y|X_i=\text{const}))}{\text{var}(Y)}$$

with Y being a result vector of n function evaluations. The sensitivity ranges from $S=0$ (no influence) to $S=1$ (only influential part). Figure 1 shows an example where RBE is assumed to be a function of the biological parameters (alpha, beta) for ions and the dose per fraction (d).

The major advantage of SA methods is that the function is not just evaluated at a single, fixed input parameter set but over the whole range of all input parameter uncertainties. The quantification (Eq.(1)) allows to display and to compare several input uncertainties at once. A further advantage is that SA can be performed with arbitrary numerical functions.

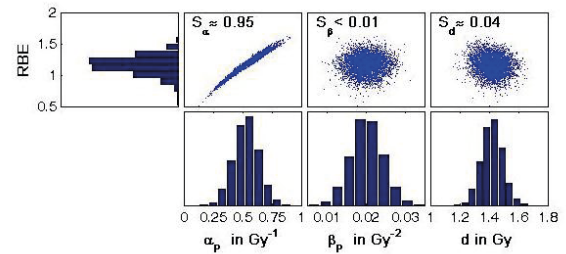


Figure 2: Example Sensitivity Analysis of RBE as a function of alpha, beta and d for ions. Their uncertainty is simulated using a normal distribution with a standard deviation of 20% (for alpha and beta) and 5% (for d) relative to the mean value. The Sensitivity S of RBE on the three input parameter is marked in the respective scatter plot.

We present here the application of SA for biological functions relevant in Carbon ion therapy (RBE and EQD2) using biological models. This is used in a second step for the systematic discussion of the respective impact of variations in the input parameters.

Variance-based SA is a powerful tool to evaluate the impact of (biological) uncertainties in Carbon ion therapy. The presented analysis is independent of the biological models. The number of input parameters that can be examined at once is only limited by computation time.

Keywords: carbon ions, biological modeling, sensitivity

102

Expression of common or species specific DNA damage-repair pathway related genes in thymus of low-dose-rate irradiated AKR/J and ICR mice

H.S. Kim

Radiation Health Research Institute, KHNP, Seoul, Republic of Korea

Purpose: we have been investigated the effect of low-dose-rate radiation (LDR, ^{137}Cs , 0.7 mGy/h) on DNA repair and damage pathway related genes in the process of cancer development in AKR/J mice carrying the mouse leukemia viral oncogene that died of thymic lymphoma within 1 year of age.

Material/methods: in this study, we studied the expression of common and/or species specific DNA repair and damage related genes in the thymus of LDR irradiated AKR/J and ICR mice (total dose: 1.7 Gy). Same sized thymuses compared to before irradiation were collected at 100th day and analyzed using whole-genome microarray, quantitative reverse transcription polymerase chain and western blot.

Results: the thymus weight was decreased and survival rate was increased in LDR irradiated AKR/J mice, but not in ICR mice. The expressions of tumor suppressor *Plxnc1* and *Rnd3* were up-regulated, whereas the expression of *Cyp11a1*, a gene contributes to tumor immune escape, was down-regulated in LDR irradiated AKR/J mice, but not ICR mice.

Conclusions: these results suggest that LDR radiation suppressed early stage of carcinogenesis and removed cancer cells from body by stimulated apoptosis and immune mechanisms.

Keywords: Low-dose-rate, radiation, DNA, repair, genes

103

Can particle beam therapy be improved using helium ions? - A treatment planning study focusing on pediatric patients

B. Knäusl, H. Fuchs, D. Georg

Department of Radiation Oncology, Division Medical Radiation Physics & CD Laboratory for Medical Radiation Research for Radiation Oncology, Medical University of Vienna/AKH Vienna, Austria

Purpose: To explore the potential of scanned helium ion (He^4) beams compared to proton beam therapy (PT). He^4 was not investigated in a treatment planning study before, due to the lack of a suitable treatment planning system (TPS). For paediatric patients He^4 is a promising candidate and the superior biological and physical properties could increase the local tumour control and the sparing of adjacent organs at risk (OARs).

Materials/methods: A pencil beam algorithm [1] for PT and He^4 was employed allowing biological dose optimization. The relative biological effectiveness (RBE) of He^4 was described using a 'zonal' model including different LET.

For paediatric patients (Neuroblastoma (NB), Wilms, Hodgkin and brain tumour) intensity modulated treatment plans were created using the TPS Hyperion. The same beam configuration (2 or 3 beams from anterior-posterior or lateral direction) was used for both particle species.

So far treatment plans for 3 NB patients were created. The clinical target volume (CTV) included the preoperative GTV and areas of local lymph node enlargement. Dose prescription to the planning target volume (PTV = CTV + 1 cm isotropic margin) was 21 Gy(RBE). Myelon, kidneys and liver were considered as OARs.

Plan quality was analyzed by evaluating dose difference maps, conformity and homogeneity index (CI, HI), $V_{95\%}$, $D_{2\%}$, $D_{98\%}$ and $D_{50\%}$ according to ICRU83. For OARs dose-volume histogram related parameters ($D_{2\%}$, $D_{50\%}$ and V_d values) were investigated.

Results: Plans optimized for PT were directly applicable for He^4 and resulted in slightly improved treatment plan quality. This could be even further optimized using more stringent constraints during inverse planning.

The PTV size ranged from 163 - 232 cm^3 . $V_{95\%}$ was covered by the 95% isodose and $D_{50\%}$ fulfilled the prescription of 21 Gy for all treatment plans. $D_{2\%}$ never exceeded 22.1 Gy (RBE) and $D_{98\%}$ was always above 18.9 Gy (RBE). The CI (0.88) and HI (0.13) were comparable for PT and He^4 .

For the myelon $D_{50\%}$ was reduced from 2.2 ± 0.3 Gy (RBE) to 1.7 ± 0.2 Gy (RBE) comparing He^4 to PT plans. $D_{2\%}$ was 6.5 Gy (RBE) at maximum and lower by 0.8-1.5 Gy (RBE) for He^4 .

Due to overlapping volumes of the kidney and the PTV, $D_{50\%}$ varied between 0.1 and 6.9 Gy (RBE) whereas on average He^4 delivered 26% less dose to the kidneys than PT. The liver was spared equally for He^4 and PT with $D_{50\%} < 1$ Gy (RBE).

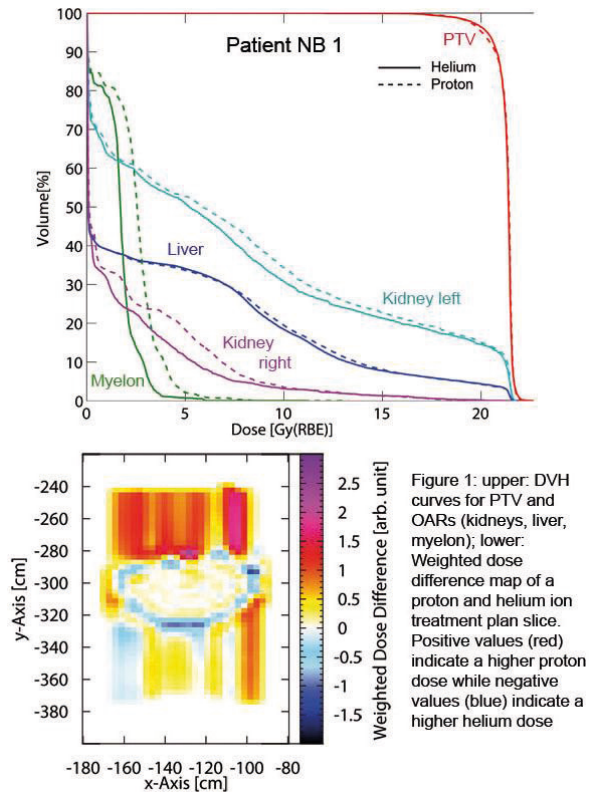
Dose weighted difference maps showed reduced entrance doses for He^4 as can be seen in Figure 1 for patient NB1. Regarding the PT plan for this patient 4% of the voxels received a higher dose than in the corresponding He^4 plan (difference > 1 Gy (RBE)).

Conclusions: The dose distribution outside the PTV was notably different and an improved OAR sparing was observed for He^4 . The results motivate a more thorough investigation of He^4 , also with respect to RBE verification measurements in order to improve biological dose optimisation.

Keywords: Helium ions, Protons, children

References:

[1] Fuchs et al (2012) MedPhys 39:6726-37



104

Vimentin (EMT Marker Protein) Score As One of Predictors Resistance to Erlotinib and Radiotherapy for Patients with Stage III Non-Small Cell Lung Cancer on A Prospective Phase II Trial

R. Komaki, Y.B. Kim, I. Wistuba, X. Tang, R. Meyn, P.K. Allen, X. Wei, I.J. Lee, M.S. O'Reilly, G. Blumenschein, W. Hong

M.D. Anderson Cancer Center, Houston, TX, USA

Background: Although erlotinib has shown radiosensitization effects, 20% of patients who were treated by erlotinib and radiotherapy following chemoradiotherapy have failed to respond in our prospective phase II trial for inoperable stage III NSCLC. We have examined predictive factor of resistant to this treatment by using Vimentin IHC which is a strong multigene signature indicative of epithelial to mesenchymal transition (EMT).

Materials/Methods: We have conducted a prospective phase II study for patients with stage III NSCLC patients. Eligibility included good PS, weight loss $\leq 5\%$, adequate lung, hematologic, hepatic, and renal functions. ChT/RT was given every Monday followed by erlotinib/RT on Tuesday-Friday and erlotinib alone over the weekend. RT (63 Gy in 35 fractions) with weekly paclitaxel ($45\text{mg}/\text{m}^2$) / carboplatin (AUC=2) and erlotinib (150 mg p.o. daily except on the day of chemotherapy) were given for 7 weeks followed by 2 cycles consolidation of paclitaxel (AUC=6) and carboplatin ($200\text{mg}/\text{m}^2$). The response was measured by RECIST criteria (v3.0) by CT scan after completion of ChT/RT. Fisher's exact and Kaplan-Meier's estimates were used for the statistical analysis. Primary endpoint was to determine efficacy of erlotinib/radiotherapy after ChT/RT measuring time to progression (TTP). The second end points were overall survival (OS), local recurrence-free survival (LRFS), distant metastasis free survival (DMFS) and their pretreatment biopsy specimens correlated between biomarkers and patients' outcome.

Results: 48 patients enrolled from 3/2008 through 6/2010 and 46 completed the entire treatment and are evaluable for response. 17 (37%) were female, 23 adenocarcinoma, and 87% former or current smokers, with median age 63 year-old (range: 46-81). Of 46 patients (96%) evaluable for response, 40 were former or never smokers; 23 had adenocarcinoma; and 41 were evaluable for EGFR mutations (37 wild-type [wt] and 4 mutations [all adenocarcinomas]). Median time to progression was 14.5 months and did not differ according to EGFR status. At a median follow-up time for all patients of 30.6 months (range, 3.4-54.6 months). OS rates were 82.6% at 1 year, 67.4% at 2 years, 48.5% at 3 years, and 32.2% at 4 years. Responses showed 14 (30%) CR, 23 (50%) PR and 9 (20%) SD or PD. Pretreatment specimens of 22 patients who failed or minimal response on this trial were analyzed for Vimentin IHC. All of the Vimentin Cytoplasm Score (VCS) < 100 (15 pts) vs. \geq 100 (7 pts) were compared regarding TTP, OS, PFS, LRFS and DMFS in 4 years. There were significant differences between the groups of VCS <100 vs. \geq 100 regarding TTP (14.7 months vs. 7 months, $P=0.04$), OS (28.4 % vs. 0 %, $P=0.03$), PFS (28.7% vs. 0%, $P=0.04$) and LRFS (82.5% vs. 0%, $p<0.008$), but not DMFS (35.9 vs. 0%, $p=0.08$), respectively.

Conclusions: This prospective phase II clinical study demonstrated an excellent 4 -year OS 32.2 %. Higher VCS predicted poor TTP, OS, PFS and LRFS but not DMFS. VCS might be used as a predictor for patients with NSCLC who are resistant to erlotinib and radiotherapy combined with chemoradiotherapy, although we need validation with larger number of patients.

Keywords: Erlotinib, Vimentin, Radiotherapy

Acknowledgment: This study was supported by US department of defense funding.

105

Reprogramming metabolism with metformin to improve radiation response

M. Koritzinsky

Princess Margaret Hospital, Toronto, Canada

Tumor hypoxia is a negative prognostic factor in multiple cancers, due in part to its role in causing resistance to radiotherapy. Hypoxia arises in tumor regions distal to blood vessels as oxygen is consumed by more proximal tumor cells. Reducing the rate of oxygen consumption is therefore a potential strategy to reduce tumor hypoxia. We hypothesized that the anti-diabetic drug metformin, which reduces oxygen consumption through inhibition of mitochondrial complex I, would improve radiation response by increasing tumor oxygenation.

Here we show that metformin treatment significantly improved tumor oxygenation in two xenograft models as measured by IHC, flow cytometry and PET imaging. Metformin also led to improved radiotherapy responses when mice were administered metformin immediately prior to irradiation. Clinically, metformin use was associated with an independent and significant decrease in early biochemical relapse rates ($p=0.0106$) in 504 localized prostate cancer patients treated with curative-intent, image-guided radiotherapy (IGRT). Mutations in p53 and LKB1 as well as expression of OCT1-3 may represent biomarkers of metformin response.

Our data demonstrate that metformin can improve tumor oxygenation and response to radiotherapy. Our study suggests that metformin may represent an effective and inexpensive means to improve radiotherapy outcome with an optimal therapeutic ratio.

106

A Beam Control System for an Experimental Beam Line Operated Parallel to a Therapeutic Beam Line

T. Kormoll¹, A. Duplity², W. Enghardt¹, S. Helmbrecht¹, F. Hueso Gonzalez¹

¹OncoRay, TU Dresden

²IBA

Purpose: At the OncoRay - National Center for Radiation Research in Oncology, in Dresden, Germany, an IBA Cyclone[®] 230 has recently been installed. The facility is equipped with a treatment room including an isocentric gantry featured with a universal nozzle delivering scattered and scanned therapy beams. In addition, there is an experimental area dedicated to radiation research. This opens the possibility to perform experiments in parallel to the medical treatment without interfering with the clinical routine. Experiments can be done during the day while the beam is not needed in the treatment room, e.g. while the patient is being positioned. This worldwide unique setup allows to make efficient use of the proton beam. A dedicated control system is required for setting the beam parameters for the experimental beam line and, most importantly, to assure that beam requests from the treatment beam line are handled with the appropriate priority. This system is currently under development and is presented in this work.

Materials and methods: The most important requirements on a beam control system for the experimental bunker are as follows:

Allocate beam automatically to the experimental area as soon as the treatment system signals that beam is not currently needed in the therapy room.

Check whether the treatment system has requested the beam and release it in an appropriate manner.

Restore former beam settings and resume the irradiation in the experimental room automatically as an interruption by the treatment system ends.

The software is supposed to interact with additional hardware which is installed in the experimental bunker where the beam line does not feature a scanning system, it is planned to install a movable table which mimics a scanning system. The interface to this table will be controlled directly by the software, which will be able to perform irradiation plans without modification of the experimental beam line.

Results: The interface to the Cyclone[®] 230 soft- and hardware is accomplished through the BSSGateway provided by IBA. This system exposes a bidirectional signaling mechanism to external software. The beam control system will be composed of several threads which communicate through a signal and slot mechanism.

In figure 1, the basic architecture is illustrated. It is aimed to be a cross-platform software and to run without any hardware present to provide a version to the future users of the OncoRay facility, which allows to simulate an irradiation for testing purpose. **Discussion:** The official start-up of the cyclotron was on the 17th of September 2013. The development on the beam control system is divided into several stages. The first stage is scheduled to be finished in February 2014 with a working version which handles the beam priority correctly and can actually be used for irradiations. Further stages include an extended setting of beam parameters, the inclusion of monitor detectors, and the extension with the movable table. To take full advantage of the unique infrastructure of the OncoRay center, the beam control system will provide convenient tools to internal and external users.

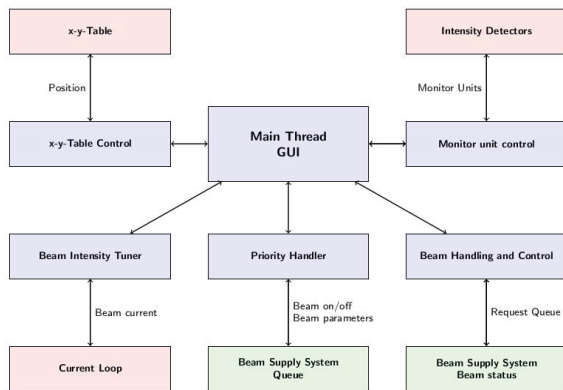


Figure 1: Schematic structure of beam control system. Software components are drawn blue, hardware components red and the IBA Beam Supply System (BSS) green.

Figure 1.

Keywords: Proton Therapy, Instrumentation, Software Development

107

Radioisotopes: the “fuel” for nuclear medicine

J. Köster

Institut Laue-Langevin, Grenoble, France

Nuclear medicine provides essential and in many cases even unique tools for diagnostics and therapy of a large variety of illnesses. Every year over 30 million nuclear medicine procedures are performed worldwide and new promising applications are under development.

Radioisotopes are the key ingredient for any radiopharmaceutical and can be considered as the “fuel” that is driving all nuclear medicine applications. The choice of a radioisotope with appropriate nuclear decay characteristics and chemical properties can be decisive for the outcome of the procedure.

Today the vast majority of all diagnostic procedures is performed with ^{99m}Tc (for scintigraphy and SPECT) and ^{18}F (PET) respectively. ^{18}F is produced in a decentralized way by a fleet of over 800 medical cyclotrons. For the last 30 years the supply of ^{99m}Tc relied exclusively on a centralized production chain distributing convenient $^{99}\text{Mo}/^{99m}\text{Tc}$ generators. However, recent ^{99}Mo supply perturbations triggered several projects that try to implement alternative production schemes of ^{99}Mo or ^{99m}Tc respectively.

Due to their excellent nuclear decay properties and their chemical versatility, ^{99m}Tc and ^{18}F will undoubtedly maintain their leading role in the future. They are complemented by other radioisotopes that are advantageous in specific diagnostic applications. In particular the generator-derived PET isotopes ^{68}Ga and ^{82}Rb , as well as longer-lived PET isotopes like ^{44}Sc , ^{64}Cu , ^{89}Zr , etc. are experiencing a rapidly rising demand.

For long time therapeutic applications of nuclear medicine were dominated by ^{131}I , used in the treatment of hyperthyroidism and thyroid cancers. However, with the advent of new targeted therapies such as radio-immunotherapies (RIT) and peptide receptor radionuclide therapies (PRRT), radiometals were found to be more appropriate than radioiodine. Today ^{177}Lu is considered as the “gold standard” for such applications, but for particular applications radioisotopes emitting radiation with even shorter range are sought. The recent FDA approval of Xofigo (^{223}Ra -chloride) for the treatment of bone metastases is now paving the way for the large scale clinical use of alpha emitters.

The demand and supply prospects of important medical isotopes will be discussed. A particular emphasis will be put on examples where nuclear and particle physics laboratories

can support the radioisotope supply with their special infrastructure or technologies.

108

Beam monitoring and dosimetry tools for radiobiology experiments at the cyclotron ARRONAX

C. Koumeir^{1,2}, M. Cherel⁴, A. Guertin², F. Haddad^{1,2}, V. Métivier², N. Michel^{1,2}, F. Poirier^{1,2}, L. Schwob¹, N. Servagent², N. Varmentot^{1,3}

¹GIP ARRONAX, Saint Herblain, France

²SUBATECH, Ecole des Mines de Nantes, CNRS/IN2P3, Université de Nantes, Nantes, France

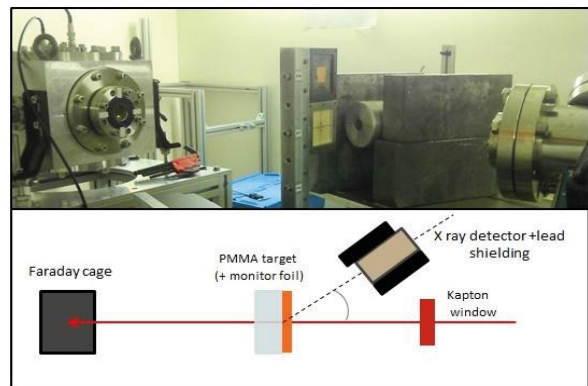
³Institut de Cancérologie de l'Ouest (R. Gauducheau), Saint Herblain, France

⁴INSERM, CRCNA, Nantes, France

Purpose: The ARRONAX (Accélérateur pour la Recherche en Radiochimie et Oncologie à Nantes Atlantique) cyclotron in Saint Herblain - France is a facility delivering α particles at 68 MeV (¹). One of its purposes is to become a platform for radiobiological studies. The radiobiological studies evolve around two axes: the low energy range (<10MeV) in order to optimize radio-immunotherapy (RIT) treatments, and the high energy range (30-68 MeV) in order to puzzle out the fundamental mechanisms generated by cells in response to ionizing radiations.

The ARRONAX platform for radiobiology is currently preparing to use a time lapse fluorescence confocal microscope suitable for the irradiation of cell wells. This platform should contain tools for beam intensity checks to enable accurate and repeatable irradiation conditions and a device to monitor the delivered dose.

Materials and Methods: A system has been developed to monitor the beam intensity using an X-ray spectrometer. It is based on the online measurement of the bremsstrahlung (>1keV) produced by the interaction of the incident particle with the medium. Experiments were made using PMMA targets bombarded with 63MeV alpha particles, in order to characterize this continuous X-ray spectrum. A simulation code of the bremsstrahlung has been built.



For relative dosimetry, experiments were performed to get Gafchromic EBT3 films response to alpha particles (1 - 30 Gray). To quantify the alpha darkening, the relative efficiency (*RE*) defined as the delivered dose ratio between photons and alpha particles for the same optical density was used. The same EBT3 lot was used and an identical protocol for scanning and analysing was applied.

Results: A good agreement has been found between experimental and simulated spectra of bremsstrahlung. The intensity of the bremsstrahlung spectrum allow the beam monitoring with an accuracy <3% for 1 Gray delivered dose. The measured spectrum presents variations with the target thickness, showing a good sensibility for thin target (<1000 μm) and a saturation for thicker ones. Bremsstrahlung

spectrum also shows a sensibility with the chemical composition of the target.

For EBT3 study, an effect of polymerization saturation has been observed compared to a photon response curve. The (RE) factor found was about 0.7.

Conclusions: Tools for a radiobiological platform are developed at ARRONAX. Bremsstrahlung measurement would allow a control of the beam intensity on the target directly without the use of an additional medium disrupting the beam. Sensibility on the chemical nature can be used for precisely modelling the dose evolution in medium with the beam direction.

The data of EBT3 response to an irradiation with alpha particles is new and necessary. We will run equivalent experiments using different beams available at ARRONAX to compare the EBT responses by varying the LET, the ionization density, the charge of incident particle.

Keywords: Beam monitoring, dosimetry

References:

[1] F. Haddad et al., Eur. J. Med. Mol. Imaging 35, 1377-1387 (2008)

109

New challenges for biologically adapted ion beam treatment planning: single and multi-ion approaches

M. Krämer¹, M. Durante^{1,2}, Y. Furusawa³, R. Hirayama³, E. Scifoni¹, W. Tinganelli^{1,2,3}

¹GSI, Darmstadt, Germany

²IOL

³NIRS

Purpose: Ion beam radiotherapy, in addition to the well known physical and radiobiological benefits of particular ion species like ¹²C, offers unique additional advantages in terms of effective dose shaping.

Multimodality, i.e. the use of multiple fields of different ion species in the same treatment plan, introduces additional degrees of freedom, allowing to distribute high- and low-LET radiation arbitrarily. This is particularly attractive in order to selectively target hypoxia and potentially other types of intra-tumour biological heterogeneity. In order to exploit these advantages, specific treatment planning tools are required.

Materials and methods: To this end, we have extended the TRiP98 code, the first treatment planning system for particles, in several directions.

The optimization engine has been modified to allow the inverse planning of different ion modalities simultaneously.

The biological effect calculation was extended beyond the RBE-weighted dose, including the oxygen enhancement ratio (OER).

An experimental in-vitro survey at NIRS with the irradiation of specific hypoxic targets with various ions supports this approach with the benchmarking of the OER-LET model newly implemented in TRiP98.

This way the first complete database for the OER-LET dependence in the region of intermediate pO₂ has been generated.

Additionally we performed extended target irradiation of an inhomogeneous target to test the model in realistic geometries.

Results: Biological dosimetry measurements performed at NIRS and GSI revealed a good agreement of the model developed to handle OER in treatment planning.

Physical and radiobiological base datasets for ion beam modalities from protons to oxygen have been established.

Treatment plans with single and multiple ion species have been produced allowing to restore the prescribed survival level across the entire target in the presence of hypoxic subvolumes.

The impact of different fractionation schemes for different ion beam modalities is also critically evaluated.

Conclusions: We present the first treatment planning system optimizing several ion species as well as allowing biological effect painting across inhomogeneous targets. The OER model is validated experimentally. TRiP98 is effective in restoring a given uniform cell killing, by scaling and redistributing beam components accordingly.

We give an outlook on the possibilities of ion beams in this respect.

Keywords: (Particle therapy, biological dose optimization, hypoxia)

110

Biomarker for stratification in radiotherapy - preclinical and early clinical models

M. Krause^{1,2,3}

¹German Cancer Consortium (DKTK) Dresden and German Cancer Research Center (DKFZ) Heidelberg, Germany

²Dept. of Radiation Oncology and OncoRay - National Center for Radiation Research in Oncology, Medical Faculty and University Hospital C.G. Carus, Technische Universität Dresden, Germany

³Helmholtz Center Dresden-Rossendorf, Germany

Within the last centuries, major advances have been achieved in radiotherapy technique as well as in combined radiation treatments. Thereby, tumour control and survival of patients improved. However, it is known for a long time that radiation response varies from patient to patient, even in the same tumour entity and stage. Predictive biomarkers that have always been used in radiation oncology are tumour site and histology, stage, differentiation and tumour size. With increasing knowledge in tumour biology, genetics and pathophysiology the tools are now available to establish more precise biomarkers that can in future help to define groups of patients for individual interventions like radiation dose escalation, decision between radiochemotherapy or radiotherapy with molecular targeted drugs or the application of hypoxic cell radiosensitisers. The talk will give an overview on the current status of knowledge on potential biomarkers e.g. of tumor hypoxia, tumor cell metabolism, DNA repair and biomarkers for combining radiotherapy with inhibition of the epidermal growth factor receptor using monoclonal antibodies.

111

Real-time monitoring of the ion range during hadrontherapy:

An update on the beam tagging hodoscope

J. Krimmer¹, L. Caponetto^{1,2}, X. Chen¹, M. Chevallier¹, D. Dauvergne¹, M. De Rydt^{1,3}, S.M. Deng^{1,2}, J.-L. Ley¹, H. Mathez^{1,2}, C. Ray¹, V. Reithinger¹, E. Testa¹, Y. Zoccarato^{1,2}

¹Université de Lyon, Université Claude Bernard Lyon 1, CNRS/IN2P3, Institut de Physique Nucléaire de Lyon, 69622 Villeurbanne, France

²MICRHAU pôle de Microélectronique Rhône Auvergne, France

³Instituut voor Kern- en Stralingsfysica, K.U.Leuven, Celestijnenlaan 200D, 3001 Leuven, Belgium

Purpose: For an improvement of the quality control during hadrontherapy an online monitoring of the ion range is highly desired. For this purpose several modalities are under development, using the detection of emitted prompt gamma rays [1,2,3] or secondary protons (IV) [4,5,6] in the case of incident carbon ions.

For all modalities, the nuclear interaction vertices (whose distribution is strongly correlated with ion ranges) are determined by intersecting the incident ion trajectory with various geometries provided by secondary radiation, e.g. planes (collimated cameras), cones (Compton cameras) or

lines (IVI). A beam tagging hodoscope is therefore an essential component which provides position information of the incident ions and can also serve as a time reference. Several hodoscopes have been developed both for fundamental research and hadrontherapy [7]. The present project aims for developing a device able to count at 10^8 Hz with timing and spatial resolutions of the order of 1 ns and 1 mm, respectively.

Materials/methods: The beam tagging hodoscope consists of square scintillating fibers (1mm x 1mm) coupled to multi-anode photomultipliers (Hamamatsu H-8500) via optical fibers. Two prototypes have been built at IPNL, a small (2x32 fibers) and a large one (2x128 fibers). The scintillating fibers of the large hodoscope are read from both ends providing a higher efficiency and an improvement in time resolution.

Dedicated front-end electronics has been developed for the readout of the hodoscope and integrated in an ASIC. The first version of these ASIC implements 8 channels, each with a high-speed current buffer, a charge sensitive amplifier and a current comparator [8], the second version integrates also a TDC providing the timing information.

Results and conclusions: Both prototypes of the hodoscope have been successfully tested in proton or carbon-ion beams, respectively. A time resolution of 1 ns FWHM has been measured. This is important for the modality of prompt gamma ray detection where the use of time of flight (TOF) information reduces background significantly.

The present methods for an online monitoring of the ion range rely on the registration of individual incident ions, or ion bunches. 10 MHz count rates have already been achieved, without optimization of the readout capability.

In fall 2013 measurements of the hodoscope in combination with the first version of the ASIC have been performed in a beam of carbon-ions. Results in terms of efficiency and count rate capability will be given.

Acknowledgments: This work is supported by the FP7-ENVISION program (WP3 and WP6), the FP7-ENTERVISION program, the FP7-ULICE program, the INSERM-Physique Cancer QAPIV project, the ANR Gamhadron project, the Rhone-Alpes Regional Program for Hadrontherapy Research, the MIZB GDR, and the LabEx PRIMES.

Keywords: hadrontherapy, online ion range control

References:

- [1] C.H. Min et al. Appl. Phys. Lett. 89 (2006) 183517
- [2] M. Testa et al., Radiat. Environ. Biophys. 49 (2010) 337-343
- [3] F. Roellinghoff et al., Nucl. Instrum. Meth A 648 (2011) S20-S23
- [4] U. Amaldi et al., Nucl. Instrum. Meth A 617 (2010) 248-249
- [5] P. Henriquet et al., Phys. Med. Biol. 57 (2012) 4655-4669
- [6] V. Reithinger et al., IEEE-NSS-MIC (2012) Anaheim
- [7] D. Lo Presti et al., JINST 8 (2013) 04015
- [8] S. Deng et al. Nucl. Instr. Meth. A 695 (2012) 390

112

Dosimetric considerations to determine the optimal technique for localized prostate cancer

P. Kuess^{1,2}, D. Berger¹, D. Georg^{1,2}, P. Georg^{1,2}, G. Golder^{1,2}, J. Gora¹, J. Hopfgartner^{1,2}, G. Kragl¹

¹Department of Radiation Oncology, Medical University of Vienna, Vienna Austria

²Christian Doppler Laboratory for Medical Radiation Research for Radiation Oncology, Medical University of Vienna, Vienna, Austria

Purpose: To assess the dosimetric differences for treating localized prostate cancer between VMAT, scanned proton therapy (IMPT), scanned Carbon-ion therapy (IMIT), LDR and

HDR brachytherapy (BT). For these modalities excellent local control and moderate side effects have been reported.

Methods and Materials: Ten patients were considered for this planning study. For external beam therapy (EBRT) the planning target volume (PTV) was created by adding a margin of 5mm (lateral/anterior-posterior) and 8mm (superior-inferior) to the CTV. The following organs-at-risk were considered: bladder wall (BW), rectal wall (RW), femoral heads, urethra, and pelvic tissue. For VMAT and IMPT 78 Gy (RBE)/2Gy were prescribed. IMIT was based on 66Gy(RBE) in 20 fractions. The CTV planning aims for HDR-BT (Ir-192) and LDR-BT(I-125) were $D_{90\%} \geq 34$ Gy in 8.5 Gy per fraction and $D_{5\%} \geq 145$ Gy, respectively. All assumed total doses and fractionation schemes are clinically used. The physical as well as the RBE weighted dose distributions for protons and Carbon-ions were converted to dose distributions based on fractions of 2Gy(IsoE). From these dose distributions various dose and dose volume parameters were extracted. An example of the dose distribution for a selected patient for all five treatment techniques after radiobiological conversion is shown in Figure 1.

Results: RW exposure 30-70Gy (IsoE) was reduced for IMIT, LDR and HDR-BT when compared to VMAT and IMPT. The high dose region of the BW DVH above 50Gy (IsoE) of IMPT resembled the VMAT shape, while all other techniques showed a significantly lower high dose region. For all three EBRT techniques similar urethra mean doses around 74 Gy(IsoE) were obtained. LDR-BT results were by about 30 Gy(IsoE) higher, HDR-BT 10 Gy(Iso) lower. Normal tissue and femoral head sparing was best with BT.

Conclusion: Despite the different prescription and fractionation schemes of the EBRT techniques, the high dose regions of BW and RW expressed in Gy(IsoE) were in the same order of magnitude. BT techniques were clearly superior in terms of bladder, rectum and normal tissue sparing.

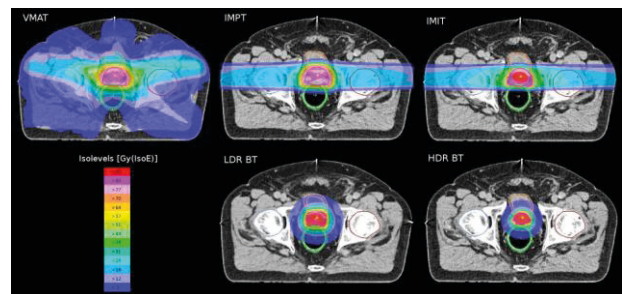


Figure 1. Representative dose distributions for a selected patient for all five treatment techniques after radiobiological conversion.

Keywords: prostate cancer, combined treatment modalities

113

The Advantages of Improved Gd DRZ Screens Compared to Gd₂SO₄ and CsI in Patients Exposure Dose Reduction during the Chest Radiography

L. Aslamova¹, N. Melenevska¹, N. Miroshnichenko^{1,2}, I. Kulich¹, S. Miroshnichenko²

¹Taras Shevchenko National University of Kyiv, Training-Research Centre for Radiation Safety, Volodymyrska str., 64/13, 01601, Kyiv, Ukraine,

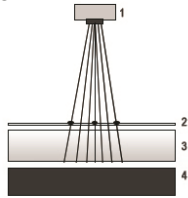
²Production-Research Association "Teleoptic", Dmytrivska str., 58, 01054, Kyiv, Ukraine

Purpose: The improved gadolinium (Gd DRZ) screens provide a strong possibility to reduce exposure dose delivered to patient during the radiographic diagnostics of lung cancer and tuberculosis. The disadvantage of cesium-iodide (CsI) screens is expensiveness which actual problem due to numerous chest screen procedures in Ukraine required to be

performed. The aim of the study was to find an optimal solution for patient exposure dose reduction using different X-ray absorbing screens and image post processing.

Materials/methods: Radiographic X-ray chest screening system included photons generator, digital receiver Iona-R4000, and ionizing chamber. Image conversion effectiveness criteria was estimated due to contrast of test-object image. Focus-to-source distance as 125 cm. In the experiments three types of X-ray absorbing screens: Gd₂SO₂, Gd DRZ, and Csl were used. The digital X-ray image processing was performed with ContextVision CVIE-teleoptic-XR2-ADI (based on the principle of non-linear signal filtering). The patient chest was simulated with water chest phantom.

1. X-ray tube;
2. Al test-objects;
3. water chest phantom;
4. digital receiver.



Results: As demonstrated in Table 1 Csl screen has higher absorption factor compared to Gd DRZ and Gd₂SO₂. Table 2 shows the exposure doses required to obtain images with proper contrasts which are also different, depending on screen type. Gd DRZ screens allow proposing of reasonable balance between exposure dose and price of the screens. During the experiments the exposure dose delivered to the standard patient (water chest phantom 9 cm thickness) under the condition of Gd DRZ screen application was 33.0 mR (compared to 27.0 mR obtained with Csl and 45.0 mR with Gd₂SO₂). These doses were required to obtain images with visual contrast of 1.8%. The next image software post processing improved image contrast up to 5.0%.

U, kV	I, mAs	D, cm	Dose, mR		
			Gd ₂ SO ₂	Gd DRZ	Csl
50	95	0	7,8	6,5	5,6
70	22	0	8,6	7,4	7,1
90	9	0	9,2	8,2	7,7
120	4	0	9,3	8,5	8,4
81	11	9	45,0	33,0	27,0

Table 1. U, tube potential; I, tube current; D, water phantom thickness

U, kV	I, mAs	K _{ABS}		
		Csl	Gd DRZ	Gd ₂ SO ₂
50	95	0,72	0,59	0,45
70	22	0,48	0,39	0,30
90	9	0,35	0,29	0,22
120	4	0,27	0,22	0,17

Table 2. K_{ABS}, X-ray absorption factor

Conclusions: The optimal solution for reduction of exposure dose delivered to the patients (approx. in 1.5 times) under the conditions of mass screening can be provided with application of improved Gd DRZ screens and image post processing.

95 MeV/A carbon fragmentation studies for hadrontherapy: measurements and comparisons with GEANT4 simulations

M. Labalme¹, J. Colin¹, D. Cussol¹, J. Dudouet¹, C. Finck², J. M. Fontbone¹, P. Henriquet³, D. Juliani², J. Krimmer³, M. Rousseau², M.G. Saint-Laurent⁴, S. Salvador¹

¹LPC Caen, ENSICAEN, Université de Caen, CNRS/IN2P3, Caen, France

²IPHC, Université de Strasbourg, CNRS/IN2P3, Strasbourg, France

³IPN Lyon, Université Claude Bernard Lyon 1, Villeurbanne, France

⁴CEA/Saclay, DSM/Irfu/SPhN, Gif-sur-Yvette, France

⁵GANIL

The increasing interest for hadrontherapy can be attributed to the great accuracy of ion beams to target the tumor while sparing the surrounding healthy tissues as well as their biological advantage. To keep the benefits of carbon ions, a very high accuracy on the dose location is required. The dose deposition is affected by the fragmentation of the incident ions that leads to a consumption of the projectiles with their penetration depth in tissues and to the creation of lighter fragments having different biological effectiveness. Up to now, the constraints on nuclear models and fragmentation cross sections in the energy range used in hadrontherapy are not yet sufficient to reproduce the fragmentation processes with the required accuracy for clinical treatments.

In this context three experiments have been performed at GANIL (France) to study the fragmentation of ¹²C. The experimental set-up was made of five three stages ΔE-E telescopes mounted on rotating stages to cover angles from 0 to 43°.

The first experiment, on thick water equivalent targets, was performed in 2008 [1]. The goals were the measurements, behind different thicknesses of PMMA, of energy and angular distributions of the fragments produced by the nuclear reactions of 95 MeV/A ¹²C. Comparisons between experimental data and Geant4 simulations exhibited discrepancies for the fragment production rates, angular and energy distributions.

To improve the nuclear reaction models and reach the accuracy required for a reference simulation code for hadrontherapy, two experiments have thus been performed on thin targets in 2011 and 2013 at GANIL. The double differential cross sections (d²σ/dE.dΩ) of 95 MeV/A ¹²C on H, C, Al, O and Ca targets have been obtained for fragment isotopes from p to ¹¹C [2]. The results show an increase of the cross sections with the mass of the target. The angular distributions of heavy fragments are more forward-focused and Z=2 fragments are predominant at low angles (<10°). The energy distributions of the fragments at forward angles are peaked close to the beam energy.

Geant4 simulations have been done using Binary Intra-nuclear Cascade (BIC), Quantum Molecular Dynamics (QMD) and Liege Intra-Nuclear Cascade (INCL) as entrance channel models coupled to either Generalized Evaporation Model (GEM) or Fermi Break-Up (FBU) as exit channel models.

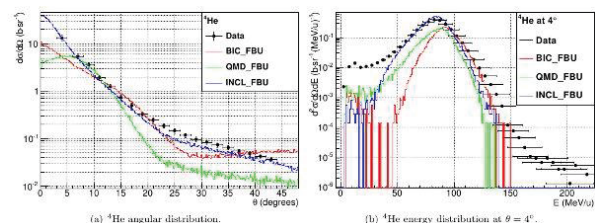


Figure 1. An example of the results obtained for ⁴He fragments with the three entrance channel models using the Fermi break-up as exit channel model. Comparisons with

experimental data show discrepancies for both energy and angular distributions.

Experimental results and GEANT4 simulations of 95 MeV/A ^{12}C cross sections on the different targets will be presented. The prediction capabilities of the different models applied to a 95 MeV/A ^{12}C beam will be discussed.

Keywords: fragmentation, GEANT4, hadrontherapy

References:

- [1] B. Braunn et al., Nucl Inst Meth B 269 (2011)
 [2] J. Dudouet et al., Phys Rev C 88 (2013)

115

Targeting carbonic anhydrase IX by nitroimidazole based sulfamides enhances the therapeutic effect of tumor irradiation and doxorubicin treatment: a new concept of dual targeting drugs

P. Lambin^{1,2}, S.G.J.A. Peeters¹, S.J.A. van Kuijk¹, A. Yaromina^{1,2}, N.G. Liewes¹, R. Saraya¹, R. Biemans¹, M. Rami³, N.K. Parvathaneni^{1,3}, D. Vullo⁴, M. Vooijs¹, C.T. Supuran⁴, J.Y. Winum³, L. Dubois¹,

¹Dept. of Radiation Oncology (MAASTRO Lab), GROW - School for Oncology and Developmental Biology, Maastricht University Medical Centre, Maastricht, The Netherlands

²OncoRay - National Center for Radiation Research in Oncology Medical Faculty and University Hospital Carl Gustav Carus Technische Universität Dresden, Germany

³Institut des Biomolécules Max Mousseron, UMR 5247 CNRS, University of Montpellier1 & 2, Montpellier, France

⁴Dept. of Chemistry, Laboratory of Bioinorganic Chemistry, Università degli Studi di Firenze, Florence, Italy

Carbonic anhydrase IX (CAIX) is a membrane-bound, hypoxia-inducible enzyme highly expressed in solid tumors, with restricted expression in normal tissues. CAIX plays an important role in processes critical for tumor cell growth and metastasis. Several carbonic anhydrase inhibitors have been developed that selectively inhibit hypoxic CAIX activity, thereby reducing extracellular acidosis. The aim of this study was to evaluate the antitumor activity of a newly designed class of dual targeting nitroimidazole based sulfamide drugs (DD) with high affinity for CAIX. We hypothesize that these compounds specifically block CAIX activity, reduce tumor growth and sensitize tumors to irradiation in a CAIX dependent manner.

Methods: Colorectal carcinoma cells harboring a shCAIX (KD) or control shRNA (EV) construct were incubated with DD at varying oxygen levels and extracellular acidification was determined. Tumor-bearing mice received DD (1x/day 10 mg/kg for 5 days) at a volume of 250 mm³ and tumor irradiation (single dose 10Gy) was performed at day 3 of the injection period. Tumor growth, volume doubling time (VDT) and potential treatment toxicity were monitored.

Results: From a series of nitroimidazole based sulfamides we identified a novel nanomolar DD (N-[2-(2-methyl-5-nitroimidazol-1-yl)ethyl]sulfamide; DH348) which showed the most pronounced in vitro reduction in hypoxia-induced extracellular acidosis. In vivo, irradiation as a single treatment resulted in an increased doubling time ($P < 0.001$) in both tumor models. Animals treated with DH348 monotherapy showed a significant slower growth (VDT = 6.32; $P = 0.004$) in the EV tumor (vehicle VDT 3.01) as well as a sensitization for radiotherapy (VDT = 8.59; $P = 0.019$). Therapeutic sensitization was only observed in the CAIX expressing tumors, proving the absence of any "off-target" effect. In vivo testing of the lead molecule in the sulfamide series, in cotreatment with doxorubicin, demonstrated a chemosensitization of CA IX containing tumors. Our interpretation is that the more acidic tumour cells (pH_i) increase the uptake of the more basic doxorubicin.

Conclusion: A newly designed nitroimidazole and sulfamide dual targeting drug is able to reduce hypoxic extracellular acidification, increase intracellular acidification, slows down tumour growth at nontoxic dose and sensitizes tumors in a CAIX dependent manner to irradiation and doxorubicin. The dual drug enhances sensitization towards radiotherapy and certain chemotherapeutic drugs compared to single published CAIX targeting compounds. Our data therefore indicate the potential utility of a dual drug approach as a new strategy for tumor-specific targeting. Dual drugs of the second generation are under development.

Keywords: Carbonic Anhydrase IX, sulfonamides, dual targeting drugs

References:

- L. Dubois, et al. (2013). Radiother Oncol 108(3):523-8
 M. Rami, et al. (2013). J Med Chem. Oct 31

116

Dual energy CT to reduce range uncertainties in hadrontherapy

G. Landry^{1,2}, J. Seco³, K. Parodi¹, F. Verhaegen²

¹LMU, Garching, Germany

²Maastr clinic, The Netherlands

³MGH

Purpose: The full exploitation of the advantageous dose deposition characteristics of protons and carbon ions in hadrontherapy can be marred by uncertainties in the calculation of their range in heterogeneous body tissues. The conversion of single energy CT (SECT) data to stopping power ratio (SPR) is considered a major source of uncertainty in the treatment planning process. While in-vivo range verification techniques based on PET imaging to estimate ^{15}O or ^{11}C production rates have shown promise of reducing range uncertainties by estimating range during treatment, the difficulty in assigning tissue elemental composition (TC) required to predict production rates from SECT data is a confounding factor. Dual energy CT (DECT), which yields estimates of the relative electron density ρ_e and effective atomic number Z_{eff} , shows promise of reducing range uncertainty by providing better estimates of 1) SPR through higher ρ_e accuracy and 2) TC through Z_{eff} .

Materials/methods: A DECT calibration procedure based on scans of a Gammex 467 phantom was developed to obtain estimates of ρ_e and Z_{eff} without the need of prior CT scanner spectral knowledge. By employing a fit of the mean ionization potential to Z_{eff} and the Bethe Bloch equation, DECT estimates of SPR were obtained for each insert of the calibration phantom. The DECT procedure was compared to the conventional SECT procedure. Furthermore TC was assigned on the basis of DECT and SECT scans. Accuracy in SPR and TC were compared for DECT and SECT. All SECT and DECT acquisitions were performed with matched imaging radiation dose levels to enable noise comparison.

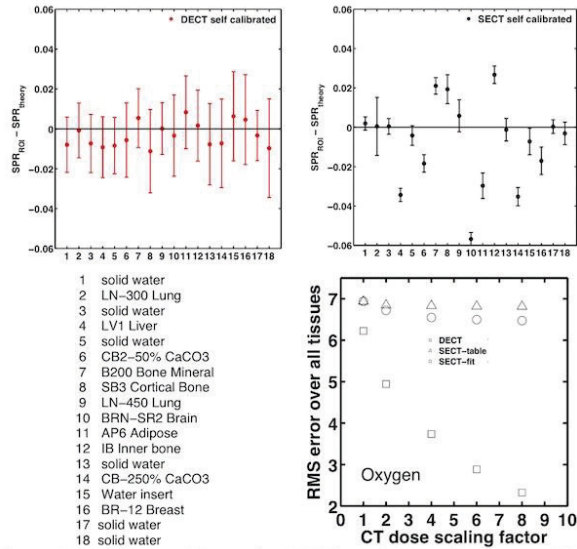
Results:

Figure 1. Top left proton SPR error from DECT for each insert of the Gammex RMI 467 phantom. Top right proton SPR error from SECT scans of the phantom. Bottom axis tick labels correspond to insert IDs listed at Bottom left. Bottom right Root mean square error averaged over all human tissues on oxygen concentration estimation from DECT and SECT.

Figure 1 presents the accuracy (mean and standard deviation) on SPR obtained for regions of interest (ROIs) centered on each insert of the Gammex 467 phantom for DECT and SECT scans obtained using equivalent exposures. SPR errors are limited to less than 0.02 units of SPR when using DECT, as opposed to errors of up to -0.06 units of SPR with SECT. On the other hand at equivalent imaging dose DECT data is significantly noisier. Figure 1 also shows that, depending on the radiation dose employed in DECT imaging, the error on TC assignment (oxygen concentration in this case) can be reduced compared to SECT. The higher noise sensitivity of DECT based TC assignment may require higher imaging radiation dose than SECT to achieve optimal results for the technique.

Conclusion: DECT performs better than SECT for the tasks of estimating proton SPR and TC and shows promise of contributing to the reduction of range uncertainties in proton and carbon ion radiotherapy.

Keywords: dual energy CT, proton therapy, range uncertainty

117

Identification of DNA sequence variants associated with a gene expression profile predictive for radiation induced fibrosis

L.V. Laursen, J. Alsner, C.N. Andreassen, J. Overgaard
Department of Experimental Clinical Oncology, Aarhus University Hospital, Denmark

Purpose: It was previously shown that risk of radiation induced fibrosis can be predicted based on gene expression patterns in cultured fibroblasts irradiated *in vitro* (1). The aim of this study is to identify DNA single nucleotide polymorphisms (SNPs) associated with these gene expression patterns by expression quantitative trait loci (eQTL) analysis.

Materials and methods: Fibroblast cultures established from skin biopsies from 48 head and neck cancer patients were irradiated *in vitro* using a fractionation scheme of 3 X 3.5 Gy. Based on a 9 gene classifier (2) 24 patients were previously identified as having a 'resistant gene expression profile' and 24 had a 'sensitive gene expression profile'. RNA from irradiated cells as well as non-irradiated control cells was isolated and gene expression analysis was performed using Illumina BeadArray HT12 microarrays. Genomic DNA from 47

of the patients was extracted from buffy coats and genotyped using Illumina OmniExpressExome BeadChips.

Results: Genes differentially expressed between the 'resistant' and 'sensitive' gene expression profile groups were identified by prediction analysis of microarrays (PAM). PAM was performed on the difference in gene expression between irradiated and non-irradiated cells (differential gene expression) as well as the gene expression in non-irradiated control cells. For the differential gene expression PAM identified 282 probes and for control cells 121 probes were identified. 48 probes were found in both analyses whereas 234 probes were unique for the differential gene expression and 73 were unique for gene expression in control cells. The majority of genes found in our PAM analyses encode proteins involved in cell cycle, DNA replication, and DNA repair as shown by enriched Gene Ontology (GO) term categories. For probes unique for differential gene expression enriched GO term categories also include 'calcium ion binding' and 'extracellular region'. eQTL analyses (Bioconductor 'MatrixEQTL' and 'iBMQ' packages) were performed using the genes identified in PAM analyses, and a number of candidate SNPs associated with the gene expression profile predictive for radiation induced fibrosis were identified.

Conclusion: We have identified DNA sequence variants associated with a gene expression profile predictive for radiation induced fibrosis. These will have to be independently validated in a larger patient cohort.

Keywords: radiation induced fibrosis, SNPs, eQTL

References:

- [1] Alsner J, Rødningen OK, Overgaard J. Differential gene expression before and after ionizing radiation of subcutaneous fibroblasts identifies breast cancer patients resistant to radiation-induced fibrosis. *Radiother Oncol* 2007;83:261-266.
- [2] Andreassen CN, Overgaard J, Alsner J. Independent prospective validation of a predictive test for risk of radiation induced fibrosis based on the gene expression pattern in fibroblasts irradiated *in vitro*. *Radiother Oncol* (in press).

118

Ultimate Time Resolution in Time-of-Flight PET

P. Lecoq, E. Auffray, S. Gundacker
CERN, Switzerland

Purpose: Highest time resolution in scintillator-based detectors is becoming more and more important, in particular for High Energy Physics and for medical Imaging applications. In medical detector physics L(Y)SO scintillators are commonly used for time of flight positron emission tomography (TOF-PET). Coincidence time resolutions (CTRs) smaller than 100ps FWHM are desirable in order to select a centimeter range region of interest, to consequently improve the image signal to noise ratio and thus give benefit to the patient by smaller injected doses or shorter scanning times. To achieve these goals it is important to study the whole chain, i.e. the gamma-ray interaction in the crystal, the scintillation process itself, the scintillation light transfer in the crystal, the light extraction efficiency, the conversion process in the photodetector and the readout electronics.

Materials and methods: This study aims at determining the experimental and theoretical limits of timing using L(Y)SO based scintillators coupled to silicon photomultipliers (SiPMs). Measurements are based on the time-over-threshold method in a coincidence setup utilizing the ultra-fast amplifier-discriminator NINO and a fast oscilloscope. Because of their slightly better timing performance LSO:Ce codoped 0.4% Ca crystals grown by Agile and coupled to a commercially available SiPM (Hamamatsu S10931-050P MPPC) have been chosen for this study.

Results: For 2x2x3mm³ crystals we achieve a CTR of 108±5ps FWHM at an energy of 511keV. Under the same experimental conditions an increase in crystal length to 5mm deteriorates the CTR to 123±7ps FWHM, 10mm to 143±7ps FWHM and 20mm to 176±7ps FWHM. This degradation in CTR is caused by the light transfer efficiency (LTE) and light transfer time spread (LTTS) in the crystal. To quantitatively understand the measured values, we developed a Monte Carlo simulation tool in MATLAB incorporating the timing properties of the photodetector and electronics, the scintillation properties of the crystal and the light transfer within the crystal simulated by SLITRANI. In this work, we show that the predictions of the simulation are in good agreement with the experimental data. We can also derive what is the best time estimator for the case of fully digital readout as a function of the SiPM characteristics, level of dark count noise and scintillation signal shape.

Conclusions: Very good timing resolution has been obtained and the influence of the crystal length has been quantitatively assessed. Moreover these data allowed us to validate a very detailed Monte Carlo model that helps us now, by switching on and off the different contributions to understand their relative influence and to optimize the overall timing resolution. Future investigations will be on the role of photonic crystals to further improve these results.

Keywords: PET, Time-of-Flight, Time resolution

119

Simulation of a coupled Silicon Photomultiplier & LYSO scintillator detector system for prototype PET detector development

E.J. Leming¹, A.D. Santo¹, F. Salvatore¹, B. Camanzi^{2,3}, A. Lohstroh⁴

¹University of Sussex, Brighton, UK

²STFC UK

³University of Oxford, UK

⁴University of Surrey, UK

In recent years the silicon photomultiplier (SiPM) has been investigated as an alternative to the traditional photomultiplier tube (PMT) in a range of applications. In this work we build a simulation to explore the potential application of SiPMs in Time-of-flight (TOF) Positron Emission Tomography (PET). A Geant4 simulation framework has been developed and is used here to simulate the response of Hamamatsu Multi Pixel Photon Counter (S10362-33-50C) coupled to LYSO scintillating crystals. A comparison between experimental data, taken with a dedicated test stand, and simulation is used to validate the physics model adopted for the SiPM & LYSO system. This simulation has been developed to drive the design of a scalable prototype being designed and built at the Rutherford Appleton Laboratory (RAL), Oxford.

Keywords: SiPM, TOF-PET, Simulation

120

From bench to bedside: development and early clinical results of ¹⁸⁸Re-SSS/Lipiodol for HCC treatment

N. Lepareur¹, V. Ardisson¹, E. Garin¹, N. Noiret²

¹CRLCC Eugène Marquis, Rennes, France

²ENSCR

Purpose:

Hepatocellular carcinoma (HCC) is the 5th most common tumour worldwide and has a dark prognosis. Lipiodol labelled with β^- -emitters has shown promising results for radionuclide therapy of inoperable HCCs. The anti-cancer centre Eugène Marquis and the national school of chemistry of Rennes (ENSCR) have jointly developed a stable and efficient labelling of Lipiodol with rhenium-188 ($E_{\beta\text{max}} = 2.1 \text{ MeV}$). The

different phases of this development, from the first syntheses to the recent first-in-human injections, are described here.

Radiotracer development:

Re-SSS (bis(perthiobenzoato) (dithiobenzoato) rhenium) chelate, used to label Lipiodol, has first been synthesized and fully characterized at the mg-level with non-radioactive rhenium. The synthesis has been transposed at tracer level first with technetium-99m, then with rhenium-188, after modification of the operating conditions. Automation of the preparation, for high-activity therapeutic doses, has been done, and its impact on personnel exposure has been studied.

Pre-clinical results:

¹⁸⁸Re- (and ^{99m}Tc-) labelled Lipiodol has been injected, intra-arterially, in healthy pigs, to assess its preferential hepatic uptake, then in HCC-bearing rats, to check tumour uptake. Results showed a good selectivity of the tracer, with a tumour-to-non-tumour ratio of 2.9 ± 1.5 at 1h and increasing to 4.1 ± 0.7 at 48h. In parallel, optimisation and combination studies have been realised, in vitro and in vivo. A toxicity study - acute and chronic - has been done and demonstrated lack of toxicity of Re-SSS/Lipiodol, opening the way for the injection in human.

Clinical trial - Conclusion:

After plenty of work to optimise the concept, check lack of toxicity and secure the preparation of the injected tracer, competent authorities validated our clinical trial file. The phase-escalation study is planned to consist of 4 dose stages, including 3 to 6 patients each. We are currently at the second stage, with 5 patients injected up to now. Preliminary results show a good tumour uptake.

In conclusion, we have developed, in less than 10 years, a potential HCC treatment by radioembolisation, which is the result of a multidisciplinary and fruitful collaboration between chemists, biologists, physicists and physicians.

Keywords: Hepatocellular carcinoma; Radionuclide therapy; rhenium-188

121

Trigger optimization for *in-beam* PET dedicated to particle therapy range verification

L. Lestand, P. Force, B. Joly, D. Lambert, M. Magne, F. Martin, G. Montarou, A. Rozes, P.-E. Vert
LPC-Clermont Ferrand - Université Blaise Pascal/CNRS-IN2P3, France

Purpose: Proton and carbon ion therapies are a very attractive treatment modality thanks to their well-defined range in matter and specific depth dose characteristics. However, it is very hard to precisely predict the exact location of the depth dose steep fall-off in the patient. This is mainly due to inaccuracies and non-uniqueness in the conversion from the Hounsfield Unit into ion stopping power, anatomical changes, patient positioning and movement. Because of these uncertainties, *in-vivo* ion range verification would be a key issue which would allow improvement in the precision of such methods of treatment delivery.

Materials and methods: Different Research and Development projects are currently under progress in order to provide such *in-vivo* range verification. Among these techniques, PET imaging performed during beam delivery has been already investigated but was abandoned for the benefit of *in-room* PET imaging. As a matter of fact, during *in-beam* PET imaging acquisitions, a large number of false coincidences due to secondary particles emitted by inelastic nuclear collisions makes the image very noisy.

Monte Carlo simulations using the Geant4 9.5.01 toolbox have been performed in order to identify some criteria which would allow to improve signal to noise ratio and to reduce dead time of data acquisition system. The chosen test case is the following:

- Incident particles: protons

- Beam intensity: 3.10^8 protons. s^{-1}
- Physical dose: 1 Gy
- Target: PMMA
- Range modulation: 3.5-6.5 cm
- Energy modulation: 69.4-98.7 MeV
- Total number of primary protons: 42.10^9
- Irradiation time: 14 s

Only the 14 s irradiation period was considered, in order to fully exploit the induced B^+ activity available for an *in-beam* PET acquisition. Different detector geometries have been considered in order to investigate the impact of PET sensitivity.

Results: We have identified an objective trigger criterion which allows selection of true coincidences coming from B^+ annihilation based on the knowledge of the beam position. Thanks to the know-how acquired from high energy physics, we are currently developing an *in-beam* PET device based on fast analogue sampling modules and multiple layer trigger using μ TCA standard. Such technology is able to handle a large flow of data and process them quickly thanks to the serial backplanes and high-speed busses provided by μ TCA standard.

Conclusion: It appears feasible to implement such trigger condition into a dedicated μ TCA serial point-to-point topology. This would provide a fast data acquisition system with low dead-time, able to reject nuclear induced false coincidences.

Keywords: in-beam PET, particle therapy, range verification

122

Development of a Time-Of-Flight Compton Camera for Online Control of Ion Therapy

J.-L. Lev¹, M. Dahoumane¹, D. Dauvergne¹, N. Freud², B. Joly³, J. Krimmer¹, J.M. Létang², L. Lestand³, H. Mathez¹, G. Montarou³, C. Ray¹, M.-H. Richard¹, E. Testa¹, Y. Zoccarato¹

¹Université de Lyon, Université Claude Bernard Lyon 1, CNRS/IN2P3, Institut de Physique Nucléaire de Lyon, 69622 Villeurbanne; MICRHAU pôle de Microélectronique Rhône Auvergne, France

²Université de Lyon, CREATIS; CNRS UMR5220; Inserm U1044; INSA - Lyon; Université Lyon 1; Centre Léon Bérard, France

³Laboratoire de Physique Corpusculaire de Clermont-Ferrand, France

Purpose: The aim of irradiation monitoring during a treatment in ion therapy is to control in real time the agreement between the delivered dose and the planned treatment. In fact, the discrepancies might come from uncertainties such as the planning accuracy by itself, or by variations due to the positioning or the anatomical changes of the patient. This can lead to ion-range variations of a few millimeters. Several devices are under development over the world to detect secondary radiations, which are correlated to the dose deposited by incident ions [1]. Compton cameras are in particular investigated for their potential high efficiency to detect prompt-gammas [2-5]. The present work aims at discussing the clinical applicability of a Compton camera design by means of Monte Carlo simulations validated against measurements of single and coincidence rates.

Materials/methods: A Compton camera with electronic collimation was designed by GEANT4 9.4 simulations, in order to optimize the detection of prompt gammas and to discriminate the neutrons by the time of flight [6]. According to the Monte Carlo design, a prototype, which is composed of three parts, is under development: a hodoscope (2x128 square scintillating fibers), a scatterer and an absorber (100 blocks of streaked BGO of 38x35x30 mm³). The hodoscope is used to tag the incident ions in time and position. The scatterer is a stack of seven double-sided silicon strip detectors of 90x90x2 mm³. Each silicon

layer has 2x64 strips with a pitch of 1.41 mm. Dedicated electronic-readout systems have been designed at IPNL and LPC for the three detection systems. A micro-TCA acquisition system is under development.

Single and coincidence rates have been measured at HIT (Germany), with 160 MeV protons and 311 MeV/u carbon ions impinging on a cylindrical PMMA phantom (diameter 15 cm, length 20 cm) with the intention to assess the simulation predictions and to scale real signal and background count rates.

In order to simulate coincidence rates with GEANT4, the time structure of an IBA cyclotron has been modeled (ion bunches every ~10 ns in the case of protons).

Results: Single and coincidence rates provided by simulations are in good agreement with measurements. For a discussion of the clinical applicability of the Compton camera, the prompt gamma profiles of real to random coincidences have been analyzed.

We also present the different detector developments together with their associated electronics.

Conclusions: The simulations and the experiments give us a preliminary idea of the applicability of the Compton camera in hadrontherapy. Further tests are now required to scale up the prototype for clinical conditions.

Keywords: hadrontherapy, online ion range control, Compton camera

References:

- [1] A.-C. Knopf and A. Lomax, Phys. Med. Biol. 58 (2013) R131-R160
- [2] S.W. Peterson et al., Phys. Med. Biol. 55 (2010) 6841-6856
- [3] G. Llosa et al., NIMA 695(2012)105-108
- [4] T. Kormoll et al., IEEE-TNS (2011) 3484 - 3487
- [5] S. Kurosawa et al., Current Applied Physics 12 (2012) 364-368
- [6] F. Roellinghoff et al. NIM A 648 (2011) S20

123

Multigap Resistive Plate Chambers as a Positron Emission Tomography detector

L. Litov¹, G. Georgiev¹, V. Kozhuharov¹, N. Ilieva², B. Pavlov¹, P. Petkov¹

¹University of Sofia St. Kliment Ohridski, Bulgaria

²Institute for Nuclear Research and Nuclear Energy, Bulgaria

The Resistive Plate Chambers (RPC) are gaseous parallel plate detectors for charged particles that are widely used in large-scale high energy physics experiments as fast trigger detectors for muon spectrometers. The RPC's main advantages are the high time and spatial resolution and their ability to work in strong magnetic fields. RPC technology allows building a device with a large field of view, increasing drastically the geometrical acceptance in comparison to the standard PET devices. The RPC's excellent position resolution for the gamma quanta impact point and the time-of-flight measurement accuracy will allow reconstruction of the image with precision better than 1 mm. Transforming the resistive plate chambers from charged-particle into gamma-quanta detectors opens the way towards their application as a basic element of a hybrid imaging system, which combines positron emission tomography (PET) with magnetic resonance imaging (MRI) in a single device.

The detector design is chosen after detailed GEANT based simulations. Special care is taken to decrease the registration efficiency for Compton scattered photons, while keeping relatively high efficiency for 511 keV photons. The detector photon efficiency is increased by adding a thin (50 μ m) lead-paint layer on the resistive plates. This layer increases photons-to-electrons conversion probability and thus the detector efficiency. Compton suppression is achieved by

adding a layer of floating glass on the lead paint. The glass acts as a filter, preventing low energy electrons to enter the active gas volume. Successful Compton suppression is crucial for the construction of RPC-based PET detectors. Detector prototypes have been build and tested using cosmic muons and ^{22}Na source. The RPCs working in avalanche mode with a Freon-based gas mixture are coupled to front-end electronics, used by the CMS experiment and the signals are fed to a custom made DAQ board or to a fast TDC. A LYSO crystal coupled to SiPM is used to trigger on 511 keV photons. We present results towards the development of a hybrid imaging system based on multigap glass resistive plate chambers. It is show that a stack of multigap RPC detector modules could achieve efficiency for 511 keV photons up to 30% and could ensure signal-to-background ratio (511 keV photons to photons with energies below 380 keV) better than 6:1. We present also test results for the performance and stability of a single multigap RPC module.

The results from the tests are in a good agreement with the simulation predictions and justify the next step - investigation of a full-size single-stack prototype in MRI environment.

Keywords: PET-MRI, Resistive Plate Chambers

124

Ongoing investigations on ion-based radiography and tomography

L. Magallanes^{1,2}, V. Bernd³, S. Brons⁴, O. Jäkel^{1,4}, K. Parodi^{1,2}, I. Rinaldi^{1,2}, M. Takechi³

¹Department of Radiation therapy and Radiation Oncology, Heidelberg University Clinic, Heidelberg, Germany

²Ludwig Maximilians University Munich, Munich, Germany

³GSI Helmholtz Center for Heavy Ion Research, Darmstadt, Germany

⁴Heidelberg University Clinic and German Cancer Research Center, Heidelberg, Germany

Purpose: The major advantage of ion therapy is the conformal dose distribution with the characteristic inverted depth dose profile (Bragg peak) and the finite ion beam range. However, full therapeutic exploitation of ion beams requires a precise determination of the distal dose fall-off in the tissue, which is currently challenged by major range uncertainties. Innovative imaging techniques have to be integrated in the ion beam therapy work-flow in order to minimize such uncertainties. Ion-based transmission imaging (radiography and tomography) is suitable to be applied at different stages of the treatment work-flow. During the planning phase, the distribution of the relative stopping power can be reconstructed and introduced as input of the treatment planning system. Moreover, during the delivery phase, transmitted planar or volumetric images can be used *in-vivo* and prior to treatment for confirming patient anatomy/position and range verification.

Materials and methods: The investigated imaging modality relies on ion beams at higher energy and lower fluence than therapeutically used, so that the transmitted ions can be detected after they exit the phantom, thus providing information on the residual beam range. To this aim, a prototype detector system consisting of a stack of 61 parallel ionization chambers with PMMA absorber plates, which was originally assembled at GSI Helmholtz Center for Heavy Ion Research for dosimetric purposes, has been slightly modified. The setup is being characterized with carbon ion beams at the Heidelberg Ion Beam Therapy Center to assess its potential use in ion-based transmission imaging. The ongoing experimental investigations are supported by Monte Carlo simulations.

Results: The experiments carried out with energetic, low scattering, carbon ion beams show promising images of phantoms of different complexity and composition. A

detailed characterization of the detector, in terms of setup and read-out electronics, has been completed. It revealed the importance of further optimization of the actual detector system, supported by Monte Carlo simulations, to improve image resolution, efficiency of fast data acquisition and image reconstruction, towards the potential application in the clinical routine.

Conclusions: This contribution will present the status and outlook of the ion-based radiographic and tomographic imaging technique which is being developed in the framework of a joint project between the University Clinic in Heidelberg, the Ludwig-Maximilians University in Munich and the GSI Helmholtz Center for Heavy Ion Research.

Keywords: ion-based transmission imaging, ion radiography/tomography

125

Interstitial Detectors for Synchronized Radiation Quality and Range Verification in Ion-Beam Therapy

G. Magrin¹, L. Grevillot¹, M. Dominietto², R. Mayer¹

¹EBG MedAustron, Wiener Neustadt, Austria

²ETH Zurich

Purpose: The accurate conformation of the dose to the tumor volume and the detailed characterization of the biological effectiveness are important challenges of ion-beam therapy that still need to be fully addressed. A poor performance in fulfilling one or both results in an un-necessary dose delivered to healthy tissue and organs at risk.

The single-event-energy-deposition spectra (microdosimetry) are continuously modified when the beam penetrates the tissue and the most drastic changes are located in the region of the Bragg peak (for both, protons and carbon ions). Combining the spectrum information with measurements of dose will virtually make it possible to recreate the Bragg peak, or at least a fraction of it, in the region close to the detector. A feasible result is the estimation of residual range when the device is placed in the distal part of the tumor.

Non-standard microdosimeters inserted in the irradiated region during treatment could perform this task maintaining also the capability of estimating the biological effectiveness.

Materials/methods: Single crystal chemical vapor deposition (SC-CVD) diamonds with tissue equivalent thickness ranging from 0.8 to 18.7 μm were developed and tested in the framework collaborations of MedAustron and INFN Tor Vergata and Legnaro, AIT, and ENEA with alpha radiation of 5.5 MeV and below.

Monte Carlo simulations (Fluka and Gate/Geant4) supported the design of superficial and interstitial radiation detectors for the characterization of the radiation in terms of quality and of absorbed dose.

Ex-vivo studies to assess the compatibility of the detectors with biological tissue and magnetic resonance imaging (MRI) have been initiated in collaboration with ETHZ.

Results: SC-CVD diamonds have been simulated to optimize their characteristics of thickness and transversal section and improve the performances. A self-calibration method has been identified.

Measurements with alpha particles and calibrated gold absorbers have been done using different diamond prototypes. The feasibility of miniaturizing the device has been verified by manufacturing detectors with sensitive volumes of 150 μm in diameter and 230 nm in thickness and reaching virtually 100% of charge collection efficiency for lineal energies over 60 keV/ μm .

Animal studies proved the compatibility of the device with MRI and gave preliminary indication for physiological compatibility.

Conclusions: The devices based on SC-CVD diamond have shown compatibility with interstitial measurement of dose and parameters which can be associated to radiation quality

and biological effectiveness in order to improve accuracy in the definition of the irradiated volume and the radiation residual range.

Future improvements of the technique and optimization of the detector design will be based on additional simulation studies and in-vivo experimental tests.

Keywords: Ion beam therapy, Radiation quality, Residual range

126

The Radiation Oncology Group of EORTC: From the past to the future

P. Maingon

Centre Georges-François LECLERC, Dijon, France

The ROG is one of the funding members of EORTC. Over the last decades, the EORTC Radiation Oncology Group (ROG) has concentrated its efforts into conducting practice-changing randomized phase III studies in many tumors sites such as brain, head and neck, breast, prostate, and rectal tumors. The ROG is a highly productive and welcome almost 300 members. Actually, it is working in close collaboration with disease-oriented groups as well as with non EORTC research groups throughout the world (RTOG, TROG, Unicancer). Even if the historical role of the ROG aiming at answering clinical question which directly contributes to the definition of new standards of care remains a major component, some ways of development are still ongoing. Novel radiotherapy combination strategies are highly promising and the challenges of combining targeted therapies and radiotherapy need to be overcome. By the implementation of a robust methodology based on the expertise of the EORTC Data Center, assessing the potential benefits and toxicities of the possible combinations in relevant preclinical models, a comprehensive development strategy that aims at clinical translation in the most promising settings has been implemented in the STAR program (Synergy of Targeted Agents and Radiotherapy). A stringent evaluation early in the development that will help to prioritize Radiotherapy settings, agents and tumor sites could be realized in a collaboration of academic institutions, collaborative groups and industry. With the objective to foster the development of these combined treatments the EORTC ROG has created the STAR working group that established and coordinates a unique European multicentric platform based on a rigorous radiation therapy quality assurance program via a digital central review facility. All partners involved in research strategies from proof of concept to clinical trials are approached to demonstrate the safety and the efficacy of such new transparent partnership building a new business model in the field of treatment of cancer.

127

Development of a technique to speed up the simulation of PET and SPECT

C. Mancini Terracciano^{1,5}, G. Battistoni², T.T. Boehlen³, F. Cerutti¹, M.P.W. Chin¹, A. Ferrari¹, C. Morone⁴, R. Nicolini², P.G. Ortega¹, P.R. Sala², V. Vlachoudis¹

¹CERN, Geneva, Switzerland

²INFN Milano, Italy

³MedAustron, Wiener Neustadt, Austria

⁴University Rome Tor Vergata, Italy

⁵Dipartimento di Fisica, Università degli studi Roma Tre, IT-00146 Roma, Italy

Techniques for a tomographic dosimetry, preferably in real time are highly desirable for quality assurance of hadrontherapy. Therefore the use of positron emission tomography (PET) and single photon emission tomography (SPECT) is expanding beyond traditional clinical diagnostics.

PET imaging during therapy with charged hadron beams is possible thanks to β^+ -radioactive nuclides emerging as by-product of irradiation. SPECT, on the other hand, detects photons produced directly by nuclear reactions. Accurate prediction of positron emitter production and a reliable simulation of the nuclear interactions is then needed to infer information about the dose distribution and for the design of new detectors. This, and similar analyses could be accomplished by Monte Carlo (MC) codes.

For those reasons, a dedicated package for PET scanner simulation was developed [1] using the general purpose MC code FLUKA [2]. FLUKA is a fully integrated particle physics Monte Carlo simulation package, widely used for an extended range of applications (accelerator shielding, detector and target design, calorimetry, activation, dosimetry, medical physics, radio-biology, etc.). Its use for medical applications and activation studies is broad and recent model developments make it a suitable tool for nuclear medicine and hadron-therapy simulations.

One of the limitations of using MC in PET and SPECT is the time needed to run the code. In this work we present several techniques that increase the efficiency of the MC simulation in this field:

Biasing the direction of emission of photons from the electron-positron annihilation and of single photons from nuclear interactions so that they preferentially point to the detector

Artificially increase the probability of nuclear interactions

Produce multiple replicas of radioactive decays and of the de-excitation photons

All these techniques rigorously preserve the physics of the code, without introducing any approximation.

We will also present some typical applications and the gain obtained in each of them.

References:

- [1] P.G. Ortega, Till T. Boehlen, F. Cerutti, Mary PW Chin, A. Ferrari, C. Mancini, C. Morone, P.R. Sala, V. Vlachoudis, "Development of a PET scanner simulation package for FLUKA", abstract for ICTR-PHE 2014.
- [2] A. Ferrari, P. R. Sala, A. Fasso , and J. Ranft, "FLUKA: a Multi-Particle Transport Code," CERN, INFN, SLAC, CERN-2005-10, INFN/TC_05/11, SLAC-R-773, 2005.

128

4D dose calculations and 4D PET image reconstruction using deformable tetrahedral models of moving organs

P. Manescu¹, J. Azencot¹, M. Beuve², H. Ladjal¹, B. Shariat¹

¹Claude Bernard University Lyon 1, LIRIS, UMR 5205 F-69622, France

²Claude Bernard University Lyon 1, IPNL, UMR 5822 F-69622, France

Purpose: Respiratory-induced organ motion is a technical challenge to nuclear imaging and to particle therapy dose calculations for lung cancer treatment in particular. Internal organ tissue displacements and deformations induced by breathing need to be taken into account when calculating Monte Carlo dose distributions or when performing tomographic reconstructions for PET imaging.

Current techniques based on Deformable Image Registration (DIR) cannot fully take into account complex internal deformations of the lungs nor the fact that respiratory motion is not reproducible [1].

This study proposes a method to calculate dose distribution and to reconstruct PET activities over adaptive tetrahedral meshes which deform with time. As an illustration, biomechanical modeling based on Finite Element Analysis (FEA) was used for motion field computation [2], [3], [4].

Methods: Contrary to DIR-based methods where motion is described by relative voxel displacement, each organ is represented as a deformable grid of tetrahedra where

internal motion is described by mesh vertex transformations. Figure 1 summarizes this approach of 4D dose calculation and PET reconstruction. For each organ of a patient with a lung tumour, the voxelized CT attenuation values were converted into tetrahedral density maps respecting the principle of mass conservation. Internal lung transformations were computed using non-linear FEA with a hyper elastic behavior. The Monte Carlo code GEANT4 [5] was used to simulate a proton passive beam targeting the lung tumour. The deposited energy was accumulated over each deforming tetrahedral element.

In order to compensate for respiratory motion for PET the 4D List-Mode

Maximum Likelihood Estimation (LM-MLEM) reconstruction algorithm was adapted to reposition the B^+ radiation activity on tetrahedral meshes. A radioactive source was simulated inside a moving lung tumor using the GATE platform [6].

Results: First, we evaluated the dose calculated using the computed tetrahedral density map by comparing it to the dose calculated on the original CT image. The gamma test was performed with a distance-to-agreement criterion of 3 mm and a 3% dose difference [7] resulting in 98% of the gamma values lower than 1.

Then, we were interested in evaluating the impact of the motion on the 4D PET reconstruction method by comparing the original simulated radiation activity with the reconstructed one using the Pearson Correlation Coefficient (PCC) [8]. The results are significantly improved when motion information is integrated with (PCC = 97%), compared to when no motion correction is applied (PCC = 75%).

Conclusions: We have presented a new approach to include respiratory motion in hadron therapy dose calculation and in PET reconstruction using a tetrahedral representation of the human anatomy. Before it can be used in clinical cases, this method needs to be validated and calibrated with real measurements using specific physical phantoms.

Keywords: Dosimetry, Tetrahedron, 4D PET

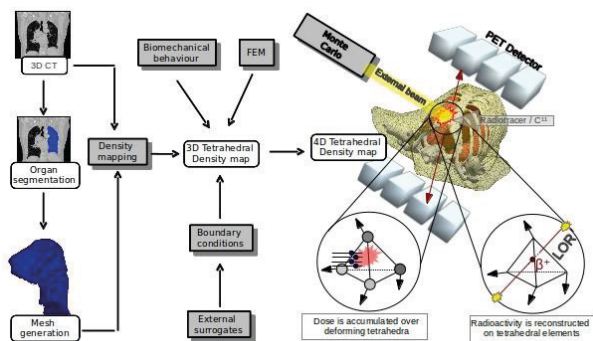


Figure 3. Flowchart of the 4D dose calculation and PET reconstruction methods using tetrahedralized representation of the human anatomy.

References:

- [1] Seppenwoolde Y, Shirato H, Kitamura K, Shimizu S, Van Herk M, Lebesque J, Miyasaka J, Precise and real-time measurement of 3d tumor motion in lung due to breathing and heartbeat, measured during radiotherapy, *Int. J. Radiation Oncology Biol. Phys.* 53(4), 822-834, 2002.
- [2] Saade J , Didier A.L, Villard P.F Buttin R , Moreau J.M , Beuve M, Shariat B, A preliminary study for biomechanical model of the respiratory system, *VISAPP*, 2010.
- [3] Al-Mayah A, Moseley J , Velec M, Brock K , Toward efficient biomechanical-based deformable image

registration of lungs for image-guided radiotherapy, *Phys. Med. Biol.* 56(15), 2011.

- [4] P.S Manescu, H. Ladjal, J. Azencot, M. Beuve, E. Testa, B. Shariat. , 4D radiotherapeutic dose calculation using biomechanical respiratory motion description. *International Journal of Computer Assisted Radiology and Surgery*, Springer. 2013.
- [5] Agostinelli S, Allison J, Amako Ke, Apostolakis J, Araujo H, Arce P, Asai M, Axen D, Banerjee S, Barrand G, et al Geant4 a simulation toolkit. *Nuclear instruments and methods in physics research section A: Accelerators, Spectrometers, Detectors and Associated Equipment* 506(3):250, 2003.
- [6] Jan, S., Benoit, D., Becheva, E., Carlier, T., Cassol, F., Descourt, P., Frisson, T., Grevillot, L., Guigues, L., Maigne, L., et al., Gate v6: a major enhancement of the gate simulation platform enabling modelling of ct and radiotherapy. *Physics in medicine and biology* 56, 881, 2011
- [7] Daniel A Low and James F Dempsey. Evaluation of the gamma dose distribution comparison method. *Medical Physics*, 30:2455, 2003.
- [8] Lee Rodgers, J., Nicewander, W.A., 1988. Thirteen ways to look at the correlation coefficient. *The American Statistician* 42, 59-66.

129

Implementation of a GPU Monte Carlo protons transport code for dose calculations: methods and challenges

D. Maneval¹, B. Ozell², P. Després³

¹Université Laval, Quebec, Canada

²École polytechnique de Montréal, Canada

Hadrontherapy is an advanced technique of external radiotherapy. Ions have a finite path in matter with a maximum deposit energy in their distal range called Bragg peak. This allows a better ballistic treatment than conventional techniques with better sparing of organs at risk and healthy tissues. Currently, hadrontherapy uses low Linear Energy Transfer (LET) ions such as protons or high-LET ones such as carbon ions. The most accurate dose calculations in protontherapy stem from Monte Carlo algorithms. However, their clinical implementation remains problematic due to long computation times. Recently, Graphics Processing Units (GPU) were used to significantly accelerate dose calculation algorithms in external beam radiotherapy and brachytherapy. While GPUs offer unprecedented parallel computing capabilities, implementing a Monte Carlo code on these devices remains challenging.

This work is aimed at presenting these challenges as well as implementation strategies used to address them in the context of Monte Carlo proton transport. It relies on GPUMCD, a validated GPU Monte Carlo code for photons and electrons. Proton physics was integrated into GPUMCD based on Geant4, which serves as a gold standard for comparison in the work we are presenting. Besides, Geant4 is also used to statistically quantify the thread divergence, paving the way for counteract this effect.

Methods to reduce thread divergence and memory bandwidth problems will be presented, along with preliminary results of the accuracy and timing performances of the GPU code.

The ultimate objective of this work is to allow the clinical use of Monte Carlo methods for dose calculations in order to improve the treatment control and quality in protontherapy.

Keywords: GPU, Monte Carlo simulations, protontherapy

130

Rediscovering grid therapy: new approachesI. Martínez-Rovira¹, G.R. Fois², Y. Prezado¹

¹Laboratoire d'Imagerie et Modélisation en Neurobiologie et Cancérologie (IMNC), Centre National de la Recherche Scientifique (CNRS), Campus universitaire, Bât. 440, 1er étage, 15 rue Georges Clemenceau, 91406 Orsay cedex (France)

²Dipartimento di Fisica, Università degli Studi di Cagliari, Strada provinciale Monserrato Sestu km 0.700, Monserrato, 09042 Cagliari (Italy)

Purpose: Grid therapy (GT) refers to a type of spatially fractionated radiotherapy technique that uses mega-voltage photon beams to deliver high radiation doses in a grid-pattern, with field sizes of around 1 cm² [1]. GT has proven to be useful in the management of large deeply seated tumours since it allows delivering high doses with reduced side effects [2]. The success of this technique lies on the fact that areas receiving low doses serve as regrowth centers for normal tissues.

The resulting dose profiles consist of a pattern of peaks and valleys, with high doses along the beams paths and low doses between them. The ratio between the peak dose and the valley dose (PVDR) is an important dosimetric parameter in these techniques since it plays an important role in biological response [3]. In particular, high PVDRs and low valley doses are requested for healthy tissue sparing.

The main drawback of GT is the important lateral scattering of high-energy photons. As a consequence, PVDR values are low (2-5). In order to further improve GT techniques, we propose to combine them with other innovative techniques that use: (i) submillimetric field sizes (from 500 µm to 1 mm), which allow to explore the dose-volume effects [4]; and (ii) other beam energies and particles (protons, electrons).

In particular, three new approaches were studied by means of Monte Carlo (MC) methods: grid synchrotron radiation therapy (gSRT), grid proton therapy (gPT) and grid high-energy electron radiotherapy (gHEERT; 150 MeV to 300 MeV). **Materials/methods:** In photon (gSRT) and electron (gHEERT) dose computations, the MC code PENELOPE (v. 2008) was used. Instead, for proton (gPT) dose calculations, the Geant4 code (v. 9.4) was employed.

Peak and valley doses and PVDR values were assessed in several irradiation configurations (grid field sizes, beam spacings, beam energies, etc.).

Results: In gSRT, PVDR values ranging from 30-70 can be found in the first millimeters and between 10-30 in depth, depending on the field size. In the case of gHEERT, extremely high surface PVDR values are observed (more than 2000), but low values are found in depth (1-2). However, higher PVDR values can be achieved by modifying the beam energy, the c-t-c distance and the beam width. Finally, in gPT, PVDRs around 300 are obtained in the first centimeters, while a uniform dose distribution is achieved in the target. These values are higher than typical PVDR values in GT.

Conclusion: Several new grid radiotherapy modalities were evaluated in this dosimetric study. Preliminary results show that high PVDR values can be achieved in normal tissue, while a uniform dose distribution may be obtained at the target. This indicates a potential gain in tissue sparing. Biological experiments are warranted.

Keywords: grid therapy, Monte Carlo dosimetry.

References:

- [1] H Marks, Radiology 58, 114 (1952)
- [2] J L Huhn et al Technol Cancer Res Treat 5, 607 (2006)
- [3] F A Dilmanian et al Neuro Oncol 4, 26 (2002)
- [4] H J Curtis, Rad Res Suppl 7, 258 (1967)

131

Effect of the washout processes in quality assurance of carbon therapy treatments by means of PET: a Monte Carlo study

I. Martínez-Rovira, C. Jouvie, S. Jan

Service Hospitalier Frédéric Joliot, Commissariat à l'Énergie Atomique et aux énergies alternatives (CEA/DSV/I2BM/SHFJ), 4 place du général Leclerc, F-91401 Orsay Cedex (France)

Purpose: The development of a reliable dose monitoring system in hadrontherapy is essential in order to verify the correct delivery of the planned dose. The imaging of B⁺ emitting isotopes produced during patient irradiation by means of Positron Emission Tomography (PET) is the only method used in clinics nowadays [1]. Among other factors, the accuracy of this method is limited by the loss of signal due to the metabolic decay processes (named washout) [2]. The objective of this study consisted in evaluating, by means of Monte Carlo (MC) methods, the influence of these processes in the resulting PET B⁺ activity maps used for dose verification.

Materials/methods: In this work, the washout processes were incorporated into the GATE code [3]. Following this implementation, Geant4/GATE is able to accurately simulate the full chain from the hadrontherapy irradiation to the PET dose monitoring, including biological effects.

In order to assess the influence of the washout processes, MC simulations were divided into two parts. First, a human head phantom was irradiated with a ¹²C beam, so that an homogeneous dose distribution was achieved in the tumour. In this simulation, ¹¹C distribution maps were generated. These maps were used as B⁺ sources in a second simulation, where the PET scanner (HR+ Siemens) was modelled following a full MC approach. PET activity distributions obtained with or without washout processes were compared for several clinical situations: various tumour dose depositions (0.5 to 3 Gy), duration of the PET acquisitions (5 to 20 min) and tumour washout parameters.

Results: A remarkable reduction of the activity distributions (a factor of 3) was observed in the presence of washout, showing the relevance of these effects (see Figure 1). However, parameters leading to low-statistics PET images (inclusion of the washout processes and short PET acquisition times) do not have a large influence on the distal activity falloff depth (less than 1 mm) for high tumour dose depositions (3 Gy). For low tumour dose depositions (0.5 Gy) differences on the distal activity falloff position can reach values of 3 mm. Finally, the influence of the tumour washout parameters, which depend on the biological state of the tumour, was also evaluated.

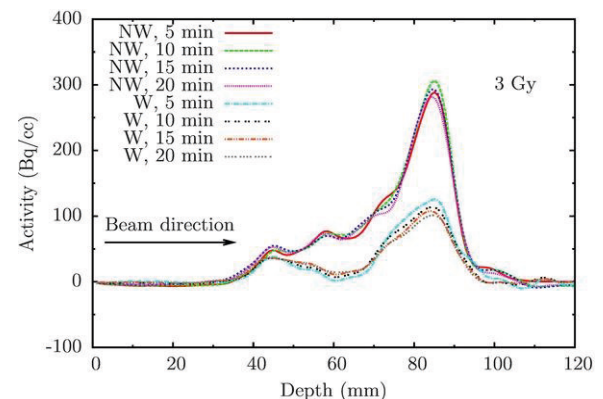


Figure 1: Depth activity profile in a human head phantom in the absence (NW) and presence (W) of washout processes

considering a tumour dose deposition of 3 Gy and several acquisition times (from 5 to 20 min).

Conclusion: It was observed that these parameters play an important role on the activity quantification and thus, on the final dose monitoring in hadrontherapy. Both the development of accurate models and experimental measurements for the assessment of the washout processes are essential and they are in progress nowadays.

Keywords: biological washout processes, PET dose monitoring, carbon therapy

References:

- [1] W Enghardt *et al Nucl Instr Meth Phys Res A* **525** (2004) 284
 [2] H Mizuno *et al Phys Med Biol* **48** (2003) 2269
 [3] S Jan *et al Phys Med Biol* **56** (2011) 881

132

Monitoring of carbon ion beams using secondary ions: investigations in inhomogeneous targets

M. Martiskova¹, G. Arico¹, T. Gaa², B. Hartmann^{1,2}, O. Jäkel^{1,2}, J. Jakubek³, S. Pospisil³, M. Reinhart²

¹Heidelberg University Hospital, Heidelberg, Germany

²German Cancer Research Center, Heidelberg, Germany

³Institute of Experimental and Applied Physics, Czech Technical University in Prague, Czech Republic

Purpose: Radiation therapy with ion beams provides highly conformal dose distributions. These are sensitive to possible variations of the beam settings and changes of the tissue in the beam path, which can deteriorate the dose distribution in the patient. To monitor the ion beam, it was suggested in [Amaldi *et al. NIM A* 617, 2010] to exploit the information carried by prompt secondary ions produced within the patient during irradiation. Our initial experimental investigations of monitoring the beam position, width and energy in a homogeneous phantom have been published in [Gwosch *et al. PMB* 58, 2013]. In this contribution we address the performance of the method in phantoms with inhomogeneities.

Materials and Methods: The experiments were performed at the Heidelberg Ion-Beam Therapy Center using beam energies and widths typical for therapy. Secondary charged particles emerging from phantoms during irradiation were registered by the pixelated semiconductor detector Timepix [Llopert *et al. NIM A* 581, 2007], which was developed by the Medipix Collaboration at CERN. Its multi-layered version (3D voxel detector) [Soukup *et al. JINST* 6, 2011] was used to determine the direction of single particles. Using an anthropomorphic head phantom containing real bones, it was tested whether the distributions of secondary ions around the phantom are sensitive to variations of the beam parameters. In a plastic slab phantom it was studied how changes of its structure affect the secondary ion distribution.

Experiments and Results: The measured particle directions were projected to the vertical beam plane. An example of such a projection is shown in figure 1 (inset). Changes of this projection with the beam parameters and phantom structure were analysed. This new imaging modality [Jakubek *IEEE*, 2011] was found to be capable of detecting lateral beam shifts, changes of the beam energy (affecting the range) and beam width (see figure 1) of a few millimeters in the head phantom. In a homogeneous plastic phantom, missing slabs of 1cm thickness were found to influence the distribution of secondary ions significantly.

Conclusion: The presented experimental investigations demonstrate that measurements of charged particle tracks around phantoms irradiated with carbon ion beams enable to detect missing slices of 1cm thickness in an otherwise homogeneous phantom. In the head-phantom it was shown

that the method provides an attractive source of information on the actual beam delivery, despite the inherent tissue inhomogeneities.

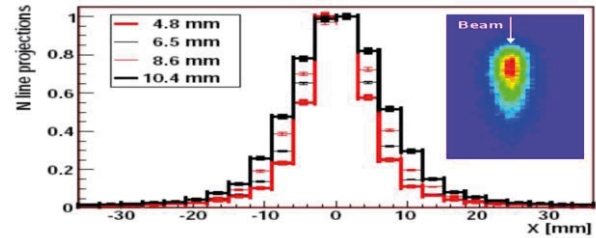


Figure 1: Distributions of the measured tracks in the phantom across the direction of the beam ($E=213$ MeV/u) for four clinically used beam widths given at the entrance of the phantom. The 2D image of the ^{12}C beam in the head phantom obtained by back-projection is shown on the right side.

Keywords: heavy ion radiotherapy, ion tracking, Timepix detector

Acknowledgements: This research was carried out in frame of the Medipix Collaboration.

133

How will we develop the evidence base for biologically individualised radiotherapy?

T. Maughan

Gray Institute for Radiation Oncology & Biology, University of Oxford, UK

Personalised medicine, the widely held paradigm for oncology treatment, implies tailoring the individual's treatment based on a detailed understanding of their tumour biology and possibly their germline characteristics. Radiotherapy treatment is of course individualized in its anatomical deposition of dose. The modulation of radiotherapy based on increased dose, altered fractionation or combination with differing conventional or targeted drugs requires the identification and validation of biomarkers which predict outcome. To date we have no routinely applied biomarker which provides such prediction of outcome, so how will we achieve biologically individualized treatments? Discovery of potential biomarkers originate in a detailed understanding of the changes in biology which affect outcome. Characterization of hypoxia either through imaging or measurement of hypoxia related gene expression has been shown to identify subsets of patients in clinical trials who have benefited from targeted interventions. Similarly, tumours carry highly variable deficiencies in DNA repair capacity. While single markers are shedding some light on this, broader tests providing functional readout of DNA repair capacity are required. In order to validate such measures, retrospective testing in large phase 3 trials is required and is underway for some studies. Subsequently, randomized trials in which the imaging or biomarker is undertaken prospectively and patients randomized into trials with the power to detect treatment biomarker interactions will be the next critical step. Collection of samples from randomized trials of radiotherapy is a critical requirement for such validation. Therefore, ensuring that every radiotherapy trial is associated with a sample collection of the diagnostic sample is a minimum recommendation. Funding for such ancillary translational studies is challenging and requires collaboration with high quality biology laboratories and consortium based approaches to discovery and validation of the requisite biomarkers to change clinical practice.

134

Data models for the Compton camera acquisition and their influence on the reconstructed images

V. Maxim¹, D. Dauvergne², E. Hilaire¹, J.L. Ley², X. Lojaco¹, E. Testa²

¹CREATIS, INSA de Lyon, France

²IPNL, Université Lyon 1, France

SPECT imaging of prompt-gamma radiation with Compton cameras is currently investigated over the world as a relevant candidate to hadron therapy monitoring. The acquisition principle of the camera is based on Compton scattering of gamma photons on a first detector followed by absorption in the camera. The emitting point of a detected photon lies on the surface of the cone having its apex at the scattering point, the axis direction opposite to the direction of the scattered photon and the half-opening angle defined by the energies involved in the detection process. To date, several different approaches have been proposed for the modeling of the direct problem. In some models the Compton projections are integrals of the intensity of the source on conical surfaces. Weights are then given to the intensities upon the position of the point on the conical surface. In other models, the projections are the sum of the integrals of the intensity on the generatrices of the cone. Models also differ by the way they account for the measurement uncertainties. The reconstruction of the image of the source is then an important challenge which faces complexity of the model, memory load and computing time issues.

We simulated data acquired by a Compton camera from sources of gamma photons with various geometries. The simulations are performed with the software MEGAlib, based on the Monte Carlo simulation toolkit Geant4. We reconstructed images of the source with a list-mode MLEM algorithm that implements various models in the system matrix. In a first experiment we stated the role of the inclusion of a model on the energy measurement uncertainties. In a second, we tested the dependency of the probability for a photon to be scattered in a point on the solid angle subtended by the element of detector at the source.

On the one side, modeling the uncertainties on the measurements obviously improves the images. On the other side, we noticed that including the solid angle in the calculation of the system matrix deteriorates the results (Fig. 1, top versus bottom row). In both cases, the sensitivity factors were arbitrarily set to one in the entire image. Preliminary results from a large simulation show that the detection probability decreases with the square of the distance from the emitting point to the scattering point. For a thin scatterer, the probability also decreases with the cosine of the incident angle of the photon on the camera. The latest does not seem verified for a detector having a thickness superior to its lateral resolution.

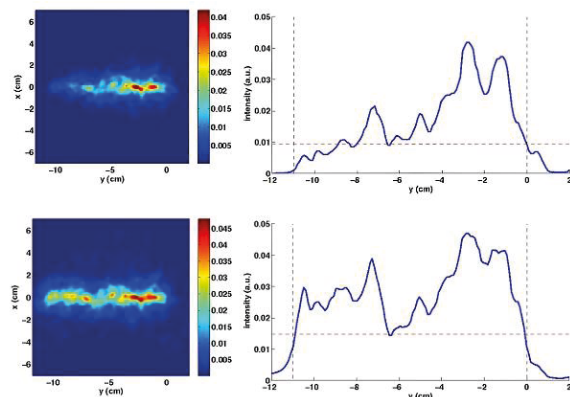


Figure 1. 3D reconstructions of a line source with end points $(0,-11,0)$ and $(0,0,0)$, using 5000 detected events. The camera is parallel to the line and centered at $(0,0,0)$.

Monte Carlo simulations allow refining the models available for Compton camera imaging. In a future work, we will investigate the variation of the sensitivity factors through the voxels and the improvement they may bring to the reconstructed images.

Keywords: image reconstruction, Compton camera, hadron therapy monitoring

135

Log file based dose calculations as a quality assurance tool in scanned beam proton radiotherapy

G. Meier, A. Nanz, R. Besson, S. Safai, A. J. Lomax

Centre for Proton Therapy, Paul Scherrer Institut, Switzerland

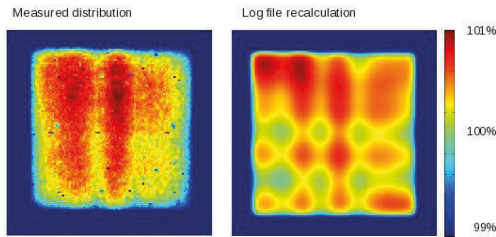
Purpose: Proton therapy with actively scanned beams requires time consuming quality assurance procedures. To reduce these, we propose an independent calculation system based on pre- and post-treatment data to reconstruct the planned and delivered dose.

Materials/methods: Our treatment control system consists of an active treatment delivery system (TDS) and passive treatment verification system (TVS). Both systems are driven by 'steering' files generated via the treatment planning system. From these, pre-treatment doses can be reconstructed. In addition, post-treatment doses can be reconstructed from log files written by the TVS which contain the actual measured parameters of the delivery (position, MU etc). Both reconstruction methods have been used to reconstruct doses for real and simulated delivery.

For post-treatment validations, gamma analysis was used to assess successful delivery, with 95% of points with a dose larger than 30% of prescription dose required to fulfill a gamma criterion of 2%, 2mm.

Results: Reconstructed dose distributions based on log files for uninterrupted deliveries fulfill the above defined gamma criterion. The reconstructed dose is sensitive to delivery errors (e.g. deviations of single spot positions of the order of a tenth of a millimeter) and can illustrate the effect of small systematic errors, which are not picked up by a spot by spot comparison of log and steering file data. The reconstructed doses agree with measurements done with a scintillating foil-CCD system within calculation accuracy. Recalculations were used qualitatively to check the origin of measured inaccuracies, allowing for a distinction of error sources between the dose delivery and the measurement system (see figure). For the example shown, systematic errors in delivered spot positions with maximal deviations of 0.17mm were detected by both the log file calculation and the measurement, indicating the sensitivity and usefulness of such an approach.

Conclusion: Steering and log file based dose calculation were shown to be an accurate tool for assessing the correct delivery of dose both before and after treatment. Furthermore, they are a potential tool in the definition of tolerances for quality checks by exploring the clinical significance of possible delivery errors. In conjunction with measurements (e.g. commissioning), reconstructed dose distributions can be used to assess the source of measured differences to a planned distribution, as illustrated for the case of a planned flat field.



Keywords: Proton therapy, pencil beam scanning, quality assurance

136

Adoptive T cell therapy potentiates efficacy of alpha radio-immunotherapy

J. Ménager^{1,2,3}, J.B. Gorin^{1,2,3}, S. Gouard^{1,2,3}, C. Maurel^{1,2,3}, M. Chérel^{1,2,3,4}, A. Morgenstern⁶, F. Bruchertseifer⁶, F. Davodeau^{1,2,3}, J. Gaschet^{1,2,3}, Y. Guilloux^{1,2,3}

¹INSERM, U892 - CRCNA, Nantes, France

²Université de Nantes, Nantes, France

³CNRS UMR 6299, Nantes, France

⁴Institut de Cancérologie de l'Ouest, Saint-Herblain, France

⁵CHU Nantes, Nuclear Medicine Department, Nantes, France

⁶Institute for Transuranium Elements, Karlsruhe, Germany

Purpose: Alpha radio-immunotherapy (α -RIT) is a cancer therapy that allows delivery of α radionuclides to tumour cells. α -RIT is currently evaluated in the treatment of different solid as well as disseminated cancers. *In vivo*, investigation of α -RIT mechanisms is rare and very few combined treatments have been performed. Therefore, as for external beam radiotherapy, optimizing α -RIT efficacy may be considered to foster immunity against cancer. Combining α -RIT with adoptive T cell transfer (ACT) is one way to boost the immune system. Multiple myeloma (MM) is a malignant proliferation of plasma cells spreading throughout bone marrow and therefore untreatable with external beam radiation. Despite the evolution of the treatments, this cancer remains incurable and development of new therapies is necessary. Thus, this study aims to investigate the therapeutic association between α -RIT and ACT with tumor specific T lymphocytes to treat MM.

Materials/Methods: The therapeutic association is performed in the immunocompetent C57BL/KaLwRij / 5T33 MM mouse model. 5T33 MM cells express CD138 and were transduced to express Ovalbumin (OVA). Thus, α -RIT targets isolated scattered MM cells using an anti-CD138 antibody labelled with bismuth-213, an α emitter. The adoptive transfer consists in the injection of OVA specific CD8⁺ T lymphocytes (OT-I).

Results: We showed that OT-I efficiently recognized 5T33-OVA, *in vitro*. Mice, injected with 5T33-OVA and treated with α -RIT combined with OT-I transfer, demonstrated significant better tumour growth control and improved survival compared to α -RIT or OT-I alone (median survival: 95,5 vs. 68 days for α -RIT alone and 55,5 days for OT-I alone). Monitoring of injected cells showed that OT-I migrate to the tumour site. Only the animals receiving the combined treatment, exhibited stimulation of their immune system, as demonstrated by delayed tumour growth and increased immune cell infiltrates in the tumours.

Conclusions: Altogether, our data demonstrate efficacy of the therapeutic association and a significant impact on the immune system. This preclinical study provides encouraging results to combine ACT of tumour specific T lymphocytes with α -RIT for cancer treatment.

Keywords: Radio-immunotherapy, adoptive cell transfer, immunobiology

137

A new elastic image fusion model for lung deformation simulation in 4D dose calculations

S. Milz¹, J. Flake¹, W. Ullrich¹, J.J. Wilkens²

¹Brainlab AG, Feldkirchen, Germany

²Department of Radiation Oncology, Technische Universität München, Klinikum rechts der Isar, Ismaninger Str. 22, 81675 Munich, Germany

Purpose: Respiration induced motion is not negligible for Stereotactic Body Radiation Therapy (SBRT) for lung cancer treatments. The intrafractional motion influences the dose distribution delivered to the underlying patient geometry. The quality of any 4D planning procedure depends on the used elastic image fusion. A model with accurate motion estimation is inevitable to generate realistic 4D dose distributions. This study introduces a novel, precise model.

Methods: The new method is a combination of common deformation simulation approaches to exploit the advantages of different strategies. For motion estimation 4DCT image data is used. The free form deformation (FFD) algorithm according to Rueckert *et al.* generates spatial relationships between every time slice covering the full thorax geometry. A set of vector fields v_{ij} connects coordinates of different time slices (x_i, x_j):

$$\vec{x}_i = v_{ij}(\vec{x}_j) \quad (1)$$

In a second deformation step the vector field is optimized for lung areas (Fig. 1.a). A specially filtered part of the already calculated deformation data is used to physically deform the three dimensional organ. For this, a mass spring model (MSM) is implemented (Fig. 1.b). It simulates for a large number of time steps the deformation of the lung. Due to its physical approach, the model spatially optimizes areas closed to the shape of the lung where FFD mostly underestimates the motion. The accuracy in such areas, lung slipping zones (LSZ), is verifiable with landmarks l , which were defined especially for LSZ in several time slices (l_i, l_j). The target registration error (η_{TRE}) measures the difference of the defined and the estimated landmarks:

$$\eta_{TRE} = |\vec{l}_i - v_{ij}(\vec{l}_j)| \quad (2)$$

The influence of the model on the final 4D dose distribution is measured with the 2D gamma index. Two dose distributions were transformed (exhale \rightarrow inhale), one with FFD and one with the optimized deformation model (FFD+MSM).

Results: The spatial optimization is proven by the analysis of the deformation fields v_{ij}^{FFD} and $v_{ij}^{FFD+MSM}$ for i =inhale and j =exhale. The difference vector field plot ($\Delta v_{ij} = v_{ij}^{FFD} - v_{ij}^{FFD+MSM}$) shows additional motion prediction especially for LSZ (Fig. 1.c). The accuracy is proven by the η_{TRE} test. 20 landmarks were matched. While FFD achieves a median value of 5.3mm, FFD+MSM improves the median to 2.0mm. The full error distribution is optimized:

Table 1.

η_{TRE} [mm]	FFD	FFD+MSM
mean	5.1	2.6
median	5.3	2.0
upper quartile	7.1	3.6
lower quartile	2.8	1.4
maximum	10.0	5.3

The motion has a direct influence on the 4D dose. The difference of both transformed dose distributions (exhale→inhale) is clearly visible in the sagittal view (Fig. 1.d). The 2D gamma test revealed that only 89.5% passed the criterion (2mm DTA, 2% DD). The gamma distribution in Fig. 1.d shows large differences with values up to 1.5 notably for LSZ.

Conclusion: The new model spatially optimizes deformation prediction in LSZ. A direct influence on a 4D dose distribution was demonstrated with a failed gamma test. Thus, the accuracy of the deformation model is crucial for the quality of 4D dose calculations.

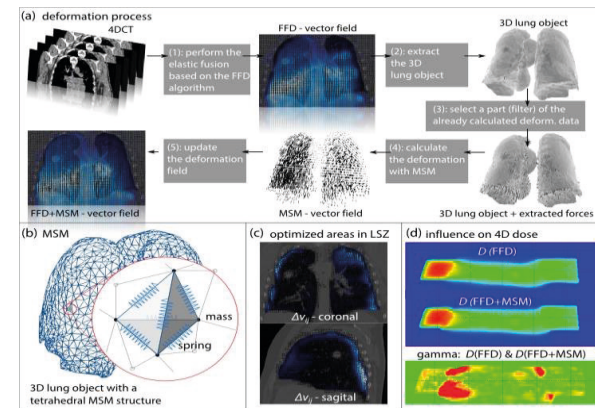


Figure 1

Keywords: Elastic image fusion, 4D dose calculation

138

Rectal cancer and fractionation sensitivity in the neoadjuvant radiation therapy setting: a project of meta-analysis and radiobiological modeling from individual patient data in randomized and observational data-sets

R. Miralbell¹, B. Glimelius², E. Zubizarreta³, A. Renehan⁴, J. Hendry⁴, S. Roberts⁵

¹HUG, Geneva, Switzerland

²University of Uppsala, Sweden

³IAEA, Vienna, Austria

⁴Christie, Manchester, UK

⁵University of Manchester, UK

Rectal cancer has a risk for local recurrence after curative surgery and therefore either neoadjuvant or adjuvant radiotherapy is delivered before or after surgery, respectively if the risk is substantial. Two approaches of neoadjuvant therapy have been formally tested in randomized trials; a short course (1 week, 5x5Gy) vs. a protracted (5-6 weeks, 25-28x1.8-2.0Gy). The former approach is more frequently used in Northern and Central Europe while the latter one is more frequently used, associated with chemotherapy, in Southern Europe and the US. Clinical outcome is probably similar with both treatment approaches. Nevertheless, the radiobiological basis for these isoeffective fractionation schedules has never been substantiated. If the therapy is appropriately targeted then the optimum schedule depends on the radiobiological parameters of the tumors, particularly fractionation sensitivity (α/β ratio) and overall treatment time. Although, a good estimate of the fractionation sensitivity for rectal cancer cure is needed, accelerated tumor cell repopulation during preoperative standard fractionated radiotherapy difficult the estimation of a reliable α/β value especially in protracted treatment settings.

There have been around seven relevant trials comparing RT schedules in the modern era, enrolling some 10,000 patients. Agreement in principal has been obtained for access to

individual patient data (IPD) from the above seven modern trials with the data in electronic form. Large numbers of observational (non-randomized) IPD are also needed in order to obtain a critical mass of patients and have the highest chances to obtain a reliable estimation of the radiobiological parameters in question. An electronic format for observational IPD will be more difficult to obtain as prospective coding in a data base is unusual outside a study. Rectal cancer reference centers are presently being targeted with this purpose. The Swedish registry has already committed to participate with 30,000 observational rectal cancer patients from their electronic data base. Manchester, Barcelona, Rome, and Toronto are targeted with the same purpose. The aim is to build-up the largest data base possible with a number far above 40,000 patients (a mega-study) in order to:

1. Estimate the radiobiological parameters for rectal adenocarcinoma after neoadjuvant XRT +/- chemotherapy followed by radical surgery, specifically the α/β ratio for local failure-free survival and time factor from multiple sources of data
2. Explore the effect of other patient and treatment factors (e.g., toxicity) on these parameters
3. Explore differences between estimates derived from different data sources (trial and observational data, prescribed and delivered doses) and the potential to combine these estimates to increase precision.
4. Explore the use of alternative methodologies (aggregated and individual patient data, different radiobiological models) and the sensitivity of the radiobiological estimates to methodology.

Tumor control will be modeled according to local control and complete remission prior to surgery. Unified definitions will be developed across all the datasets. The primary analyses will utilise the standard LQ model. Models are fitted by direct maximisation of the likelihood and compared using likelihood ratio tests. As in this previous work we will test the impact of inter-patient heterogeneity using beta-binomial models and by fitting heterogeneity models using MCMC methodology. Where the data allow we will also fit the Roberts and Hendry heterogeneity model (red journal 1998), and any other formulations that are potentially useful identified from the literature review.

Keywords: rectal cancer, neoadjuvant treatment, fractionation sensitivity

139

Robust Optimization of IMPT Dose Distributions

R. Mohan

MD Anderson Cancer Center, Houston, TX, USA

Intensity-Modulated Particle (proton and heavier ion) Therapy (IMPT) is potentially the most powerful tool for radiation therapy. It derives this potential from the physical and biological characteristics of particles and the availability of an additional degree of freedom, that of incident energy. However, particles are vulnerable to a significantly greater degree than photons to uncertainties introduced by such factors as inter- and intra-fractional anatomy variations, inadequacies of methods to compute dose distributions accurately or to estimate stopping power ratios of the tissues in the paths of the particle beams, uncertainties in relative biological effectiveness, etc. Presumably, heavier ions are more vulnerable than protons. As a consequence, the biologically effective dose distributions delivered to the patient may be substantially different from what may appear on a treatment plan. Some of the sources introduce uncertainties that are random in nature, while others introduce systematic uncertainty. In other words, the dose distributions are not robust in the face of uncertainties. Thus, the treatment may lead to unanticipated outcomes. In the traditional practice of photon therapy, the combined

effect of uncertainties is incorporated into margins for the planning target volume (PTV) and organ at risk volume (ORV), a practice that is not transferable to particle therapy in part because of uncertainties in the ranges of particles and, in part, due to the perturbation in dose distributions within, and not just at the boundaries, the anatomic structures caused by the factors mentioned above.

Particle dose distributions can be made less sensitive to uncertainties by using larger numbers of beam, making spot sizes larger, degrading distal edges and by reducing uncertainties in general. However, in order to account for residual uncertainties, it is necessary to resort to robust optimization. Robust optimization methods, which have long used in many fields such as statistics, finance, manufacturing, medicine, etc., can also be applied effectively in the optimization of IMPT to make the resulting dose distributions substantially more resilient to uncertainties. Several different IMPT robust optimization approaches are being explored. Examples include voxel-by-voxel worst-case, mini-max worst case and statistical approaches. Illustrative examples comparing results of different approaches with the traditional PTV-based approach will be presented. Current approaches have so far dealt with setup and range uncertainties only. Research to incorporate inter- and intra-fractional anatomic variations and uncertainties in biological effectiveness is just starting. Such research is essential to fully realize the potential of particle therapy.

140

Parameterization of lateral dose profiles for proton therapy application at CNAO

M. Mori¹, M. Ciocca², A. Fontana³, A. Mairani^{2,4}, K. Parodi^{5,6}, A. Rotondi^{1,3}

¹Dipartimento di Fisica, Università di Pavia, Italy

²Fondazione CNAO, Pavia, Italy

³INFN Sezione di Pavia, Italy

⁴HIT, Heidelberg, Germany

⁵Heidelberg University Clinic, Heidelberg, Germany

⁶Ludwig Maximilians University, Munich, Germany

The main purpose of this work is to parameterize the FLUKA calculated lateral dose beam profiles for protons in water at CNAO (Centro Nazionale Adroterapia Oncologica). The CNAO Treatment Planning System (TPS) currently calculates plans using a double Gaussian model with a database of parameters that was customized for the Heidelberg Ion Beam Therapy Center (HIT). Before patients' treatment, studies have been performed in order to understand the impact of different beam profiles on dose calculations [1] and the results have been considered acceptable for therapy. After these studies, CNAO decided to improve dose calculations by introducing a more accurate database for its TPS, obtained by the FLUKA Monte Carlo (MC) [2,3] simulations accounting for the CNAO beamline. The second purpose of this work consists in the investigation of alternative models for the fitting function, to obtain a more accurate description of the tails of lateral dose distributions in water.

The analysis was performed for all the 147 TPS energies ranging from about 60 to 230 MeV. The work has been done with the ROOT framework [5], exploiting Minuit features [6] for a detailed error evaluation. For each beam energy we have fitted the lateral beam profiles at 124 depths along the longitudinal direction. For each energy and depth, the best fit gives four parameters for the TPS double Gaussian model [4]:

$$D(r) = N \left[(1 - w) \frac{1}{2\pi\sigma_1^2} e^{-\frac{r^2}{2\sigma_1^2}} + w \frac{1}{2\pi\sigma_2^2} e^{-\frac{r^2}{2\sigma_2^2}} \right]$$

Where σ_1 and σ_2 are the sigma, w is the relative weight and N represents the normalization factor. For the second purpose

we have studied two alternative fitting functions. The first one makes use of four parameters and is a sum of a Gaussian and a Rutherford hyperbole to describe the peak and the tails of the distribution, respectively. The second one depends on six parameters and adds a third Gaussian to the TPS model to better describe the tails of lateral dose profiles.

Best fit parameters have been obtained by optimizing the minimization procedure with different algorithms (gradient, simplex and MC) and the final values were compared with the HIT ones.

Comparing the actual TPS database and the one obtained in this work we have found a promising solution for upgrading the CNAO TPS for patient treatments.

References:

- [1] K. Parodi et al, J. Rad. Res. 54 (2013) 91
- [2] G. Battistoni et al, AIP Conference Proceeding 896 (2007) 31
- [3] A. Ferrari et al, CERN-2005-10 (2005), INFN/TC_05/11, SLAC-R-773 (2005)
- [4] R. Fruhwirth and M. Regler, Nucl. Inst. Met. A456 (2001) 369
- [5] R. Brun and F. Rademakers, Nucl. Inst. Meth. in Phys. Res. A 389 (1997) 81
- [6] F. James, CERN Computing and Data Processing School, 1972

141

A novel TOF-PET detector based on organic scintillators

P. Moskal¹, T. Bednarski¹, P. Białas¹, E. Czerwiński¹, Ł. Kapłon¹, A. Kochanowski¹, G. Korcyl¹, J. Kowal¹, P. Kowalski², T. Kozik¹, W. Krzemien¹, M. Molenda¹, Sz. Niedźwiecki¹, M. Pałka¹, M. Pawlik¹, L. Raczyński², Z. Rudy¹, P. Salabura¹, N.G. Sharma¹, M. Silarski¹, A. Stomski¹, J. Smyrski¹, A. Strzelecki¹, W. Wiślicki², M. Zieliński¹, N. Zoń¹

¹Jagiellonian University, Cracow, Poland

²Świerk Computing Centre, National Centre for Nuclear Research, Poland

A new concept of TOF-PET detection system developed at the Jagiellonian University [1,2] will be presented. The novel solution opens unique possibilities of combining PET with CT and PET with NMR, so that the same part of the body can be scanned at the same time with both methods without moving the patient [3]. The method allows also for three dimensional reconstruction of the gamma quantum interaction point [3] enabling significant reduction of parallax errors in reconstruction of PET images.

The novelty of the concept lies in employing large blocks of polymer scintillators instead of crystals as detectors of annihilation quanta, and in using predominantly the timing of signals instead of their amplitudes for the reconstruction of Lines-of-Response. The low efficiency for detection of annihilation quanta and low probability for photoelectric effect in polymer scintillators can be compensated by large acceptance and very good time resolution achievable with this kind of detectors. To take fully advantage of the fast signals a novel front-end electronics allowing for sampling in a voltage domain was developed [3], and new methods for the reconstruction of hit position of the gamma quantum based e.g. on the Compressing Sensing theory are elaborated [4]. The solutions are subject of ten patent applications submitted this year [3] which will be presented for the first time. The talk will include an overview of the novel detector, electronics and signal reconstruction concepts.

Two different designs of the diagnostic chamber will be presented. First, referred to as the Strip-PET [5], contains plastic scintillator strips read out by pairs of photomultipliers arranged around a cylindrical surface. The second solution, referred to as the Matrix-PET [6], uses plastic scintillator plates read out by arrays of photomultipliers. In both cases a

sampling of signals in voltage domain allow for localization of the interaction point.

The project is supported by the Foundation for Polish Science and the Polish National Center for Development and Research.

Keywords: Time-of-Flight Positron Emission Tomography, Plastic Scintillators, Signals Sampling

References:

- [1] P. Moskal, Patent applications (2010): PCT/PL2010/00062, PCT/PL2010/00061
- [2] P. Moskal et al., Bio-Algorithms and Med-Systems 7 (2011) 73
- [3] P. Moskal et al., Patent applications (2013): P405178, P405179, P405181, P405182, P405183, P405184, P405185, P405186, P405187, P405188
- [4] L. Raczynski et al., Acta Phys. Pol. B Proc. Supp. 6 (2013) 1121
- [5] P. Moskal et al., Nuclear Medicine Review 15 Supp. (2012) C81
- [6] P. Moskal et al., Nuclear Medicine Review 15 Supp. (2012) C68

142

From Bench to bedside: experience of the glioblastoma model for optimization of radiosensitization

E.C. Moyal

INSERM U1037, CRCT, Toulouse, France

Department of Radiation Oncology, Institut Claudius Regaud, Toulouse, France

Radioresistance of glioblastoma (GBM) is dependent on intracellular radioresistance but also on factors controlling the micro-environment both potentially being activated by irradiation. More recently, tumor heterogeneity and presence of GBM stem cells have been fully implicated in modulation of GBM radiosensitivity. Our team is involved since several years in translational research in radiobiology/radiotherapy in the aim to optimizing the efficacy of radiotherapy of patients treated for glioblastoma by studying and deciphering biological pathways controlling intracellular radioresistance but also angiogenesis, hypoxia and invasion. We have first shown that FGF2 controls radioresistance through the farnesylated form of RhoB and that integrins $\alpha\text{v}\beta\text{3}$ and $\alpha\text{v}\beta\text{5}$ control GBM radioresistance but also hypoxia and angiogenesis *in vitro* and *in vivo* through RhoB. More recently we demonstrated that FGFR inhibition by a specific FGFR inhibitor led to *in vitro* and *in vivo* GBM radiosensitization as well as inhibition of the expression of HIF-1 α . We also recently shown that irradiation as hypoxia induced HIF1 α in GBM through ILK that we previously demonstrated to mediate $\alpha\text{v}\beta\text{3}$ and $\alpha\text{v}\beta\text{5}$ integrins- induced radioresistance and that inhibiting HIF-1 α led to GBM radiosensitization. We then showed that inhibiting farnesylation of RhoB with the farnesyltransferase inhibitor Tipifarnib induced *in vitro* radiosensitization as well as oxygenation and vascularisation normalisation *in vivo*. Based on these preclinical studies we designed a Phase I-II clinical trial associating Tipifarnib with radiotherapy in newly diagnosed GBM patients, all the patients being followed by MRI spectroscopy as well as perfusion MRI. Expression of the proteins that we showed to control GBM radioresistance through RhoB were studied by immunohistochemistry in the tumor of all the patients included in the trial. This study allowed us to confirm in the patients the vascular normalisation after Tipifarnib and radiotherapy treatment and to show for the first time that expression of $\alpha\text{v}\beta\text{3}$ integrin and FGFR1 were correlated with poor overall survival and shorter time to progression confirming that FGFR1 and $\alpha\text{v}\beta\text{3}$ integrin pathways are of interest to target in association with radiotherapy in the aim to radiosensitizing glioblastoma.

Our team is pursuing this translational research including the study of the involvement of these pathways in GBM stem cells radioresistance.

143

Potential of radiation response by a novel EGFR/DNA targeting molecule in a triple negative breast cancer model
T.M. Muanza, J.-C.J. Bertrand, M. Heravi, S. Kumala, Z. Rachid, D. Radzioch
Jewish General Hospital, Segal Cancer Centre, McGill University, Montreal, Canada

Purpose and objectives: Epidermal growth factor receptor EGFR is often overexpressed in human malignancies and it is associated with the activation of the AKT pathway leading to anti-apoptotic effects. This also includes the lack of sensitivity of some tumours to several existing cytotoxic therapies such as radio and chemotherapies. Therefore, it is of great importance to develop novel anti-cancer drugs effective against EGFR-overexpressing cancer cells.

ZRBA1 is a binary targeting molecule, which not only blocks EGFR at the TK domain but also induces DNA breaks. However, the binary property of this molecule can be limited by DNA repair mechanisms in cancer cells. Therefore to further increase the efficacy of treatment we combined ZRBA1 with ionizing radiation.

Methods: Using MDA-MB-468 breast cancer and 4T1 mouse mammary cancer cells, we performed colony forming assay to determine the radio-modulating effect of ZRBA1. The combined treatment was tested at multiple schedules (before radiation, concurrent and after radiation). Using Western blot analysis, flow cytometry and comet assay we have also evaluated the effect of each of the treatments alone and in combination on the level of apoptosis and cell cycle arrest as well as DNA damage induction. Finally, we have confirmed our *in vitro* data in a syngeneic breast cancer model by performing a tumour growth delay assay.

Results: Our colony forming assay showed a radiation dose enhancement factor (DEF) of 1.5 when ZRBA1 (22 μM) is combined with radiation. Moreover, our flow cytometry analysis showed a significant increase in G2/M cell cycle arrest when ZRBA1 and radiation are combined ($p < 0.046$). Similarly, MDA-MB-468 cells treated with ZRBA1 and radiation showed increase in both single and double strand breaks. Western blot results demonstrated the highest level of cleaved PARP when radiation and ZRBA1 are combined as a late response. Importantly, our *in vivo* tumour growth delay assay strongly suggests that ZRBA1 potentiates the radiation response in our 4T1 breast cancer model. In addition, tumour growth delay was nearly doubled in combined treated group compared to irradiated only group (26 days in irradiated group vs. 47 days in combined treatment group) with a statistical significance of 0.0456 on day 31 post-treatment (radiation+ ZRBA1 vs. radiation alone).

Conclusion: Our results have shown that ZRBA1 potentiates the radiation response in a triple negative breast cancer model *In vitro* and *In vivo*. The higher potency of this combination is due to increased cell DNA damage, cell cycle arrest and apoptosis.

144

Head motion correction in positron emission tomography using point source tracking system

B. Nazarpour¹, H. Rajabi²

¹Department of Electrical Engineering, East Tehran Islamic University, Tehran, Iran

²Department of Medical Physics, School of Medical Sciences, Tarbiat Modares University, Tehran, Iran

Aim: The motion of the head during brain positron emission tomography (PET) acquisitions has been identified as a source of artifact in the reconstructed image. In this study, a

method is described to develop an image-based motion correction technique for correcting the post-acquisition data without using external optical motion-tracking system such as POLARIS.

Method: In this technique, GATE has been used to simulate PET brain scan using point sources mounted around the head to accurately monitor the position of the head during the time frames.

Result: The measurement of head motion in each frame showed a transformation in the image frame matrix, resulting in a fully corrected data set.

Conclusion: Using different kinds of phantoms and motions, the accuracy of the correction method is tested and its applicability to experimental studies is demonstrated as well.

Keywords: Motion correction, Point sources, PET, MAF (multiple acquisition frame), GATE

145

Comparison of 4 MV and 6 MV photons for whole breast irradiations

M. Nesteruk, M.K. Fix, D. Frauchiger, L. Henrich, K. Lössl, P. Manser, M. Schmücking, D. Terribilini
Inselspital, Bern University Hospital, and University of Bern

Purpose: Several studies were conducted to investigate potential benefits on dose distribution by using 4 MV photon beams compared to higher photon energies. These works were mainly focused on phantom studies, showing differences mainly at the air-water interfaces [1]. However, so far there are not many studies carried out on clinical cases showing a real benefit of using this energy. A potentially favourable location of the target volume investigated in this study is the whole breast. Thus, the aim of this work is to examine possible benefits of using 4 MV instead of 6 MV for whole breast irradiations.

Materials and methods: Using golden beam data provided by Varian, the AAA algorithm (11.0.31) was configured for 4 MV photon beams in our treatment planning system Eclipse. Further, 10 patients with breast tumour treated in our clinic with 3D conformal radiotherapy (3DCRT) were chosen. The prescribed dose was 50 Gy in all these plans and for each patient the skin structure was created as a 5 mm margin from the body structure. For each of these plans, a 4 MV plan has been generated by switching the beam energies from 6 MV to 4 MV, while the beam setup and beam modifiers were kept the same. For these cases dose volume histograms for the target as well as for the organs at risk were compared.

Results: Our study shows that better coverage of superficial target volumes in 3D conformal plans can be achieved using 4 MV beams. For the whole breast patients the minimum dose to the PTV was increased by (6.28 ± 2.11) % of the prescribed dose, while the maximum dose increased only by (1.80 ± 0.91) %. However, maximum dose to the skin increased by (1.60 ± 0.56) Gy for a prescribed dose of 50 Gy.

Conclusions: The results of this study suggests that for the considered cases the usage of 4 MV lead to equivalent or in some cases to improved dose distributions when compared to the treatment plans using 6 MV.

Keywords: 4 MV, whole breast irradiation, dose calculation

References:

[1] C F Behrens, Dose build-up behind air cavities for Co-60, 4, 6 and 8 MV. Measurements and Monte Carlo simulations, Phys. Med. Biol. 51 (2006) 5937-5950

146

Present status of CNAO

R. Orecchia^{1,2}, M.R. Fiore¹, P. Fossati^{1,2}, A. Iannalifi¹, S. Ronchi¹, B. Vischioni¹, V. Vitolo¹, M. Krengli^{1,4}, C. Bono¹, G. Fontana¹, B. Tagaste¹, M. Riboldi^{2,3}, A. Pella³, G. Baroni^{1,3}, M. Ciocca¹, S. Molinelli¹, G. Vilches Freixas¹, A. Mirandola¹, Denis Panizza¹

¹*Italian National Center for Oncologic Hadrontherapy, Pavia, Italy*

²*European Institute of Oncology, Milan, Italy*

³*Politecnico di Milano University, Milan, Italy*

⁴*University of Piemonte Orientale, Novara, Italy*

The clinical activity at the Italian National Center for Oncologic Hadrontherapy (CNAO) started in September 2011 with proton treatments, followed by carbon ion treatments in November 2012. At the beginning of the clinical activity two treatment rooms were operational. Now also the central room with both horizontal and vertical beam lines is available. Before the Ministry of Health authorizations to start patient treatment with protons and carbon ions, a preclinical phase with radiobiological and dosimetric tests had been performed with good results. Up to date (end November 2013), about 170 patients have been treated in the frame of a wide range of clinical trials. Patients are referred to our Center from almost all the Italian Regions, and soon treatments for foreign patients will be possible.

So far 15 clinical trials, 6 on proton and 9 on carbon ion therapy, have been approved by the CNAO Ethical Committee. The evaluation of the clinical results of these trials in terms of toxicity and tumor control will be part of the certification procedure to which CNAO has to undergo in order to acquire the EC label for routine patient treatment. The efficiency of the CNAO synchrotron and the patient safety for clinical use are evaluated primarily through the clinical results. As a consequence, the main aim of both the ongoing and closed trials is the evaluation of the toxicity of particle therapy treatments on patients, assessed based on the CTCAE toxicity scale v.4.

In the last months the trials on 1) skull-base chordoma and chondrosarcoma treated with proton therapy, 2) carbon ion therapy for bone and soft tissue sarcoma of head and neck, 3) carbon ion therapy for bone and soft tissue sarcoma of trunk, had been closed with minimal toxicity of grade 3 and 4. These trials had demonstrated the safety of the CNAO particle therapy. In particular, the low incidence of complications is promising, especially considering published data from other particle therapy centres worldwide. As a consequence of the excellent clinical results, CNAO has obtained so far the EC labeling issued by the Istituto Superiore di Sanità, the Italian Health Ministry notifying body, on the three clinical trials previously mentioned.

Keywords: hadrontherapy, patients, safety

147

First results with a new detection system for complex radiotherapy treatment verification

M.C. Ovejero¹, Z. Abou-Haidar², M.A.G. Alvarez⁶, R. Arráns³, C. Battaglia², M.A. Cortés-Giraldo¹, J.M. Espino¹, M.I. Gallardo¹, R. Núñez⁴, A. Pérez Vega-Leal⁴, J.M. Quesada¹, A. Selva⁵

¹*Department of Atomic, Molecular and Nuclear Physics, University of Seville, Seville, Spain*

²*National Center of Accelerators (CNA), Seville, Spain*

³*Virgen Macarena University Hospital, Seville, Spain*

⁴*Department of Electronic Engineering, University of Seville, Seville, Spain*

⁵*Department of Physics and Astronomy, University of Padova, Padova, Italy*

⁶*Physics Institute, University of Sao Paulo, Sao Paulo, Brazil*

The purpose of this contribution is to show the first results obtained with a new detector prototype for complex radiotherapy treatment verification, obtained after a critical reviewing of a previous one [1,2], in order to improve its performance. The results shown here correspond to the characterization of the new prototype; this is a necessary step prior to obtaining dose maps in axial planes, which is the final aim of the system.

One of the main improvements has been the change of the detection system. The new prototype includes a "Dual chip SSSSD BB7" detector manufactured by Micron Semiconductor, Ltd, made up of two single sided silicon strip detectors (SSSD), separated by a dielectric layer of kapton, in a "back to back" configuration. In each SSSSD, the outer surface is segmented in 32 strips, 2mm width each. The active area is 64×64 mm² and the active thickness of each SSSSD is 500 µm. While the detector of the first prototype was a commercial one [1,2], the new detection system has been designed with specific criteria for absorbed dose measurements.

The measurements have been carried out with a Siemens Primus clinical linac, working at photon mode with a nominal beam energy of 6MV, at the Virgen Macarena University Hospital in Seville. The detector is placed inside a plane phantom and is irradiated with a beam perpendicular to the active area. The phantom has been built with polyethylene, since its density is nearly equivalent to that of water, with a size big enough to house the detector and accomplish the electronic equilibrium conditions. Several irradiations of the detector within this configuration, with different radiation field sizes and doses, have been carried out in order to study its behavior.

A preliminary study of linearity, reproducibility, uniformity, resolution, percent depth dose (PDD), dose calibration and output factor of the detection system has been performed; the new system has an improved performance in comparison to the first prototype. As an example of these first results, we can state that the experimental data taken with the new detection system and those obtained with an ionization chamber (regularly used at the Hospital) agree within 1%.

References:

- [1] M. A. Cortés-Giraldo, M. I. Gallardo, J. M. Quesada, R. Arráns and A. Bocci, "Geant4 Simulation to Study the Sensitivity of a MICRON Silicon Strip Detector Irradiated by a SIEMENS PRIMUS Linac" *Progress in Nuclear Science and Technology* vol. 2 (2011) 191-196
- [2] A. Bocci, M. A. Cortés-Giraldo, M. I. Gallardo, J. M. Espino, R. Arráns, M. A. G. Alvarez, Z. Abou-Haidar, J. M. Quesada, A. Pérez Vega-Leal, F. J. Pérez Nieto, (2012) *Nuclear Instruments and Methods in Physics Research A* 673 98-106.

148

Auger electron emitters labeled to monoclonal antibodies trigger cell membrane-mediated bystander effects

S. Paillas¹, F.-X. Arnaud², T. Chardès¹, R. Mairs³, I. Navarro-Teulon¹, A. Pèlerin¹, J.-P. Pouget¹

¹IRCM, INSERM, Montpellier, F-34298, France

²Laboratoire Laplace, UMR 5213, Toulouse, F-31400, Université de Toulouse, France.

³Cancer Research UK, Beatson Laboratories, Glasgow, Scotland.

The observation of radiation-induced bystander response has important implication for understanding the efficiency of radiotherapy particularly after low-dose exposure. We investigated the role of bystander phenomena in cells exposed to low-dose radioimmunotherapy (RIT) using ¹²⁵I-monooclonal antibodies (mAb).

Contribution of bystander effects was assessed using standard medium transfer experiments between donor and receiver cells. In order to identify the role of mAbs' internalization in

bystander response, cells were incubated in the presence of sodium azide, a drug blocking the internalization of antigens. The role of cell membrane rafts in ¹²⁵I-mAbs-induced bystander effects was investigated by incubating cells exposed to RIT with either Methyl-β-cyclodextrine or Filipin, two lipid raft disruptors. Subsequently, we also analyzed signaling pathways activated by lipid raft formation in treated cells. Finally, the potential role of oxidative processes in bystander effects was tested using N-Acetyl-L-Cystein (NAC) or DMSO, two radical scavengers.

Following treatment with anti-CEA or anti-HER1 ¹²⁵I-mAbs, we observed a decrease in survival of both donor (to 60% of control) and receiver cells (to 25% of control), confirming the presence of bystander effects. No cell killing in receiver cells was observed after donor cells were treated with the non-targeting mAb¹²⁵I-PX, indicating the specificity of the latter response. Importantly, when anti-CEA or anti-HER1 ¹²⁵I-mAbs were trapped at the surface of donor cells, no significant difference in survival was observed, compared with the above results, obtained in response to internalized ¹²⁵I-mAbs, both for donor or receiver cells. These results suggest that internalization of ¹²⁵I within the cell is not required for the generation of a cytotoxic bystander response. In addition, the disruption of lipid rafts significantly increased clonogenic survival in donor ($P < 0.001$) and receiver cells ($P < 0.05$). We observed also an inhibition of the activation of ERK and Akt signaling pathways, indicating the important role of the cell membrane and more specifically of lipids rafts in the production of bystander effects. Furthermore, the observation that NAC increased the survival of donor and receiver cells indicated the involvement of oxidative stress in bystander effects associated with treatment using ¹²⁵I-mAbs. These results provide evidence that the cell membrane plays an essential role in the mediation of bystander responses induced by ¹²⁵I-mAbs.

Keywords: auger electron emitters, bystander effect, cell membrane

149

Nuclear translocation of FTS (Fused Toes Homolog) is required for EGFR phosphorylation and confers radiation resistance on uterine cervix cancer

W.-Y. Park¹, A. Anandharaj¹, S. Cinghu¹, J.-R. Yu²

¹Department of Radiation Oncology, Chungbuk National University College of Medicine, Cheongju, Republic of Korea

²Department of Environmental and Tropical Medicine, Konkuk University College of Medicine, Chungju, Republic of Korea

Purpose: Radiation therapy (RT) is the major treatment modality for uterine cervix cancer. However, about one third of the patients especially with locally advanced disease (FIGO IIIB-IVA) suffer from recurrence. Defining the molecular events that contribute to radiation resistance is of critical importance to improve the treatment results. Fused Toes Homolog (FTS) is a member of a group of proteins termed as E2 variants and this group of proteins lacks an active cysteine residue that is required for ubiquitin transfer. Here we evaluated the role of nuclear translocation of FTS in radiation resistance of cervix cancer.

Materials and methods: The expression of FTS was studied by immunohistochemistry from the formalin-fixed paraffin-embedded cervix cancer tissues of patients received curative RT. The point mutation constructs of FTS were made by using site directed mutagenesis and the change of translocation of FTS and its downstream signaling were studied by transfecting normal FTS and its mutants into the normal and cervix cancer cell lines.

Results: Immunostaining of cervix cancer tissues revealed that FTS was located in the nucleus of the cancer cells of the patients with recurrence after RT. In vitro study also revealed that this protein was translocated into nucleus from

cytoplasm upon irradiation. Among the six mutants of possible phosphorylated sites of FTS only the threonine into alanine (T190A) mutant failed to translocate into nucleus. The cells transfected with this mutant FTS (T190A) showed decreased phosphorylation of EGFR, p38 and JNK.

Conclusions: Nuclear translocation of FTS confers radiation resistance on uterine cervix cancer. Threonine residue of FTS at position 190 is essential for its nuclear translocation, which is related with EGFR phosphorylation and its downstream effects.

Keywords: FTS (Fused Toes Homolog), Nuclear translocation, Radiation resistance

150

Experimental characterization of acoustic detection and imaging for Bragg peak localization in proton therapy

K. Parodi¹, W. Assmann¹, S. Kellnberger^{2,3}, M. Omar^{2,3}, C. Gäbisch⁴, S. Reinhardt¹, P.G. Thirolf¹, M. Moser⁵, G. Dollinger⁵, T. Hellerer⁴, G. Sergiadis^{2,3}, V. Ntziachristos^{2,3}

¹Ludwig Maximilian University, Chair for Medical Physics, Munich, Germany

²Technical University Munich, Chair for Biological Imaging, Munich, Germany

³Helmholtz Center Munich, Institute for Biological and Medical Imaging, Munich, Germany

⁴Munich University of Applied Science, Institute for Micro- and Nano-technologies, Munich, Germany

⁵Universität der Bundeswehr, Institute for Applied Physics and Instrumentation, Munich, Germany

Purpose: Range uncertainties still represent a main obstacle to full clinical exploitation of the ballistic advantages offered by ion beams for radiation therapy. Currently, several techniques based on the emission of nuclear reaction products are being explored. However, remaining challenges include complex instrumentation and not straightforward correlation between the underlying electromagnetic energy deposition and nuclear reaction processes. In this work, we investigate direct acoustic detection and imaging of the ion energy deposition that peaks within the Bragg peak.

Material/methods: Experiments were performed with proton beams at the Tandem accelerator of the Maier-Leibnitz-Laboratory in Munich. The low energy of 20 MeV was specifically chosen to probe the maximum achievable accuracy in Bragg peak determination for a very well confined energy deposition. A wide range of beam parameters (intensity and time structure) were varied to explore the systematics of the signal and extrapolate applicability to clinical-like scenarios. In addition to homogeneous water targets, measurements were also performed with a range degrader and a metallic wire emulating an implanted marker.

The thermoacoustic signals were captured using different piezoelectric transducers. A cylindrically focused 3.5 MHz ultrasound transducer was employed to characterize various parameters of operation, while imaging of the Bragg peak was performed by using a high frequency, spherically focused transducer at 10 MHz central frequency. Acoustic signals were amplified with a low-noise 63 dB amplifier before digitization with a digital oscilloscope, which was triggered by the beam-chopper signal. To enhance the sensitivity, an averaging of 16 pulses per measurement was used. Data analysis was performed with MATLAB.

Results: For beam intensities exceeding 10^5 protons/pulse, a clear signal could be acquired, revealing the expected Bragg-peak position with sub-millimeter accuracy. Moreover, 1 mm range differences introduced by a 0.5 mm thick Al absorber could be clearly resolved. The 2D transversal image of the Bragg peak was also found in reasonable agreement with Gafchromic film measurements. Following the very promising proof-of-principle experiments, additional measurements in

the frequency domain are planned in fall 2013, and available results will also be presented.

Conclusions: Acoustic detection offers a more direct way to observe the energy deposition of an ion beam in matter. Although the idea is not novel, state-of-the-art instrumentation primarily developed for photo-acoustic imaging promises to make real-time 3D imaging of scanned ion beams within the patient feasible. The technique holds particular promise for application to next-generation high dose-rate accelerators (e.g., synchro-cyclotrons and lasers), where larger thermoacoustic signals are expected to be produced.

Keywords: Ion beam therapy, Acoustic imaging, Range verification

151

Training the next generation of experts in hadron therapy: the PARTNER training network

The Partner training network

The Particle Training Network for European Radiotherapy, PARTNER, was launched in 2008 with the support of the European Commission. This 4-year Marie Curie Initial Training Network focused on training a new generation of highly specialised professionals in the multidisciplinary field of hadron therapy. In fact, the steadily growing number of proton and ion beam centres generates a critical need of experts who will operate these facilities and carry out the necessary research to achieve a more reliable and cost effective therapy.

Ten academic institutes and research centres, as well as two leading companies in the field of particle therapy, have been involved in PARTNER, which was coordinated by CERN. Over the course of the project, 29 Marie Curie researchers were trained in a wide range of subjects, such as physics, medicine, radiobiology, and information technology. They also performed excellent research in these fields, as demonstrated by their numerous publications, prizes, and awards. The latest results from many of the PARTNER research projects have been published in open access form in a special issue of the Journal of Radiation Research

Besides the scientific and technical courses, an important part of the PARTNER training portfolio was devoted to developing soft skills such as leadership, communication, project writing. These complementary skills are meant to boost the researchers' career opportunities, and indeed many of the PARTNER researchers are now working in various institutes and hospitals involved in hadron therapy around the world.

Keywords: hadrontherapy, cancer, radiotherapy

Acknowledgment: The PARTNER project is funded by the European Commission under FP7 Grant Agreement N. 215840.

152

An integrated monitoring system for the on-line assessment of particle therapy treatment accuracy

V. Patera¹, G. Battistoni², N. Belcari^{3,4}, M.G. Bisogni³, N. Camarlinghi⁴, P. Cerello⁵, F. Ciciriello^{6,7}, G.A.P. Cirrone⁸, S. Coli⁵, F. Corsi^{6,7}, G. Cuttone⁸, E. De Lucia⁹, A. Del Guerra^{3,4}, P. Delogu^{3,4}, R. Faccini^{1,10}, S. Ferretti^{3,4}, E. Fiorina⁵, G. Giraud⁵, A. Kraan^{3,4}, F. Licciulli^{6,7}, B. Liu^{3,4}, N. Marino⁴, C. Marzocca^{6,7}, G. Matarrese^{6,7}, C. Morone^{1,11}, M. Morrocchi^{3,4}, S. Muraro², R. Nicolini², C. Peroni^{5,12}, L. Piersanti^{1,10}, M.A. Piliero^{3,4}, G. Pirrone^{3,4}, A. Rivetti⁵, F. Romano⁸, V. Rosso^{3,4}, P. Sala², A. Sarti⁹, A. Sciubba^{1,10}, G. Sportelli^{3,4}, R. Wheadon⁵

¹University Roma La Sapienza, Italy

²INFN Milano, Italy

³University of Pisa, Italy

⁴INFN Pisa, Italy

⁵INFN Torino, Italy

⁶Politecnico Bari

⁷INFN Bari

⁸INFN LNS

⁹INFN LNF

¹⁰INFN Roma La Sapienza, Italy

¹¹INFN Roma Tor Vergata, Italy

¹²University of Torino, Italy

The quality assurance of cancer therapy treatment with hadron beams ask for a new standard in dose release monitoring. The task of on-line dose profile monitoring must be faced by developing novel imaging modalities related to dose deposition and the assessment of reliable indicators of correctness of the treatment plans.

The INSIDE (INnovative Solutions for Dosimetry in hadrontherapy) project is research program funded by the Italian Minister for University and Research that aims at building an integrated on-line monitoring system of the treatment accuracy. The system is made of a dedicated PET scanner operated in-beam combined with a tracking system able to provide the beam profile within the target volume (see figure 1).

PET imaging is a well assessed method to verify the dose deposition after the hadrontherapy treatment that exploits the correlation between the activity distribution of the short living radionuclides produced by the beam nuclear reactions and the dose distribution. State-of-art PET monitoring systems follow two approaches. The off-line approach consists of moving the treated patient in a clinical PET/CT scanner located outside the irradiation site. In the in-room concept the PET examination is carried out immediately after the treatment by means of a stand-alone scanner installed nearby. A step forward is the so-called in-beam PET monitoring where a dedicated PET imaging system is integrated in the gantry and operates during the irradiation to provide an immediate feedback of the dose deposition. Following such innovative approach, the INSIDE project aims at building an in-beam PET scanner designed to reconstruct the particles range with 1 mm resolution in less than 5 minutes after the first dose delivery. The scanner, tailored for the monitoring of head and neck tumors, is composed of two planar heads, each of 10 cm (axially) x 20 mm (transaxially), to be placed at 50 cm distance around the patient. The detectors are built using the latest technology of Silicon Photomultipliers with 3x3 mm³ granularity and one-to-one coupling to LYSO crystal pixels. A custom designed FE and DAQ system is being developed to cope with the rates typical of a therapeutic beam.

The PET activity map is complemented with the profile of the beam within the target, obtained by tracking the secondary particles (protons) coming from scattering of the primary beam with the target nuclei and from projectile fragmentation in case of C12 therapeutic beams. In fact the emission point of the secondary charged particles is correlated with the Bragg peak position and it can be reconstructed by back-pointing the particle tracks toward the beam path. The tracking system is composed of 6 planes of orthogonal squared scintillating fibers coupled to a 1 mm² SiPM. An electromagnetic calorimeter made of LYSO crystal arrays coupled to Position Sensitive PMTs is placed downstream the tracker and provides the residual energy of the charged particles.

This paper describes the implementation details of the project and provides an update of the status and of the experimental achievements.



Figure 1. Conceptual design of the monitoring system composed of two opposite PET heads located above and below the patient head, under the patient bed, and of the particle tracker located at an angle close to the upper PET head. The beam nozzle is visible on the right side of the picture.

Keywords: Hadron Therapy, In-Beam PET, Silicon Photomultiplier (SiPM)

153

Antitumor activity of combination therapy with TH-302 and irradiation in a rat rhabdomyosarcoma model

S. Peeters¹, R. Biemans¹, L. Dubois¹, C.P. Hart², P. Lambin¹, N.G. Lieuwes¹, R.G.P.M. van Stiphout¹, C.M.L. Zegers¹

¹Department of Radiation Oncology (MAASTRO Lab), GROW - School for Oncology and Developmental Biology, Maastricht University Medical Centre, Maastricht, Netherlands

²Threshold Pharmaceuticals, South San Francisco, CA, USA

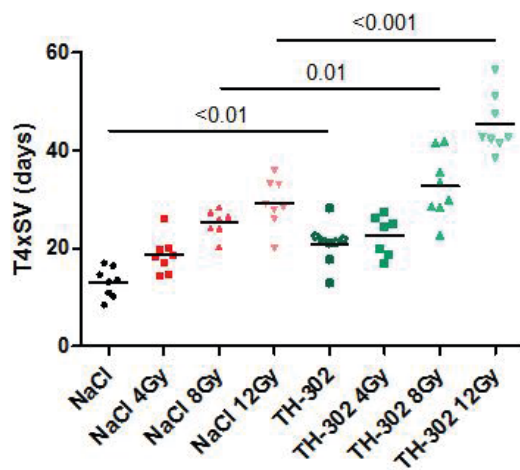
Purpose: Radiotherapy treatment of cancer patients is often impaired by the presence of regions with low oxygen concentration (hypoxia) within the tumor. In order to target and kill the cells within the hypoxic regions additional treatment is needed. Hypoxia-activated prodrugs are specifically directed against the hypoxic regions of tumors and are converted into cytotoxic or cytostatic agents in regions of tumor hypoxia. TH-302 selectively releases the DNA cross-linker bromo-isophosphoramidate mustard (Br-IPM) in the presence of certain reductases and under hypoxic conditions. In a rodent model of rhabdomyosarcoma, we first determined the optimal dose of TH-302, and then investigated the activity of TH-302 combined with a single dose of irradiation under varying oxygen conditions.

Materials & methods: Wag/RIJ rats bearing rhabdomyosarcoma R1 tumors (4.2 ± 1.0 cm³) were injected interperitoneally (i.p.) with either vehicle (0.9% NaCl) or TH-302 (25, 50, or 75mg/kg) for 4 consecutive days. A single dose of irradiation [(IR) 4, 8 or 12Gy] was applied on the third day of TH-302 treatment (2-3 hours after the TH-302 dosing). During the treatment period, oxygen status was altered either by exposing the animals for 4 hours to 7% oxygen breathing or carbogen (95% oxygen) plus nicotinamide

(500mg/kg, i.p.) breathing conditions. Animals were exposed to the altered oxygen environment for 2 hours, dosed with TH-302, and exposed to the altered oxygen environment for an additional 2 hours. Tumor growth was monitored using caliper measurements until a volume of 4 times start volume (T4xSV) was reached (n≥7 per group).

Results: Treatment with 25mg/kg TH-302 led to a significant increase in the number of days to reach T4xSV compared with vehicle-treated rats ($P<0.01$, by Mann Whitney test) and was tolerated in contrast to doses of 50 and 75 mg/kg, which were toxic in tumor bearing rats. The study was continued using 25mg/kg TH-302 combined with IR. An IR dose-dependent effect was observed in both vehicle- and TH-302-treated animals (see figure). A significant delay in tumor growth was observed in animals treated with TH-302 plus 8Gy and 12Gy compared with vehicle-treated animals ($P=0.01$ and $P<0.001$, respectively). Furthermore, the combined treatment of TH-302 and 12Gy caused a synergistic effect (two-way ANOVA $P=0.018$). Increasing the tumor hypoxic fraction by 7% oxygen breathing did not influence the T4xSV. Exposure to nicotinamide plus carbogen reduced the hypoxic fraction and the effect of TH-302 was not significantly different from the vehicle controls ($P>0.1$) under this condition.

Conclusions: Treatment with the hypoxia-targeted drug TH-302 reduced tumor growth in a rat model of rhabdomyosarcoma. Combining TH-302 and IR therapy delayed tumor growth, an effect which was abolished after increasing the oxygenation status of the tumor. These data support clinical testing of TH-302 in combination with radiotherapy.



Keywords: Bioreductive drug TH-302, Hypoxia, Anti-tumor activity

154

Clinical testing of an in-room imaging system for patient setup verification in particle therapy

A. Pella¹, G. Fontana², B. Tagaste², M. Desplanques¹, M.R. Fiore², P. Fossati^{2,3}, A. Iannafi², B. Viscioni², V. Vitolo², C. Bono², M. Riboldi^{1,2}, G. Fattori¹, P. Cerveri^{1,2}, G. Baroni^{1,2}, R. Orecchia^{2,3}

¹Politecnico di Milano University, Milan, Italy;

²Italian National Center for Oncologic Hadrontherapy, Pavia, Italy

³European Institute of Oncology, Milan, Italy

In case of radiation therapy (RT) with accelerated particles, stable patient immobilization and accurate positioning are required to provide a precise target alignment to the beam

line. Recent facilities are equipped with systems devoted to minimize the occurrence of errors in patient repositioning, relying on image guidance techniques as state of the art approach. Images are acquired daily to guide translational/rotational setup corrections to the ideal planned isocenter. Correction vectors (CVs) are calculated comparing in-room imaging with the nominal condition captured in treatment planning images, and then used to improve patient setup accordingly. The Italian National Center for Oncologic Hadrontherapy (Centro Nazionale di Adroterapia Oncologica, CNAO; Pavia, Italy) offers RT with protons and carbon ions. The last room being commissioned for clinical activities (room #2, R2) adopted a custom approach for X-ray setup verification, composed by an articulated robot with six joints which carries a C-arm structure equipped with an X-ray tube and a flat panel. The system is optimized to provide both orthogonal static projections and three dimensional (cone beam CT, CBCT) imaging modalities. Pre-clinical commissioning have been previously addressed. Clinical testing of this system will be presented here.

32 patients have been treated in R2 since the beginning of clinical activities (April 2013). In order to evaluate the clinical performance of the setup verification system, geometric residual errors after image-guided setup correction are reported, operating as follow: (a) rough patient alignment at nominal position; (b) acquisition of double (latero-lateral, LL and antero-posterior, AP) kV X-ray image projections for setup verification; (c) setup correction in accordance with the CV provided by the automatic registration; (d) new acquisition of LL and AP images for residuals evaluation. According with this procedure, results will be presented as median and interquartile range (75th and 25th percentile difference) of residuals recorded during the treatment fractions of 13 patients.

Results are summarized in Table I, and subdivided among head and neck (n=6), pelvis (n=5) and prostate gland (n=2) cases. The maximum median value was recorded in pelvis district (0.33 mm). As expectable, the obtained head residuals are in general slightly lower than extra-cranial districts.

		CC [mm]	LL [mm]	AP [mm]	pitch [°]	roll [°]	rot [°]
Head (n=6)	Median	0.05	-0.13	0.00	-0.10	-0.01	0.00
	Interquartile	0.32	0.53	0.44	0.51	0.36	0.27
Pelvis (n=5)	Median	0.33	-0.03	-0.21	0.00	-0.02	-0.12
	Interquartile	1.02	0.58	0.54	0.40	0.23	0.45
Prostate (n=2)	Median	0.10	0.03	0.00	0.04	0.10	0.00
	Interquartile	0.82	0.43	0.27	0.17	0.21	0.22

Table I: Residuals (Median values and Interquartile range) after setup verification and correction of first 13 patients treated in R2 at CNAO. CC=Cranio-Caudal direction; LL=Lateral direction; AP=Antero-Posterior direction. Residuals are referred to beam eye view.

We report the clinical testing of a custom in-room system for patient setup verification in RT with accelerated particles. Residuals provided by the registration software were found to be consistent with clinical needs.

Keywords: Setup verification, in-room imaging, particle therapy

155

Cardiac toxicity induced by radiotherapy. Role of the GEF, Epac, in hypertrophy and amyloidosis but not in fibrosis

B. Petit¹, D. Azria², C. Bourcier^{2,3}, J. Bourhis^{1,4}, A. Bridier³, W. Dörr^{5,6}, B. Escoudet^{7,8}, P. Fenoglietto², A.M. Gomez², S. Gourguou², A. Llach⁹, V. Monceau⁴, E. Morel⁹, C. Strup-Perrot¹⁰, V. To⁴, M.C. Vozenin^{1,4}

¹Laboratoire de Radio-oncologie, CHUV, Lausanne, CH

²Department of Radiation Oncology, CRLC Val d'Aurelle, Montpellier, France

³Département de radiothérapie, Institut Gustave Roussy, Villejuif, France

⁴INSERM U1030, LabEx LERMIT, Villejuif, France - Faculté de Médecine Paris-Sud, Université Paris-Sud 11, Le Kremlin-Bicêtre, France

⁵Dept. Radiotherapy and Radiation Oncology, Med. Faculty, Technical University, Dresden, Germany

⁶Dept. of Radiation Oncology & Christian Doppler Laboratory for Medical Radiation Research in Radiooncology Medical University, Vienna, Austria

⁷Département de Physiologie, Explorations Fonctionnelles, Assistance Publique-Hôpitaux de Paris, Hôpital Bichat, Paris, France - Université Paris Diderot, Paris 7, France

⁸INSERM U872, Paris France

⁹INSERM U769, IFR141, LabEx LERMIT, Faculté de Pharmacie, Châtenay-Malabry, France

¹⁰LRTE/SRBE/DRPH/IRSN, Fontenay-aux-Roses, France

Background: Cardiac toxicity is a side-effect of anti-cancer treatment including radiotherapy and this translational study was initiated to characterize radiation-induced cardiac side effects in a population of breast cancer patients and in experimental models: The aim was to identify of novel therapeutic target.

Methods: The size of the heart was evaluated in CO-HO-RT patients by measurement of the Cardiac-Contact-Distance before and after radiotherapy (48 months of follow-up). In parallel, fibrogenic signals were studied in a severe case of human radiation-induced pericarditis. Lastly, radiation-induced cardiac damages were studied in mice and in rat neonatal cardiac cardiomyocyte.

Results: In patients, time dependant enhancement of the CCD was measured suggesting occurrence of cardiac hypertrophy. In the human radiation-induced pericarditis, activation of fibrogenic (CTGF, RhoA) and remodeling (MMP2) signals were measured. In irradiated mice, decreased contractile function, enlargement of the ventricular cavity and long-term modification of the time constant of decay of Ca²⁺ transients were reported. Both hypertrophy and amyloid deposition were timely correlated with the induction of Epac-1; whereas radiation-induced fibrosis correlated with Rho/CTGF activation. Transactivation studies support Epac contribution in hypertrophy's stimulation and showed that radiotherapy and Epac displayed specific and synergistic signals.

Conclusion: Epac-1 has been identified as a novel regulator of radiation-induced hypertrophy and amyloidosis but not fibrosis in the heart.

Keywords: Radiotherapy, Cardiotoxicity, fibrosis

156

Research and development of a TOF-based multi-slit collimated camera for online hadrontherapy monitoring

M. Pinto¹, D. Dauvergne¹, N. Freud², J. Krimmer¹, J.M. Letang², C. Ray¹, F. Roellinghoff^{1,2,3}, E. Testa¹

¹IPNL, Université de Lyon, F-69003 Lyon, France; Université Lyon 1 and CNRS/IN2P3, UMR 5822 F-69622 Villeurbanne, France

²CREATIS, Université de Lyon, F-69622 Lyon, France; Université Lyon 1 and CNRS UMR 5220; INSERM U1044; INSA-Lyon; Centre Léon Bérard, France

³Ion Beam Applications SA, Chemin du Cyclotron 3, B-1348 Louvain-la-Neuve, Belgium

Purpose: Hadrontherapy is an innovative radiotherapy modality that allows for high tumour conformality due to the characteristic Bragg peak in the dose-depth profile. However, the high precision involved also makes the monitoring of dose delivery more critical. Currently, only positron emission

tomography is clinically implemented but other techniques may also provide clinically-relevant information, namely the ones relying on prompt-radiation emission. This work addresses the research and development (R&D) of a TOF-based multi-slit collimated camera, one of the possible devices that use prompt-radiation information to monitor dose delivery in particular for proton and carbon ion treatments. This camera involves the detection of prompt gammas emitted during the treatment along the beam axis, for which the correlation with the range of particles in matter has been extensively demonstrated [1,2].

Materials and methods: The development of a multi-slit collimated camera for hadrontherapy monitoring faces unique circumstances mainly because 1) the background events present during an irradiation and 2) the energy of the prompt gammas that may be greater than 10 MeV. Such physical aspects lead to the need of using particle transport Monte Carlo tools instead of analytical approaches to perform the development of such a device. Geant4 toolkit was chosen for this purpose. However, Geant4 overestimates the prompt-gamma emission for this specific application. Moreover, the amount of background events during a typical irradiation scenario may play an important role on showing the benefits of using TOF techniques. Such techniques aim at improving the signal-to-background ratio, thus allowing for a better retrieval of the signal information.

This work used experimental data from several single-slit collimator experiments in order to have irradiation scenarios as close as possible to reality. After the simulations, a procedure was implemented to obtain an analytical prediction of the camera precision based on both the geometrical parameters and the characteristics of the simulated longitudinal profile for a given device.

Results: Following this process, it was possible to both benchmark Geant4 simulations with experimental data and propose several designs for a TOF-based multi-slit collimated camera. The analytical prediction procedure provides an important benefit by greatly decreasing the development time for further optimisations. The results demonstrate the advantage of using TOF in such a device. Experimental results with first prototypes of multi-slit collimated cameras will also be discussed.

Conclusions: The R&D process leading to a TOF-based multi-slit camera will be presented and the various steps and considerations required to attain a monitoring device for hadrontherapy treatments will be discussed.

Keywords: hadrontherapy, prompt-gammas monitoring, collimated camera

Acknowledgements: This work is being carried out within FP7-ENTERVISION network with the Grant Agreement number 264552, being as well in the framework of ETOILE's research programme (PRRH) at Université Claude Bernard Lyon 1 (UCBL) and supported by the FP7-ENVISION programme (Grant Agreement number 241851) and by the LabEx PRIMES ANR-11-LABX-0063/ANR-11-IDEX-0007.

References :

- [1] C. H. Min et al., Applied Physics Letters 89 (2006)
- [2] E. Testa et al., Applied Physics Letters 93 (2008)

157

ClearPEM-Sonic: a multimodal PET-ultrasound mammo-graphy system

M. Pizzichemi¹, R. Bugalho², L. Cao³, G. Cucciati¹, N. Di Vara¹, F. Farina⁴, N. Felix⁵, B. Frisch⁶, A. Ghezzi¹, E.A. Hillemanns⁶, V. Juhán⁷, D. Jun⁸, P. Lasaygues⁹, P. Lecoq⁶, S. Mensah⁹, O. Mundler¹⁰, J. Neves², M. Paganoni¹, J. Peter³, P. Siles⁷, J.C. Rasteiro Da Silva², R. Silva-Silva², S. Tavernier⁸, L. Tessonnier⁷, J. Varela²

¹University of Milano Bicocca, Italy

²Laboratório de Instrumentação e Física Experimental de Partículas Lisboa, Portugal

³DKFZ, Germany

⁴Consortium GARR

⁵SuperSonic Imagine

⁶CERN, Switzerland

⁷Assistance Publique Hôpitaux Marseille, France

⁸Vrije Universiteit Brussels, Belgium

⁹Laboratoire de Mécanique et Acoustique Marseille, France

The ClearPEM-Sonic is a multimodal system dedicated to mammography, capable of providing co-registered metabolic, anatomical and structural information through combination of positron emission tomography with ultrasound elastographic imaging. The project is aimed to improve early stage detection of breast cancer through the high-resolution and high-sensitivity metabolic information provided by PEM, and the high-resolution anatomic information from US. Further improvements in the specificity of the system is provided by the ability to rule out non-cancerous findings from PEM, taking advantage of elastography imaging information.

The ClearPEM-Sonic has been developed by the Crystal Clear Collaboration and is currently installed at Hôpital Nord, Marseille, in the frame of CERIMED, the European Centre for Research in Medical Imaging. The detector is based on LYSO:Ce crystals, each of 2x2x20 mm³, grouped in 192 matrices of 8x4 crystals. BaSO₄ is used as coating material and reflector. Read out is performed individually on both 2x2 mm² faces of each crystal, using avalanche photodiodes (APDs), allowing therefore Depth Of Interaction (DOI) computation. Image registration between PEM and US modalities is performed by custom developed software, exploiting information provided by the magnetic tracking system.

The detector performance has been thoroughly tested during the commissioning phase, confirming a spatial resolution of 1.3 mm. A good DOI resolution has been shown, with asymmetry ratio better than 4%/mm. The co-registration software developed has proved to accurately superimpose images coming from the different modalities with a precision better than 2mm. The clinical trial (phase 1) is being carried out on 20 patients with a known breast lesion who have been injected with FDG for a whole-body PET/CT as part of their diagnostic process. Clinical results are compared to conventional imaging and MRI, with biopsy as a golden standard, to validate the use of ClearPEM-Sonic as a clinical imaging instrument for early detection of breast cancer. An example is shown in Figure 1.

Detector performance and clinical results obtained by ClearPEM-Sonic will be discussed in this presentation.

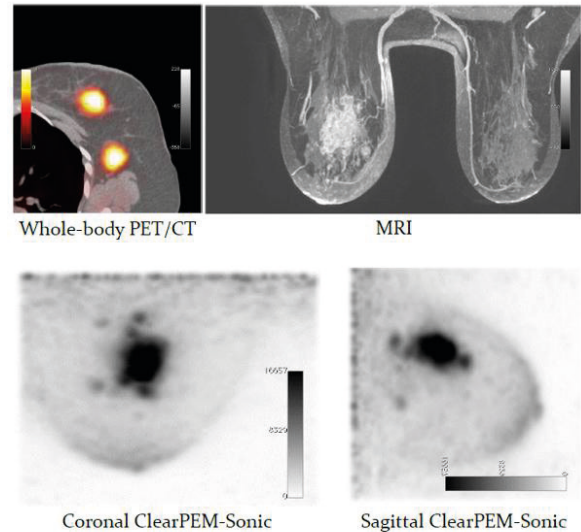


Figure 4. Comparison of standard Whole Body PET/CT, MRI and ClearPEM-Sonic imaging of a multifocal breast cancer.

Keywords: PET, multimodality, breast cancer

158

Time resolved portal dosimetry for Volumetric Modulated Arc Therapy (VMAT) in lung cancer patients with atelectasis

M. Podesta¹, L.C.G.G. Persoon¹, S.M.J.J.G. Nijsten¹, E.G.C. Troost¹, F. Verhaegen^{1,2}

¹Department of Radiation Oncology (MAASTRO), GROW - School for Oncology and Developmental Biology, Maastricht University Medical Centre, Maastricht, the Netherlands

²Medical Physics Unit, Department of Oncology, McGill University, Montréal, Canada

Purpose/Objective: In lung cancer patients, the geometry can rapidly change due to atelectasis or pleural effusion. These changes can result in differences between the planned and delivered dose. Currently, portal dosimetry for VMAT allows verification of integrated arc delivery. Due to the dynamic nature of VMAT and the changes that can occur, integrated arc fields may be insufficient to detect all but major discrepancies between planned and delivered dose, and require more experience to interpret. Time resolved portal dosimetry may provide a solution to this problem. We present a method to analyze portal dosimetry data in a time resolved manner to detect dose differences and facilitate the identification of their causes.

Methods and Materials: In this study we present 15 lung cancer patients with geometrical changes analyzed with time resolved dosimetry. In our clinic, 2D integrated and 3D portal dosimetry are routinely used for VMAT which was extended to allow for verification of the treatment from time-point to time-point (also called control-points). The time resolved doses are compared with a gamma (γ) evaluation (criteria: 3%, 3mm).

Results: A patient with a squamous cell cancer of the lower lobe of the left lung developed an atelectasis after 11 fractions resulting in tissue displacement and an increased dose to the clinical target volume (CTV) of the tumor (from 106% to 118% of the prescribed dose) while the dose to the affected mediastinal lymph nodes dropped drastically (from 100% to 85%). With time-resolved dosimetry the failing arc angles were identified (Figure 1). In the original plan (plan 1), the highest fail rates are present for the beams angled through the newly formed atelectasis. Following a first plan adaptation a second adaptation was necessary due to further

tissue changes. Finally, a third plan was calculated and remained unchanged during the remainder of the treatment course as it agreed well with the measured time resolved dose.

Conclusions: Time resolved dosimetry for VMAT treatments in lung cancer patients shows that dose differences can be detected at any point in time of the delivery, providing more information (e.g. geometry) to the clinician or physicist. Time resolved dosimetry enables the detection of dose delivery differences and provides more information to discern the cause of discrepancies. With this, more appropriate plan adaptations may be feasible resulting in improved coverage of the target and sparing of surrounding organs at risk.

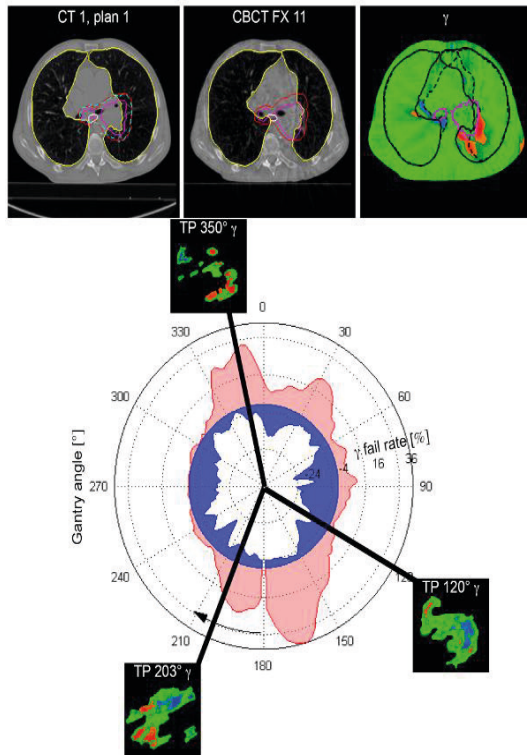


Figure 1. Top panels: the planning CT for the 1st treatment plan is shown with delineated lungs (yellow), esophagus (white), PTV (red), CTVs (purple), and the 95% isodose line (cyan dashed line). In the second panel, the re-delineated CBCT of fraction 11 is shown. The third panel indicates the γ evaluation for the corresponding slices with the lungs (black) and the CTVs (magenta), the dashed and solid lines are the CBCT and planning CT delineations respectively. For the γ evaluation, pixels violating the 3%,3mm criteria are shown in blue ($\gamma < 1$) and red ($\gamma > 1$), pixels within the criteria ($1 < \gamma < 1$) are shown in green. Below these three panels the time-resolved γ fail rate is plotted with 2D γ evaluations at 120, 203 and 350°.

Keywords: Dosimetry, VMAT, EPID

159

²¹²Pb-labeled mAbs targeting CEA or HER2 during α -RIT of small peritoneal carcinomatosis - Dose effect relationship?

J.-P. Pouget¹, A. Pichard¹, V. Boudousq¹, L. Bobyk¹, R. Ladjohounlou¹, S. Paillas¹, M. Le Blay¹, M. Busson¹, C. Lozza¹, P. Maquaire², J. Torgue², I. Navarro-Teulon¹

¹INSERM U896, Montpellier, France

²AREVA Med LLC

Purpose: We investigated the role of monoclonal antibodies (mAbs) internalization on the final outcome (efficacy/toxicity) of mice treated with alpha radioimmunotherapy (α -RIT) using ²¹²Pb-labeled mAbs. The relationship between distribution of radioactivity at the tissue level and subsequent biological radiobiological effects was also assessed.

Materials/methods: Nude mice bearing 2-3 mm peritoneal nodules obtained by xenograft of A-431 tumor cells, expressing low and high level of HER2 and CEA receptors, were intraperitoneally (i.p.) injected with increasing activities (370-1480 kBq; 37 MBq/mg) of either 35A7 (non-internalising anti-CEA), Trastuzumab (internalizing anti-HER2) or PX (non-specific) ²¹²Pb-labeled mAbs. Control groups were injected with corresponding amount of unlabeled mAbs or with NaCl. Tumor growth was followed by bioluminescence and median survival (MS) of control and treated mice was determined. ²¹²Pb-35A7 and ²¹²Pb-Trastuzumab biodistribution was used to determine the cumulative uptake of radioactivity (UOR) in organs and tumors. Mean absorbed doses were calculated using the MIRD formalism. Hematological, liver and kidney toxicities were also assessed. Distribution of radioactivity at the tissue level was determined by digital micro-autoradiography and the relationship with biological markers of tissue damage was investigated using immunohistological approach.

Results: A mild and transient hematological toxicity in groups treated with the highest amount of activity was observed. MS of the groups treated either with internalizing or non-internalizing ²¹²Pb-labeled mAbs was significantly improved compared to those treated with non-specific ²¹²Pb-PX or those only given unlabeled mAbs or just NaCl. MS ranged from 42 d to 94 d using various activity levels of anti-CEA ²¹²Pb-35A7 while MS was not reached over the follow-up period of 130 d for mice treated with anti-HER2 ²¹²Pb-Trastuzumab. However, UOR and absorbed doses were shown to be higher for ²¹²Pb-35A7 mAb than for ²¹²Pb-Trastuzumab (35.5 Gy versus 27.6 Gy, respectively). Investigation of potential relationships between distribution of radioactivity at the tissue level and biological parameters is ongoing.

Conclusions: We investigated the therapeutic efficacy of ²¹²Pb-labeled mAbs in i.p. α -RIT of small tumors. A higher efficacy per decay, of internalizing versus non-internalizing ²¹²Pb-labeled mAbs was found. Heterogeneous distribution of radioactivity in tissues or bystander effects could be involved in the observed lack of absorbed dose/therapeutic efficacy relationship.

Keywords: alpha-radioimmunotherapy, Pb212, bystander effects

160

Nanoparticles and protontherapy: disentangling possible physical effects

Y. Prezado, S. Beilla

IMNC-CNRS, Orsay, France

The challenge in RT is to deposit a tumoricidal dose in the target while keeping the healthy tissues under tolerances. With that aim, new strategies like the use of nanomedicine to improve the performances of the hadrontherapy are being developed. Experiments performed at molecular scale (using plasmid DNA as a probe) have proved that the addition of

platinum or gadolinium nanoparticles (NPs) of 3 nm diameter during fast carbon ions or proton irradiations amplifies the induction of strong biological damages [1]. The enhanced effect has been ascribed to physical processes (ionizations and electron emission), which are activated in the NPs by incident ions and secondary electrons emitted in the tracks. In particular, the production of Auger electron cascades is considered to be highly effective in generation of cellular damages. The consequence of this fast excitation phenomenon would be a neat amplification of the radiolysis induced in the nanometric volume around the NPs. Our goal was to verify that hypothesis.

In this work, Monte Carlo simulations (GATE 6.1) were performed to assess the increase of production of secondary secondary electrons (including Auger electrons) when a cell sample is irradiated by 200 MeV protons in the presence of gold NPs. Two different concentrations of AuNPs, 0.6 and 10 mg/mL, were evaluated.

The number of secondary electrons produced does not significantly differ when nanoparticles are employed, even for the highest concentration studied. A slight increase of Auger electrons production is observed at very low energies (< 100 eV) for the highest concentration (10 mg/mL).

Physical effects seem not to be the main responsible for the enhanced radiosensibilisation of tumor cells in the presence of AuNPs when the irradiation is performed with protons. Other (biological/chemical) mechanisms might be the dominant ones in the amplification of damage.

Keywords: nanoparticles, protontherapy, Monte Carlo simulations

References:

[1] E. Porcel, S. Liehn, H. Remita, et al, Platinum nanoparticles: a promising material for future cancer therapy? *Nanotechnology*. 2010 Feb 26; 21(8):85103. Epub 2010 Jan 26.

161

RBE and DNA damage variation along monoenergetic and modulated Bragg peaks of a 62 MeV therapeutic protons beam

K.M. Prise¹, P. Chaudhary¹, T. Marshall¹, F.M. Perozziello², L. Manti², F.J. Currell¹, S.J. McMahon¹, J.N. Kavanagh¹, G.A.P. Cirrone³, F. Romano³, G. Schettino^{1,4}

¹Centre for Cancer Research and Cell Biology, Queen's University Belfast, UK

²Department of Physics, University of Naples Federico II and INFN, Italy

³Istituto Nazionale di Fisica Nucleare, LNS, Catania, Italy.

⁴National Physical Laboratory, UK

Background and Purpose: Biological optimization of proton therapy can only be achieved through detailed evaluation of RBE variations along the full range of the Bragg curve. The routinely utilized clinical RBE value of 1.1 represents a broad average which disregard the steep rise of Linear Energy Transfer (LET) at the distal end of the Spread-Out Bragg Peak (SOBP). With particular attention to key endpoints of cell survival and DNA damage, a comparative investigation studied cell killing RBE variation along monoenergetic (pristine) and modulated (SOBP) beams using normal and radioresistant human cells.

Material and Methods: Human fibroblasts (AG01522) and glioma (U87) cells were irradiated at six depth positions along monoenergetic and modulated 62 MeV proton beams at the INFN-LNS (Catania, Italy). Clonogenic assays were used to quantify cell killing, with Monte Carlo simulations and the Local Effect Model (LEM) employed to critically evaluate the data. DNA damage measurements were also made at two of the positions and repair assessed upto 24 hours after irradiation.

Results: Significant cell killing RBE variations were observed along the beam path, particularly in the distal region, with a

strong dose dependence. Experimental RBE values were in good agreement with the LEM, indicating dose averaged LET as a suitable predictor of proton biological effectiveness.

Conclusion: The predicted biological dose delivered to a tumor region based on the variable RBE, inferred from the data, varies significantly from clinical profiles based on a generic RBE of 1.1.

Keywords: RBE, LET, Bragg Peak

162

Radiosensitization of Non-Small Cell Lung Cancers by Targeting Ionizing Radiation-Induced Activation of ADAM17
M. Pruschy¹, S. Bender^{1,2}, A. Brogini-Tenzer¹, O. Riesterer¹, A. Sharma^{1,2}

¹Laboratory for Molecular Radiobiology, University Hospital Zurich, Switzerland

²Cancer Biology PhD Program, Life Science Zurich Graduate School, University of Zurich (UZH)/Swiss Federal Institute of Technology Zurich (ETH Zurich), Switzerland

Purpose: Inherent and acquired resistance to the cytotoxic effects of ionizing radiation (IR) is increasingly recognized as a significant impediment to the efficacy of radiotherapy. Primary therapeutic response of IR is imparted by genomic instability and DNA damage, however IR also triggers multiple intracellular signaling processes that lead to the secretion of various para- and autocrine factors into the tumor microenvironment. These secreted factors then loop back (autocrine fashion) to modulate multiple pathways eventually driving acquired resistance. Here we investigated treatment-dependent secretion of various auto- or paracrine factors, which might drive acquired rescue mechanisms and determine the overall radiation sensitivity of the tumor.

Material and methods: Exhaustive secretome analysis was performed using antibody arrays for a wide range of secretory factors impacting different phenotypes. Secretion kinetics of selected factors was determined across different established tumor cell lines in response to increasing doses of ionizing radiation and in murine blood serum, derived from irradiated tumor xenograft-carrying mice. To determine the relevance of the specific factors, clonogenic survival assays in response to IR were performed with siRNA-targeted tumor cell lines and in presence of respective inhibitors.

Results: We performed an exhaustive IR-dependent secretome analysis (>300 factors) and investigated in detail the effect of increasing doses of IR on the expression and tumor cell secretion of amphiregulin, transforming growth factor- α and ALCAM, which represent top hits in the array screening. All these factors were secreted in a dose dependent way from several non-small cell lung cancer (NSCLC) cell lines in response to IR. No changes were observed at the transcriptional level implying potential modulation at the posttranslational level. Interestingly, irradiation induced an acute, dose-dependent increase in ADAM17 activity, which correlated with substrate shedding. Ex vivo analysis of murine blood serum derived from irradiated tumor xenograft-carrying mice support our in vitro results. Targeting ADAM17 with the small molecular inhibitor TMI-005 and siRNA-mediated silencing confirmed that ADAM17 is driving a pro-survival response with subsequent treatment resistance. Pharmacologic inhibition or siRNA-mediated downregulation of ADAM17 in combination with IR reduced proliferation and clonogenicity of the NSCLC cells. Analysis of in vivo experiments is ongoing.

Conclusions: Our findings demonstrate that IR significantly activates ADAM17, which results in shedding of multiple survival factors, growth factor pathway activation and treatment resistance in NSCLC cells. We provide a sound rationale for positioning ADAM17 inhibitors as radiosensitizers to improve the treatment of NSCLC.

Keywords: Secretome, Radiosensitization, ADAM17

163

The REQUITE project: validating predictive models and biomarkers of radiotherapy toxicity to reduce side-effects

T. Rancati¹, D. Azria², A. Brookes³, T. Burr⁴, J. Chang-Claude⁵, S. Davidson⁶, D. De Ruyscher⁷, A. Dunning⁸, R. Elliott⁹, S. Gutiérrez Enríquez¹⁰, P. Lambin¹¹, L. Lozza¹², B. Rosenstein¹³, R.P. Symonds³, H. Thierens¹⁴, R. Valdagni¹², A. Vega¹⁵, F. Wenz⁵, M. Yuille⁹, C. West⁹

¹Fondazione IRCCS Istituto Nazionale dei Tumori, Italy

²University of Montpellier, France

³University of Leicester, UK

⁴Source Bioscience, Nottingham, UK

⁵German Cancer Research Centre, Heidelberg, Germany

⁶The Christie NHS Foundation Trust, Manchester, UK

⁷University Hospitals Leuven/KU Leuven, Belgium

⁸University of Cambridge, UK

⁹University of Manchester, UK

¹⁰Vall d'Hebron Institute of Oncology-VHIO, Barcelona, Spain

¹¹Stichting Maastricht Radiation Oncology, Maastricht, The Netherlands

¹²Fondazione IRCCS Istituto Nazionale dei Tumori, Milan, Italy

¹³Mount Sinai School of Medicine, New York, USA

¹⁴Universiteit Gent, Belgium

¹⁵Fundación Pública Galega Medicina Xenómica, Santiago de Compostela, Spain

Purpose: Recently the first replicated genetic associations for adverse reactions to radiotherapy (RT) have been reported. These will help to build predictive statistical models for optimising RT delivery or interventions to alleviate the side effects. It is now timely to start a project that aims to validate known predictors of adverse reactions and develop the statistical models to become clinically useful. The REQUITE project is a European Union funded FP7 project that aims to do this.

Materials/methods:

REQUITE's objectives:

1. Perform a multi-centre, cohort study collecting: blood samples, epidemiology and treatment data, longitudinal side-effect and QOL data (before and after treatment, years 1 & 2).
2. Produce a centralised biobank of DNA from 5,300 patients and a centralised data management system.
3. Validate published biomarkers of radiosensitivity.
4. Validate clinical predictors of RT toxicity in breast, prostate and lung cancer and incorporate biomarker data.
5. Design interventional trials to reduce long-term side-effects.
6. Provide a resource for dissemination and exploitation to the RT community.

Results: REQUITE is funded for 60 months and organised into seven work packages (see figure). WP1 is responsible for overall management and scientific oversight run by Manchester.

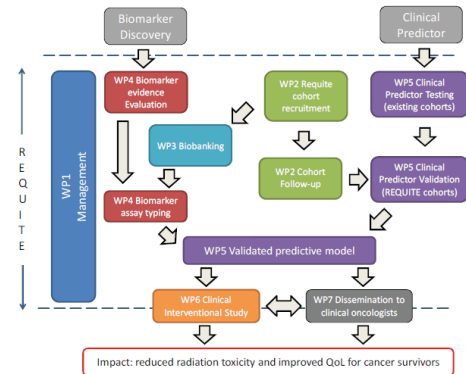
The central activity of the project is a multi-centre, observational study organised through WP2, led by DKFZ. Enrolment will proceed for 2 years in nine clinical centres, with 2 years follow-up. The primary endpoints are change in breast appearance; rectal bleeding (prostate); pneumonitis (lung). The integrated database will be designed at Leicester. Blood samples will be collected before radiotherapy. Tracking, biobanking and DNA preparation is handled in WP3 at CIGMR in Manchester. Validation of biomarkers (genetic markers and apoptosis assays) as predictive factors will be carried out in WP4 led by Leicester.

Some clinical factors have suggested predictive value for RT side-effects, but there is no consensus. In WP5 Gent will lead

in validating published models in existing cohorts, leading to replicated models that can be validated using the REQUITE cohorts.

In WP6 Leuven will use the predictive models to design clinical interventional trials and produce protocols that seek to lower RT side-effects in those individuals at high risk of developing them without affecting tumour control. Dissemination and outreach will be co-ordinated through WP7 led by MAASTRO.

Graphical presentation of the components showing interdependencies



Keywords: radio-induced toxicity, predictive models, genetic investigation

164

Influence of Double Strand Breaks Repair on Radiotherapy Induced Acute Skin Reactions in Breast Cancer Patients

B.S.S. Rao¹, K.D. Mumbrekar¹, D.J. Fernandes², H.V. Goutham¹, K. Sharan², B.M. Vadhira³, K. Satyamoorthy⁴.

¹Division of Radiobiology & Toxicology, School of Life Sciences, Manipal University, Manipal, Karnataka, India

²Department of Radiotherapy & Oncology, Shirdi Sai Baba Cancer Hospital and Research Centre, Kasturba Hospital, Manipal, Karnataka, India

³Manipal Hospital, Bangalore, Karnataka, India

⁴Division of Biotechnology, School of Life Sciences, Manipal University, Manipal, Karnataka, India

Purpose: Curative radiotherapy (RT) associated normal tissue adverse reactions poses strong limitations for the success of RT and further it worsens the quality of life in survivors. The parameter that explains when and to what extent normal tissue toxicity after RT evolves would be of clinical relevance because of its predictive value and may provide an opportunity for a personalized treatment approach.

Materials/methods: DNA double strand breaks and its repair were analyzed by microscopic γ H2AX foci analysis in peripheral lymphocytes from 80 pre RT breast cancer patients. The peripheral blood lymphocytes were exposed *in vitro* to a challenge dose of X-rays (2 Gy). The actual damage (AD, at 0.25, 3 and 6 hrs) and percentage residual damage (PRD, at 3 and 6 hrs) were used as parameters to measure cellular radiosensitivity and correlated with RT induced acute skin reactions in patients stratified as non-over responders (<2 RTOG grade, NOR) and over responders (\geq 2 RTOG grade, OR).

Results: The results indicated that the mean foci level in lymphocytes from the patients before exposure to 2 Gy, and after exposure (at 0.25, 3 hrs) were non-significant ($p > 0.05$), between NOR and OR groups. However, analyzing the increased PRD at 6 hr was found to be correlated with increasing RTOG grades ($r = 0.2392$; $p = 0.0326$). Furthermore, trend analysis clearly indicated an increase in the acute toxicity with that of increasing PRD starting from the lower quartile to the upper quartile groups ($p < 0.0001$).

measurements obtained with homogeneous and heterogeneous target.

Materials and methods: The IVI (Interaction Vertex Imaging) method relies on charged particles produced in the fragmentation of incident ions to obtain information on the beam range [3]. The principle is to reconstruct trajectories of emitted particles (mainly protons) and to extrapolate them back to point of creation, called vertex. To reconstruct protons trajectories, a three dimensional tracking system based on thin CMOS sensors [4] was used. Geant4 simulations were used for comparison with experiment.

Results: In order to study the sensitivity of the IVI to small variations of the ion range and the influence of heterogeneities on longitudinal vertex distributions, an experiment was performed at HIT (Heidelberg Ion-beam Therapy center). The target was a head-size PMMA cylinder (16 cm diameter), with cylindrical holes placed in various positions; holes could be filled with inserts of different materials: PMMA, cortical bone ($\rho = 1.82 \text{ g/cm}^3$) and air were used in this study. Typical treatment beam ranges were used, considering various insert configurations.

A realistic simulation of the experimental setup was performed, including detector response and reconstruction efficiencies. Longitudinal vertex distributions obtained with homogeneous and heterogeneous target were compared in order to study the method sensitivity to small range variations with and without the presence of heterogeneities. In all cases, range variations of less than 2 mm at 100 mm could be detected. Finally, the influence of beam ranges on vertex distributions, in the case of heterogeneous target, was studied, in order to explore the advantages and the limit of this method.

Conclusion: The IVI method for a real-time ion range monitoring was investigated, by experiments and simulations, using heterogeneous targets. Experimental and simulated data are in good agreement, particularly in the Bragg peak region. We will discuss the clinical relevance of IVI in terms of real-time control at a pencil-beam scale.

Keywords: carbon therapy, online range control, proton vertex imaging

References:

- [1] P. Henriquet et al., *Phys.Med.Biol.* 57 (2012) 4655-4669;
- [2] K. Gwosch et al., *Phys.Med.Biol.* 58 (2013) 3755-3773;
- [3] U. Amaldi et al., *Nucl. Instrum. Meth A* 617 (2010) 248-249;
- [4] C. Hu-Guo et al., *Nucl. Instr. Meth. A* 623 480(2010) 150;

167

Geant4 simulation of a dedicated beam line at the CNAO facility for the study of uveal melanomas

A. Rimoldi^{1,2}, A. Fontana^{1,2}, C. Riccardi^{1,2}, P. Piersimoni^{1,2}, M. Ciocca³, S. Molinelli³

¹University of Pavia, Italy

²INFN

³CNAO

One of the most successful fields of application of hadrontherapy (in particular protontherapy) is the treatment of uveal melanomas. The CNAO facility (Centro Nazionale di Adroterapia Oncologica) in Pavia (Italy) is a synchrotron based medical center where it is possible to treat tumors with proton or carbon ion beams when they are accelerated at energies ranging from 60 MeV to 250 MeV (protons) and from 120 MeV/u to 400 MeV/u (Carbon ions).

The aim of this work is to check the possibility to optimize the CNAO present experimental setup in order to make it suitable for ocular treatments, without dramatically change the present operational beam-line settings. For this purpose a Geant4 application was developed, by which a simulation of

the entire CNAO transport beam line was realized. Realistic eye-modeled detectors were implemented and a simulation of an ocular treatment on a use-case was performed.

The results obtained with the simulation are presented. As a first step we show the comparisons between experimental beam characteristics and Geant4/Fluka simulated data at different spatial positions. The optimization of the CNAO beam line is illustrated and the introduction along the line of some passive elements is justified. An ad-hoc detector implementation is also presented (a detailed model of an human eye) as well as other detectors used in the application for optimization studies. Additional studies refer to the direct use of a CT scan as detector for a right irradiation on a damaged ocular tissue. Dose volume histograms obtained with the optimized simulation are also shown.

This work is a starting point to confirm the possibility to plan a new dedicated beam line for ocular tumor treatments at the CNAO Laboratories and to validate treatment plans for the optimization of all the parameters for the treatments in real clinical cases. This feasibility study could also be used in future as a core development to check the reliability of the treatment planning systems for current clinical cases .

Keywords: simulation, Geant4, hadrontherapy

168

Gadolinium based nanoparticles for radiosensitization of head and neck squamous cell carcinoma

C. Rodriguez-Lafrasse¹, M.-T. Aloy¹, I. Miladi², E. Armandy¹, L. Sancey², A. Berniard², C. Billotey², O. Tillement², F. Lux², P. Perriat³, M. Janier²

¹Laboratoire de Radiobiologie Cellulaire et Moléculaire, EMR3738 Lyon1-HCL, Faculté de Médecine Lyon-Sud, Université de Lyon, Université Lyon 1, 69921 Oullins cedex - France

²Institut Lumière Matière, UMR 5306 CNRS, Université Lyon 1, 69622 Villeurbanne cedex - France

³INSA-Lyon, MATEIS CNRS UMR551, CNRS, Université Lyon 1, 69621 Villeurbanne cedex - France

Purpose: Head and neck squamous cell carcinoma (HNSCC) is an aggressive and recurrent malignancy that displays intrinsic resistance to radio- and chemotherapy. The aim of this study is to radiosensitize these tumors using gadolinium based nanoparticles (GBN) made of a polysiloxane matrix and surrounded by gadolinium chelates. The nanoparticles in the tumors should enhance the efficacy of radiotherapy (thanks to the high Z of gadolinium) through the generation of electron Auger cascade and secondary electrons.

Materials/Method: GBN were synthesized by the procedure described in P. Mowat et al., *J Nanosci Nanotechnol.*, 2011.

SQ20B HNSCC cell line was established from a patient with squamous cell carcinoma from the larynx.

Cells were incubated with different concentrations of GBNs (0.1-2 mM) 1 hour at 37°C before irradiation with 250 kV photons or 33.6 keV/μm carbon ions.

SQ20B tumour bearing mice were assigned in four groups: vehicle alone (n=11), vehicle +10 Gy photons (n= 20), GBNs (n=12), GBNs + 10 Gy photons (n=21)

Results: The association of 0.6 mM GBNs with photon or carbon ion irradiation decrease significantly SQ20B cell survival. Radiosensitization goes through the increase in non-reparable DNA double-strand breaks, the shortening of G2/M phase blockage, the inhibition of cell proliferation, each contributing to the commitment to apoptosis. The combined treatment of GBNs with irradiation can also overcome the resistance of SQ20B stem-like cells. Combination of GBNs with carbon ion irradiation shows a Relative Biological Efficiency (2.5) higher than the one obtained with combination of GBNs with photon irradiation (1.6).

Using an SQ20B tumor-bearing mouse model, we also demonstrate that GBNs in conjunction with photon irradiation

significantly retard tumor growth compared with radiation alone, with complete remission in some mice. Significantly, an increase in apoptosis and decrease in cell proliferation is also detected within tumors in the combined treatment group.

Conclusions: This study demonstrates the high radiosensitizing properties of GBNs *in vitro* and *in vivo* for HNSCC tumors. In combination with their imaging properties (contrast agent for MRI due to the presence of gadolinium) GBNs can be used for theranostic applications (i.e. image guided radiotherapy).

Keywords: Theranostic, Nanoparticles, Radiosensitization

Acknowledgement: This project was conducted under the framework of LANTHARAD (PDC019 CLARA 2010), PRRH-ETOILE and LABEX PRIMES (2012)

169

Homologous recombination deficiency and radio-curability in mouse models for BRCA1/2-deficient breast cancer
S. Rottenberg, G. Borst, A. Gasparini, M. Barazas, C. Guyader, W. Sol, A. Kersbergen, M. Verheij, J.J. Sonke
The Netherlands Cancer Institute, Plesmanlaan 121, 1066CX Amsterdam, The Netherlands

More than 50% of the cancer patients undergo irradiation as part of their cancer treatment. Although radiotherapy significantly contributes to cancer cure, local therapy resistance and the subsequent emergence of distant metastasis remain major obstacles for the success of radiotherapy. Despite the long-standing use of cultured cancer cell lines or the transplantation of human tumor cells into immunodeficient mice, we do not fully understand the precise mechanisms that cause radiotherapy escape. To investigate radioresistance and metastatic spread in an *in vivo* model that closely resembles human cancer, we have studied radiotherapy responses in new generation mouse models for BRCA1/2-mutant breast cancer. For this purpose, radiotherapy interventions were carried out using a small-animal dedicated Cone-Beam CT (CBCT) equipped micro-irradiator.

Due to the BRCA inactivation, the tumors that arise in our genetically engineered models (GEMMs) lack homology-directed DNA repair; an Achilles heel that provides a therapeutic opportunity to eradicate tumors locally with radiotherapy. However, similar to the situation in cancer patients, we observe that cancer cells in these models can escape the lethal effects of high dose radiotherapy. In contrast to several xenotransplantation models tested, eradication was usually not achieved with clinically relevant doses in our BRCA GEMMs. Instead, we observed the development of acquired radioresistance, which was stable upon re-transplantation and re-treatment. To our knowledge, this is the first model in which such secondary radioresistance can be studied. Interestingly, in our BRCA1-deficient GEMMs we also observed another type of therapy escape: the development of metastatic tumors, which showed increased radioresistance in several cases. Thus, these new radiotherapy escape models that we have established provide a unique opportunity to explore the basic underlying mechanisms.

170

Targeting hypoxia through autophagy

K. Rouschop

University of Maastricht, the Netherlands

Hypoxia is a common feature of tumors and an important contributor to malignancy and treatment resistance. We and others have shown that a lysosomal degradation pathway, autophagy, which enables cells to recycle and redirect

nutrients to adapt to metabolic stresses, is required for the survival of hypoxic cells. Consequently, autophagy inhibition sensitized tumors to irradiation as determined by tumor growth delay experiments.

Our research focuses on unraveling the molecular mechanisms that are required for the activation of autophagy during hypoxia and to exploit these for therapeutic purposes. During this presentation, I will elaborate on some of our recent findings regarding autophagy targeting and targeting of autophagy associated mechanisms and their potential application in increasing treatment efficacy.

Keywords: Autophagy, hypoxia

171

Initial Qualification of the Irradiation Uncertainties in Ion Beam Therapy of Prostate Cancer

A. Rucinski^{1,2}, S. Brons¹, O. Jäkel^{1,2}

¹Heidelberg Ion Beam Therapy Centre, Germany

²Department of Radiation Oncology, Heidelberg University Clinic, Germany

Purpose: Ion beam therapy is expected to be an efficient method for treating prostate cancer due to its high dose conformity and radiobiological effectiveness. This high precision tumor therapy technique is particularly sensitive to inter and intrafractional anatomy variations, which affect dose delivery to the different extent depending on the selected irradiation protocol. The goal of the presented study is to order the factors influencing the quality of prostate irradiation according the clinical relevance criteria by analyzing their dosimetric effect.

Materials/methods: The presented robustness analysis included Computed Tomography (CT) images of 20 patients (117 CT scans). Treatment plan (TP) optimizations and dose distribution calculations were performed for several irradiation protocols. As a reference, the irradiation protocol used at Heidelberg Ion Beam Therapy Centre (HIT) was used. Volume of clinical target volume (CTV) receiving the dose higher than 95% of prescribed target dose (V95-CTV) and rectal volume receiving dose higher than 90% (V90-Rectum) of prescribed target dose were used as the quality indices of TP. The robustness analysis investigated the following aspects:

- Daily patient anatomy variation.
- Application of spacer gel, enlarging the distance between the target (prostate) and the most critical organ at risk (rectum).
- Image registration methods for patient position verification.
- Protocol-specific safety margin concepts (Planning Target Volume - PTV).
- Selection of a representative TP CT
- Role of biological assumptions regarding the α/β -ratio which characterizes radio-resistance of the cells
- Treatment plan optimization settings: ion sort (carbons or protons), optimization algorithms (conventional or with intensity modulation), scan grid, and gantry angles.

Results: The initial results indicate that in term of dosimetric changes of V95-CTV and V95-Rectum, the daily target dose distribution could be mostly affected by (in order of relevance): daily patient anatomy variations, application of spacer gel, selection of a representative CT image, and the biological assumptions used in TP process. Further mentioned factors demonstrate a minor clinical relevance.

Conclusions: The presented study indicate which aspects of ion therapy irradiation protocol might influence the patient safety. The dosimetric effects of interfractional patient anatomy variations are specific for patient and treatment fraction and could be mitigated, e.g., by the application of spacer gel. It could be beneficial for the patient to develop

and incorporate in the clinical protocol methods (e.g. adaptive TP techniques), which allow to recognize prior the irradiation different than on TP-CT anatomy distribution and therefore, avoid incorrect dose delivery. Not negligible is the dosimetric effect of biological assumptions regarding the tumor tissue used in the TP process.

Keywords: ion therapy, prostate cancer, spacer gel

172

Quantitative study of clinical SPECT: image reconstruction and sensitivity

H. Saikouk^{1,2}, N. El Khayati¹

¹Université Mohammed5-Agdal, Faculté des Sciences, Rabat, Morocco

²Nuclear Medicine Department, Oncology and Hematology Center, Mohammed VI Hospital, Marrakech, Morocco

Purpose: SPECT (Single Photon Computed Tomography) gamma camera is being a remarkable device for diagnostic in nuclear medicine department. The quantitative studies represent a significant part of the investigations carried out. The verification of the accuracy of its performances becomes then imperative.

Our purpose is to investigate quantitatively the image quality for tomographic acquisition of a double headed clinical SPECT gamma camera and its sensitivity.

Materials and methods: A line source, containing ^{99m}Tc radioisotopes, was used to evaluate the sensitivity and its variation with tomographic acquisition. The tomographic acquisition was performed for a 128x128 matrix, 1.80 mm² pixel size and 8 projections per head.

A Jaszczak phantom (filled with ^{99m}Tc solution) was used for the image quality study with a matrix 128x128, 2.40 mm² pixel size and 64 projections per head.

We evaluated different parameters like the tomographic non-uniformity, the contrast, and the impact of scatter or attenuation corrections in the enhancement of the image quality. The contrast and the non-uniformity were calculated considering the most visible cold spheres in Jaszczak phantom. For scatter correction, the double window method is used with energy window of 15 % centered at 140 keV for ^{99m}Tc, and a CT acquisition has been done for attenuation correction.

In other side, Monte carlo simulations were performed using GATE (Geant4 Application for Tomographic Emission) platform which is mainly dedicated to emission tomography. Calculating on the Moroccan grid computing "MaGrid" was a good way to enhance statistics and spend less time in simulation. The goal being to reproduce the experimental results concerning the parameters studied in this work, in order to further study in the future.

Results: Measured values of contrast regarding to the four visible cold spheres of diameters 31.8 mm, 25.4 mm, 19.1 mm, and 15.9 mm, are respectively: 0.71, 0.58, 0.42 and 0.25. The tomographic non-uniformity value is 7.4%. These results are comparable to those recommended in the AAPM (American Association of Physicists in Medicine) report N° 52. The sensitivity value obtained, in the case of static acquisition, is 80.35 cps⁻¹MBq⁻¹ and the tomographic sensitivity value is 76.45 cps⁻¹MBq⁻¹. The data are in a good agreement with those recommended in the literature, for parallel hole collimator used in the present work. The attenuation and scatter corrections, significantly improves the image quality (fig.1).

The last part of results concerns Monte Carlo simulations for sensitivity and for the image reconstruction and relative discussion.

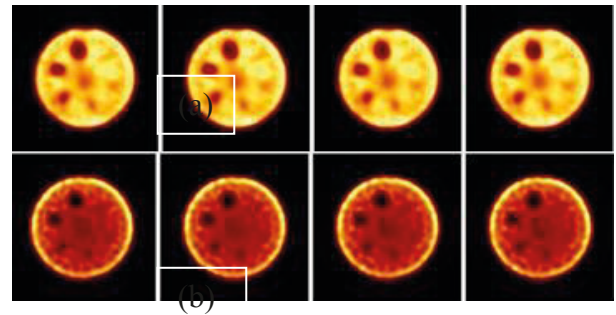


Figure 1: Image reconstruction: (a) considering scatter and attenuation corrections, (b) considering scatter correction without attenuation correction.

Keywords: SPECT-CT, quantification, GATE

173

Dosimetric comparison between Agility and MLCi heads for nasopharyngeal IMRT plans created by two different treatment planning systems

A. Sakumi¹, A. Haga¹, Y. Iwai², K. Nakagawa¹, K. Yamamoto¹, K. Yoda²,

¹University of Tokyo Hospital, Japan

²Elekta K. K. Ltd.

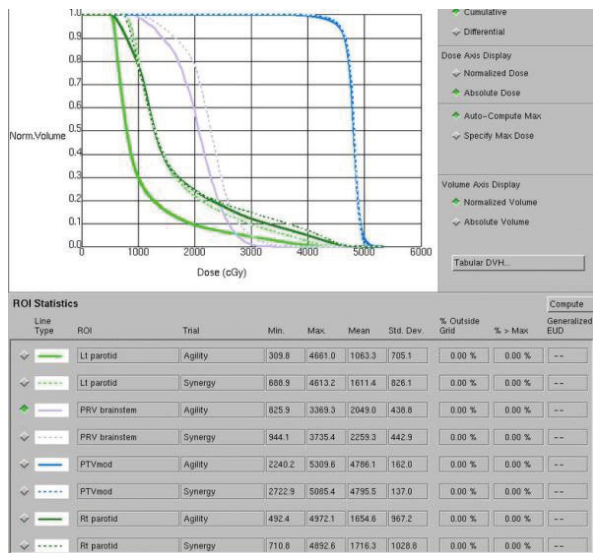
Purpose: In order to spare the organs at risk (OARs) under the same homogeneity index (HI) of PTV for nasopharyngeal IMRT, we installed a new MLC, Agility (Elekta Ltd.) having a reduced leaf transmission and an interleaf leakage. Dosimetric comparisons were performed between the Agility and a traditional MLCi heads for nasopharyngeal IMRT plans created by two different treatment planning systems.

Materials and methods: The Agility has 80 pairs of MLC leaves with a leaf width of 5mm at the isocenter and an extremely low leaf transmission (< 0.5%). IMRT plans for five nasopharyngeal carcinoma patients were created by Pinnacle3 (Philips Ltd.) v9.2 and Monaco (Elekta Ltd.) v3.3, with the Agility and the MLCi head models.

Results: Figure shows comparisons of dose volume histograms for a patient case, where the solid and the dotted lines correspond to the Agility and the MLCi plans, respectively. Under the same HI, the maximal dose to brainstem with the Agility was 4 Gy less than that with the MLCi head, and the mean dose to parotid gland with the Agility was 15% less than that with the MLCi.

The beam delivery time for the Agility plan was 10% shorter than that for the MLCi plan.

Conclusions: We have confirmed that IMRT plans created by the Agility head resulted in less mean doses to OARs compared to the MLCi plans under the same HI. It was also shown that the beam delivery time was reduced with the Agility head.



Keywords: Nasopharyngeal carcinoma, IMRT

174

The recent developments of the FLUKA Monte Carlo code oriented to its applications in hadrontherapy

P. Sala¹, G. Battistoni¹, T. Boehlen², F. Cerutti³, M. Chin³, A. Ferrari³, A. Mairani⁴, C. Mancini-Terracciano³, C. Morone^{5,6}, R. Nicolini¹, P. Ortega¹, V. Patera^{6,7}, V. Vlachoudis³

¹INFN Milano, Italy

²MedAustron

³CERN

⁴CNAO

⁵Universita "Tor Vergata" Roma

⁶INFN Roma

⁷Universita Roma "La Sapienza" Roma

Purpose: One of the most important applications of the FLUKA Monte Carlo code concerns medicine, and in particular nuclear medicine, radiotherapy and hadrontherapy. For the latter FLUKA is used for different purposes. Among them: generation of libraries for TPS, forward calculations for TPS verification in actual patient cases, predictions of relevance for monitoring, like production of prompt gammas and charged particles, or beta+ emitters to be detected by PET tomography.

In the recent years several developments have been introduced in the code in order to improve its accuracy and reliability when computing predictions for the health physicist and the clinician. Such improvements concern different aspects: physics models, calculation techniques and auxiliary tools, as those needed to manage medical images.

A summary of the most relevant achievements will be presented together with some comparison with data and examples of the code application in hadrontherapy.

Materials and methods: FLUKA is a general purpose tool for calculations of particle transport and interactions with matter. It handles all hadrons, ions, and electromagnetic particles.

The FLUKA applications range from LHC or cosmic energies down to hadron-therapy and microdosimetry. It is the standard tool at CERN for beam-machine interactions and radioprotection. All FLUKA models and algorithms are subject to continuous development and verification which benefits to a wide range of applications.

FLUKA has the ability to run either in fully analogue mode, or in biased mode exploiting a rich variety of variance reduction techniques.

The code is jointly developed by the European Laboratory for Particle Physics (CERN), and the Italian National Institute for Nuclear Physics (INFN).

The user can now manage the code through a very powerful and flexible graphic interface (FLAIR) developed using the Python programming language. It allows to edit commands, inspect output files, post-process results, generate plots (interfacing to gnuplot), access documentation, nuclear data and a library of materials including the standard references from ICRU and ICRP. The most recent developments concern the capability of importing DICOM images in order to build automatically patient geometries and assign elemental compositions and densities voxel by voxel according to the measured Hounsfield units.

Results: The developments for medical applications include, in first place, refinements to the ionization energy loss treatment. In addition improved treatments for Compton scattering and positron annihilation have been introduced which account for individual atomic shells and associated momentum distributions. Concerning nuclear models, significant developments include the interactions of alpha particles below 150 MeV/A and the improvements in the latest stages of nuclear reactions. Overall the calculations of prompt gamma ray emission compare favorably with experimental results and it is mature enough for the intended applications. New features in the modeling of proton induced nuclear interactions now provide reliable cross section predictions for the production of radionuclides like ¹¹C, ¹⁵O, etc.

From the point of view of calculation techniques, most recent developments are aimed at achieving a significant acceleration of computing time. At present we are considering specific biasing techniques and threshold optimization which are the subject of another abstract for this Conference.

Of great interest are the developments introduced in the FLAIR Graphical User Interface. Among them we have the automatic inclusion of different types of existing PET scanner devices.

Conclusions: The FLUKA code is being continuously improved in order to match the needs required in several applications. The case of hadrontherapy, and of medical application in general, remains one of the most important and challenging examples. In this contest the participation to dedicated European projects, like PARTNER, ENVISION and ENTERVISION, turned out to be very beneficial.

The development of models and calculation techniques useful for medical applications will continue in the future.

Keywords: Monte Carlo, hadrontherapy, Treatment Planning, PET, SPECT

175

Measurements of Carbon ion fragmentation on thin C and Au targets from the FIRST collaboration at GSI.

A. Sarti^{5,10}, Z. Abou-Haidar^{16,24}, C. Agodi⁶, M.A.G. Alvarez¹⁶, T. Aumann¹, F. Balestra^{8,11}, G. Battistoni², A. Bocchi¹⁶, T.T. Böhlen^{22,23}, A. Boudard²¹, A. Brunetti^{3,9}, M. Carpinelli^{3,13}, G.A.P. Cirrone⁶, M.A. Cortés-Giraldo¹⁷, G. Cuttone⁶, M. De Napoli⁴, M. Durante¹, J.P. Fernández-García¹⁷, C. Finck¹⁸, B. Golosio^{3,13}, E. Iarocci^{5,10}, F. Iazzi^{8,11}, G. Ickert¹, R. Introzzi⁸, D. Juliani¹⁸, J. Krimmer²⁰, A.H. Kummali^{8,12}, N. Kurz¹, M. Labalme¹⁹, A. Lavagno^{8,11}, Y. Leifels¹, A. Le Fèvre¹, S. Leray²¹, B. Liu^{25,27}, F. Marchetto⁸, V. Monaco^{8,12}, M.C. Morone^{9,14}, D. Nicolosi^{6,27}, P. Oliva^{3,13}, A. Paoloni⁵, V. Patera^{5,10}, L. Piersanti^{5,10}, R. Pleskac¹, N. Randazzo⁴, F. Romano^{6,15}, D. Rossi¹, V. Rosso^{25,26}, M. Rousseau¹⁸, R. Sacchi^{8,12}, P. Sala², S. Samuel¹⁹, C. Scheidenberger¹, C. Schuy¹, A. Sciubba^{5,10}, C. Sfienti^{6,23}, H. Simon¹, V. Sipala^{4,13}, E. Spiriti⁷, L. Stüttge¹⁸, M. Toppi^{5,28}, S. Tropea⁶, H. Younis^{8,11}

¹GSI Helmholtzzentrum für Schwerionenforschung, Darmstadt, Germany

²Istituto Nazionale di Fisica Nucleare - Sezione di Milano, Italy

³Istituto Nazionale di Fisica Nucleare - Sezione di Cagliari, Italy

⁴Istituto Nazionale di Fisica Nucleare - Sezione di Catania, Italy

⁵Istituto Nazionale di Fisica Nucleare - Laboratori Nazionali di Frascati, Italy

⁶Istituto Nazionale di Fisica Nucleare - Laboratori Nazionali del Sud, Italy

⁷Istituto Nazionale di Fisica Nucleare - Sezione di Roma 3, Italy

⁸Istituto Nazionale di Fisica Nucleare - Sezione di Torino, Italy

⁹Istituto Nazionale di Fisica Nucleare - Sezione di Roma Tor Vergata, Italy

¹⁰Dipartimento di Scienze di Base e Applicate per l'Ingegneria, "La Sapienza" Università di Roma, Italy

¹¹Dipartimento di Fisica, Politecnico di Torino, Italy

¹²Dipartimento di Fisica, Università di Torino, Italy

¹³Università di Sassari, Italy

¹⁴Dipartimento di Biopatologia e Diagnostica per Immagini, Università di Roma Tor Vergata, Italy

¹⁵Centro Studi e Ricerche e Museo Storico della Fisica "Enrico Fermi", Roma, Italy

¹⁶CNA, Sevilla, Spain

¹⁷Departamento de Fisica Atómica, Molecular y Nuclear, University of Sevilla, 41080-Sevilla, Spain

¹⁸Institut Pluridisciplinaire Hubert Curien, Strasbourg, France

¹⁹LPC-Caen, ENSICAEN, Université de Caen, CNRS/IN2P3, Caen, France

²⁰IPN-Lyon, Université de Lyon, Université Lyon 1, CNRS/IN2P3, Villeurbanne, France

²¹CEA-Saclay, IRFU/SPhN, Gif sur Yvette Cedex, France

²²European Organization for Nuclear Research CERN, Geneva, Switzerland

²³Medical Radiation Physics, Karolinska Institutet and Stockholm University, Stockholm, Sweden

²⁴Universität Mainz Johann-Joachim-Becher, Mainz, Germany

²⁵Dipartimento di Fisica, Università di Pisa, Italy

²⁶Istituto Nazionale di Fisica Nucleare - Sezione di Pisa, Italy

²⁷Dipartimento di Fisica, Università di Catania, Italy

²⁸Dipartimento di Fisica, Università di Roma "Tor Vergata", Italy

²⁹Institute of Nuclear Physics and Chemistry, China Academy of Engineering Physics

The FIRST (Fragmentation of Ions Relevant for Space and Therapy) experiment at GSI laboratory, designed and built by an international collaboration from France, Germany, Italy and Spain, took data in summer 2011, studying the collisions of a Carbon ion beam with ¹²C and Au thin targets. The experiment main purpose is the first double differential cross section measurement of the carbon ion fragmentation at energies that are relevant both for tumor therapy and space radiation protection applications.

The FIRST dataset contains carbon ions collisions on a 8mm carbon target (about 18M events) and on a 0.5 mm Au target (about 2M events). The SIS (heavy ion synchrotron) was used to accelerate the ¹²C ions at the energy of 400 MeV/u. The experimental setup covered two distinct angular regions: the small angle region, where fragments are produced with a polar angle (ϕ) with respect to the impinging beam direction (z axis) smaller than 5° and a large angle region with ϕ between 5° and 40°.

The differential cross sections as a function of angle and energy, for both Au and C target will be presented and compared to the most recent measurement in this field at different energies. The comparison with a detailed FLUKA MC simulation, that has been developed in order to validate the analysis strategy and measure the reconstruction efficiencies, will be reported as well.

Keywords: Fragmentation cross section, Carbon ion Hadrontherapy

176

Daily variation in rectal size and position during prostate radiotherapy measured from helical tomotherapy CT scans

J. Scaife¹, K. Harrison², M. Romanchikova³, M. Sutcliffe⁴, S. Thomas³, R. Jena¹, N. Burnet¹

¹Department of Oncology, University of Cambridge, UK

²Cavendish Laboratory, University of Cambridge, UK

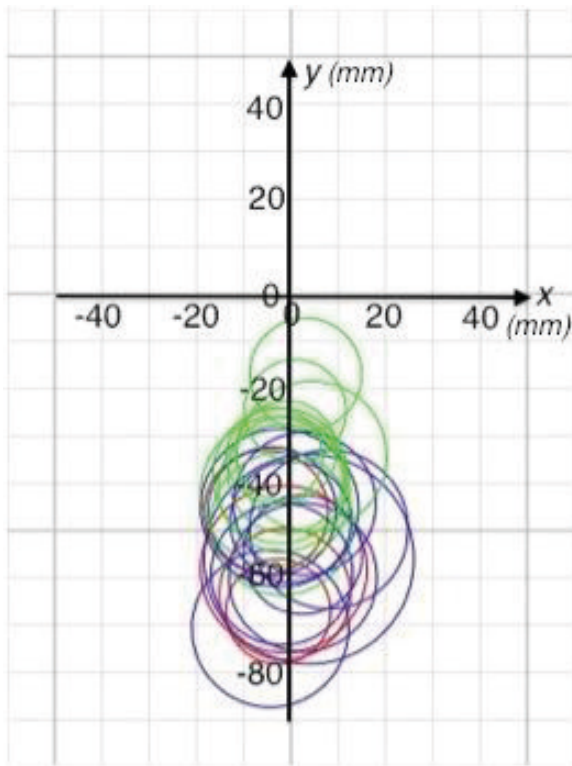
³Radiotherapy Physics, Cambridge University Hospitals NHS Foundation Trust, UK

⁴Department of Engineering, University of Cambridge, UK

We have evaluated the daily variation in the size and position of the rectum in 10 patients treated for prostate cancer. This is the first step towards exploring the idea that the dose delivered to the rectum on a particular day of treatment might be different from the planned dose.

The 10 patients were treated using the TomoTherapy HiArt™ system with daily image guidance. Their imaging data were retrieved from the TomoTherapy archive using in-house software and converted to DICOM format. A single clinician contoured the rectal circumference and femoral heads, on all slices of each MV image guidance scan, for each patient (370 scans). These DICOM data were processed using an in-house Python application. A reference point was devised as midway between the estimated centres of the femoral heads, using a polygon centroids method. The distances from this reference point to the anterior, posterior, left and right extents of the rectum were then measured for each slice of each scan for each patient. Subsequent analysis was performed in Excel. The daily position and size of the inferior, middle and superior thirds of the rectum were established. The magnitudes of daily movements of the centre of the rectum in both anterior-posterior (AP) and left-right (LR) directions were then calculated.

Extents of the rectum were produced for 99% and 100% of scans for the middle and superior thirds. Only 51% of scans extended low enough to allow determination of the extent of the inferior rectum; 6 patients were therefore excluded from analysis of this third. Mean rectal radius was calculated, mean AP and LR dimensions being almost identical. The figure shows the mean rectal circumference for each patient for each third of the rectum (red inferior, blue middle and green superior) with 0,0 being the reference point. This illustrates the variation in position and size of the rectum between thirds, and between patients within thirds.



The magnitude of the daily changes in position and size for the 10 patients are summarised in the table:

	Mean of mean daily anterior-posterior movements of centre of rectum in mm (Mean of Standard Deviations)	Mean of mean daily left-right movements of centre of rectum in mm (Mean of Standard Deviations)	Mean of mean daily rectal radii in mm (Mean of Standard Deviations)
Superior rectum	7.2 (5.7)	1.8 (1.5)	13.1 (2.2)
Middle rectum	4.0 (3.3)	3.0 (2.4)	15.7 (2.7)
Inferior rectum	3.3 (2.6)	3.3 (2.7)	13.9 (2.8)

We have devised a novel method for quantifying the size and position of the rectum during image-guided radiotherapy. This allows its location to be tracked daily within a patient, and permits comparisons to be made between patients. Differences were seen in the magnitude of movement between the different thirds of the rectum, and also between the relative movements in AP and LR directions. The greatest movements were seen in the superior third of the rectum in the AP direction, with an average move between any two consecutive treatment days of 7.2mm. This confirms the idea that the delivered dose to the rectum is likely to vary on a daily basis, particularly in the superior rectum, and calculation of this is underway. We plan future work using scans extended further inferiorly, and to develop automated methods for contouring.

Keywords: Image-guided radiotherapy, Prostate cancer, Rectum

177

Ultrafast PET Detectors Based on Digital SiPMs and Their Use in In-Situ PET and Prompt Gamma Ray Imaging

D.R. Schaart

Delft University of Technology, The Netherlands

The use of time-of-flight (TOF) information in positron emission tomography (PET) has been shown to enable significant improvement in image noise properties, especially in larger patients. Silicon photomultipliers (SiPMs) are solid-state photosensors offering high internal gain while being compact, essentially transparent to gamma rays, and insensitive to magnetic fields. Since several years a number of manufacturers are offering reliable and practical devices. This has spurred many research groups to explore their potential use in scintillation detectors for PET, aiming at e.g. compactness, high spatial resolution, depth-of-interaction (DOI) correction, MRI-compatibility, and improved TOF performance. At the same time, SiPM technology itself is undergoing rapid development. For example, a fully digital implementation of the SiPM, the so-called digital photon counter or dSiPM, has been introduced recently. SiPMs and dSiPMs enable excellent timing resolution, with coincidence resolving times (CRTs) well below 200 ps FWHM having been demonstrated by several groups already. This paper presents an overview of recent developments in dSiPM-based TOF-PET detectors as well as recent results obtained with these devices in in-situ PET and prompt gamma imaging for particle therapy treatment monitoring. It is discussed how the favorable properties of dSiPMs can be exploited to provide realistic solutions for in-vivo particle therapy monitoring concepts proposed by various groups in recent years. In particular, it is shown how the excellent timing performance of dSiPM based scintillation detectors can be used to improve sensitivity and to reduce artifacts in in-situ PET devices, as well as to reduce background noise in prompt gamma imaging.

Keywords: digital silicon photomultipliers, in-situ PET, prompt gamma imaging

178

Enhanced RBE of sub-micrometer focused low-LET protons

T.E. Schmid¹, G. Dollinger², S. Girst², C. Greubel², G.

Multhoff¹, J. Reindl², E. Schmid³, J. Seel², C. Siebenwirth²

¹Klinikum Rechts der Isar, Technische Universität München

²Universität der Bundeswehr München, Germany

³Ludwig-Maximilians Universität München, Germany

Purpose: Due to their physical and radiobiological properties, in particular their increased relative biological effectiveness (RBE), high linear energy transfer (LET) radiation qualities are of special interest for tumour therapy. The aim of the present investigation is to quantify the influence of spatial dose distribution on the RBE of heavy ions. By focusing low LET 20 MeV protons (LET in water of 2.65 keV/μm) the spatial dose distribution of protons can be modified towards that of heavy ions where the dose is concentrated around the ion tracks.

Methods: In this work the influence of spatial dose distribution is studied on the endpoint of induction of dicentric chromosomes. Human-hamster hybrid (AL) cells were irradiated with focused 20 MeV protons in a quadratic matrix pattern with certain point distances and certain numbers of protons per matrix point. Three different matrices were used: 5.4×5.4 μm², 7.6×7.6 μm² and 10.6×10.6 μm² with protons per point of 117, 232 and 451. All three irradiation modes deposit a mean dose of 1.7 Gy. For comparison cells are also irradiated with randomly distributed protons or 55 MeV carbon ions in a 5.4×5.4 μm² matrix pattern and one ion per point, applying the same dose of 1.7 Gy.

Results: Figure 1 shows the pooled results from two independent experiments. The RBE for induction of dicentric chromosomes after irradiation with randomly distributed protons is calculated to 1.33 ± 0.19 and increases with higher numbers of protons per point up to 2.60 ± 0.27 for 451 protons applied at each point of a $10.6 \times 10.6 \mu\text{m}^2$ matrix. The RBE of carbon ions (3.21 ± 0.27) is about 25% higher than the RBE of 451 focused protons. The enhanced RBE of focused protons is attributed to their inhomogeneous dose distribution, similar to heavy ions, where dose and hereby DNA double strand breaks (DSB) are concentrated around the matrix points. Thus the probability for joining wrong DSB ends, a prerequisite for induction of dicentric chromosomes, increases due to the decreasing mean distances to neighbouring DSB

Conclusion: These findings demonstrate the influence of spatial dose distribution to RBE and show the potential of using focused low LET protons as a model system for further understanding RBE of heavy ions.

Supported by the DFG-Cluster of Excellence 'Munich-Centre for Advanced Photonics', by the by BMBF-project 02NUK031 "LET-Verbund".

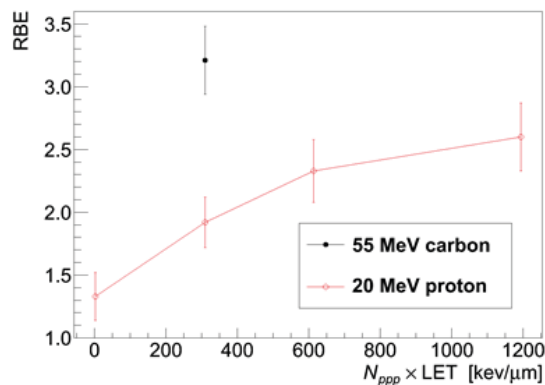


Figure 1. RBE of 55 MeV carbon ions and 20 MeV protons versus the number of particles per point multiplied by the LET.

Keywords: proton irradiation, microchannel, skin

179

Characterization of wireless personal dosimeter prototype for Interventional Radiology medical operators

L. Servoli¹, M. Biasini^{1,2}, L. Bissi¹, A. Calandra², B. Ceccucci¹, S. Chiocchini², R. Cicioni², E. Conti^{1,2}, R. Di Lorenzo^{1,3}, A.C. Dipilato², N. Forini², D. Magalotti^{1,4}, A. Maselli³, M. Paolucci^{1,3}, D. Passeri^{1,2}, A. Pentiricci^{1,5}, P. Placidi^{1,2}, M. Scarpignato³, A. Scorzoni^{1,2}

¹INFN Perugia, Italy

²Università degli Studi di Perugia, Italy

³Azienda USL Umbria 2, Italy

⁴Università degli Studi di Modena, Italy

⁵Azienda USL Umbria 1, Italy

Purpose: A personal wireless dosimeter prototype, to be worn by medical staff during Interventional Radiology procedures, has been characterized.

Materials and methods: The prototype is composed by a sensing element (a CMOS silicon pixel device), a real-time data reduction system (a CPLD), a control system, a wireless transmission module, a remote station for prototype configuration, control and data storage.

The prototype has been irradiated in laboratory using monochromatic X-ray photons to calibrate the sensing element, then using the angiography system with a PMMA phantom, to diffuse the direct radiation, in all the working conditions (continuous/pulsed, fluoroscopy/fluorography, different systems) and with different sensor settings. The prototype has also been exposed to certified X-ray beams to obtain a relative calibration. Finally the prototype has also been used during medical procedures, mounted over the protective vest worn by the medical staff. All the results have been compared with two dosimetric control systems, a set of TLDs and an UNFORS EDD-30 system.

Results: Two sensor quantities have been used to verify the linearity of the prototype's response: the number of detected photons and the total detected signal in a frame. The appropriate data reduction strategies have then been implemented in CPLD to obtain a limited amount of data to be transmitted to the remote station with a 1-10 Hz frequency, lowering the needed throughput of the wireless system, and hence the power consumption. The prototype has been capable of measuring the dose and dose-rate following closely the time structure of the X ray beam during the full duration of the procedure. The uncertainty on the dose and dose-rate measurements is below 10%, and the wireless transmission protocol has been found to be adequate also in the capability of establishing the connection through the operating room walls, allowing the control station to be outside the operating room and simplifying considerably the entire system.

Conclusion: The wireless dosimeter prototype, produced in the framework of the RAPID project, for personnel dosimetry of the medical staff during Interventional Radiology procedures, has been tested and found to be satisfactory from the point of view of the power consumption, the wireless transmission capability, the precision in dose and dose-rate measurements.

Keywords: wireless dosimeter, Interventional Radiology, CMOS sensor.

180

A radionuclide generator of Erbium-165, an isotope for Auger Therapy

G.W. Severin, K.M. Jensen

Hevsey Laboratory, NUTECH Technical University of Denmark

Purpose: Internal targeted radiotherapy with Auger emitting radioisotopes, 'Auger Therapy', is a tool for the treatment of both local and diffuse disease. The benefit of Auger Therapy is the high LET and short range of the low energy Auger electrons. This results in high ionization density in targeted cells, and relatively small doses to non-targeted tissues.

¹⁶⁵Er is a candidate nuclide for Auger therapy because of three important characteristics. First, ¹⁶⁵Er decays by electron capture to stable ¹⁶⁵Ho, and the only ionizing radiations from this decay are atomic emissions, i.e. Auger electrons and x-rays. Second, it has an appropriate half-life, 10.4h, for targeted internal radiotherapy with peptides and fast circulating mAbs. And third, erbium chelation chemistry is identical to that of the other rare earths, allowing radiolabeling to targeting molecules through well-known chelation schemes.

Due to its suitability for Auger therapy, a reliable and high-specific activity production method for this isotope is required for preclinical, and eventually translational use. We present a radionuclide generator for the production of carrier free ¹⁶⁵Er. The generator is based upon the Szillard-Chalmers reaction of DOTA bound ¹⁶⁵Tm as previously described for the similar radiolanthanide pair ¹⁴⁰Nd/¹⁴⁰Pr [1].

Methods: For preclinical applications and development, ¹⁶⁵Tm is produced by proton irradiation of unenriched Er foil at 16MeV on a GE PETtrace cyclotron. The bulk non-radioactive

erbium is removed by ion exchange chromatography, and the Tm isotopes are concentrated and reacted with DOTA at elevated temperature (90°C). The electron capture decay of ¹⁶⁵Tm disrupts the DOTA chelation, and frees the daughter ¹⁶⁵Er. An activation barrier prevents the newly formed ¹⁶⁵Er from binding to excess DOTA, or participating in exchange reactions at room temperature [2]. After suitable in-growth time, 10-24 h, the ¹⁶⁵Er is 'milked' from the Tm-DOTA solution on a small volume of DOWEX-50, eluted in aqueous ammonium hydroxy isobutyrate, and reacted with suitable targeting molecules. For the purpose of this study, DOTATATE was used as a labeling representative for targeting peptides.

Results: The produced ¹⁶⁵Er has activity ranging up to 200 MBq at specific activities of up to 43 GBq/μmol vs. non-radioactive Er (ICPOES). ¹⁶⁵Er-DOTATATE was successfully labeled.

Conclusions: A ¹⁶⁵Tm/¹⁶⁵Er generator, produced with a low energy cyclotron, provides the Auger emitting therapeutic isotope ¹⁶⁵Er in sufficient quantity and specific activity for preclinical studies. There are no obstacles in scaling up the production for clinical application.

Keywords: radionuclide production, isotope generator, auger therapy

References:

- [1] Zhernosekov et al, *Radiochim Acta* 2007 **95** 319-327
 [2] Jang et al, *J Am Chem Soc* 1999 **121** 6142-6151

181

The new business model of the European Organization for Research and Treatment of Cancer (EORTC)

E. Shash

European Organization for Research and Treatment of Cancer (EORTC)

In the past decade, increasing understanding of the mechanisms and pathways of tumor biology, clinical cancer research has truly entered a promising era filled with exciting new possibilities. Innovative options for prevention, diagnosis and treatment of cancer patients are under development, and these, combined with advances in technology, means there is still a lot more to come. However, the current clinical trial landscape cannot fully embrace these advances. In order to harness these possibilities and turn dreams into reality, stakeholders need to work together within an integrated cancer clinical research environment that is able to address the questions that are relevant today.

Facing rising health care costs and an unsustainably high attrition rate for candidate drugs, there is an urgent need to reshape the European clinical research landscape.

The approval process needs to be streamlined, to accommodate advances in molecular biology, and drug development has to move away from the old fashioned trial-and-error approach.

More effort is needed to understand disease mechanism and the mechanisms of action of the new molecular agents so that we can bridge the translational gap and avoid exposing patients to unnecessary toxic agents and avoid costly late drug failure.

The real benefit of drugs needs to be assessed independently to make evidence-based strategic decision about reimbursement possible. As there is no universal definition of what is considered a 'beneficial treatment', all stakeholders need to be involved in such a discussion.

A pan European approach would reduce duplication of effort and delays and lead to a harmonized healthcare landscape across Europe.

Keywords: Pay for performance, Real life data, Private Public Partnership

References:

- [1] Lacombe D, Burock S, Meunier F. Academia-industry partnerships: are we ready for new models of partnership?: the point of view of the EORTC, an academic clinical cancer research organisation. *Eur J Cancer* 2013.
 [2] Burock S, Meunier F, Lacombe D. How can innovative forms of clinical research contribute to deliver affordable cancer care in an evolving health care environment?. *Eur J Cancer* 2013

182

Octavius 4D measurements For RapidArc™ : What are clinically Acceptable Gamma- Index Pass Rates?

H. Sidhique¹, N. Ramar², J. Cramb³, M. Muthukumarn⁴, D. Manigandan⁵

¹Continental Hospitals Limited, Hyderabad, India

²Apollo Hospitals, Bangalore, India

³Peter MacCallum Cancer Centre, Melbourne, Australia

⁴Apollo Hospitals, Chennai, India

⁵Shri Shiddivinayaka Cancer Centre, Miruj, India

Purpose: The aim of this investigation was to compare the minimum gamma pass-rate of RapidArc™ pre-treatment patient specific quality assurance (QA) using Octavius 4D dosimetry system in static and rotational mode of measurements.

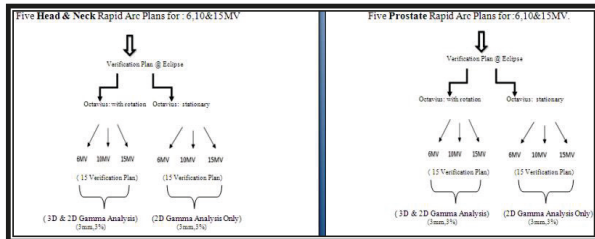
Materials and Methods: In this retrospective study 5 patients in each site of head-and-neck and prostate cases were taken into consideration. RapidArc (RA) treatment plans were generated using Varian Eclipse™ V. 11 treatment planning system (TPS) pre-configured of TrueBeam STx for photon beam energies of 6, 10 and 15 MV. Octavius 4D dosimetry system from PTW, Germany installed at Apollo Hospitals, Bangalore, was employed in this study. Eclipse TPS using 2 different sets of CT images during calculation of verification plans and Octavius 4D phantom was at 2 different set-up during delivery of same verification plans for all cases and beam energy as follows:

4D Phantom is static during RA QA plan delivery- S1 (set-up1); Verification plans were generated using Scanned images of Octavius 4D phantom at site (presence of built-in air cavity)
 4D Phantom rotates during RA QA plan delivery- S2 (set-up2); Verification plans were generated using PTW produced DICOM CT images (no-air cavity)

2 dimensional (2D) and 3 dimensional (3D) Gamma Index (GI) were analyzed for S1 and S2 set up of deliveries respectively. For 2D GI analysis, isocenter planar dose was chosen for all cases and beam energy where as 3D GI analysis were performed between TPS calculated and measured/reconstructed dose cubes from Verisoft, PTW. Both 2D and 3D GI were analyzed with universal criterion of 3% delta dose (Δd) and 3mm distant-to-agreement (DTA). In addition, TPS planned dose planes for S1 were also compared with detector dose planes extracted from the measurements of S2.

Results and Conclusion: Total of 60 QA verification plans were delivered (5 Head-and-Neck patients for three photon energies in S1 and S2; 5 prostate patients for three photon energies in S1 and S2). 3D gamma index analysis between TPS and measured dose cubes were better in agreement for 3mm DTA & 3% Δd with the pass-rate more than 96% for both head-and-neck and prostate cases for all the three photon beam energies. The minimum 2D gamma pass-rate from S1 were 97.3%, 97.5% and 97.9% in prostate; 96.3%, 98.6% and 97% in head-and-neck for 6, 10 and 15 MV respectively. The minimum 2D gamma pass-rate of reconstructed dose planes from S2 measurements with TPS dose at detector plane was 92.3%, 96.1% and 97.8% in prostate; 93.9%, 98% and 90.4% in head-and-neck for 6, 10 and 15 MV respectively. Our study shows that Octavius 4D phantom computed tomography images can be used to create patient specific QA verification plan and it could be delivered whilst the Octavius 4D

phantom is in static mode to achieve clinically acceptable gamma pass rate values (> 95%) for head-and-neck and prostate with pelvic lymph node RapidArc delivery verification using 6, 10 and 15 MV photons.



Keywords: RapidArc, Octavius 4D, Rotational Dosimetry

183

The use of the Golden Triangle paradigm for Knowledge Exchange for Computational Radiotherapy: a Case Study

M. Simmons¹, N. Burnet², A. Parker³

¹Cavendish Laboratory, University of Cambridge, UK

²Department of Oncology, University of Cambridge, UK

³High Energy Physics Group, Cavendish Laboratory, University of Cambridge, UK

Purpose: Cern initiatives in developing medical applications for its technology have been significant drivers enabling us to develop collaborations in this field, where experts from particle physics, medical physics, computer science, engineering, and medicine are working together to make advances in radiation oncology. Such interdisciplinary teams, we argue, are able to spark innovation in ways which otherwise would be impossible.

We present the development of collaborative Computational Radiotherapy initiatives as a Case Study. These collaborations at Cambridge and beyond are examples of “[those] most exciting collaborations [which] arise as a result of like-minded people getting together - sometimes by chance - to address a problem.” (From the UK Treasury Lambert Review of 2003.)

Methods: The talk presents the powerful and novel Golden Triangle paradigm for Knowledge Exchange (KE) - encompassing people, ideas and funding. Our application of this paradigm has underpinned the instigation and growth of Computational Radiotherapy, and our concomitant strategies for facilitating effective knowledge exchange. The creation and maintenance of a web of effective relationships has been indispensable. Scientists from different disciplines do not routinely meet nor speak the same ‘language’, any successful application of knowledge exchange must address this and break down silos. We make a persuasive case that KE is overwhelmingly a human-centric art rather than a data-centric science. We present evidence which suggests that undue reliance and interfacing with data systems is positively detrimental to effective knowledge exchange. Examples cited will include the effectiveness, or otherwise of email.

Results: The talk looks at progress so far. It will also discuss our mutually beneficial links with companies and other organisations.

The talk covers the highlights of the collaborations built on the human web, as well as some of the lessons learnt. These include the contribution of Cern techniques in warehousing and managing extremely large volumes of data, critical in our winning the bid for our flagship research project, VoxTox, and an essential elements in our other two projects, Accel-RT and GHOST. We assess the overall impact of our collaborations in radiation oncology.

Conclusions, and the future: Finally, we scan the horizon for future possibilities in computational radiotherapy. Additional

challenges include public education and information about the societal value of physics research and radiation oncology research. Also, how can we build on our experience of human network building so far to make them more effective?

We have learnt that knowledge cannot simply be encoded as digitised data, but must be communicated between humans if any sustainable progress is to be made. Good human-centric facilitation is essential for effective knowledge exchange.

Keywords: people-centric, data-centric, collaborations

184

Prompt gamma imaging of proton pencil beams at clinical beam current

J. Smeets¹, A. Celani², E. Clementel³, C. Fiorini^{4,5}, T. Frizzi², S. Henrotin¹, G. Janssens¹, I. Perali^{4,5}, D. Prieels¹, F. Roellinghoff¹, F. Stichelbaut¹

¹Ion Beam Applications SA, Louvain-la-Neuve, Belgium

²XGLab, Milano, Italy

³iMagX Project, ICTEAM Institute, Université Catholique de Louvain, Louvain-la-Neuve, Belgium

⁴Politecnico di Milano, Dipartimento di Elettronica, Informazione e Bioingegneria, Milano, Italy

⁵INFN, Sezione di Milano, Milano, Italy

Thanks to its concentrated dose deposition pattern, proton therapy offers precision and consequently demands accuracy. In order to further improve feedback on treatment delivery, different concepts of cameras are being designed in view of instantaneous range verification by imaging prompt gammas emitted along the proton tracks in the patient.

Prompt gamma imaging is a simple concept applied in most challenging conditions. Technical requirements include (1) large dynamic range for the broad, continuous, multi-MeV energy spectrum of prompt gammas, (2) high detection efficiency to take most benefit of the few prompt gammas emitted per individual proton pencil beam spot, (3) low sensitivity to the uncorrelated neutron background and (4) very high count rate to score several thousand counts in the typical millisecond duration of a beam spot.

The present study reports on the development and test of a prompt gamma camera relying on a slit collimator to produce a reversed 1-dimensional projection of the last centimeters of the beam path on a segmented LYSO detector for treatments delivered in pencil beam scanning mode. The geometry was optimized by means of simulations to reach millimeter accuracy on range estimation for doses compatible with single pencil beams by comparison of a measured profile with a reference simulated one.

In order to meet the demanding specification on the count rate capability, a dedicated, cost-effective photodetection system was designed. This very-fast, 1-dimensional, high-energy gamma imaging device relies on two rows of 20 LYSO crystal slabs, directly coupled to SiPMs’ arrays and readout by 40 independent acquisition channels in fast counting mode.

A first prototype limited to 3 channels was implemented and validated in April 2013 during proton irradiations of a PMMA target at the West German Proton Therapy Centre in Essen. This prototype was, to our knowledge, the very first to achieve successful acquisitions of correlated prompt gamma profiles at clinical beam currents of several nA at nozzle exit. These performances were reached at close distances and up to the maximum clinical beam energy of 230 MeV, demonstrating the technical feasibility of prompt gamma imaging with both sufficient sensitivity and counting speed for application in pencil beam scanning mode.

Leveraging this proof of concept, the full-size photodetection system equipped with the first of its two rows of 20 slabs was assembled and tested in October 2013. Correlated profiles were recorded for individual pencil beams of a few milliseconds duration. A count rate of 1 MHz per individual slab was even reached above a 2 MeV threshold for a beam

energy of 230 MeV and a beam current of 27 nA, i.e. 10 times more than a typical clinical beam current for IBA C230 cyclotron. Further characterization results will be presented.

Keywords: Proton therapy, Range verification, Prompt gammas

Acknowledgment: This project received funding from the European Union Seventh Framework Program (FP7/2007-2013) under grant agreement nos 241851 (ENVISION) and 264552 (ENTERVISION).

185

Fat percentage and hand grip strength in lung cancer: the influence on survival and toxicity

K.M. Smits, G. Nalbantov, R. Houben, C. Oberije, J. Paulissen, E. Troost, P. Lambin
Department of Radiation Oncology (MAASTRO), GROW-School for Oncology and Developmental Biology, Maastricht University Medical Center, the Netherlands

Purpose: To determine the influence of fat percentage and hand grip strength before start of radiotherapy (RT) on overall survival (OS) and radiation-induced toxicity in patients with non-small cell lung cancer (NSCLC). In addition, the association with World Health Organisation (WHO) performance status was evaluated to assess whether these variables could be used as surrogates for WHO performance status.

Materials and methods: Analyses were performed using data of 392 stage I-III NSCLC patients that were treated with RT alone or combined with chemotherapy in the period 2002-2011. Fat percentage and hand grip strength were measured at two time points (baseline and halfway through RT), 299 patients were staged and treated according to the 6th edition and 93 according to the 7th edition of the TNM classification system. OS was defined as time from first visit to our clinic until death or end of follow-up (October 2013), toxicity was scored using the Common Toxicity Criteria version 3.0 (CTCv3.0). Severe toxicity was defined as lung toxicity grade 3 or higher, at any time point during or after RT. Kaplan-Meier curves and log-rank tests, and multivariate Cox proportional hazards models were used to assess the influence of fat percentage and grip strength on survival. The association with toxicity risk measured was assessed using multivariate logistic regression.

Results: Median baseline fat percentages or grip strength measurements did not differ from measurements during RT (Table 1). Baseline fat percentage and grip strength was associated with WHO performance status in men ($p=0.010$ and 0.0002 respectively) but not in women (Figure 1A). Median survival in the population was 19 months (18 months for males, 22 for females), at the end of follow-up 72% of the patients was deceased. There was no influence of fat percentage on OS in either men ($p=0.534$) or women ($p=0.563$). For grip strength, however, a higher baseline and during RT grip strength was associated with a better outcome in men ($p=0.006$) (Figure 1B and Table 1).

Information on lung toxicity was available for 142 patients, 47 of these had a CTC score > 2 at any time point after treatment. For men, a high baseline fat percentage was associated with a lower risk of post-RT dyspnea ($p=0.039$). A baseline grip strength higher than the median was associated with a lower risk of post-RT dyspnea in female patients ($p=0.042$), but this group was small.

Conclusion: Our results suggest that a higher baseline grip strength is associated with superior survival outcomes in male NSCLC patients treated with radiotherapy alone or combined with chemotherapy. A higher baseline fat percentage in men and baseline grip strength in women appears to be associated with lower dyspnea risk but these groups were small, and results need to be replicated in future studies. Nevertheless,

our results indicate that grip strength might be useful as an easy, low-cost prognostic marker in NSCLC.

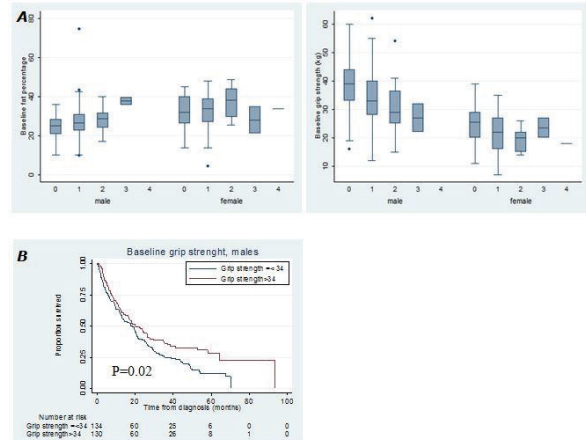


Figure 1

A: A higher baseline fat percentage was associated with increasing WHO performance scores in men ($p = 0.010$) but not in women ($p=0.587$). Decreasing grip strength was associated with increasing WHO performance scores in men ($p=0.0002$) but not in women ($p=0.114$); **B:** Kaplan-Meier analyses for grip strength below and above the median value for male NSCLC patient, $p=0.020$

Table 1: The influence of fat percentage and hand grip strength on overall survival and dyspnea risk CTC grade > 2

	Median	Survival, HR (95%-CI)		Dyspnea risk CTC >2 , OR (95%-CI)				
		\leq median	$>$ median	\leq median	$>$ median			
Men	Baseline							
	Fat, %	26.2	1 (ref)	0.89 (0.67-1.18)	0.99 (0.97-1.01)	1 (ref)	0.66 (0.28-1.56)	0.92 (0.87-1.00)*
	Grip strength, kg	35.0	1 (ref)	0.76 (0.56-1.04)	0.98 (0.96-0.99)*	1 (ref)	0.69 (0.27-1.74)	0.96 (0.91-1.02)
	During RT							
	Fat, %	26.5	1 (ref)	0.99 (0.71-1.37)	0.99 (0.97-1.02)	1 (ref)	0.51 (0.20-1.30)	0.94 (0.87-1.01)
	Grip strength, kg	35.0	1 (ref)	0.63 (0.44-0.88)*	0.98 (0.96-0.99)*	1 (ref)	0.72 (0.27-1.90)	0.96 (0.91-1.01)
Women	Baseline							
	Fat, %	33.5	1 (ref)	1.05 (0.68-1.63)	1.01 (0.98-1.03)	1 (ref)	0.73 (0.15-3.44)	1.03 (0.94-1.14)
	Grip strength, kg	24.0	1 (ref)	0.85 (0.52-1.39)	0.97 (0.94-1.01)	1 (ref)	0.10 (0.01-0.92)*	0.85 (0.71-1.03)
	During RT							
	Fat, %	32.9	1 (ref)	1.02 (0.64-1.64)	0.99 (0.96-1.03)	1 (ref)	0.67 (0.10-4.65)	0.98 (0.88-1.10)
	Grip strength, kg	23.0	1 (ref)	1.15 (0.68-1.94)	0.99 (0.94-1.03)	1 (ref)	0.20 (0.01-2.82)	0.95 (0.79-1.15)

* $p < 0.05$

Keywords: non-small cell lung cancer, fat percentage and hand grip strength, prognostic markers

186

A combined electrical impedance tomography and cone beam CT for radiation therapy monitoring

M. Soleimani, C. Yang
University of Bath, Avon, UK

Purpose: Cone Beam Computed Tomography (CBCT) is an imaging modality that has been used in image-guided radiation therapy (IGRT). For applications such as lung radiation therapy, CBCT images are greatly affected by the motion artefacts. This is mainly due to low temporal resolution of CBCT. We have proposed a dual modality of Electrical Impedance Tomography (EIT) and CBCT as a mean for motion compensated CBCT.

Materials/methods: The main aim of this work is to investigate the effectiveness of the motion-compensated CBCT using proposed conjugate gradient least square (CGLS) algorithm together with the EIT system for limited projection data reconstruction. In this set up, the EIT will provide information about the movement of the organ(s) and this motion data will be used to enhance the CBCT images. In this work the motion-compensated CGLS was developed and tested for the improvement of CBCT image reconstruction using one-fourth projection data.

Results: Figure 1.a shows a CBCT reconstruction of a circular inclusion with motion and Figure 1.b shows motion compensated image using EIT motion data.

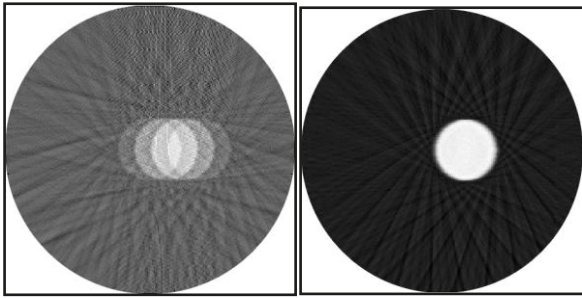


Figure 1. CBCT image with simulated motion and motion compensated reconstruction

Conclusions: The motion-compensated CGLS was applied to dual modality of CBCT/EIT, which uses the motion signal extracted from EIT images to compensate in CBCT image reconstruction. The results showed that the motion signal extracted from EIT images could be used to compensate the motion artefact in CBCT image reconstruction by using proposed motion-compensated CGLS algorithm.

Keywords: Electrical impedance tomography, lung radiation therapy, cone beam CT

187

Different detector concepts for several imaging scenarios: from hadrontherapy monitoring to clinical imaging

P. Solevi¹, J. Barrio¹, J. Cabello^{1,2}, J. Gillam^{1,3}, C. Lacasta¹, G. Llosá¹, J. F. Oliver¹, M. Rafecas¹, C. Solaz¹, I. Torres-Espallardo¹, M. Trovato¹

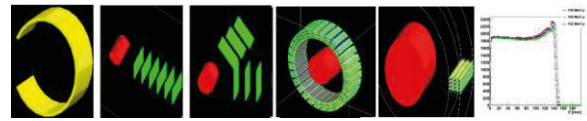
¹IFIC (CSIC/UV), Valencia, Spain

²Klinikum rechts der Isar der Technischen Universität München, Germany

³Brain & Mind Research Institute, University of Sidney, Australia

Purpose: Emission Tomography (ET) covers a wide number of applications, from the standard clinical imaging to the more recent Hadrontherapy (HT) treatment monitoring. For all aforementioned applications different trends in detector have been explored, attempting to find the optimal one. We present a comprehensive study of conventional and novel detector concepts crystal based, employed for Positron Emission Tomography (PET) and Single Photon Imaging, mostly developed within the ENVISION network. Defining the detector of choice over a wide dynamic range is one of the main objectives of the presented work.

Materials and methods: ET employs crystal based detectors given their capability to merge high detection efficiency, good energy and spatial resolution with fast timing. We compare monolithic crystal detectors an LaBr3 crystal block read out by a Silicon Photo-Multipliers matrix and AS-PET, a novel detector with axially oriented crystals. The latter is based on individually read out LYSO crystals, 10 cm long, axially arranged. Both systems have been experimentally validated and extensively studied at simulation level by means of dedicated Geant4 and GATE Monte Carlo, for different applications, further optimizing the geometry and readout. HT monitoring requires special detector arrangement and acquisition, in order to minimize the background mostly due to nuclei fragments and gammas uncorrelated with the original hadron path in the patient. Some of the geometries and systems investigated are shown in Fig. 1 ((a) to (c)) for the monolithic crystal, (d) and (e) for the AX-PET system).



(a) (b) (c) (d) (e) (f)

Results: Different sources are simulated in order to evaluate the systems capability with respect to different scenarios: mono-energetic hadron beams (as in Fig.1, (f)), more complex hadron treatment plans and linear sources for both 511 keV back-to-back gammas and single photons at different energies. The discretized geometry of AX-PET yields a large tracking capability of the photons within the detector matrix, partially lost in continuous crystals. Therefore it provides a larger sensitivity, important for both clinical and HT PET, and exhibits a potential for single photon detection. Still the individual crystal readout poses some limitations to the dynamic range of the detector, thus moving to higher energy prompt-gamma detection would imply further adjustments, feasible thanks to the flexible design. Monolithic crystals, with a concept pretty far from the highly granular AX-PET, still perform very well, offering a wider dynamic range. Both detectors provide a few millimeters spatial resolution in PET modality, in the hadron range determination too.

Conclusions: Two very different detector concepts have been extensively studied and compared, the compact monolithic crystal and the highly granular AX-PET device. Both detectors perform well in the investigated applications, PET and Single Photon Imaging.

Keywords: hadrontherapy, PET, Single Photon Imaging

188

Hpv Status and Effect on Radiosensitivity in Head and Neck Cancer Tumor Xenografts

B.S. Sørensen¹, M. Busk¹, A. Minchinton², A. Kyle², M. Horsman¹, J. Alsner¹, J. Overgaard¹

¹Department of Experimental Clinical Oncology, Aarhus University Hospital, Aarhus, Denmark

²BC Cancer Research Centre, Department of Integrative Oncology, Vancouver, Canada

Purpose: HPV associated Head and neck squamous cell carcinoma (HNSCC) represent a distinct subgroup of HNSCC characterized by a favourable prognosis and a distinct molecular biology. Previous data from the randomized DAHANCA 5 trial indicated HPV positive tumours did not benefit from hypoxic modifications by Nimorazole during radiotherapy, whereas a significant benefit was observed in the HPV negative tumours. However, more studies, have demonstrated equal frequencies of hypoxia amongst HPV-positive and HPV-negative tumours. We have in an in vitro study demonstrated that hypoxia lowers radiosensitivity in both HPV positive and HPV negative HNSCC cell lines and that sensitivity can be partly restored by Nimorazole treatment. However, HPV positive HNSCC cell lines shows significantly elevated inherent radiosensitivity compared to HPV negative cell lines.

The aim of the study was to confirm that the demonstrated difference in radiosensitivity observed in vitro also applies to tumour xenografts grown from HPV positive and HPV negative HNSCC cells. Moreover, the aim was to identify and quantify differences in the microenvironment related to HPV-status.

Methods: Tumor xenografts were established from HPV negative (FaDu_{bb}, UTSCC33) and HPV positive (UD2 and UMSCC47) HNSCC cell lines.

Tumors were treated with 10 Gy or 20 Gy and the effect on the tumour microenvironment was studied at different timepoints after treatment. Cryosections were imaged for

factors such as apoptosis, necrosis, cell proliferation, hypoxia, vessel density and vessel perfusion.

To assess the spatial distribution of hypoxia in response to the treatment in the different tumour models two hypoxia markers were used. EF5 was administered prior to treatment, whereas PIMO was injected at different time points after irradiation.

Results: The HPV positive and HPV negative tumour xenografts displayed comparable pre-treatment levels in vessel density and hypoxic fraction. With the observed endpoints, HPV positive tumour xenografts were found to be more radiosensitive than HPV negative tumours.

Conclusion: There is a range of unresolved questions regarding the different biology and clinical outcome of HPV positive HNSCC, the purpose of the present project was to obtain insight into the biology of treatment responsiveness of HPV-related HNSCC. The markedly higher radiosensitivity, which may account for the favourable clinical prognosis, previously found in vitro in HPV positive cells, was also observed in vivo in tumour xenografts in the present study.

Keywords: HPV, HNSCC, Radiosensitivity

189

Nuclear techniques for studying soft matter at ISOLDE/CERN

M. Stachura¹, A. Gottberg¹, L. Hemmingsen², K. Hohnston³, M. Kowalska¹

¹CERN, Geneva, Switzerland

²University of Copenhagen, Denmark

³University of Saarland, Germany

Due to the complexity of “living systems” nuclear techniques are not commonly used in biology and biochemistry even though they offer powerful insights to local properties. The ISOLDE facility is, however, a perfect place to carry out experiments with Perturbed Angular Correlation of γ -rays (PAC) spectroscopy. This technique is suitable for addressing different biological problems, such as: heavy metal ion - protein interaction, dynamics of protein folding or protein - protein interaction, providing information on the molecular and electronic structure at the metal site [1]. A short overview of recent ISOLDE studies on *de novo* designed peptides, natural proteins, plants and bacteria will be presented.

Furthermore, recently a new avenue of research in the fields of wet chemistry and biochemistry has been opened at ISOLDE: β -NMR spectroscopy has been successfully applied in the first ever experiment on liquid samples. The method is over a billion times more sensitive than conventional NMR on liquids and thus may be applied to elements which are otherwise difficult to explore spectroscopically, such as Mg^{2+} , Zn^{2+} or Cu^+ . The setup and the first β -NMR results of ^{31}Mg implanted into an ionic liquid will be shown [2].

Keywords: PAC, NMR, soft matter

References:

[1] L. Hemmingsen *et al.*, Chem. Rev. 2004, 104, 4027.

[2] A. Gottberg *et al.*, manuscript in preparation.

190

The (non-) detectability of failures in motion mitigated ion beam delivery by means of in-beam PET

K. Stützer¹, W. Enghardt¹, M. Priegnitz², C. Bert³, N. Saito³, K. Parodi⁴, F. Fiedler²

¹OncoRay - National Center for Radiation Research in Oncology, Dresden, Germany

²Helmholtz-Zentrum Dresden-Rossendorf, Germany

³GSI Helmholtzzentrum für Schwerionenforschung Darmstadt and University Hospital Erlangen, Germany

⁴Heidelberg University Clinics and LMU Munich, Germany

Purpose: The qualitative positron emission tomography for the dose monitoring in ion beam therapy (PT-PET) has been approved for static tumors under clinical conditions. The detection of dose deviations is based on a comparison between the measured and an anticipated β^+ -activity distribution. Also for intra-fractionally moving targets, the 4D simulation [1] as well as the 4D reconstruction [2] of in-beam PET data has been established. Within dedicated experiments the results of the comparison between measured and anticipated activities were investigated with regard to the detection of failures in the motion mitigated ion beam delivery.

Materials/methods: PMMA targets have been irradiated with ^{12}C ion beams at GSI Darmstadt, and the induced β^+ -activity distributions were determined by in-beam PET measurements using the installed double-head scanner BASTEI [3]. The targets were periodically moved perpendicular to the incident ion beam direction. Motion mitigation by means of beam tracking or gating has been applied. In some measurements, failures in motion mitigation were induced systematically or by chance. The reconstructed activity distributions were compared to those measurements with static targets or with correct motion mitigation or to the anticipated distribution from a 4D simulation.

Results: Failures in beam tracking are manifested in a lateral and distal broadening of the β^+ -activity distribution, but an algorithm for such an automatic quantitative evaluation is still missing.

The breakdown of a gating sensor led partly to an irradiation without motion compensation. In such a case, an activity distribution with similar shape is anticipated by the 4D simulation (cf. figure 1). Only a deeper search in the simulation input data or a static target simulation could reveal the treatment error.

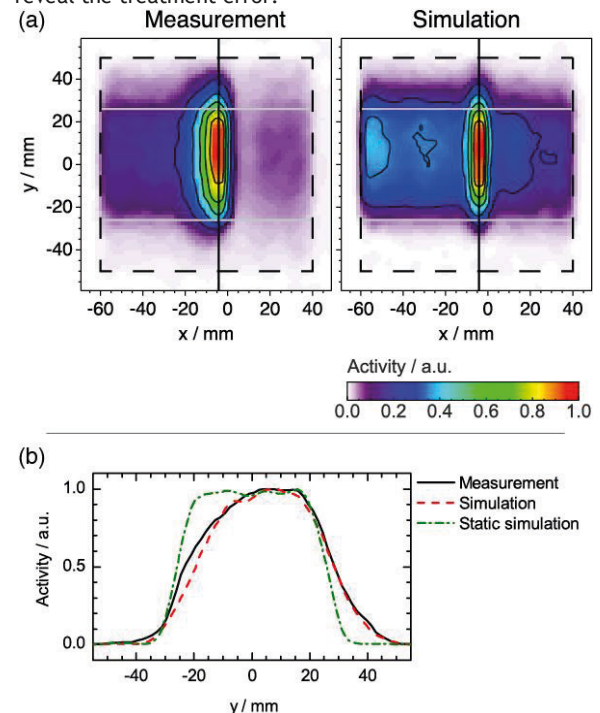


Figure 5. Bird's eye view of the measured and the simulated activity distribution (a) within a target (dashed) irradiated with mono-energetic beams (impinging from the left). Motion mitigation (parallel y) was insufficient due to a gating breakdown. Profiles taken along the vertical lines show similar progression (b) which differs clearly from the symmetric profile gained from a static target simulation.

Conclusions: In 4D PT-PET data evaluation, on the one hand, similar activity distributions might be found from measured and simulated data, although a crucial motion mitigation error occurred like the selection of a wrong gating window or an undetected gating breakdown. On the other hand, there might be differences which are still non-detectable in a quantitative way. Thus, caution needs to be paid when interpreting 4D in-beam PET data.

Keywords: particle therapy, intra-fractional target motion, dose monitoring

Acknowledgement: The work was supported by the FP7 ENVISION project (241851).

References:

- [1] Laube et al. (2013) Phys Med Biol 58(3) 513-33
- [2] Stützer et al. (2013) Phys Med Biol 58(15) 5085-111
- [3] Enghardt et al. (2004) Nucl Instr Meth Phys Res A 525 284-8

191

Automatic beam dose profiler for scanned pencil beams (protons and carbon ions) at the CNAO hadrontherapy facility

A. Tamborini^{1,2}, L. Raffaele^{3,4}, M. Ciocca⁵, A. Mirandola⁵, C. Viviani⁵

¹University of Pavia, Italy

²INFN-Section of Pavia, Italy

³National Laboratories of South (LNS)

⁴INFN-Section Of Catania

⁵CNAO Foundation, Pavia, Italy

Purpose: At the National Centre for Oncological Hadrontherapy (CNAO) we are developing a 2D scintillation detector for beam line characterization and Quality Assurance (QA). The aims are the *online* reconstruction of beam lateral profiles and the verification of the accuracy of beam deflection.

Also the radiation field homogeneity will be investigated through measurements of planar relative dose distributions.

The use of this system will allow to perform periodic dosimetric quality checks and commission of beam lines with a relevant time and cost saving, with respect to the currently used method (EBT3 films), at least at the same level of accuracy and reproducibility.

Materials/Methods: The detector consists of a thin plastic scintillating screen (EJ212, 250 x 250 x 2 mm³) coupled with a CCD camera through an optical mirror. The CCD camera collects the visible light emitted from the scintillator when exposed to the particle beam. An external covering box has been provided to fully protect the system from the environmental light.

The machine-triggered acquisition and data processing is performed by a Labview application: the program acquires each image as a 12-bit matrix. The CCD acquisition time is set at 2 s to fully include the synchrotron spill duration (1 s). Once optimal working distances were set, we measured the pixel size of the CCD-acquired image to be 0.254 mm (corresponding to the detector's spatial resolution), comparable with EBT3 films scanned using an EPSON scanner (0.2 mm). No geometrical image distortion was observed using a test object, while signal intensity inhomogeneity within the image was corrected by applying a flat field filter. Before image analysis, a routine performs the background removal.

Results: The system characterization, using both proton and carbon ion pencil beams, included dosimetric tests of linearity (see Figure 1), short-term reproducibility and homogeneity and gave satisfactory results.

The detector was positioned at the isocenter to measure the lateral profiles of the pencil beams and their Full Width at Half Maximum (FWHM) value.

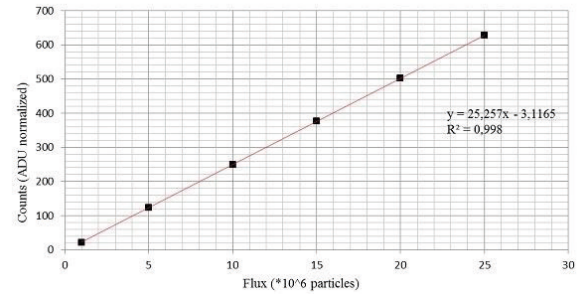


Figure 1: Light yield (normalized on a Region Of Interest - ROI) as a function of carbon ions flux. The behaviour is linear.

A cross-check with profiles measured with EBT3 films was done to verify the detector's performance and reliability. Results are very promising since the measurements obtained with the two methods are compatible within the spatial resolution.

Conclusions: First results have shown nice agreement between the scintillator and EBT3 films, both for individual pencil beams and scanned fields, for different energies.

Further investigations to improve the detector performances and to achieve a more compact system are ongoing. Particularly, the expected quenching effect of the plastic scintillating screen under particle beams close to the Bragg peak depth is currently under testing, both for protons and carbon ions.

Keywords: Scintillator, Dosimetry, Radiation

192

Novel detectors for range assessment in particle therapy

P.G. Thirolf

Faculty of Physics - Medical Physics, Ludwig-Maximilians University Munich, Germany

Purpose: The stopping characteristics of ion beams for hadron therapy, as manifested by the Bragg peak, provide an obvious advantage for a highly conformal dose delivery. However, range uncertainties pose the key challenge that still limits the full exploitation of this technique, in particular in the vicinity of critical organs at risk. Thus a reliable online ion-beam range verification needs to be developed, requiring also optimized innovative detection concepts.

Materials/Methods: Presently, several complementary approaches are pursued to evaluate the perspectives for online ion beam range verification in hadron therapy. Currently, monitoring of the dose delivery within the patient solely relies on the imaging of annihilation photons from β^+ -decaying nuclear reaction products during therapeutic irradiation via positron emission tomography (PET) during or shortly after treatment. In addition, alternative signatures are being explored, targeting prompt γ rays or secondary charged particles from nuclear reactions, or even acoustic signals induced by ion-beam excitations. Several groups embarked on the development of novel gamma cameras, either using conventional mechanical collimation or electronic collimation, as realized in various Compton camera prototypes presently under study. Novel detector materials (new scintillation materials like LaBr₃ or room-temperature semiconductors like CdZnTe, CZT) are being investigated. Also hybrid detectors, combining prompt (during treatment)

and delayed (in treatment interrupts) photon detection via (□)-PET imaging is discussed.

Results: Following extensive simulation studies, Compton camera prototypes are presently being developed in several laboratories (e.g. Dresden, Garching, Lyon, Valencia) and corresponding novel detector components are being developed, partly aiming also for tracking of the Compton electrons to improve the reconstruction efficiency. Pixelated silicon detector systems (e.g. Timepix) have proven to provide an imaging performance for tracking of secondary particles, which is attractive for therapeutic applications. Promising signals from an acoustic detection of the energy deposition by a proton beam have been observed in a water phantom with sub-mm sensitivity to the Bragg-peak position.

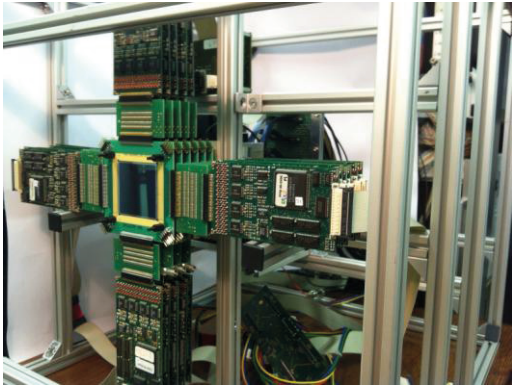


Figure1: Prototype of the Compton camera developed in Garching for ion beam range monitoring (visible is the scatter component, consisting of a stack of double-sided silicon-strip detectors together with the corresponding readout electronics).

Conclusions: Complementary messengers (prompt photons, charged particles, acoustic signals) from the Bragg peak of an ion beam in hadron therapy are presently being investigated in view of their potential to solve the urgent challenge to allow for an online ion beam range verification. Novel detector systems are being developed and characterized, aiming at a localization of the Bragg peak with mm accuracy.

193

Imaging for Prescription Function

D. Thorwarth

Section for Biomedical Physics, University Hospital for Radiation Oncology Tübingen, Germany

Purpose: To review the current state of the art concerning functional imaging strategies to derive dedicated prescription functions for biologically individualized radiotherapy (RT).

Methods and Materials: A clinical phase II trial on hypoxia dose painting (DP) is presented. To date, n=25 head-and-neck cancer (HNC) patients were included into this study. Patients received in addition to a planning CT scan and a conventional ¹⁸F-FDG PET/CT a dynamic ¹⁸F-FMISO PET/CT examination. Based on the FMISO PET/CT data, a voxel-based analysis for tumor hypoxia was performed. Patients that presented with hypoxic tumors were randomized into two treatment arms: (1) Standard IMRT with 70 Gy or (2) a dose escalation of 10% into the hypoxic sub-region of the tumor.

Data of patients randomized into the standard treatment arm were used to validate a tumor control probability (TCP) model derived in an earlier study from dynamic FMISO PET/CT information. This model forms the basis of a dedicated prescription function for individualized hypoxia DP. **Results:** n=5 patients did not show significant levels of tumor hypoxia and were thus not randomized whereas n=20 patients

could be randomized into two arms. Hypoxic volumes (HV) derived from dynamic FMISO PET/CT ranged from 0-49.2mL with a mean HV of 8.1mL. As a consequence, tumors with HVs smaller than 5-10mL did not receive the intended dose escalation of 77 Gy as the volumes were too small with respect to the finite dose gradients yielded by photon RT. The functional FMISO PET/CT information from the patient group randomized into the standard treatment arm could be used to validate a TCP model and thus a dedicated prescription function for hypoxia DP in HNC.

Conclusion: Individualized RT in terms of DP can only be appropriately applied if dedicated prescription functions are available. Such prescription functions can only be generated by functional imaging studies with a correlation of the results to RT outcome.

194

Investigation of Irregular Motion Influence for Future 4D In-Beam PET Imaging

Y. Tian¹, K. Stützer¹, W. Enghardt^{1,2}, M. Priegnitz², S. Helmbrecht¹, F. Fiedler²

¹OncoRay-National Center for Radiation Research in Oncology, Technische Universität Dresden, 01307 Dresden, Germany

²Helmholtz-Zentrum Dresden-Rossendorf, P.O. Box 510119, 01314 Dresden, Germany

Purpose: Particle therapy PET (PT-PET) has been established for dose monitoring and particle range assessment in hadron therapy¹. Imaging is up to now restricted to static organs. However, by means of phantom irradiation it has been shown that a 4D maximum likelihood expectation maximization (4D MLEM) reconstruction method is able to compensate for blurring artefacts of regular motion in in-beam PET images². Nevertheless, respiratory curves often show inconsistent amplitude variation, frequency modulation and baseline drift during radiotherapy. Since the anatomical information is not updated by a CT scanner during treatment, transformation of data from each phase could only rely on the 4D CT obtained prior to irradiation, which might be incorrectly transformed. Based on that clinical situation, this study aims to investigate the effect of irregularity in motion on 4D PET image reconstruction.

Materials and methods: The influence of irregular motion onto 4D PET images has been investigated by a ²²Na source experiment, using the double-head PET scanner at GSI, Darmstadt, Germany. The radioactive source was placed on a motion table driven by varied motions. A regular $y(t) = \cos^4$ motion with 20 mm peak-to-peak amplitude and 4 s time period was supposed to be the respiratory motion for treatment planning and a 4D-CT was generated according to it. Irregular motions were based on the regular one, combining with different parameters, to perform variations in amplitude, frequency and drift. PET list-mode data obtained were sorted into 9 phases and transformed according to the transformation matrix of the regular motion to reconstruct PET images using 4D MLEM.

Results: A compilation of the reconstructed images in fig. 1 shows that 4D-MLEM is robust for irregular motions with relatively small amplitude elongation and frequency variation. However, artefacts occur in PET image of data sets with ≥ 4 mm amplitude elongation and drift. The reconstructed activity distribution of the sodium source was elongated from a circular shape to an ellipse due to the unmatched transform information. For statistical evaluation, full width at tenth maximum (FWTM) along the motion direction in y (FWTM_y) as well as the non-motion direction in x (FWTM_x) are calculated. For baseline drift between 2 and 10 mm, FWTM_y of calculated B⁺-activity distribution increases from 8.62 mm to 15.30 mm. Also the FWTM_y/FWTM_x ratio ranges from 1.09 to 1.90, which indicates substantial

increase of artefact compared to the regular motion with a ratio of 1.01.

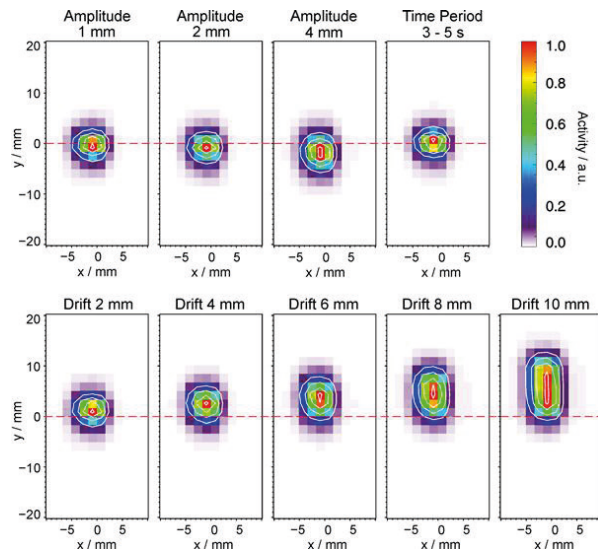


Figure 1. 4D reconstruction images for moving ^{22}Na sources applying different irregular motion pattern.

Conclusion: This study has investigated the robustness of 4D PET approach in terms of varied irregular motions expected from respiration. Since irregular motion causes image artefacts, a strategy is requested to ensure correct recording of motion data beyond the needs for beam delivery control.

Keywords: 4D in-beam PET, Respiratory motion artefact, particle therapy monitoring

Acknowledgments: This work has been supported by the ENTERVISION project which is funded by the European Commission under FP7 Grant Agreement N. 264552.

References:

- [1] W. Enghardt et al., Nucl. Instr. Meth. A 525, 284-288 (2004)
- [2] K. Stützer et al., Phys. Med. Biol. 58, 5085-5111 (2013)

195

PIP: a compact recirculating accelerator for the production of medical isotopes

A. Toader, R. Barlow, R. Edgecock
Huddersfield University, UK

PIP is a proposed proton non-scaling fixed-field alternating-gradient (nsFFAG) accelerator which uses an internal target for the production of medical isotopes. Conceptually the FFAG provides strong focusing, avoiding the losses experienced by cyclotrons. For many medical isotopes the production cross-section peaks strongly as a function of beam energy, and the recirculating beam of PIP gives high efficiency of production as protons which lose energy in the target foil will have this energy replaced for the next pass. The energy can be selected (in the range of MeV to tens of MeV) by altering the radial position of the target foil, and beam extraction is also possible. We discuss the production of ^{11}C , ^{13}N , ^{15}O , ^{18}F , $^{99\text{m}}\text{Tc}$, and other isotopes

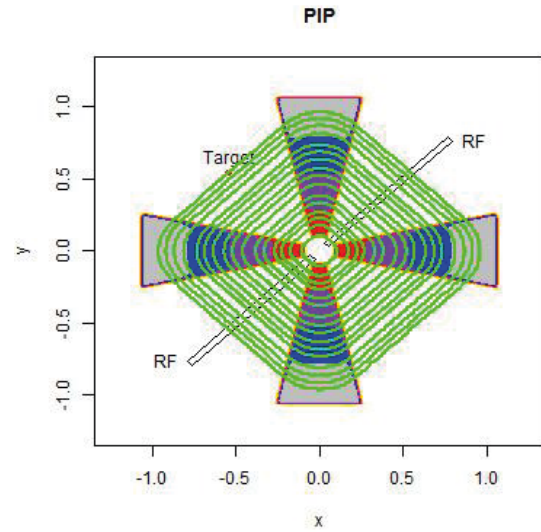


Figure 1. The figure shows the field map for a 4 MeV version of PIP, and reference orbits from 50 keV upwards. The machine design and its performance (acceptance and acceleration) are described.

We show that PIP's compact, cost-efficient and simple design means that the machine can be installed to service a single hospital, producing doses on demand, as and when needed by patients.

Keywords: Radioisotope, FFAG

196

From CERN to PET/MR

D. Townsend

A*STAR-NUS Clinical Imaging Research Centre, Singapore

The use of multi-modality imaging to stage patients with cancer has now become standard practice in many places. The benefits of assessing disease processes with combined imaging modalities is widely recognized and extensively documented. Such instrumentation for molecular imaging is also finding a role in designing appropriate therapies for individual patients and for monitoring their response to personalized treatment. However, the appearance in the clinic of purpose-specific multi-modality instrumentation is relatively recent and is still under development. The demand to improve spatial resolution and image quality at increasingly lower radiation dose is a challenge that requires innovative hardware and software methodology. Such improvements must be achieved within the constraints imposed by cost and clinical acceptability. The recent introduction into the clinic of simultaneous PET/MR has stimulated the development of solid-state photodetectors that are insensitive to magnetic fields. While the research and clinical utility of PET/MR is still being explored, fast, compact, silicon photomultiplier-based PET detectors have recently appeared for the first time in a clinical PET/CT scanner. The current trend in PET instrumentation is therefore in the direction of compact, field-insensitive detectors that are common to both PET/CT and PET/MR scanners. This, and other developments over the past decade such as the introduction of time-of-flight, are changes that have led to multi-modality devices offering high performance in terms of sensitivity, spatial resolution, count rate capability, image quality and reconstruction methodology. Some of these developments in medical imaging that will be highlighted are consequences of technology originating from CERN and the particle physics community. This presentation

will therefore assess the various technological milestones that have been attained over the past several years and the extent to which they offer a future direction for multi-modality instrumentation.

Keywords: Multi-modality

197

Preclinical Assessment of Efficacy of Radiation Dose Redistribution Based on Intratumoral FDG-PET Uptake

D. Trani, L. Dubois, S. Peeters, M. Granzier, N. Lieuwes, R. Biemans, B. Reniers, G. Nalbantov, E. Troost, G. Bosmans, F. Verhaegen, P. Lambin

Dept. of Radiation Oncology (MAASTRO), GROW - School for Oncology and Developmental Biology, Maastricht University Medical Centre, Maastricht, the Netherlands

Purpose: Clinical studies have shown that high pre-treatment intratumoral levels of ^{18}F -deoxyglucose (FDG) uptake, determined by positron emission tomography (PET) imaging, resulted in lower survival in patients with non-small cell lung cancer (NSCLC). Moreover, after radiotherapy (RT) residual FDG-uptake areas in the primary lesion significantly correspond to high FDG-uptake regions in the pre-RT scans. In this study, we aimed to assess pre-clinically whether radiation dose redistribution based on intratumoral FDG-PET uptake could lead to improved treatment efficacy compared to uniform irradiation.

Materials/Methods: Forty adult male WAG/Rij rats were implanted subcutaneously with syngeneic rhabdomyosarcomas in the lateral flank. When tumours reached a size between 5 to 8 cm³, animals were imaged with a FDG-PET -computed tomography (CT) scan (2 hours post-injection). The gross tumour volume (GTV) was defined on CT scans, while biological target volumes (BTV) corresponding to the 30% of the GTV with the highest ["hot" BTV] or the lowest ["cold" BTV] FDG-uptake were delineated on the corresponding PET images. Animals were randomly assigned (n=10 per group) to 1) uniform irradiation (Fig. 1A), 2) dose redistribution with the FDG-"hot" BTV receiving 40% higher dose than the rest of the GTV (Fig. 1B), 3) dose redistribution with the FDG-"cold" BTV receiving 40% higher dose than the rest of the GTV, and 4) sham irradiation (control). The mean tumour dose (MTD) was maintained at 12 Gy for all treatment groups. RT planning was performed with Eclipse 10 (Varian, CA). On the same day of the FDG-PET-CT scan, animals were individually irradiated on a TrueBeam High Definition 120 Leaf MLC. Toxicity and tumour growth after treatment were monitored until three-times the start volume was reached.

Results: Radiation toxicity was not observed in any of the treatment groups, regardless of the irradiation protocol. For the uniform and FDG-"hot" BTV irradiation groups, we observed a significant growth delay compared to the control group (27 days vs. 12 days respectively, $p < 0.01$). However, in the current experimental set-up we did not observe a clinically meaningful difference between uniform and heterogeneous "hot" BTV irradiation groups ($p = 0.8$).

Conclusion: Our results suggest for the first time *in vivo* that no clinically meaningful differences may exist between dose redistribution based only on high FDG-PET uptake regions and uniform irradiation. We are currently completing analysis of the FDG-"cold" dose redistribution arm and performing the same experiments with 8 Gy as MTD to ensure that our current observations are not dependent on saturation of the tumour control probability for our experimental model. In the future, it will be important to test other biological features of the tumour microenvironment (e.g. hypoxia and drug uptake) for image guided radiation dose painting.

Keywords: preclinical image-guided radiotherapy, radiation dose redistribution, intratumoral heterogeneity

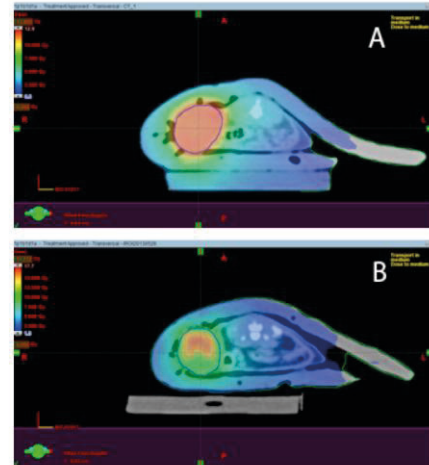


Figure 1. Representative dose colour wash for a homogeneous (A) and a FDG-"hot"-BTV-based dose redistribution (B) plan for two different rat rhabdomyosarcomas. The gross tumour volume (GTV; blue contour) and the body (rat body+bolus; green contour) were delineated on the CT scan for both animals (A and B). For the heterogeneous dose the FDG-"hot" BTV (red contour) was delineated on merged PET-CT image. Mean tumour dose (MTD) was 12 Gy for both plans. In the FDG-"hot"-BTV-based dose redistribution plan the BTV received a mean dose of 15 Gy and the rest of the GTV received a mean dose of 11.2 Gy.

198

Large Momentum Acceptance NS-FFAG superconducting gantry for Carbon Ion Cancer Therapy for PAVIA

D. Trbojevic, B. Parker, M. Pullia
Brookhaven National Laboratory, USA

A new design of the superconducting Non-Scaling FFAG (NS-FFAG) carbon isocentric gantry is presented. It could be applied for the PAVIA facility. The small light superconducting magnets replaced a large and heavy warm magnet. The patient treatment for the carbon-ion therapy is done with fixed magnet current settings for a large energy range: either from 200 - 400 MeV/u or from 70 - 200 MeV/u. The scanning is provided downstream of the 90 degrees bend and the beam arrives to the patient with infinite value of the S.A.D.

Keywords: superconducting gantry for carbon-therapy

199

Compton Telescope Prototype Based on Continuous LaBr₃ Crystals and Silicon Photomultipliers

M. Trovato¹, J. Barrio¹, P. Botas¹, J. Cabello², J.E. Gillam³, C. Lacasta¹, G. Llosá¹, J.F. Oliver¹, M. Rafecas¹, C. Solaz¹, P. Solevi¹, V. Stankova⁴, I. Torres-Espallardo¹

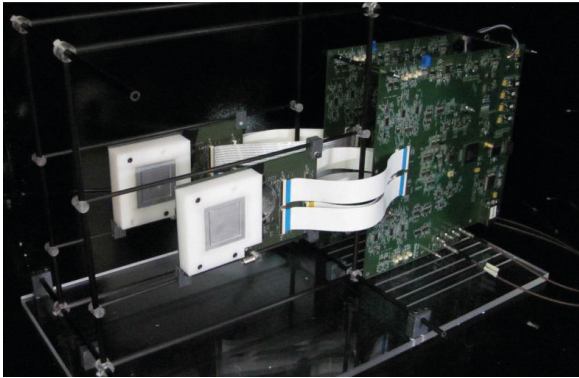
¹IFIC-CSIC/UV, Valencia, Spain

²Klinikum rechts der Isar der Technischen Universität München, Germany

³Brain and Mind Institute - University of Sydney, Australia

⁴Kirchhoff-Institute for Physics

Purpose: Hadrontherapy is a precise form of radiotherapy that uses a beam of protons or ions to target the cancer cells. During the treatment, prompt gammas are emitted along the proton or carbon ion tracks in the patient, from nuclear de-excitation of the target tissue nuclei. Compton camera systems are being investigated to detect those gamma rays and reconstruct the origin of the photons for treatment monitoring. A three layer Compton telescope prototype for treatment planning in hadron therapy is under development at IFIC - Valencia, in the framework of the European ENVISION project.



Material and Methods: The Compton telescope will consist of three detector layers and each layer will be made of a continuous LaBr₃ crystal coupled to four Silicon Photomultiplier (SiPM) arrays.

A two layer prototype of the telescope has already been built up and tested. Each layer is composed of a 32x36 mm² LaBr₃ crystal coupled to four SiPM arrays. The first detector (placed closer to the radioactive source) is 5 mm thick, the second one is 10 mm thick. Each SiPM array, from Hamamatsu Photonics (S11064-050P(X1)), consists of 16 (4x4) Multi Pixel Photon Counter (MPPC) with elements of 3 mm x 3 mm size, each one composed of 3600 microcells of 50 μm x 50 μm size. The MPPC arrays are placed in a custom made hybrid board that provides mechanical support, the bias for the MPPC arrays and also hosts a VATA64HDR16 ASIC from Gamma Medicas-Ideas, employed to read-out the 64 detector channels. Each hybrid board is connected to a data acquisition system (DAQ) developed at IFIC and equipped with an FPGA that provides the configuration for the ASIC and the control of the acquisition process. A third detector layer of the telescope, made of a 27.2x26.8x5 mm³ LaBr₃ crystal coupled to four SiPM arrays, has been assembled and tested. Each SiPM array consists of 16 (4x4) MPPC from Hamamatsu (S11830-3344MF), with elements of 3 mm x 3 mm size. The energy resolution obtained in the preliminary tests with the third detector layer is 6.6% FWHM at 511 keV.

Results: Coincidence tests have been carried out with the two layer telescope, placing the two detectors 41 mm apart and a ²²Na source 49 mm far from the first detector. Photons emitted by a ²²Na source that are Compton scattered in the first detector and interact also in the second, have been collected. Images of a ²²Na point-like source have been reconstructed employing a ML-EM algorithm, determining the correct functioning of the prototype.

Conclusions: A two layer Compton Camera with continuous LaBr₃ crystals coupled to SiPM arrays has been assembled and tested. Coincidence tests have been successfully performed and allow the reconstruction of a ²²Na point-like source. In-beam tests have been performed at the CNA (National Accelerator Center) in Seville. A cyclotron providing an 18 MeV proton beam, was used to irradiate quartz and graphite targets. The in-beam coincidence data processing is ongoing.

200

Current Status of Carbon-Ion Radiotherapy at NIRS

H. Tsujii

National Institute of Radiological Sciences (NIRS), Chiba, Japan

Introduction: In June 1994, the NIRS initiated carbon ion radiotherapy (C-ion RT) with HIMAC that was built as a part of the nation's "Overall 10-year anti-cancer strategy in

Japan". Since then, the HIMAC has served as a multipurpose facility that is jointly used for cancer therapy and fundamental studies. In 2010, a new treatment building with three rooms was built to use beam lines extending from the HIMAC. This was designed to administer adaptive charged particle therapy with pencil beam scanning, as well as to develop a compact rotating gantry [1]. Treatment with the scanning method started in 2011, and its indications have since been expanded to many types of tumors [2].

Materials/Methods: Initially, phase I/II trials were performed in order to confirm the safety and efficacy of C-ion RT, with the fraction number and treatment time being fixed for each tumor. In this way, the total dose was escalated in successive increments of 5 to 10%. Consistent efforts have been made to provide C-ion RT on an ethically and scientifically sound basis under a number of Committees.

Results: As of August 2013, the total number of patients registered is more than 7,700. The experiences to date indicate that C-ion RT is advantageous for the following tumors: skull base tumors, head and neck cancer (adenocarcinoma, adenoid cystic carcinoma, malignant melanoma), NSCLC (early stage, locally advanced tumors), hepatocellular cancer, pancreatic cancer, prostate cancer, rectal cancer (postoperative pelvic recurrence), bone/soft tissue sarcoma of the pelvis, paraspinal region and head/neck, and uterine cervix adenocarcinoma. Tumors located in the vicinity of critical organs such as the eye, spinal cord and digestive tract with a relatively large size and/or irregular shape have also been effectively treated. However, tumors that infiltrate or originate in the digestive tract are difficult to control with C-ion RT.

Regarding dose fractionations, a significant reduction in fractions has been obtained with acceptable toxicities in most cases. For example, stage I lung cancer and liver cancer can be treated with only one or two fractions, respectively. Even for prostate cancers, 12 to 16 fractions have been sufficient. Currently, the number of irradiation sessions per patient averages 12 fractions spread over approximately three weeks.

Conclusions: Clinical advantages have been demonstrated in the treatment of several types of tumors with C-ions, in particular, non-squamous cell type of tumors, and locally advanced, large tumors with acceptable morbidities. The physical and biological benefits of C-ions have permitted significantly shorter-course radiotherapy.

References:

- [1] Tsujii H, Minohara S, Noda K: Heavy-particle radiotherapy: System design and application. Reviews of Accelerator Science and Technology Vol 2 (ed. by Chao AW), Imperial College Press, UK, pp1-19, 2009.
- [2] Tsujii H, Kamada T.: A review of update clinical results of carbon-ion radiotherapy. *Jpn J Clin Oncol.* 2012; 42(8): 670-685.

Keywords: Carbon-ion, Radiotherapy

201

The ULICE project

The ULICE Consortium

The ULICE project was launched in 2009 with the aim to develop appropriate instruments for high-performance hadron-therapy (with a special attention to carbon ion therapy) and to foster the collaboration among existing and future centres, as well as between all the actors involved in this research field.

ULICE is funded for four years by the European Commission with 8.4 million Euros and involves 20 European institutions coordinated by CNAO. All the existing and planned European ion therapy facilities are involved in the project, together

with two research centres (CERN and GSI) and two industrial companies (Siemens and IBA).

The project is built on 3 pillars, each coordinated by a different institution and focusing on one aspect of the composite objective pursued by the ULICE project. The first pillar is the ‘Joint Research Activities’ and aims at improving the performances of hadron-therapy facilities by developing new tools and protocols. In particular, a novel adaptive treatment planning, a computer assisted programme to select the patients, as well as new protocols, would give the possibility to perform the best treatment for every tumour, possibly combining different types of irradiation.

Reducing the dimensions and costs of the gantry, the structure that gives the possibility to direct the beam from any directions out of 360° degrees, is another important goal for this section of the project.

The second pillar, called ‘Network Activities’ focuses on the necessity for interaction and know-how sharing between the partners involved in the project, as well as on dissemination activities, which goes from workshop and training for researchers, to publications and outreach events.

Finally, the third pillar, ‘Transnational Access’, aims at providing access for external users to hadron-therapy facilities in order to use the particles beam for research purposes, besides treatments. Beam time will be allocated to external researchers on the base of the impact of the proposed project, after evaluation by a dedicated review committee.

Keywords: hadrontherapy, cancer, radiotherapy

Acknowledgment: The ULICE project is co-funded by the European Commission under FP7 Grant Agreement N. 228436.

202

Mediators associated to the inflammatory response in prostate cancer patients undergoing RT: preliminary results

R. Valdagni¹, P. Allavena², B. Avuzzi¹, N. Bedini¹, T. Magnani¹, S. Morlino¹, S. Pesce², T. Rancati¹, S. Villa¹, N. Zaffaroni¹

¹Fondazione IRCCS Istituto Nazionale dei Tumori, Italy

²Clinical and Research Institute Humanitas, Rozzano, Italy

Purpose: A very recent ‘hot topic’ in prostate cancer (PCa) radiotherapy (RT) is the observed association between late rectal toxicity (tox) and the presence of abdominal surgery (surg) before RT. The exact mechanism is unclear. It has been speculated that previous surgery may act throughout a limitation in blood supply and/or in reducing bowel movements. The important role that cytokines play in inflammation, fibrosis, and tissue restitution has been elucidated by Okunieff et al (2008) and some investigators have even shown that the levels of inflammatory cytokines in individual animals of the same strain affects the severity of tox from animal to animal (Liang 2003). It is also well established that patients (pts) with intrinsically high inflammatory states (e.g., collagen vascular disease, autoimmune disease) are at extremely high risk of severe fibrosis after pelvic RT (Willett 2000). Thus, we could expect that the variability of these cytokines among pts might explain the wide variability of clinical tox.

Our working hypothesis was that surg may influence plasma level of inflammatory molecules and this fact might result in an enhanced radiosensitivity.

We here present preliminary results on monitoring the expression of inflammatory molecules during RT.

Material and Methods: Plasma levels of a panel of soluble mediators associated to the inflammatory response were measured in PCa pts undergoing RT. The blood was collected before starting RT (day 0), after 8Gy and after 50Gy, at the end of RT, at 1, 6 and 12 month followup. We measured 4 primary cytokines (IL-1, IL-6, IL-8, TNF), a chemokine (CCL2)

and PTX3. The expression of inflammation markers and their kinetics were correlated with pts’ characteristics.

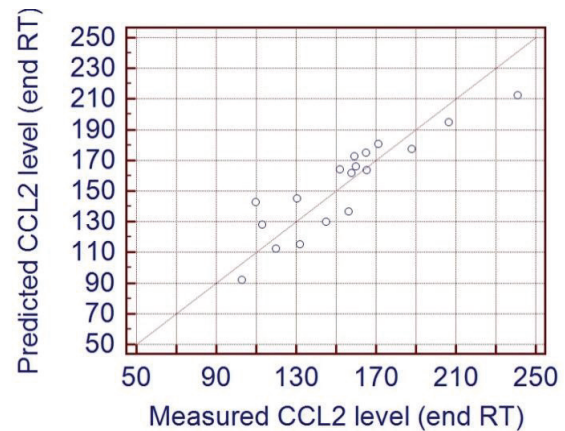
Results: 20 pts were enrolled in this preliminary evaluation. All pts were treated with IMRT at 78Gy. 3/20 pts reported grade2-3 acute rectal tox.

CCL2 was the most interesting marker showing significant increase during and after RT. Median values were: 127 (day 0), 135 (8Gy), 146 (50Gy), 158 (RT end), 143 (1month), 163 (6months) and 146 (12months), p range: 0.002-0.04.

CCL2 levels at RT end could be modelled using linear regression including the following variables: basal CCL2 (p=0.0001), age (p=0.0013), surg (p =0.03), hypertension (p=0.006) and use of anticoagulants (p=0.03), multiple correlation coefficient=0.89 (see plot).

Study of correlation between inflammation markers and acute tox was not possible, due to the low number of events.

Conclusions: This preliminary study identified a correlation between CCL2 levels at the end of RT and basal CCL2, age and surg, hypertension and use of anticoagulants, suggesting a response to RT which is modulated by pts’ characteristics. Larger accrual is needed to confirm this preliminary result and to analyse its correlation with radio-induced tox.



Keywords: Prostate cancer, radio-induced toxicity, inflammatory markers

203

Moving forward in radionuclide development in Switzerland

N. Van der Meulen^{1,2}, R. Schibli¹, A. Türler²

¹Paul Scherrer Institut, Center of Radiopharmaceutical Science, Villigen, Switzerland

²Paul Scherrer Institut, Laboratory of Radiochemistry and Environmental Chemistry, Villigen, Switzerland

Paul Scherrer Institut (PSI), recently celebrating 25 years of existence, has been the pioneer of many radiochemical and physics projects over the years. PSI produced radionuclides commercially, such as ⁸²Sr, but has since concentrated on radionuclide production for research purposes.

PSI has recently shown interest in radionuclides such as ¹⁶¹Tb [1, 2], ¹⁵⁵Tb [2, 3], ⁴⁴Sc [4], ⁶⁴Cu and ⁸⁹Zr [5] for diagnostic and therapeutic purposes, respectively. The related research is hoping to provide proof that ¹⁶¹Tb can match the therapeutic value of ¹⁷⁷Lu, while ⁴⁴Sc may be more effective in diagnosis than ⁶⁸Ga, again putting PSI at the forefront of nuclear medicine research with new radionuclidic possibilities. A mandate has recently been announced, prioritising nuclear medicine and it is hoped that the necessary funding can be acquired to upgrade the facilities in this regard.

A number of possibilities can be provided to cement the future of PSI in the world of radionuclide production: the first would be the upgrade the current target facilities to

handle an increase in beam intensity. The 72 MeV injector cyclotron currently supplies CRS with a beam intensity of 70 μA [5] and it is felt that this could be upgraded to at least 200 μA to increase production yields. A second option is the possible upgrade of another vault to handle an increase in beam intensity in an attempt to provide ^{68}Ge and ^{82}Sr to a demanding market.

With the local authorities sanctioning the construction of a technical park in the future, it is hoped that technical support, along with some private investment, will enhance the research towards new radionuclides products at PSI.

Keywords: radionuclide production, cyclotron

References:

- [1] Lehenberger S. *et al.* The low-energy beta⁻ and electron emitter ^{161}Tb as an alternative to ^{177}Lu for targeted radionuclide therapy. *Nucl. Med. Biol.* 2011; 38: 917-924.
- [2] Müller C. *et al.* A unique matched quadruplet of terbium radioisotopes for PET and SPECT and for α - and β -radionuclide therapy: An *in vivo* proof-of-concept study with a new receptor-targeted folate derivative. *J. Nucl. Med.* 2012; 53: 1951-1959.
- [3] Müller C. *et al.* Future prospects for SPECT imaging using the radiolanthanide terbium-155 - production and preclinical studies in tumor bearing mice. *Nucl. Med. Biol.* 2013; Proc. of WIPR2013.
- [4] Müller C. *et al.* Promises of cyclotron produced ^{44}Sc as surrogate for ^{68}Ga and diagnostic match for ^{177}Lu : *In vitro* and *in vivo* study of a ^{44}Sc -DOTA-folate conjugate. *J. Nucl. Med.* Submitted.
- [5] Hohn A. *et al.* Production and separation of „non-standard“ PET nuclides at a large cyclotron facility: the experiences at the Paul Scherrer Institute in Switzerland. *Q. J. Nucl. Med. Mol. Imaging* 2008; 52: 145-150.

204

Influences of aberrant mitochondrial DNA in cancer and cancer therapy

M. van Gisbergen¹, L. Dubois¹, R. Hoffmann², P. Lambin¹, H. Smeets³, A. Voets^{1,3}

¹Department of Radiation Oncology (MaastRO) Lab, GROW - School for Oncology and Developmental Biology, Maastricht University Medical Center, Maastricht, The Netherlands

²Department of Genetic Instability and Ageing, European Research Institute for the Biology of Ageing, University of Groningen, University Medical Center Groningen, The Netherlands

³Department of Clinical Genomics, GROW - School for Oncology and Developmental Biology, Maastricht University Medical Center, Maastricht, The Netherlands

Purpose: Mitochondrial DNA is mainly encoding for 13 subunits of the oxidative phosphorylation (OXPHOS) system. Since the primary OXPHOS function is aerobic ATP production, we hypothesize that OXPHOS dysfunction, through mutations and gene variations, results in decreased ATP production, increased oxidative stress, reduced DNA repair capacity and increased apoptosis, all contributing to increased normal tissue radiation toxicity.

Materials and methods: mtDNA depletion (ρ^0) of BEAS-2B cells was accomplished by culturing BEAS-2B parental cells in medium supplemented with ethidium bromide (50 ng/ml) for a minimum of 8 passages. Characterization of the ρ^0 cells was performed by fluorescent confocal imaging using mito tracker Deep Red (mitochondria) and picogreen (dsDNA) staining, and PCR. HCT116 $\text{SCO2}^{-/-}$ cells, having an OXPHOS complex IV dysfunction, were obtained from Paul Hwang. Proliferation was assessed using the IncuCyte FLR using either glucose-rich medium or ketogenic medium consisting of glucose depleted medium, additionally supplemented with 5mM lithium acetoacetate. Metabolic profiles were generated using the

Seahorse XF96. A mitochondrial stress test was established using 1 μM oligomycin, 0.6 μM FCCP and 1 μM mixture of rotenone and antimycin A. A glycolysis stress test was performed by sequential addition of 10 mM glucose, 1.0 μM oligomycin and 0.1 M 2-deoxyglucose.

Results: Our findings suggested that BEAS-2B ρ^0 cells proliferate slower in glucose-rich medium compared to BEAS-2B parental cells. In addition, they were not able to survive in ketogenic medium in which proliferation of parental cells seemed not to be affected. Cellular respiration analysis demonstrated an almost complete inhibition of ρ^0 cell mitochondrial respiration (oxygen consumption rate). Although BEAS-2B ρ^0 cells showed an increased extracellular acidification rate for glycolysis (46% of the total extracellular acidification rate, $P = 0.001$), compared with the parental cell line (21%), no spare capacity could be observed in this cell line. The glycolytic reserve of parental cell lines was 23%. On the other hand glycolytic capacity (44%) and non-glycolytic acidification (12%) were not altered ($P = 0.5422$, $P = 0.9883$) between cell lines. Additionally, in HCT116 $\text{SCO2}^{-/-}$ cells, used as a positive control, mitochondrial respiration was hampered in line with the ρ^0 cells.

Conclusions: Proliferation of BEAS-2B ρ^0 cells was reduced in regular medium and completely blocked in ketogenic medium. No mitochondrial respiration could be observed in these cells, compensated by an increased glycolysis and a loss of the glycolytic reserve. These data indicate that BEAS-2B ρ^0 are fully dependent on glycolysis to survive and that a ketogenic diet could be viable therapeutic option for tumors with mutations encoding for OXPHOS subunits. Preliminary results of our ongoing projects will be presented at the meeting.

Keywords: mtDNA, OXPHOS, Cancer

205

New insights in IGRT for prostate cancer

M. van Herk

Radiation oncology department, the Netherlands Cancer Institute / Antoni van Leeuwenhoek hospital, Amsterdam, the Netherlands

The technology of external beam radiotherapy has improved tremendously. Due to the development of advanced diagnostic imaging, tumor localization has greatly improved. The recognition of the presence of internal organ motion has led to development of image guidance. The unprecedented precision of image guidance, however, may lead to overconfidence in the accuracy of the total treatment chain. Target volume definition in general, however, remains difficult and is now by far the limiting factor in the accuracy. For delineation of the prostate capsule, the reported delineation variation is about 2 mm SD. The delineation of the dominant tumor lesion is not more accurate than that. These limits we may have to learn from our clinical mistakes. For instance, a group in Brussels found an almost 50% recurrence rate after introducing marker-based image guidance for low risk prostate cancer with a too small margin [1].

The main factors that affect the accuracy of treatment after image guidance has been implemented are: 1) uncertainties in target volume definition; 2) the quality of the surrogate (if any) used to localize the tumor. For the prostate these are in general nowadays gold markers, leaving uncertainty at the seminal vesicles and lymph nodes of treated; 3) intrafraction movement - this has studied in great detail with active marker technology; 4) movement that is too complex to be corrected by the image guidance solution. For the prostate the latter is mainly the large rotation of the gland and deformation of the vesicles. Some techniques exist for simple plan modification to correct for the large rotations but these are rarely used. Based on this overview, one can see that a

major step to improve this situation is to make sure that target volume definition is consistent and according to protocol. Then of course, pathology studies can help to improve knowledge of GTV and CTV delineation. Unfortunately, pathology investigations are generally impossible for the actual patient groups undergoing radiotherapy. However, these studies are very useful to obtain knowledge of the distribution of tumor nodes throughout the prostate, showing that prostate cancer is for this reason, data mining approaches may help to correlate e.g., local dose variations with outcome [2]. This study indicates a significant relation with outcome of dose cm's outside the prostate for high risk patients. Due to margins and beam arrangements, however, such regions often incidentally receive high doses anyway. A change in technique or margins may therefore have unexpected effects on outcome.

I conclude that, in spite of modern IGRT, there are still uncertainties that need to be covered by safety margins. The most important uncertainties relate to imaging and biology that are not corrected by IGRT. Even though PTV margins are designed to cover geometrical uncertainties, they also cover microscopic disease. Reducing margins after introducing IGRT may therefore lead to poorer outcome and should be done with utmost care (especially in higher stage disease). Physicists and computer scientists in the hospital have an important role to reduce these uncertainties.

References:

- [1] Conformal arc radiotherapy for prostate cancer: increased biochemical failure in patients with distended rectum on the planning computed tomogram despite image guidance by implanted markers. Engels B, Soete G, Verellen D, Storme G. *Int J Radiat Oncol Biol Phys.* 2009 Jun 1;74(2):388-91. Epub 2008 Dec 4.
- [2] Relating dose outside the prostate with freedom from failure in the Dutch trial 68 Gy vs. 78 Gy. Witte MG, Heemsbergen WD, Bohoslavsky R, Pos FJ, Al-Mamgani A, Lebesque JV, van Herk M. *Int J Radiat Oncol Biol Phys.* 2010 May 1;77(1):131-8. Epub 2009 Dec 11.

206

A single device for mechanical and radiation Quality Assurance measurements of medical accelerators

E. Velarde¹, I. Iordachita², Y. Mekuria³, K. Ding¹, J. Moore¹, J. Wong¹

¹Department of Radiation Oncology and Molecular Radiation Sciences, Johns Hopkins University, Baltimore, MD, USA

²Department of Mechanical Engineering, Johns Hopkins University, Baltimore, MD, USA

³Department of Radiation Oncology, University of Heidelberg, Mannheim, Germany

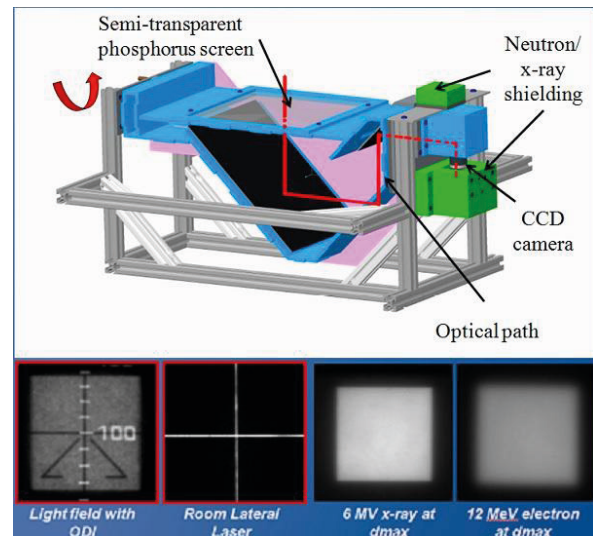
Purpose: To develop a single unifying device that will record, document and track mechanical, optical and dosimetric measurements. This will reduce the number of devices used and time spent to perform monthly and annual QA (Quality Assurance) tasks recommended in AAPM (American Association of Physicists in Medicine) Task-Group 142 Report.

Materials/Methods: This system includes a novel multi-mirror system with rotating capabilities which directs the optical and radiation sources to a stationary 1.4 megapixel camera, to acquire images of all planes centered on the isocenter. A single phosphor screen is used as the receptor for optical light imaging. A buildup sheet is added to this setup for radiation measurements. The convenience of the single setup in a single device allows us to reduce the time greatly. A computer interface will allow efficient pass/fail analysis for laser alignment, light/radiation field coincidence, flatness and symmetry tests, radiation isocenter and MLC (Multileaf Collimator) QA. In addition it will be equipped to provide

monthly reports as well as tracking tasks over any desired period of time.

Results: The system has successfully acquired novel images, such as a combination of the light field, optical distance indicator and lasers as well as radiation field. QA of mechanical motions such as table and collimator rotations is readily captured. Radiation QA measurements accommodate both x-ray and electron beams. Gantry QA can be performed by rotating the device and calculating the center of mass of the beam's intensity. This new method allows us to determine the motion of the gantry in the GT (Gun-Target) direction, which cannot be done with the standard gantry star shot. The time spent in Monthly QA according to Task-Group 142 for these tasks is reduced in half.

Conclusion: A single device has been successfully developed to unify all mechanical, optical and radiation components for required and recommended monthly QA tasks, reducing monthly machine maintenance time. The system has also been used to find the radiation isocenter and can be used for commissioning of new medical accelerators. In particular, the device records, documents and tracks optical measurements that are now only evaluated visually which will strengthen the confidence for safe patient treatment.



Keywords: QA Linear Accelerators

207

An Intensity Modulated Radiotherapy Beam Monitoring System using a Monolithic Active Pixel Sensor

J.J. Velthuis¹, R.F. Page¹, R.P. Hugtenburg², S.W. Blake³, D. Crawford³, S. Fletcher³, M. Saunders³, P.H. Stevens³

¹University of Bristol, UK

²Swansea University, UK

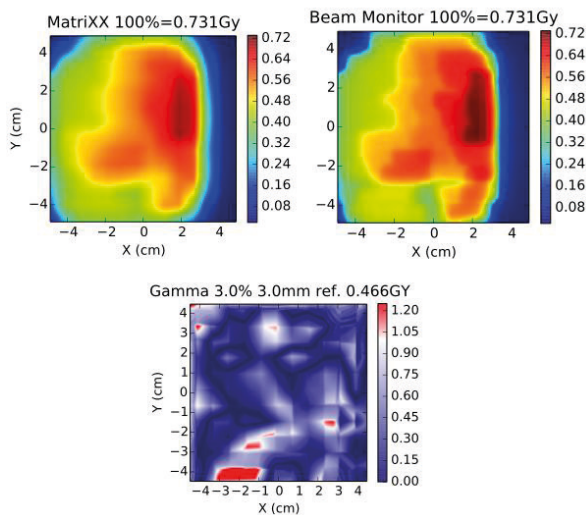
³University Hospitals Bristol, UK

Intensity Modulated Radiotherapy (IMRT) is becoming a commonly used radiotherapy technique for the treatment of solid malignant tumors. Treatment fields can be complex and are produced using Multileaf Collimators (MLC) with moving leaves. Currently the only beam monitoring is from internal systems in the linac themselves, with new independent dosimetry systems starting to emerge. These independent systems include upstream dosimeters, portal imaging devices and dosimeters fixed to the patient. The device presented here is an upstream detector. The main issues with using an upstream device are the attenuation of the beam and the surface dose caused by the generation of secondary particles. To minimize these effects such a device should be as thin as possible. Monolithic Active Pixel Sensors (MAPS) with inbuilt

amplification in the pixel make this feasible, and have thicknesses less than 50 μm . The work presented here shows the progress made towards an upstream beam monitor and dose verification system based on a MAPS camera device.

The Achilles MAPS camera was operated at 10 frames per second and mounted to an Elekta SL22 6MV linac head with either Gafchromic film or the MatriXX 2D ionization chamber array, used for MLC leaf position and dose verification, placed below. The film was positioned at 98.5 cm SSD with 1.5 cm of water equivalent buildup and the MatriXX at 95 cm SSD with 5 cm buildup. A series of exposures were then administered with different sequences of fields to allow both MLC position reconstruction and dose calculations to be performed. The reconstruction of the MLC position was based on a feature extraction technique that employs a Sobel kernel. The final position was then extracted from a linear fit to a contour that represents the mean point of the maximal intensity change in the image. The dose is extracted using a Monte-Carlo (MC) simulation of the linac head with 1 mm material upstream of the detector. The photon energy fluence was obtained by subtracting a Monte Carlo calculated charged particle signal. The fluence is converted to dose in the phantom using a pencil beam method. The results presented are for a small clinical IMRT beam.

The MLC position reconstruction was in excellent agreement with the film measurement, with the film error dominating the comparison. The resolution of the MLC reconstruction was $52 \pm 4 \mu\text{m}$ for a single frame. The dose measurement using the Achilles agreed well with the MatriXX, with a comparison using the gamma index giving a 97% pass rate for 3%/3mm, as shown in the figure.



These results demonstrate a working prototype upstream MAPS based dosimeter, which is able to extract both the dose and the MLC positions. The next stage is to push towards real-time application of these techniques for both IMRT and VMAT treatments.

Keywords: IMRT, MAPS, Real-time Beam Monitoring

Acknowledgements: The research presented here is funded by the National Institute for Health Research (NIHR) Invention for Innovation (i4i) Programme.

208

The ART of translation

M. Verheij

Department of Radiation Oncology, The Netherlands Cancer Institute, Amsterdam, The Netherlands

Translational research refers to the transfer of a new scientific concept from its basic preclinical stage to a successful clinical application. This process is bidirectional as clinical results should also be used to re-evaluate and improve their underlying experimental models. An inherent element of translational research is the use of patient material. This should, however, be interpreted widely and not be restricted to biological material. In fact, all information derived from patients - including digital and epidemiological data - is suitable for translational research. Acknowledging translational research as an essential tool to advance oncology, many research groups and funding organizations focus on this area.

NKI is a comprehensive cancer center combining hospital and research laboratories under one roof in a single independent organization with one board of Directors responsible for both clinic and research. The institute has a long tradition of integrating basic science and cancer care, and has developed several strategies to accommodate translational research since its foundation in 1913 [1]. NKI stimulates part-time research appointments of staff clinicians by “twinning” them to basic scientists on joint translational projects. A translational research fellowship program offers to young clinicians after completion of their specialty training, a 2-3 years fellowship in basic research labs to build-up their oncology careers. In addition, internal start-up funding is provided to generate preliminary data and support project proposals. Furthermore, all clinical trial proposals are screened for potential translational research elements. A Translational Research Board, consisting of staff MDs and PhDs with a track record in translational research, coordinates these activities.

Although many regard translational oncology as an interplay between fundamental biological and clinical research, this is certainly not a complete description. In radiation oncology, translational research includes many other areas of “basic” research, such as molecular biology, bioinformatics, imaging, software development, epidemiology and physics. The department of Radiation Oncology at NKI has structured its translational physics research activities in multidisciplinary groups to ensure an optimal two-way interaction between clinicians and physicists and to provide a discussion forum for linking relevant clinical questions to innovative solutions. The software development for image-guided CT-based position verification integrated with the linear accelerator represents an apposite example [2] and has been essential for Adaptive RadioTherapy, the latest piece in art of modern radiotherapy. Building on the practice-changing studies on the interaction between cisplatin and radiation in tumor and normal cells [3] and new insights in molecular effects of radiation [4], biology-driven translational research is facilitated at the departmental level by resident-PhD programs, combined clinical-research appointments and focused start-up funding.

Together, these elements form the “NKI model” of integrated basic and clinical research and provide a stimulating environment for translational radiotherapy.

References:

- [1] www.historad.nl/en
- [2] Sonke *et al.* Med Phys. 2005
- [3] Schaake-Koning *et al.* N Eng J Med. 1992
- [4] Verheij *et al.* Drug Resist Updat. 2010

209

Clinical experience with adaptive radiotherapy for muscle bladder cancer

A. Vestergaard¹, M. Hoyer², M.B. Ellegaard², J. Søndergaard², U.V. Elstrøm², J.B. Petersen¹, L.P. Muren¹

¹Department of Medical Physics, Aarhus University Hospital, Denmark

²Department of Oncology, Aarhus University Hospital, Denmark

Purpose: Large changes in bladder shape and size during a course of radiotherapy (RT) make adaptive RT (ART) appealing in treatment of muscle invasive bladder cancer. We are running a two-center clinical trial of ART for bladder cancer where the primary aim of the trial is to reduce gastro-intestinal morbidity due to sparing of the bowel and the rectum. We here report on initial clinical experience and outcome of this trial.

Materials/methods: The present study reports preliminary results on the first nine bladder cancer patients included in the ART trial. All patients received 60 Gy in 30 fractions to the bladder; in four patients the pelvic lymph nodes received 48 Gy simultaneously. Patients were set-up by use of cone-beam CT (CBCT) guidance and treatment was delivered by volumetric modulated arc therapy (VMAT). In our ART strategy, the first five fractions were delivered using large non-adaptive margins - the bladder contours from the CBCTs acquired prior to the first four fractions were used to create a library of three plans corresponding to a small, medium and large size bladder. DVHs for organs at risk were calculated by summation of the selected plans calculated on the planning CT and compared to our previous standard non-adaptive RT plans involving population-based margins.

Results: The frequency of which the small and medium size plans were selected was equal, whereas the large size plan was used on less than 27% of the (total of 225) plan selection fractions. The median rectal volume receiving 50 Gy or more was 5% [0-41%], compared to 17% [0-62%] if the patients had been treated with standard, non-adaptive RT. For the bowel cavity, the median volume receiving more than 45 Gy was 269 cm³ [83-486 cm³], compared to 337 cm³ [126-553 cm³] if not treated with adaptation. No grade 3-4 gastro-intestinal morbidity was observed.

Conclusion: Daily adaptive plan selection in RT of bladder cancer results in a considerable normal tissue sparing, and is expected to reduce the risk of gastro-intestinal morbidity.

210

ENTERVISION WP4. Biological Dosimetric Phantom. Proof of Concept Preliminary results

T. Viana Miranda Lima¹, M. Dosanjh¹, A. Ferrari¹, A. Mairani², F. Marchetto³, K. Ricketts⁴, G. Royle⁴

¹CERN

²CNAO

³INFN

⁴UCL

Development of clinical treatment protocols for radiation therapy is dependent on the availability of information on the biological efficacy of radiation doses. In order to gain robust data, multiple cell irradiation experiments must be performed at different dose points, using a range of cell lines. Therefore, it is important to be able to verify the biological effects of complex dose distributions in homeomorphic phantoms, alongside

measurements of physical dose. One of the ENTERVISION projects focuses on the development of a biological dosimetric phantom. Firstly, the phantom and desired set-ups were evaluated then its suitability for radiobiology studies were assessed during a set of cell irradiations. Status: The phantom was irradiated mimicking the patients' pathway starting with the CT scan, followed by treatment planning and being irradiated. For the irradiation, a uniform dose distribution was delivered with a proton beam and the process was repeated using a carbon ion beam. The dose was measured from pinpoint ionisation chambers readings and the uniformity was assessed with radiochromic films. The experimental results were compared with the TPS and Monte

Carlo calculations. Using MC simulations it was also investigated how the simulation of a more detailed geometry would affect the obtained results. From the radiobiology studies the cell survival by analyzing its proliferation was studied. Results: The calculated mean deviation was below 2% for both beams used. This brings the result within the acceptance threshold as desired by CNAO QA procedures. Conclusion: The experimental results obtained showed good agreement with both TPS and Monte Carlo simulations. The next step will involve a full radiobiology study with different biological inputs.

Keywords: Ion beam therapy, radiobiology, dosimetry

211

Realistic on-the-fly dose calculation for low energy X-rays Intra-Operative Radiation Therapy

M. Vidal¹, P. Guerra², E. Herranz¹, P. Ibáñez¹, J.M. Udías¹

¹Grupo de Física Nuclear, Dpto. Física Atómica, Molecular Nuclear, UCM, Madrid, Spain

²Department of Electronic Engineering, ETSIT, Universidad Politécnica de Madrid, Madrid E-28040 Spain

Purpose: The aim of this work was to develop a new algorithm to compute dose from a mobile accelerator of low energy X-rays Intra-Operative Radiation Therapy (XIORT) (ex: INTRABEAM®, Carl Zeiss) in heterogeneous conditions, such as a patient 3D volume, within 2-3 seconds. XIORT needs accurate and fast dose calculation. In this work a hybrid Monte Carlo tool is developed which takes into account all the components of the XIORT X-rays up to 50 keV and predicts in a satisfactory way the dose delivered to the patient. The tool is being included in Radiance® from GMV [1], a powerful Treatment Planning System for IORT.

Materials and methods: A few analytical algorithms exist which only consider the primary x-ray beam [2]. A hybrid Monte Carlo code which takes into account the photoelectric and the Compton effects for X-rays up to 50 keV, was developed to compute dose in 3D-CT volumes. Full Monte Carlo simulations have been generated with penEasy to validate our tool in homogeneous and heterogeneous conditions [3]. For the spherical applicators (from 0.75 cm to 2.5 cm radius) and the needle, a genetic algorithm was employed to determine the energy spectra which reproduce the measured dose distribution in water. Once the energy spectrum is obtained, it is implemented in the hybrid Monte Carlo algorithm. The absorbed dose distributions were then simulated in water and heterogeneous media both with penEasy and the hybrid Monte Carlo algorithm for the spherical applicators and the needle.

Results: The energy spectra for all the spherical applicators and the needle are similar to energy spectra from other Monte Carlo studies and measurements [4]. Dose distributions computed by the fast hybrid Monte Carlo tool are in a good agreement with penEasy full simulations in water and heterogeneous media. The algorithm gives also a good prediction of the measured dose distribution in water, and comparison to measured data in heterogeneous phantoms is being carried out. Computation time is below 5 seconds in a single core of a modern PC.

Conclusions: The hybrid Monte Carlo algorithm is a fast and robust tool to compute dose distributions in a patient geometry. It is being implemented in the Intra-Operative Radiation Therapy Treatment Planning System Radiance® from GMV, and can be used for any XIORT system.

Keywords: Intraoperative radiotherapy, Monte Carlo simulations, dose calculation

References:

[1] J. Pascau, *et al.* 2012. Int. J. Radiat. Oncol. Biol. Phys. 83(2), 287-295.

- [2] M. A. Ebert *et al.* 2003. *Med. Phys.* 30(9), 2424-2431.
 [3] J. Sempau, *et al.* 2011. *Med. Phys.* 38(11), 5887.
 [4] S. Clausen, *et al.* 2012. *Z. Für Med. Phys.* 22(3), 197-204.

212

The SMAC-mimetic Debio 1143 efficiently enhanced radiotherapy in head and neck squamous cell carcinoma models

D. Viertl¹, J. Bourhis¹, L. Kadi², O. Matzinger¹, S. Rigotti², M.-C. Vozenin¹, G. Vuagniaux², C. Zanna²

¹Lausanne University Hospital, Lausanne, Switzerland

²Debiopharm SA, Lausanne, Switzerland

The small molecule Debio 1143 (D1143) is an orally-active, SMAC-mimetic designed to promote apoptosis in tumor cells by blocking the activity of inhibitor of apoptosis proteins (IAPs). This study aimed to test the efficacy of D1143 as a single agent or in combination with radiotherapy (RT) in head and neck squamous cell carcinoma (HNSCC) models.

The effect of D1143 was assessed by the colony forming assay on a panel of HNSCC cell lines. Tumor cells were incubated at various concentrations of D1143 and treated with increasing doses of radiation. The number of surviving colonies was then recorded and compared to an untreated group. In parallel, various treatment sequences were tested, (before, during or post-irradiation) to determine the effect of D1143 on primary apoptosis (early, pre-mitotic apoptosis) and secondary apoptosis (late, post-mitotic reproductive cell death). The *in vivo* radiosensitizing effect of oral treatment with D1143 was further evaluated in nude mice bearing HNSCC tumor xenografts.

D1143 alone selectively inhibited colony formation of several cell lines. In addition, combination experiments found D1143 to be highly effective in enhancing cell death induced by RT. A synergistic effect of D1143 was observed in the majority of the tested cell lines treated by RT. Interestingly, the radiosensitizing effect of D1143 was preeminent when cells were co-incubated with D1143 24 hours after irradiation, showing that D1143 efficiently impacts late apoptosis due to mitotic catastrophe and/or other cell death events that arise after irradiation.

In mice bearing HNSCC radio-resistant tumors, D1143 given orally in combination with RT delayed the tumor growth for more than 40 days when compared to RT.

These results show that D1143 exhibits activity as a single agent and can potentiate the effects of radiotherapy in HNSCC models indicating that D1143 has a promising therapeutic potential for the treatment of HNSCC.

Keywords: SMAC-mimetic, radiosensitization, IAP inhibitor

213

Radiosensitizing effect of a RasGAP derived peptide on cell survival in human cancer cells *in vitro* and *in vivo*

D. Viertl¹, A. Annibaldi², O. Matzinger¹, M.-C. Vozenin¹, C. Widmann², J. Bourhis¹

¹Radiation Oncology, Lausanne University Hospital, Lausanne, Switzerland ;

²Physiology, University of Lausanne, Lausanne, Switzerland

In this study we used TAT-RasGAP₃₁₇₋₃₂₆, an engineered peptide derived from RasGAP and we studied its radiosensitizing properties *in vitro* on cell survival and proliferation of several human cancer cells and *in vivo* on tumor growth of xenograft tumors in mice.

Clonogenic assays with 4 human cancer cells (PANC-1, HCT116 p53^{+/+}, HCT116 p53^{-/-}, and HeLa) and a non tumorigenic cell line (HaCaT) were performed. Cells were exposed to 0, 1, 2 and 4 Gy with or without 20 µM TAT-RasGAP₃₁₇₋₃₂₆.

TAT-RasGAP₃₁₇₋₃₂₆ radiosensitizing effect was also tested in tumor xenograft mouse model. During 10 days, mice bearing

subcutaneous HCT116 (WT or p53 mutant) tumors received every day 1.65 mg/kg TAT-RasGAP₃₁₇₋₃₂₆ i.p. injected and were locally irradiated with 3 Gy.

At all the tested radiation doses TAT-RasGAP₃₁₇₋₃₂₆ showed a significant supra-additive radiosensitizing effect on all the tested tumor cell lines. By combining radiation and TAT-RasGAP₃₁₇₋₃₂₆ the cell surviving fraction at 2 Gy was decreased by a factor ranging from 2.1 to 3.8-fold. Without radiation TAT-RasGAP₃₁₇₋₃₂₆ had no effect on cell survival and proliferation. Furthermore, TAT-RasGAP₃₁₇₋₃₂₆ showed no sensitizing effect on the non tumorigenic cell line exposed to radiation.

In vivo, TAT-RasGAP₃₁₇₋₃₂₆ also induced a significantly radiosensitizing effect as shown by a significant higher reduction in tumor volume as much as by a significant tumor growth delay. Combination of TAT-RasGAP₃₁₇₋₃₂₆ and radiotherapy allowed to delay the tumor volume growth by 10 days in HCT116 p53^{+/+} tumors and by 34 days HCT116 p53^{-/-} tumors compared to the group of mice that received only radiotherapy. Like *in vitro* TAT-RasGAP₃₁₇₋₃₂₆ had no effect on tumor volume if not combined with radiotherapy.

Results showed that TAT-RasGAP₃₁₇₋₃₂₆ has a radiosensitizing effect on *in vivo* and *in vitro* cancer cells without any notable effect on healthy tissues. Therefore TAT-RasGAP₃₁₇₋₃₂₆ should be considered as a novel and attractive radiosensitizer compound.

Keywords: RasGAP, peptide, radiosensitizer

214

NOTCH and radiotherapy: does it matter?

M. Vooijs, V. Sosa Iglesias, R. Habets, J. Theys

Dep Radiation Oncology, Maastricht, The Netherlands

Purpose: Patients with advanced NSCLC have 5 year survival rates of less than 15 %. The NOTCH pathway plays an important role during lung development and physiology and is often deregulated in NSCLC. Notch inhibitors are being widely tested in clinical trials however information on the efficacy of Notch inhibition in combination treatments remains understudied. Here we investigated the prognostic and predictive impact of NOTCH signaling in human NSCLC in preclinical mouse models and *in vitro* in human and murine (KRAS/P53 GEMM) NSCLC cell lines.

Material & Methods: The expression of Notch receptors, ligands and target genes was investigated in 90 patients with early stage NSCLC and correlated with disease-free survival. Human and murine NSCLC with overexpression or attenuation of the Notch pathway were used *in vitro* and to generate xenograft tumors to investigate the role of Notch signaling in tumor progression and response to radiation therapy. The role of Notch signaling in hypoxia tolerance, radio-sensitivity and chemo-sensitivity was assessed *in vitro* and *in vivo*. Tumor perfusion, hypoxia and proliferation were analyzed in xenograft tumors and correlated to NOTCH signaling activity.

Results: Patients with high NOTCH activity in tumors showed significantly worse disease-free survival. Ectopic NOTCH1 activation did not affect the proliferation or intrinsic radio-sensitivity of NSCLC cells *in vitro*. In contrast, tumors with blocked NOTCH activity grew slower than wild type tumors while tumors with high NOTCH1 activity grew significantly faster were more hypoxic and radio-resistant. Results will be presented on the possible mechanisms by which NOTCH signaling contribute to radiation and chemo-resistance.

Conclusions: We conclude that NOTCH signaling plays an important role in NSCLC growth and response to therapy. Further knowledge into the mechanism of therapy resistance may provide improved intervention schedules/combinations if NOTCH inhibitors are applied in combination with standard of care treatment.

Keywords: notch, radiotherapy, hypoxia

215

Novel strategies to spare normal tissues from radiation damageM.-C. Vozenin*CHUV, Swiss Cancer Center of Lausanne, Departement d'Oncologie, Laboratoire de Radio-Oncologie, CH-1011 Lausanne*

Since decades, radiation oncologists are aware and concerned of the toxicities induced at the normal tissue level by anti-cancer treatment including radiation therapy. Today this question has gained much interest as the number of long-term cancer survivor is increasing. Several axis of research have been developed to improve further the therapeutic ratio of radiation therapy and avoid or reverse normal tissue complications. These therapeutic strategies are mostly targeting molecular pathways involved in the pathogenic crosstalk between epithelial, inflammatory, vascular and mesenchymal compartment but novel strategies are emerging. Our previous pre-clinical experiments demonstrated the anti-fibrotic benefit of Rho/ROCK inhibition using Pravastatin, thus providing the biological rationale for a phase II clinical trial currently ongoing. The first results are encouraging and show benefit in a subgroup of patients. In follow up studies, we investigated the relevance of two regulators of Rho activation, the two GEF: Epac 1 and Epac 2 (Exchange protein activated by cAMP) in radiation-induced cardiac toxicity and identified Epac-1 as a novel regulator of radiation-induced hypertrophy and amyloidosis but not fibrosis in the heart. Then, due to their critical biological roles in fine tuning cellular and tissue homeostasis, we investigated the possible involvement of microRNAs by molecular profiling and showed robust induction of miR-210. Furthermore, we showed that miR-210 overexpression was repressed by anti-fibrotic treatment and direct miR-210 inhibition exerted an anti-fibrotic action by itself through reduction of extracellular matrix gene expression. Lastly, we decided to modify radiotherapy procedure by itself and used hypo-fractionated radiotherapy delivered at ultra-high dose rate (FLASH, >50Gy/s). Interestingly, when applied to various preclinical models (lung, hematopoietic, brain in mice) FLASH radiotherapy induced a major differential effect, protecting normal tissues from radiation-induced toxicity while maintaining the anti-tumor action. The mechanisms involved in this differential effect are currently investigated.

Keywords: normal tissue toxicity

216

A novel dual-modality optical tomography and x-ray system for small animal radiation research platformK.K.-H. Wang¹, Y. Yang¹, S. Eslami², I. Iordachita², M.S. Patterson³, J.W. Wong¹¹*Department of Radiation Oncology and Molecular Radiation Sciences, Johns Hopkins University, USA*²*Laboratory for Computational Sensing and Robotics, Johns Hopkins University, USA*³*Department of Medical Physics and Applied Radiation Sciences, McMaster University, Canada*

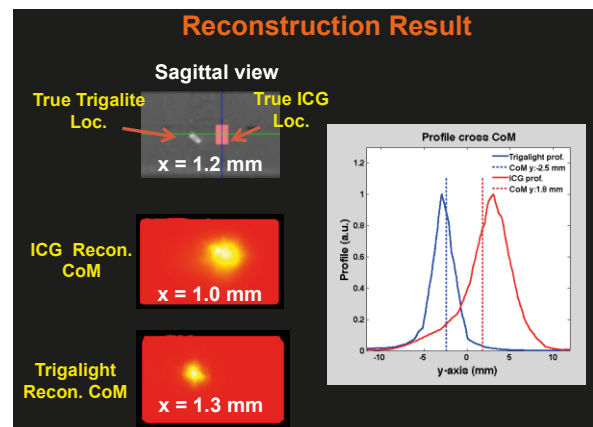
Purpose: A novel, low cost, and integrated optical tomography and x-ray system was designed and built for the small animal radiation research platform (SARRP) to provide soft tissue guidance as well as to support highly sensitive functional imaging. Our system is able to perform dual color, bioluminescence (BLT) and fluorescence tomography (FLT), images simultaneously, providing a complementary optical image modality and therefore extending radiobiological applications.

Materials & Methods: The CBCT/BLT/FT system was designed and tested in a standalone form. An optical homogeneous

phantom, in half cylindrical geometry, was placed on a rotation stage. A solid self-illuminated bioluminescence source, Triglighthouse[®], and liquid fluorescence agent, indocyanine green (ICG), were placed inside the pre-drilled holes in the phantom. Prior to the optical imaging acquisition and to simulate *in vivo* situation, the CBCT was conducted to provide geometry information and improve the optical reconstruction accuracy by limiting the solution space. The bioluminescence signal was taken at multiple wavelengths ranging from 550 to 650nm to improve the reconstruction source positioning accuracy. An optical fiber is placed at center position of the phantom to excite ICG. A mirror system capable of 90degree rotation around the object reflects the optical signal to the CCD camera.

Results: The figure shown below illustrates the true location from the CBCT, and the corresponding reconstructed Triglighthouse and ICG image at the sagittal view. The center of mass (CoM) for ICG and Triglighthouse can be reconstructed within 0.3mm at sagittal plan. The reconstructed ICG (red) and Triglighthouse (blue) profiles versus y-axis, passing through the two sources, are also shown below. The blue and red dash lines indicate the CoM position of the Triglighthouse and ICG, respectively. The true separation between the two sources is 5mm versus our reconstructed result 4.3mm.

Conclusions: We expect that this novel dual color system specially designed for SARRP will not only provide soft-tissue radiation delivery guidance but also present new opportunities for pre-clinical radiation research.

**Keywords:** Diffusive optical tomography, small animal radiation

217

Host and Tumor Immunity: Local and Systemic Opportunities to Enhance Tumor Curability by RadiotherapyR.R. Weichselbaum*M.D. Department of Radiation and Cellular Oncology, Ludwig Center for Metastases Research, University of Chicago Medicine, USA*

Success of radiation treatment depends on intrinsic properties of tumor cells, involvement of the host immune system and the crosstalk between tumor and host cells in primary and secondary (metastatic) sites. During the last decade our laboratory has investigated the role of these interactions in the ability of radiotherapy to eradicate primary tumors and metastatic disease. In the current presentation we will focus on host factors which interact with ionizing radiation (IR). The results of our studies using genetic models and specific immunological probes have identified CD8⁺ cytotoxic T cells, professional antigen presenting cells (CD11c⁺ dendritic cells), local production of

TNF α by tumor infiltrating lymphocytes (TILs), and host Type I Interferons (IFNs) as required for successful treatment by radiation^{1,2}. Transformation of the tumor microenvironment into an “immunological hub” to suppress local and distant disease is a tantalizing goal for which radiotherapy might be well suited, especially in combination with immunotherapy. Our group has recently demonstrated that the combination of radiotherapy and anti-PD-L1 antibodies decrease accumulation and function of myeloid derived suppressor cells (CD11b, Gr1+) through enhanced local production of TNF α by tumor infiltrating lymphocytes (TILs). In experimental systems^{3,4} The capacity of local radiotherapy to augment the activation TILs and drive cytokine production is, in part, due to the ability to increase tumor antigen cross-presentation by professional antigen presenting cells in the tumor stroma. Our group demonstrated host type I IFNs are essential for enhanced tumor antigen cross-presentation following radiotherapy. The critical role of type I IFNs in the host immune response to radiotherapy positions them as central components in the crosstalk between tumor cells and the host that can exert positive or negative influences depending on the context. In particular, the interaction of tumor cells with the host leads to the selection of clones resistant to the cytotoxic effects of IFNs and radiotherapy. Using transcriptomic approaches we identified a set of Interferon Stimulated Genes (ISGs) associated with tumor radioresistance.⁵ This gene set was identified in different types of primary tumors (lung, prostate, breast and glioblastoma) and termed the Interferon Related DNA Damage Signature (IRDS). Statistical training of this gene set detected a 7 gene signature which predicted response to adjuvant radio/chemotherapy for some women with breast cancer⁶. The IRDS is prognostic for patients with subsets of glioma and prostate cancer. We propose that these data indicate the presence of pro-survival genes in the IFN/Jak/Stat axis, which has been confirmed recently through a genomics approach. The Jak-Stat pathway is currently under investigation as a potential therapeutic target for radio-chemosensitization in different tumor types. Our current approaches are directed towards identification of tumor ISGs with pro-survival/radioprotective functions. These results demonstrate the requirement to investigate both tumor and the host to improve the therapeutic ratio in radiotherapy.

References:

- [1] Lee Y. et al. Therapeutic effects of ablative radiation on local tumor require CD8+ T cells: changing strategies for cancer treatment. *Blood* 114, 589-595 (2009)
- [2] Burnette BC et al. The efficacy of radiotherapy relies upon induction of type1 interferon-dependent innate and adaptive immunity. *Cancer Res.* 71, 2488-2496 (2011).
- [3] Liang H., Deng L, et. al. Radiation-induced equilibrium is a balance between tumor cell proliferation and T cell-mediated killing. *J. Immunol.* 2013; 190(11):5874-81
- [4] Deng LF. et. al. Radiation and PD-L1 blockade induce T-cell mediated depletion of myeloid-derived suppressor cells and tumor regression. *J. Clinical Investigation* (In Press) 2013.
- [5] Khodarev NN et. al. STAT1 is overexpressed in tumors selected for radioresistance and confers protection from radiation in transduced sensitive cells. *Proc. Natl. Acad. Sci. USA* 101: 1714-1719, 2004.
- [6] Weichselbaum RR et. al. An interferon-related gene signature for DNA damage resistance is a predictive marker for chemotherapy and radiation for breast cancer. *Proc. Nat. Acad. Sci. USA* 105(47):18490-18495, 2008.

218

The doorway to high specific activity of ^{195m}Pt

D. Wilmsen¹, A. Blanc², M. Jentschel², U. Köster², P. Mutti², T. Soldner², W. Urban², G. de France³, G. Simpson⁴, C. Ur⁵, D. Habs⁶, J. Jolie¹, K. Moschener¹, T. Thomas¹

¹Institute of Nuclear Physics Cologne (IKP), Germany

²ILL Grenoble

³GANIL Caen

⁴LPSC Grenoble

⁵LNL Legnaro

⁶LMU Munich

Purpose: Recently an alternative production method for the platinum isomer ^{195m}Pt by resonant (γ, γ') photo-excitation induced by intense monochromatic gamma beams was proposed [1]. This method relies on a suitable ‘doorway state’ linking the low spin ground state with the isomer. The selective population of this isomer is of special interest as it shows unique properties for diagnostic and therapeutic purposes in nuclear medicine, especially in the treatment of cancer. ^{195m}Pt has a half-life of 4 days. It emits X-rays (66 keV and 76 keV) as well as gamma rays (99 keV) useful for SPECT imaging. Thus, including ^{195m}Pt into a Pt-compound enables imaging of the biodistribution of this compound with SPECT or gamma cameras. One benefit for the use of ^{195m}Pt refers to the frequently used platinum based chemotherapeutics like cis-platin or carbo-platin. Here, ^{195m}Pt could offer a useful tool to assess the tumor cells’ uptake during the chemotherapeutical treatment.

In addition ^{195m}Pt also emits an abundant amount of Auger and conversion electrons which can be used therapeutically as their energy is deposited in a very short range (few μm to tens of μm) which concentrates the decay energy on single targeted cells.

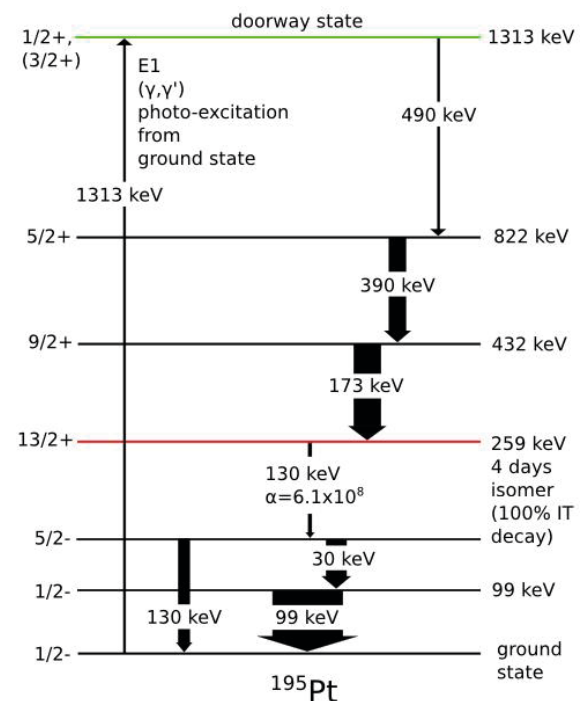


Figure: Schematic partial level scheme illustrating the selective population of the isomeric ^{195m}Pt via photo-excitation from the ground state.

Materials/methods: In November 2012 we performed a neutron capture experiment in the frame of the EXILL campaign at the Institut Laue-Langevin (ILL) by using a detector array consisting of 46 High Purity Germanium

(HPGe) detector crystals. A sample of 96% enriched ^{194}Pt was placed in the intense cold neutron beam in order to investigate the nuclear structure of ^{195}Pt via the reaction $^{194}\text{Pt}(n,\gamma)^{195}\text{Pt}$. With coincidence and angular correlation measurements the level scheme and the spins and parities of excited states ^{195}Pt were studied. Special regard was given to pathways populating the isomer.

Results: We found a 'doorway state' in ^{195}Pt at an excitation energy of 1.313 MeV which is populating the isomer ^{195m}Pt and, in addition, decays directly into the ground state fulfilling the requirements for gamma ray induced activation of ^{195m}Pt . Moreover we could observe other promising γ -transitional pathways leading to the isomer.

Conclusions: Radioisotopes play an important role in nuclear medicine. ^{195m}Pt with high specific activity offers suitable properties for diagnostics and therapeutic treatment of cancer. The newly observed 'doorway state' is a prime candidate for production of high specific activity ^{195m}Pt by selective photo-excitation reactions.

Keywords: doorway state, ^{195m}Pt , photo-excitation

References:

[1] D. Habs, U. Köster, Appl. Phys. B 103, 501-519 (2011)

219

Inhibition of tumour growth using the small molecule Cathepsin L inhibitor, KGP94

T. Wittenborn, M.R. Horsman

Department of Experimental Clinical Oncology, Aarhus University Hospital, Denmark

Purpose: The protease family known as the cathepsins are known to play an important role in tumour progression, invasion and angiogenesis. The present study evaluated the effects on growth delay of the cathepsin L inhibitor KGP94 in two different murine tumour models.

Materials and methods: Male CDF1 or C3H/HeNsd mice were inoculated on the right rear foot with a C3H mammary carcinoma or a SCCVII carcinoma, respectively. A solution of KGP94 was prepared by dissolving in a mixture of 10% Tween 80 and 90% HEPES-buffer. KGP94 solution was intraperitoneally injected at 0.01ml/g mouse bodyweight. To obtain the optimal anti-tumour treatment for the KGP94 compound, various doses (from 1-20mg/kg) were administered to mice for different periods (1-20 days) after tumour implantation; KGP94 was generally injected once/day but in one series it was given thrice daily on days 1-5. Tumour response was assessed by determining the tumour growth time, which was the time in days to reach a tumour volume of 500mm³ (TGT₅₀₀). Results are listed as Mean (\pm SEM). One-way ANOVA comparison of group means was performed, and a P<0.05 was considered significant.

Results: The TGT₅₀₀ for control animals was 18.0 days (\pm 0.3) for the C3H mammary carcinoma and 13.6 days (\pm 0.7) for the SCCVII carcinoma. Mice treated with KGP94 from days 1-5 showed significant tumour growth delay for both tumour models when doses were at 10.0 mg/kg or higher; at 5.0 mg/kg the C3H mammary carcinoma had a significantly increased TGT₅₀₀, whereas the SCCVII carcinoma did not. When KGP94 was administered in doses below 5.0 mg/kg neither of the tumour models showed significant growth delay. Additional experiments in the C3H mammary carcinoma model showed that treatment for 5 days was just as effective as treatment for 20 days, and that no additional growth delay was observed when increasing the number of treatments/day from one to three.

Conclusion: KGP94 significantly delayed tumour growth in the C3H mammary carcinoma model, and worked best when given directly after inoculation of tumour material. This suggests that KGP94 may have a more significant role in inhibiting metastatic development rather than influencing

the growth of established tumours. Significant growth delay was also observed in the SCCVII tumour model, however, it occurred with higher doses of KGP94 compared to the C3H mammary carcinoma. This could be explained by the more aggressive nature of the SCCVII tumour model (low TGT₅₀₀ when compared to C3H).

Keywords: Cathepsin inhibitor, Growth delay, Treatment optimization

Acknowledgements: Supported by The Danish Cancer Society, The Danish Council for Independent Research: Medical Sciences, and OXiGENE Inc.

220

Advancing the small animal radiation research platform for pre-clinical radiation research

J. Wong¹, P. Kazanzides², I. Iordachita², R. Jacques², N. Cho², S. Eslami², E. Velarde¹, K. Wang¹, T. McNutt¹

¹Department of Radiation Oncology and Molecular Radiation Sciences, Johns Hopkins University School of Medicine, Baltimore, USA

²Center for Computer Integrated Surgical Systems and Technology, Johns Hopkins University Whiting School of Engineering, Baltimore, USA.

Purpose: A new generation of advanced pre-clinical radiation systems is now available commercially with on-board cone-beam CT (CBCT) to guide the focal irradiation of targets in small animals using robotically controlled gantry and couch motions. Radiation can be directed to a target in an animal to within 0.2 mm accuracy. Many radiation experiments involving small radiation beams have been performed and would not be feasible previously. Continuing technical advances are being made.

Methods: For the small animal radiation research system (SARRP), a three dimensional (3D) treatment planning system (TPS) has been developed. The superposition-convolution (SC) algorithm is adopted and significantly modified for dose calculations at the kilovoltage x-ray energies. Dose calculation with heterogeneity correction is performed on a graphical processing unit. X-ray phase spaces for 21 mono-energetic bins representing the 220 kVp source spectrum are cast for dose calculations in the animal at a voxel resolution of 0.2 mm. Dose calculation for a volume consisting of 384 x 256 x 256 voxels is completed in 4 sec. Material dependent correction factors are used to allow the calculation of dose to water or dose to the medium at the point of interest. The TPS is integrated with the 3D Slicer-4 navigation platform for imaging, animal positioning and irradiation operations of the SARRP. A new double-focusing variable collimator allows any rectangular beam setting up to 4 cm x 8 cm. Finally, the SARRP is extended to incorporate on-board bioluminescence and fluorescence tomographic imaging. A novel rotating 3-mirror arrangement supports multiple projection imaging with a stationary CCD camera. The optical imaging subsystem with its light tight housing is installed on a mobile cart for docking with the gantry of the SARRP when needed.

Results: Validations in phantoms consisting of water, cork, graphite and aluminum inhomogeneities show agreement with radiochromic film (water) dosimetry and Monte Carlo calculations to within 5%. The variable collimator is set at a distance 5 cm further upstream than the small fixed-field collimators. With motorized collimator operation, CBCT imaging and conformal irradiation are performed in one continuous operation. The dosimetric performance of the variable collimator is currently being studied. The optical imaging capability of the SARRP can locate the center of mass of a molecular optical light source to within 1 mm.

Conclusions: The SARRP and similar platforms are transforming pre-clinical radiation research. Molecular optical imaging capabilities offer the exciting potential to

study the disease process in the context of radiation experiment. The continuing technological advances further enhance the capabilities of these systems with great potential for high impact discovery radiation research.

Acknowledgment: Supported in part by NCI (USA) R01-CA 158100 and Xstrahl Inc.

221

Identification of new therapeutic targets

B.G. Wouters

Princess Margaret Cancer Centre, Toronto, ON, Canada

Radiotherapy is used as a curative treatment in many types of cancer with tumour control rates that vary significantly by disease type and tumour stage. Several known biological factors adversely influence treatment efficacy in a patient specific manner, including DNA repair mechanisms, tumour cell proliferation, and tumour hypoxia. These biological phenotypes have served as the basis for development of alternative therapeutic approaches incorporating alternative treatment schedules and/or addition of chemotherapy or molecularly targeted agents. However, it is clear that each of these biological mediators of tumour radioresistance is influenced by a large number of underlying genes and cell signaling pathways, many of which are altered during carcinogenesis. Thus, there is a need for development of investigational approaches that are able to interrogate the potential of targeting individual genes and pathways to improve radiation sensitivity in a high throughput manner. To do so, we have initiated a series of functional genomic screens to identify genes that play essential roles in promoting cellular resistance to hypoxia and cellular radiosensitivity. Our approach utilizes lentiviral delivered shRNA libraries ranging in size from 200-80,000 unique shRNAs. Highly complex shRNA pools targeting ~16,000 human genes have been used to discover a series of novel genes and pathways that confer sensitivity to hypoxia and to radiation treatment in vitro. In addition, smaller focused pools targeting receptor tyrosine kinases, or the entire human kinome have been interrogated both under in vitro conditions as well as in xenografts growing in vivo. Our results reveal a number of novel targets that function in a contextual synthetic lethal manner to increase tumour radiosensitivity and which are thus potential new targets for combination therapy.

Keywords: functional genomics, hypoxia

222

Gamma Probe Based on Scintillation Crystal and Silicon Photomultiplier

A. Yagnyukova¹, T. Khabibullin¹, A. Bolozdynya¹, V. Kantserov¹, K. Zhukov²

¹National research nuclear university "MEPhI", Moscow, Russia

²P.N.Lebedev Physical Institute of the Russian Academy of Sciences

Gamma probe is a radionuclide diagnostic device designed for localization of maximal radioactive pharmaceutical concentration areas in organism. A prototype of gamma probe was developed and produced. Detector consists of an inorganic scintillation crystal and silicon photomultiplier (SiPM) [1].

The main technical characteristics were measured using the ⁵⁷Co gamma source (85% 122 keV, 10% 136 keV): spatial resolution and spatial selectivity are 8 mm and 26° respectively; sensitivity is 12 cps/kBq. Obtained results satisfy the minimal requirements for commercially available systems [2].

Table 1. Technical characteristics of gamma probe prototype

	Spatial resolution, mm	Spatial selectivity, °	Sensitivity, cps/kBq
Gamma probe, MEPhi	8	26	12
Requirements	<15	<40	>5

Registration efficiencies of gamma radiation with ⁵⁷Co and ¹³⁷Cs sources were obtained: 70% and 30% respectively. The temperature instability of SiPM compensation was implemented.

Tests on laboratory animals were performed. The result showed that the prototype of gamma probe is able to rapidly and accurately localize the 1-2 cm radiopharmaceutical concentration area (fig. 1).

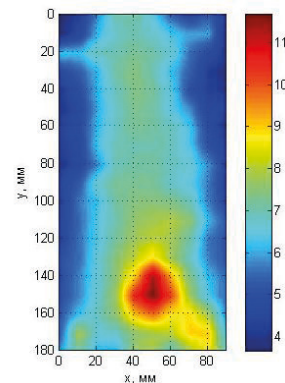


Figure 1. Distribution of radiopharmaceutical concentration in a body of a rat

Keywords: sentinel lymph node localization, gamma probe, radioguided surgery

References:

- [1] V.N.Belyaev, T.S.Brantova, K.A.Vorobyev et al. Optimization of characteristics of gamma probe based on Silicon photomultiplier for intraoperative diagnostics of oncological diseases. // Medical physics, 2012, № 2 (54), p. 49-54
- [2] H.Wengenmair, J.Kopp. Gamma Probes for Sentinel Lymph Node Localization: Quality Criteria, Minimal Requirements and Quality of Commercially Available Systems, // <http://www.sln-kompetenzzentrum.de/gammaprobes.pdf>

223

Frequency difference electrical impedance tomography for imaging lung tumour

C.L. Yang, M. Soleimani

University of Bath, UK

Purpose: Real time monitoring of lung tumour during radiation therapy of lung is a very challenging task. We aim to investigate the Electrical impedance tomography (EIT) as a mean for real time monitoring of lung tumour.

EIT is a fast and cost-effective technique to provide tomographic conductivity image of a subject from boundary current-voltage data. EIT has various potential applications in medical area, such as lung and brain function monitoring. Traditional EIT reconstruction uses time difference imaging technique. However, time difference EIT may not be useful

for monitoring lung tumour behaviour as it is difficult to obtain background data of lung while the tumour has already consisted in the region. This problem can be solved by using frequency difference reconstruction as it only requires measurement data in two different frequencies. Lung tumour has different spectral behaviour compare to normal tissues. This can be used for imaging and tracking tumour.

Methods: In this paper, a frequency difference algorithm is proposed for lung tumour monitoring. Patient's specific model can be developed using diagnostic CT images which can locate the tumour position. When the area of which tumour could possibly active has been located, the proposed EIT algorithm can then be used to observe tumour movement within an area of interest where the tumour could potentially vary.

Results: Figure 1 shows simulation results of reconstructing tumour in real human lung data.

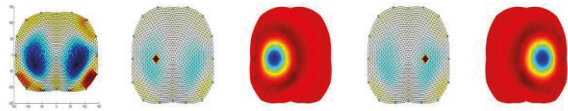


Figure 1: Reconstruction of lung tumor using frequency difference imaging.

Conclusions: EIT imaging is being developed for lung monitoring in intensive care units. For lung radiation therapy real time monitoring using EIT higher special resolution is required. In this paper we presented a frequency difference EIT imaging and local region tomography concept that shows promising results for high spatial resolution required for tumor monitoring during radiation therapy of lung.

Keywords: Electrical impedance tomography, frequency difference imaging

224

[¹⁸F]HX4 PET imaging of tumour hypoxia in HNSCC patients
C.M.L. Zegers¹, F. Hoebbers¹, W. van Elmpt¹, M.C. Öllers¹, A.D. Windhorst², B. Kremer³, F.M. Mottaghy⁴, P. Lambin¹

¹Dept. of Radiation Oncology (MAASTRO), Maastricht University Medical Centre, Maastricht, The Netherlands,

²Dept. of Nuclear Medicine and PET Research, VU University Medical Centre, Amsterdam, The Netherlands

³Department of Otolaryngology/Head and Neck Surgery, VU University Medical Centre, Amsterdam, The Netherlands

⁴Dept. of Otorhinolaryngology and Head and Neck Surgery, Maastricht University Medical Centre, Maastricht, the Netherlands.

¹Department of Nuclear Medicine, Maastricht University Medical Centre, Maastricht, The Netherlands

Purpose: Tumour hypoxia has a negative influence on treatment efficacy. Imaging of hypoxia could help to monitor or predict treatment response and to select patients for additional (anti-hypoxia) therapy. [¹⁸F]HX4 is a novel PET tracer for the evaluation of hypoxia. The aims of this study are to evaluate [¹⁸F]HX4 uptake, optimal acquisition time point and hypoxia changes during radiotherapy in HNSCC patients.

Materials/Methods: HNSCC Patients (T2-4, any N, M0) included in an ongoing trial (NCT01347281) were imaged with [¹⁸F]HX4 PET/CT, before and during (after \pm 20Gy) fractionated irradiation. Patients were treated with radiotherapy (N=1), in combination with chemotherapy (N=8) or cetuximab (N=2). PET/CT imaging was performed at 1.5h, 3h and 4h after i.v. injection of 369 \pm 59 MBq [¹⁸F]HX4. SUV_{max} was extracted from the gross tumour volumes (GTVs); primary tumour and lymph nodes). The SUV_{mean} in the trapezius muscle was used to calculate tumour-to-muscle ratios (TMR). The tumour hypoxic fraction (HF) and hypoxic volume (HV), defined as the relative fraction or absolute volume of the

GTV with a TMR>1.4, were calculated for all lesions. The relationships between image parameters were evaluated using the Pearson's correlation coefficient.

Results: [¹⁸F]HX4 PET/CT scans of 11 HNSCC patients, with in total 21 GTVs (21 \pm 25 cm³) were analyzed. On baseline [¹⁸F]HX4 PET scans, a significant uptake (TMR>1.4) was observed in 15/21 lesions (7/11 primary tumours and 8/10 lymph nodes). Within the hypoxic lesions, the average TMR increased over time from 1.6 \pm 0.3 to 1.8 \pm 0.4 and 2.1 \pm 0.5 for 1.5h, 3h and 4h, respectively. The average HF was 18 \pm 21% (range: 0-70%). The average hypoxic volume was 6.4 \pm 11.3 cm³ (range: 0-45 cm³). Lesion size was significantly correlated with baseline TMR (R=0.59 P<0.01), HF (R=0.50 P=0.02) and HV (R=0.90 P<0.01).

For 8 patients (14 GTVs) imaging was performed before and during radiotherapy treatment. 10/14 lesions were hypoxic at baseline, of which 5 showed persistent hypoxia (TMR>1.4) during treatment. One lesion without baseline hypoxia, showed a minor HF (0.2%) during treatment. All pre-treatment hypoxic lesions showed a decrease in SUV_{max}, TMR and HF, with an average decrease of 30 \pm 12% (SUV_{max}), 28 \pm 13% (TMR) and 89 \pm 22% (HF), respectively. A significant correlation was observed between the imaging parameters before and during radiotherapy treatment; SUV_{max} (R=0.65 P=0.01), TMR (R=0.54, P<0.05), HF (R=0.76, P<0.01) and HV (R=0.71, P<0.01)

Conclusions: The majority of HNSCC lesions shows significant hypoxia before treatment. The optimal imaging time point for [¹⁸F]HX4 PET in HNSCC is 4 hours p.i., expressed by the highest TMR. Pre-treatment hypoxic tumours show a decrease of [¹⁸F]HX4 uptake during radiotherapy treatment. Hypoxia during treatment is related to baseline hypoxia. The relationship with outcome will be evaluated after completion of inclusion and maturation of data.

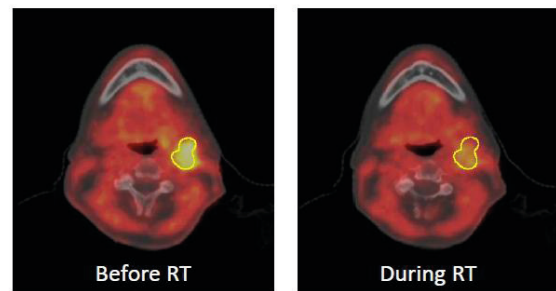


Figure: [¹⁸F]HX4 PET/CT transverse view before and during radiotherapy.

225

Circulating biomarkers for determining absorbed ionizing radiation dose & risk for radiation induced toxicity in humans

F. Zenhausern^{1,2}, M. Brengues¹, R. Korn²

¹Center for Applied Nanobiotechnology and Medicine, University of Arizona, Phoenix, AZ 85004, USA

²Scottsdale Healthcare Research Institute, Scottsdale, AZ 85258

Advances in molecular techniques have improved discovery of biomarkers associated with radiation exposure [1]. A challenge still resides in characterizing signaling pathways involved in molecular and cellular responses to radiological interactions in various biospecimens under different types of irradiation conditions.

Our team is developing the devices, biomarkers and bioassays for the accurate determination of an individual's absorbed dose of ionizing radiation within 0.5 Gy to 10 Gy [2,3]. We report the development of bioassay platforms for identifying sets of genes, whose transcriptional responses are coupled to

either radiation induced tissue specific damage or to the functional recovery of radiation damaged tissue. By using advanced “omics” assays [2-4] (e.g. DNA microarrays, capillary electrophoresis or multiplex qPCR assays) we can characterize quickly and accurately the presence and abundance of molecular species circulating in human biological fluids (e.g. blood, serum, saliva or urine). From circulating lymphocytes in peripheral blood, it is also possible to identify and characterize biomarkers of risk factors [4] for normal-tissue radiation sensitivity that can be separated into two general categories, treatment-related and patient-related factors.

We will discuss specifications and report results from validating these novel molecular diagnostics in preclinical studies to examine the predictive capacity for translating these diagnostic assays into improved clinical outcomes in personalized radiotherapy. The requirements for measuring radiobiological effects using other types of irradiation sources (e.g. protons, carbon ions) will also be discussed.

Keywords: biodosimetry, omics, biomarker

References:

- [1] Meadows SK, Dressman HK, Muramoto GG, Himburg H, Salter A, Wei Z, Ginsburg GS, Chao NJ, Nevins JR, Chute JP (2008), PLoS One, vol 3(4):e1912.
- [2] Brengues M., Paap B., Bittner M., Amundson S., Seligman B., Lenigk R., Zenhausern F., Health Physics, February (2010), 179-185
- [3] Brengues M., Liu D., Korn R. Zenhausern F., Radiation Measurements, in press.
- [4] Badie C, Kabacik S, Balagurunathan Y, Bernard N, Brengues M, Faggioni G, Greither R, Lista F, Peinnequin A, Poyot T, Herodin F, Missel A, Terbrueggen B, Zenhausern F, Rothkamm K, Meineke V, Braselmann H, Beinke C, Abend M., Radiation Research, 2013 Aug; 180(2):138-48.
- [5] Lacombe J., Azria D., Mange A., Solassol J., Expert Reviews Proteomics, 2013, 10(1), 33-43

226

Noninvasive Imaging of Radiation-Induced Lung Inflammation with Positron Emission Tomography (PET) in a Murine Model

Y. Zhang, K. Ding, C. Foss, K. Kang-Hsin Wang, M. Pomper, E. Velarde

Johns Hopkins University School of Medicine, USA

Purpose: Radiation-induced lung injury is a limiting factor in the treatment of thoracic cancers with radiotherapy. Early noninvasive diagnosis of these sequelae is still lacking in the clinic which prevents early follow-up of patients and timely intervention of disease. Translocator protein (TSPO), previously known as peripheral benzodiazepine receptor (PBR), is abundantly present in macrophages and neutrophils and has been proposed as a potent imaging biomarker for inflammation. The goal of the study is to achieve early detection of radiation-induced lung inflammation with noninvasive PET/CT imaging of TSPO expression level. Here we investigated whether ^{124}I -iodoDPA-713, a TSPO-specific radiolabeled ligand, is viable for in vivo PET/CT imaging of radiation-induced lung inflammation in a mouse model.

Materials and methods: To noninvasively monitor the variation of TSPO expression level in radiation-induced mouse lung inflammation with PET/CT imaging. ^{125}I -iodoDPA-713 will be used to identify the optimal imaging window and dose level for inducing lung inflammation. Different dose levels will be delivered and 1 mCi ^{125}I -iodoDPA-713 will be injected and SPECT imaging will be carried out for non-invasive monitoring of the inflammation window. Female Balb/c mice will be divided into irradiated (15 mice) and control (3 mice) groups. A single focal irradiation of 5 mm and 60 Gy will be delivered to the right lung of each mouse with stereotactic

frame on a novel small animal radiation research platform (SARRP) with computed tomography (CT) guidance. The mice will be imaged a day after irradiation and monitored 5 weeks following irradiation. Each mouse will be injected intravenously with 1 mCi of ^{124}I -iodoDPA-713 and then scanned in a dedicated preclinical PET/CT imaging system with the stereotactic frame so that the PET images can be co-registered with the dose map from SARRP. Regions-of-interest (ROIs) analysis will be performed on the PET images to monitor the lung inflammation process. After each imaging study, two of the irradiated animals will be sacrificed and after the last imaging study, all the remaining animals will be sacrificed for biodistribution study with gamma counter to confirm the in vivo PET quantification. The lungs and major organs will be harvested and processed for immunohistochemistry staining to validate the noninvasive imaging data. Extensive staining for TSPO, CD68 (for macrophage), and H&E will be carried out to confirm the in vivo PET findings.

Results and Conclusions: SPECT imaging with ^{125}I -iodoDPA-713 revealed that lung inflammation induced with 60Gy irradiation is TSPO-related and 24 h after irradiation offered the optimal imaging window for inflammation. Lung inflammation is an early event when compared with other events such as fibrosis in radiation-induced toxicities. Early detection of lung injury by non-invasive imaging of inflammation due to radiation is of great importance for effective cancer patient management, especially for those undergoing radiotherapy.

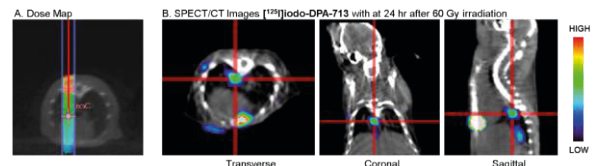


Figure 1 A. Dose map showing the Posterior-Anterior beam with 60Gy dose to the right lung. B. SPECT/CT images with ^{125}I -iodoDPA-713 at 24 hr after 60Gy irradiation to the right lung. The red cross shows the inflammation in the right lung.

Keywords: PET, Inflammation, Translocator Protein (TSPO)



This abstract book is sponsored by ULICE

The ULICE project is funded by the European Commission under Grant Agreement no 228436

